Dynamics of atmospheric ammonia exchange with intensively-managed grassland

Celia Milford

Doctor of Philosophy

The University of Edinburgh

2004

Declaration

This thesis has been composed by myself, and all work reported herein is my own except where otherwise stated. This thesis has not been submitted for any other degree.

8/6/2004

Acknowledgements

I would like to acknowledge funding of this work from the European Commission through the GRAMINAE project (ENV4-CT98-0722 and IN2O-CT98-0118) with additional contributions from the UK Department for the Environment, Food and Rural Affairs and Devolved Administrations (DEFRA). The work was carried out jointly between CEH and the University of Edinburgh.

I would like to thank both my supervisors, Dr. Mark Sutton and Dr. John Moncrieff for their encouragement, advice and enthusiasm. I would also like to thank all my colleagues at CEH, many of whom have helped me in numerous ways. Particular thanks go to Ulli Dragosits and Eiko Nemitz for their friendship and for their generous support. Many thanks also go to Mark Theobald for assisting with the field measurements, Robert Storeton-West for providing additional meteorological data, Mhairi Coyle and Sim Tang for their support and for Sim's tact in sharing an office in the final days.

I would also like to thank Dr. Benjamin Loubet for his scientific collaboration and contribution of bioassay measurements of apoplastic and foliar ammonium. I would like to thank Dr. Marcel Riedo for providing the dynamic ecosystem model and his help in my application of it. In addition I would like to thank all the GRAMINAE participants, particularly those who took part in the Braunschweig integrated experiment and contributed to the NH_3 gradient flux measurements.

Thanks also go to Lawrence Hodgson-Jones of the University of Edinburgh for providing the field site and also for providing details of all the management activities at the field site.

My heartfelt gratitude also goes to my family and friends, who have provided encouragement, support and patience throughout.

Table of Contents

List of Symbols

Symbol	Description	Units or value of constant
Latin Alphabet		
a	constant in R_w parameterisation	-
b	constant in R_s parameterisation	-
c_p	specific heat capacity of air	1.01 J g^{-1} K^{-1}
d	zero-plane displacement height	m
D_χ	molecular diffusivity of entrained property	m^2 s^{-1}
e	water vapour pressure	kPa
$e(z_0')$	water vapour pressure at the leaf surface	kPa
$e_{sat}(T)$	saturated vapour pressure at temperature T	kPa
f_e	R_s correction factor for humidity	(0-1)
f_s	R_s correction factor for differences in the molecular diffusivities of the gases	(0-1)
f_T	R_s correction factor for temperature	(0-1)
f_w	R_s correction factor for water stress	(0-1)
F_g	flux of ammonia with ground layer	ng m^{-2} s^{-1}
F_s	stomatal flux of ammonia	ng m^{-2} s^{-1}
F_t	net flux of ammonia above the canopy	ng m^{-2} s^{-1}
F_w	cuticular flux of ammonia	ng m^{-2} s^{-1}
F_χ	flux of trace gas concentration χ	ng m^{-2} s^{-1}
g	acceleration due to gravity	9.81 m s^{-2}
g_s	stomatal conductance	m s^{-1}
h_c	canopy height	m
H	sensible heat flux	W m^{-2}
$[H^+]_{apo}$	apoplastic hydronium concentration	mol l^{-1}
$[H^+]_g$	ground surface hydronium concentration	mol l^{-1}
I	electrical current	A
I_p	photosynthetically active radiation	µmol m^{-2} s^{-1}
k	von Karman constant	0.41
K_{HA}	Henry equilibrium constant	mol^2 kg^{-2} atm^{-1}
K_b	equilibrium constant for NH_3	-
K_M	eddy diffusivities for momentum	m^2 s^{-1}
K_H	eddy diffusivities for heat	m^2 s^{-1}
K_χ	eddy diffusivity for entrained property	m^2 s^{-1}
L	Monin-Obukhov length	m
m_l	mass of de-ionised water	g
m_{fw}	mass of ground leaves (fresh weight)	g
M	exponent in the power-law approximation of the wind velocity profile	-
M_{NH4}	molecular mass of ammonium	g mol^{-1}
n	exponent in the power-law approximation of the eddy diffusivity profile	-
$[NH_4^+]_{apo}$	apoplastic ammonium concentration	mol l^{-1}
$[NH_4^+]_g$	ground surface ammonium concentration	mol l^{-1}
$[NH_4^+]_{fol}$	foliar NH_4^+ concentration	µmol g^{-1}
$[NH_4^+]_{sol}$	NH_4^+ concentration of solution	µg g^{-1}
p_a	ambient air pressure	kPa
Q_{chem}	chemical production or consumption term	ng m^{-3} s^{-1}
r	shape factor	-
R	transfer resistance	s m^{-1}

R_a	aerodynamic resistance	s m^{-1}
R_{ac}	aerodynamic within-canopy resistance	s m^{-1}
R_b	boundary layer resistance	s m^{-1}
R_{bg}	ground boundary layer resistance	s m^{-1}
R_c	canopy resistance	s m^{-1}
Re_*	turbulent Reynolds number	-
R_s	stomatal resistance	s m^{-1}
R_{sE}	stomatal resistance for water vapour transfer	s m^{-1}
R_t	total resistance to transfer	s m^{-1}
R_w	cuticular resistance	s m^{-1}
Ri	Richardson number	-
RH	relative humidity	%
Sc	Schmidt number	-
t	time	s
T	temperature	°C, K
T_g	temperature of the ground surface	°C
T_s	temperature of the canopy	°C
u , $u(z)$	horizontal mean wind speed	m s^{-1}
u'	fluctuation in wind speed in direction of mean flow	m s^{-1}
u_*	friction velocity	m s^{-1}
u_{*g}	friction velocity at the ground	m s^{-1}
U	height-averaged mean horizontal wind speed	m s^{-1}
U_1	constant in the power-law approximation of the wind velocity profile	variable
V	potential difference	V
V_d	deposition velocity	m s^{-1}
V_{max}	maximum deposition velocity	m s^{-1}
w	vertical component of wind speed	m s^{-1}
w'	fluctuation in vertical wind component	m s^{-1}
x	horizontal distance	m
x_L	fetch	m
z	vertical height	m
z_0	roughness length, notional height above d at which momentum is absorbed	m
z_0'	notional height above d at which tracer is exchanged	m
z_g	height above the surface to which the in-canopy logarithmic profile extends	m

Greek alphabet

β_χ	REA empirical constant of proportionality	($\approx$ 0.56-0.6)
χ	trace gas concentration	$\mu g\ m^{-3}$
χ_a	trace gas concentration at reference height	$\mu g\ m^{-3}$
χ^+	mean concentration during updraughts	$\mu g\ m^{-3}$
χ^-	mean concentration during downdraughts	$\mu g\ m^{-3}$
χ_c	canopy compensation point	$\mu g\ m^{-3}$
χ_g	gaseous ammonia concentration in equilibrium with ground surface ammonium concentration	$\mu g\ m^{-3}$
χ_s	stomatal compensation point	$\mu g\ m^{-3}$
χ_*	scaling concentration	$\mu g\ m^{-3}$
δ	height of the constant flux layer	m
δ_0	lower boundary of in-canopy logarithmic profile	m
$\Delta F_{z,sto}$	storage error in the vertical flux	$ng\ m^{-2}\ s^{-1}$
$\Delta F_{z,adv}$	advection error in the vertical flux	$ng\ m^{-2}\ s^{-1}$
$\Delta F_{z,chem.}$	error in the vertical flux due to chemical production or consumption	$ng\ m^{-2}\ s^{-1}$
ε	ratio of molecular weights of water vapour and dry air	0.622
Φ_M	stability correction function for momentum	-
Φ_H	stability correction function for heat	-
κ	constant in the power-law approximation of the eddy diffusivity profile	-
λ	latent heat of evaporation at 10 °C	$2477\ J\ g^{-1}$
λE	latent heat flux	$W\ m^{-2}$
Γ_d	dry adiabatic lapse rate	$-0.0098\ K\ m^{-1}$
Γ_s	stomatal emission potential	-
Γ_g	ground surface emission potential	-
μ	ratio of molecular weights of dry air to water vapour	-
θ	potential temperature	K
ρ_a	density of dry air at 10 °C	$1246\ g\ m^{-3}$
σ	ratio of the density of water vapour to the density of air	-
σ_w	standard deviation of w	$m\ s^{-1}$
τ	momentum flux	$N\ m^{-2}$
τ_L	Lagrangian timescale	s
ν	kinematic viscosity of air	$m^2\ s^{-1}$
$\xi(z)$	length scale	m
Ψ_H	integrated stability function for momentum	-
Ψ_M	integrated stability function for heat	-
ζ	stability parameter	-

Abstract

Continuous measurements of atmospheric ammonia (NH_3) exchange were conducted for a period of 19 months (May 1998-November 1999) over intensively managed grassland (cut twice for silage and grazed) in southern Scotland using the aerodynamic gradient method. The mean NH_3 concentration and flux for the whole measurement period were 1.52 $\mu g\ m^{-3}$ and 13.9 $ng\ m^{-2}\ s^{-1}$, respectively.

Enhanced emissions of NH_3 were observed following four separate grass cutting events (June 1998, August 1998, June 1999 and May 2000) with peak emissions of 380, 200, 539 and 508 $ng\ m^{-2}\ s^{-1}$, respectively. The magnitude of these emissions was up to an order of magnitude greater than the emissions observed from the grassland prior to cutting. Enhanced NH_3 emissions from cut grassland have been observed, but not quantified prior to this study.

The NH_3 exchange was bi-directional with large diurnal and seasonal variation, which was strongly linked to grassland management in addition to meteorological conditions. The grassland varied from being a net sink for NH_3 during winter months (-6.0 g NH_3-N $ha^{-1}\ d^{-1}$) and prior to cutting of the grass (-4.9 g NH_3-N $ha^{-1}\ d^{-1}$) to being a net source after the grass was cut (29.3 g NH_3-N $ha^{-1}\ d^{-1}$) and after nitrogen fertilisation (153.6 g NH_3-N $ha^{-1}\ d^{-1}$). Net emission was also observed during grazing periods (33.0 g NH_3-N $ha^{-1}\ d^{-1}$). The pattern of NH_3 exchange was similar for 1998 and 1999.

The net annual budget of NH_3 exchange for the grassland for May 1998-April 1999 was emission of NH_3 of 1.9 kg N $ha^{-1}\ yr^{-1}$, equating to 1.6% of the fertiliser N applied. The gross emission flux for the year was 4.2 kg N $ha^{-1}\ yr^{-1}$. Scaling up these gross emissions across the whole of the UK improved grassland (60,500 km^2) would lead to 25 kt NH_3-N, equivalent to 9.5% of the UK total emissions. These results indicate that the gross emission from all processes in fertilised grassland, including emissions from fertilisation, grazing and from cutting, make a significant contribution to the NH_3 emission budget of the UK.

A two-layer canopy compensation point resistance model was applied to the NH_3 measurements. Close agreement between measured and modelled fluxes was obtained by introducing seasonally dependent functions of the foliar and ground layer emission potentials (Γ_s, Γ_g) for key periods. This is a significant improvement on the current use of constant emission potentials within national deposition models.

In addition to the resistance modelling approach, a fully dynamic grassland ecosystem model (PaSim) was applied to the NH_3 measurements. In PaSim, the emission potentials and NH_3 exchange are linked functionally to dynamic plant and soil N pools. Scenarios of changing climate and management were explored with the model. The simulated NH_3 emissions did not follow the expected thermodynamic response to a rise in temperature and demonstrated the complexity of the ecosystem level response of NH_3 exchange to climate change. Simulated NH_3 emissions were reduced by 15% by delaying the timing of fertiliser applications by two weeks, indicating the potential of this measure as an NH_3 abatement option.

The first major intercomparison of NH_3 gradient measurements was conducted during a field campaign over intensively managed grassland in Germany. Enhanced emissions of NH_3 after grass cutting were also observed at this site, providing additional corroboration for this emission source, while the temporal pattern of exchange was similar to that observed in Scotland.

Chapter 1: Introduction

1.1 Ammonia and its role as an atmospheric pollutant

1.1.1 Ammonia in the atmosphere

Ammonia (NH_3) is the dominant base in the atmosphere, and can exist in three phases: i) gaseous, as NH_3; ii) particulate, as ammonium (NH_4^+), for example as ammonium sulphate $(NH_4)_2SO_4$, and iii) liquid, for example as NH_4OH in cloud or fog droplets. NH_3 and NH_4^+ are collectively known as NH_x. The partitioning between the gas and particulate phase is regulated by chemical reactions with sulphuric, nitric and hydrochloric acid as follows:

$$2NH_{3(g)} + H_2SO_{4(g)} \longrightarrow (NH_4)_2SO_4 \quad (1.1)$$

$$NH_{3(g)} + HNO_{3(g)} \longleftrightarrow NH_4NO_3 \quad (1.2)$$

$$NH_{3(g)} + HCl_{(g)} \longleftrightarrow NH_4HCl \quad (1.3)$$

The reaction of NH_3 with acidic sulphate aerosol is generally seen as irreversible, because the vapour pressure of ammonium sulphates is small (Seinfeld and Pandis, 1998). However, reaction with both nitric acid and hydrochloric acid is reversible, due to the significant vapour pressures of ammonium nitrate and ammonium chloride (Pio and Harrison, 1987; Mozurkewich, 1993).

Ammonia is extremely soluble in water, although the solubility decreases with increasing temperature according to the Henry equilibrium (Eq. 1.4):

$$NH_{3(g)} \overset{K_{HA}}{\leftrightarrow} NH_{3(aq)} \quad (1.4)$$

where K_{HA} is the Henry equilibrium constant. In the presence of water, ammonia is readily protonated to ammonium, the degree of dissociation depends on the pH and temperature (Eq. 1.5):

$$NH_{3(aq)} + H_2O \overset{K_b}{\leftrightarrow} NH_4^+ + OH^-. \quad (1.5)$$

where K_b is the equilibrium constant. Both these processes are reversible and in this way, NH_3 can be volatilised from NH_4^+ in solution either from within plants or from the land surface (section 1.3.1 and 1.3.3).

Ammonia is removed from the atmosphere and transferred to the earth's surface via dry, wet or occult deposition processes. Dry deposition is the transfer of gaseous NH_3 or particulate NH_4 by turbulent transport, molecular diffusion, gravitational settling or impaction. Wet deposition is the transfer of NH_4^+ to the ground via precipitation (rain and snow). Occult deposition is the transfer of NH_4^+ present in clouds or fog coming into contact with Earth's surface or surface elements; this process is more important at high altitudes and for aerodynamically rough surfaces such as forests.

Chemical conversion and deposition deplete the atmospheric concentration of NH_3 with time. The mean residence time of a pollutant in the atmosphere multiplied by the mean wind speed gives an estimate for the transport distance of a pollutant. For example, a mean residence time of 1 day and a mean wind speed of 5 m s^{-1} equates to a mean transport distance of 430 km. Various estimates for the mean atmospheric residence time for NH_3 have been reported. Soderlund and Svensson (1976) reported a range of 1-4 days, Moller and Schieferdecker (1985) estimated 19 hours, Sutton (1990) estimated 10 hours while Flechard (1998) reported a mean residence time of 3.5 hours. The differences in these estimates reflect variations in the method used for calculation and the measurement period from which the estimates were derived. Particulate NH_4^+ has a longer atmospheric lifetime and consequently a longer transport distance. Soderlund and Svensson (1976) reported 15 ± 9 days while Moller and Schieferdecker (1985) estimated 7-19 days.

This difference in atmospheric lifetimes and the nature of the sources of NH_3 and NH_4^+ gives rise to different geographical distributions of dry and wet deposition of NH_x within the UK (Sutton *et al.*, 2001b). Large deposition fluxes of NH_3 are generally found in the lowland areas close to large emission sources, whereas wet deposition is generally largest in the remote upland areas. This is due to NH_4^+

travelling further than NH_3 and also a result of the greater amounts of precipitation in upland areas. In addition there is an orographic enhancement of wet deposition in upland areas. Orographic cloud forms over hills and generally contains a higher within-cloud concentration of pollutants as it is formed within the boundary layer. This orographic cloud is often washed out by precipitation from higher level clouds, increasing the amount of wet deposition reaching the surface (Choularton *et al.*, 1988; Fowler *et al.*, 1988).

1.1.2 Emissions of ammonia

In contrast to other pollutants such as sulphur dioxide (SO_2) and ozone (O_3), ammonia can be emitted as well as deposited to the surface. This bi-directional land-atmosphere exchange of NH_3 provides an extra complexity for measurements and modelling of NH_3.

Although non-anthropogenic emissions of NH_3 occur (from vegetation and from other sources such as wild animals and birds), the dominant source of ammonia within the UK and throughout Europe is agriculture. Since 1996 an official inventory of NH_3 emissions for the UK has been produced each year. A summary of the UK NH_3 emission inventory for 2000 is given in Table 1.1 (DEFRA, 2002).

Table 1.1. UK NH_3 emission inventory for 2000 (DEFRA, 2002)

Source of ammonia	Ammonia emission (kt NH_3)	% of total emission
Cattle	139.6	44
Poultry	45.5	14
Pigs	29.8	9
Fertilizer	26.3	8
Sheep etc[a]	18.0	6
Other agricultural sources[b]	5.7	2
Total Agricultural sources	264.9	83
Non Agricultural sources	54.9	17
Total	**319.8**	**100**

[a]includes sheep, deer and goats
[b]includes horses on farms and biomass burning

The total estimated emissions of NH_3 for 2000 are 320 ± 50 kt (DEFRA, 2002). Cattle provide the largest source of NH_3 with poultry second, and pig production and

fertilisers following. Emissions arise from all aspects of livestock husbandry such as animal housing, grazing, storage and land-spreading of animal manures. Non-agricultural sources comprise 17% of the UK emissions; these cover a large number of diverse sources. Vehicle emissions and horses (not on farms) are the two largest sources of about 11.8 and 9.3 kt NH_3, respectively (Sutton *et al.*, 2000a). Emissions of NH_3 from vehicles have increased as catalytic convertors have been introduced to reduce oxidised N emissions.

1.1.3 Ammonia: ecological concerns

Ammonia is of concern in the environment because of its acidifying and eutrophying effect on ecosystems and its role in the formation of aerosols. These processes are discussed below. Where ammonia is present at sufficient concentration levels in the atmosphere it can have direct adverse effects on plants, animals and humans (van der Eerden *et al.*, 1994; Michaels, 1999; Portejoie *et al.*, 2002; Krupa, 2003). However, concentration levels are rarely high enough to cause harmful effects except inside or in the vicinity of large intensive sources (e.g. poultry and pig farms). Consequently, it is the deposition of NH_3, and its subsequent fate in the soil or plant, that causes the largest proportion of adverse effects.

Soil acidification

Once NH_3 comes into contact with soil it generally exists in the form NH_4^+, accepting a proton from the soil solution (Eq. 1.5). NH_4^+ may be taken up by vegetation (releasing one proton) or undergo nitrification to NO_3^- (releasing two protons) thereby increasing the acidity of the soil (Van Breemen *et al.*, 1982; 1984):

$$NH_4^+ + 2O_2 \rightarrow 2H^+ + NO_3^- + H_2O \qquad (1.6)$$

However, the acidifying effect of NH_x deposition will vary on a site-to-site basis, depending on the fate of the deposited nitrogen, e.g. depending on the effectiveness of nitrification or immobilisation of NH_4^+ by soil organic matter.

Eutrophication

The additional N provided to ecosystems by NH_x deposition can also lead to eutrophication and replacement of sensitive vegetation by more nitrophyllous vegetation (Aerts *et al.*, 1990; Tilman and Wedin, 1991). This has been particularly documented in the case of heathlands, where significant proportions of heathland in agricultural regions have been taken over by grass species (Heil and Diemont, 1983; van der Eerden *et al.*, 1991; Bobbink *et al.*, 1992). Replacement has occurred either by direct competitive advantage of the nitrophyllous grasses, or as a consequence of increased N deposition increasing the sensitivity of the heathlands to drought, frost and insect stress. The species diversity of calcareous grasslands is also considered at risk from N deposition, as the competitive ability of tor-grass (*Brachypodium pinnatum*) is enhanced relative to other species (Bobbink, 1991; Pitcairn *et al.*, 1991). In response to these findings, long-term experiments of enhanced N wet deposition onto calcareous and acidic grasslands and heathlands were initiated in 1989 and are ongoing (Lee and Caporn, 1998). This research has shown large differences between initial (mostly positive) effects of additional N doses and adverse effects observed after four-five years of experimentation. These results highlight the importance of long-term experiments when investigating ecosystem responses to pollutants.

There is strong evidence that N deposition may stimulate microbial soil processes, such as mineralisation, which in turn increase N availability (Fisk and Schmidt, 1996; Lee and Caporn, 1998). Ammonia has also been implicated in aiding forest decline (Nihlgård, 1985), where it has been suggested that NH_x deposition may affect nutrient balances, drought and frost sensitivity. However, forest decline is currently accepted to be a result of many factors and the full suite of pollutants being deposited on a forest needs to be considered (e.g. NH_x, SO_2, O_3 and nitrogen oxides (NO_x)). Adverse effects of pollutant deposition on forests can be experienced either via direct foliar deposition or as a result of deposition to the soil, the relative contribution of these pathways to the overall adverse effect is still uncertain (Fangmeier *et al.*, 1994; Krupa, 2003).

Eutrophication

The additional N provided to ecosystems by NH_x deposition can also lead to eutrophication and replacement of sensitive vegetation by more nitrophyllous vegetation (Aerts *et al.*, 1990; Tilman and Wedin, 1991). This has been particularly documented in the case of heathlands, where significant proportions of heathland in agricultural regions have been taken over by grass species (Heil and Diemont, 1983; van der Eerden *et al.*, 1991; Bobbink *et al.*, 1992). Replacement has occurred either by direct competitive advantage of the nitrophyllous grasses, or as a consequence of increased N deposition increasing the sensitivity of the heathlands to drought, frost and insect stress. The species diversity of calcareous grasslands is also considered at risk from N deposition, as the competitive ability of tor-grass (*Brachypodium pinnatum*) is enhanced relative to other species (Bobbink, 1991; Pitcairn *et al.*, 1991). In response to these findings, long-term experiments of enhanced N wet deposition onto calcareous and acidic grasslands and heathlands were initiated in 1989 and are ongoing (Lee and Caporn, 1998). This research has shown large differences between initial (mostly positive) effects of additional N doses and adverse effects observed after four-five years of experimentation. These results highlight the importance of long-term experiments when investigating ecosystem responses to pollutants.

There is strong evidence that N deposition may stimulate microbial soil processes, such as mineralisation, which in turn increase N availability (Fisk and Schmidt, 1996; Lee and Caporn, 1998). Ammonia has also been implicated in aiding forest decline (Nihlgård, 1985), where it has been suggested that NH_x deposition may affect nutrient balances, drought and frost sensitivity. However, forest decline is currently accepted to be a result of many factors and the full suite of pollutants being deposited on a forest needs to be considered (e.g. NH_x, SO_2, O_3 and nitrogen oxides (NO_x)). Adverse effects of pollutant deposition on forests can be experienced either via direct foliar deposition or as a result of deposition to the soil, the relative contribution of these pathways to the overall adverse effect is still uncertain (Fangmeier *et al.*, 1994; Krupa, 2003).

Atmospheric effects

Since ammonia is the dominant gaseous base in the atmosphere, it plays a key role in atmospheric chemistry processes. Ammonium aerosols formed from the reaction of NH_3 with acids (see section 1.1.1) have a negative impact on air quality and visibility (Barthelmie and Pryor, 1998). Conversely, it is thought that ammonium aerosols play a positive role in reducing the radiation forcing potential on the global climate, either through direct light scattering effects or through the indirect effect of aerosols acting as cloud condensation nuclei (IPCC, 1996). The magnitude of this effect is currently very uncertain, however.

1.1.4 Atmospheric pollution control

National and international bodies became increasingly aware of the need to legislate in favour of environmental protection when the effects of Long Range Transboundary Air Pollution (LRTAP), particularly acid-rain from sulphur dioxide and nitrogen oxides, became apparent in the early 1970s. In recognition of the international nature of this problem and the need for international measures, the UN-ECE (United Nations Economic Commission for Europe) established the Convention on Long-Range Transboundary Air Pollution (CLRTAP) in 1979. This convention has been responsible for various protocols acting to reduce emissions of pollutants. The first was the Sulphur Protocol, which proposed a reduction of sulphur emissions by 30% from the 1980 levels by 1990. This was signed in 1985 and came into force in 1987. This was followed by a protocol on Nitrogen oxides in 1988, one on Volatile Organic Compounds (VOCs) in 1991 and a 2nd Sulphur Protocol in 1994 proposing a 62% reduction of sulphur emissions compared with the 1980 levels. These early protocols involved a blanket reduction in emissions with no real consideration of targeting the emission reductions more specifically to reduce the effect of pollution for any particular ecosystem or area.

However, consideration of the receptors was introduced with the concept of the "critical load" or "critical level". The critical load may be defined as "a quantitative estimate of an exposure to one or more pollutants below which significant harmful effects on specified sensitive elements of the environment do not occur, according to

our present knowledge" (Nilsson and Grennfelt, 1988). The critical load concerns the amount of pollutant *deposition* that is received by an ecosystem. The definition of a critical level is the pollutant *concentration* in the atmosphere, above which direct adverse effects on receptors, such as plants, ecosystems or materials may occur according to present knowledge (UNECE, 1988). Krupa (2003) reviews published values of critical levels for NH_3. Van der Eerden *et al.* (1994) suggest a critical level for NH_3 of 23 $\mu g\ m^{-3}$ for a monthly mean concentration and 8 $\mu g\ m^{-3}$ for an annual mean concentration.

Critical loads have been defined for acidification and for eutrophication with the former taking account of both sulphur and nitrogen deposition. Critical loads are set for different ecosystems as each ecosystem will react differently to pollutant inputs. For example, the critical loads for nutrient nitrogen for arctic and alpine scrub, temperate forests and sub-atlantic semi-dry calcareous grassland are 5-15 kg N ha^{-1} yr^{-1}, 10-20 kg N ha^{-1} yr^{-1} and 15-25 kg N ha^{-1} yr^{-1}, respectively (Achermann and Bobbink, 2003; Bobbink *et al.*, 2003).

The amount of deposition that an ecosystem receives over and above the critical load is known as "critical load exceedance", and pollution control measures have been introduced to target reduction in deposition in these exceeded areas. The concept of "Gap-closure", i.e. reducing the critical load exceedance but not necessarily achieving complete non-exceedance (Hettelingh *et al.*, 2001; Posch *et al.*, 2001) is central to current approaches in atmospheric pollution control. Recent air pollution control initiatives of the UNECE such as the "Protocol to Abate Acidification, Eutrophication and Ground-level ozone", known as the Gothenburg Protocol (signed in 1999), employ this approach. The Gothenburg Protocol is the first protocol to include NH_3 and sets annual emission limits for each country for ammonia, sulphur dioxide, nitrogen oxides and non-methane VOCs, which are to be met by 2010. The annual limit for NH_3 emissions for the UK, by 2010, is 297 kt yr^{-1}.

In addition to the Gothenburg Protocol, the EC National Emission Ceilings Directive (NECD) was signed in 1999. This directive sets the same limit on NH_3 emissions as the Gothenburg Protocol. The EC Directive on Integrated Pollution Prevention and

Control (IPCC), signed in 1996, requires large pig and poultry units (> 750 sows, > 40,000 birds) to introduce measures by 2007 to reduce emissions of ammonia along with other pollutants.

As a result of the dependence of air pollution control measures on the assessment of critical load exceedance, it is vital to have good estimates of the deposition of acidifying and eutrophying pollutants. Wet deposition is easily measured by collecting rainfall and analysing the concentration of the pollutant of interest in the rainfall. There is currently a UK network of 39 sites measuring the concentration of various ions in rain, which is combined with the UK Meteorological Office rainfall data to produce maps of wet deposition across the UK (NEGTAP, 2001).

Dry deposition, however, is more difficult to measure as it requires more expensive instrumentation and greater operator time and expertise. Consequently, it is not possible to have sufficient measurements of dry deposition throughout the UK and so models have been developed to estimate dry deposition. Smith *et al.* (2000) describe such a model for estimating dry deposition of NH_x. This model is based on a resistance approach (see section 2.4) and combines concentrations of NH_3 with meteorological data and parameterisation of the surface exchange of NH_3 over different land types on a 5 x 5 km grid.

A UK National Ammonia Monitoring Network was initiated in 1996 and now operates over 90 sites measuring NH_3 concentrations (Sutton *et al.*, 2001b). However, due to the large spatial variability in emissions and concentrations of NH_3, a multi-layer atmospheric transport model, FRAME (Fine Resolution Ammonia Exchange Model) (Singles *et al.*, 1998; Fournier *et al.*, 2002), is used to provide a concentration field of NH_3 across the UK for input into the deposition model. This modelled concentration field uses the spatial NH_3 emission inventory (Dragosits *et al.*, 1998) as an input and is calibrated against the concentrations from the monitoring network (Smith *et al.*, 2000; NEGTAP, 2001).

The accuracy of the dry deposition model estimates relies on the accuracy of the NH_3 emission inventory, concentration estimates, meteorological inputs and also on the parameterisation of the dry deposition process. Parameterisations are developed from

detailed micrometeorological measurements of NH_3 exchange over different land surfaces. The need for detailed measurements to underpin the modelling approach is one of the main motivations for measurements of NH_3 exchange.

1.1.5 UK Nitrogen budgets and trends

In addition to quantifying deposition to particular areas and calculating critical load exceedance, there is also interest on a national and international level in the total budget of a pollutant, i.e. the total amount emitted, deposited, exported or imported from a country. In the case of nitrogen it is also of interest to compare the budgets of reduced N (NH_x) and oxidized N (NO, NO_2, HNO_3, NO_3^-, collectively known as NO_y), as both contribute to acidification and eutrophication. UK budgets for reduced and oxidized N for 1996-1997 are shown in Fig. 1.1 (NEGTAP, 2001). This shows that although the emissions of oxidized N are greater than those of reduced N, the amount of oxidized N deposited within the UK is less due to a greater proportion being exported out of the country. This indicates the importance of reduced N deposition within the UK.

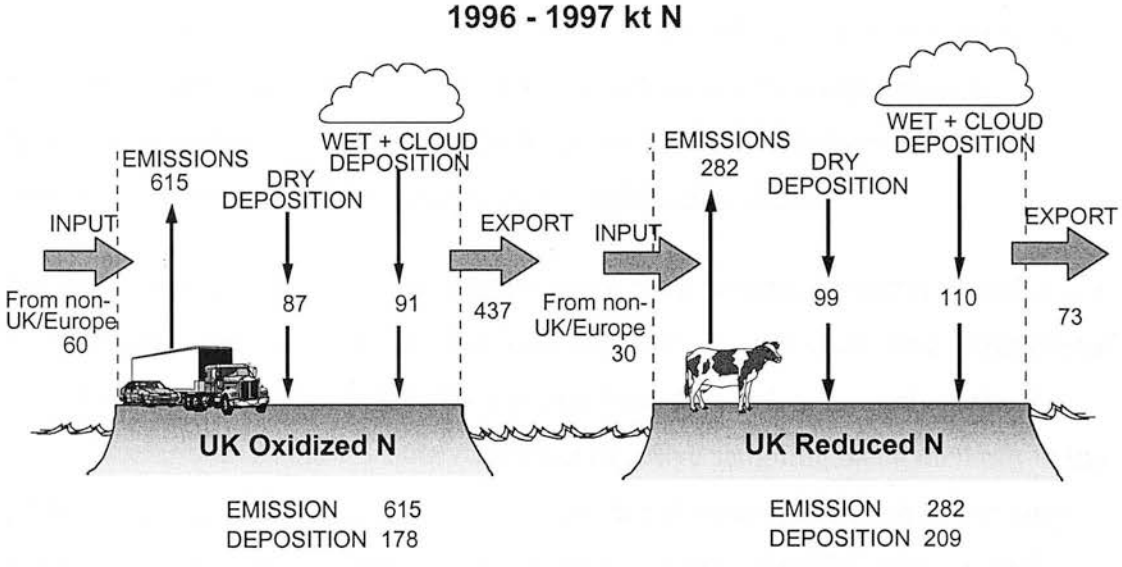

Figure 1.1. UK budgets for oxidized and reduced nitrogen (1996-1997) as kt N (from NEGTAP, 2001).

Sulphur dioxide emissions in the UK have decreased dramatically (82% reduction between 1970 and 1999) due to abatement measures and other activities such as fuel switching (Goodwin *et al.*, 2000). In the same period NO_x emissions have only decreased by 30% (Goodwin *et al.*, 2000). It is difficult to give an estimate of the

trend in NH_3 emissions, partly because inventories have only been compiled for recent years but also because the NH_3 emission inventory is the most uncertain due to the diverse nature of sources. However, NEGTAP (2001) gives a value for UK emissions of NH_3 from 1990 to 1999 and this shows a slight ($\approx$ 5%) decrease. As a result of these trends the relative contribution of reduced and oxidized N to potential acidification is increasing. In 1986, nitrogen contributed 46% of the potential acidification whereas in 1997 it contributed 65% (NEGTAP, 2001).

1.2 Measurement of ammonia

1.2.1 Measurement techniques

The development of automated techniques for measuring ammonia concentration has been slower than for some of the other trace gases. This is largely due to two main difficulties: i) the co-existence of the three phases of ammonia/ammonium and the highly variable partitioning between these phases; ii) the high solubility of NH_3 in water, leading to problems of adsorption of NH_3 onto surfaces such as sample inlets etc. Fehsenfeld (1995) concluded in a review of NH_3 measurement techniques, "much of the uncertainty associated with atmospheric NH_3 is due to the scarcity of reliable measurements, this in turn is due to a lack of sensitive measurement techniques which are easy to use in the field and can operate automatically and continuously to establish large databases for statistical analyses."

The following section briefly describes some of the measurement techniques that are available for measuring NH_x concentration. Differences exist in the time resolution of the various measurement techniques, ranging from the week to monthly scale of passive techniques to the > 1 hour resolution of active sampling batch methods to the 10 Hz sampling possible by some of the more recent techniques. Most of the early measurement techniques operate on the principle of capturing NH_3 with an acidic medium. There then remains the issue of separating the gaseous and aerosol forms of ammonia. Various methods have been developed to separate these two phases; most methods utilise one of two main principles: differential filtering or differential diffusion rates of gaseous NH_3 and aerosol NH_4^+.

Passive sampling

Passive samplers operate by passive diffusion of NH_3 (rather than active air sampling using a pump) to an acidic capturing surface. Absorption of NH_4^+ is negligible due to its low rate of diffusion. Two examples of passive samplers are diffusion tubes (Hargreaves and Atkins, 1987) and APLHA samplers (Tang *et al.*, 2001). The advantage of these samplers is their low cost and simplicity and the fact that they operate without electricity. The length of the sampling period depends on the particular design of the sampler and on the ambient NH_3 concentration. For typical ambient concentrations a sampling period of greater than one week is necessary while for high concentrations, sampling periods of less than a day may be possible. However, high-temporal resolution sampling is not possible with passive methods.

Active sampling batch methods

There are two main types of active batch sampling methods: filter packs and denuders. Filter packs consists of a collection of filters in series to separate NH_3 and NH_4^+, as well as potentially other species (Allen *et al.*, 1988; Harrison and Kitto, 1990). The principle of the method is to capture NH_4^+ aerosol on an inert pre-filter, while allowing NH_3 to pass through undisturbed to be captured on a subsequent acid-impregnated filter. Sampling rates are typically 1-24 hr and the filters are extracted and analysed in a laboratory.

Denuder samplers, in contrast, utilise the difference in diffusion rates of particulate and gaseous NH_3 to the sides of a tube or annulus in which the conditions for laminar flow are satisfied. As a small molecule, gaseous ammonia has a rapid diffusion rate and consequently passes to the sides of the denuder that has been coated with a suitable chemical adsorbant, usually an acid but sometimes a metal oxide adsorbent. Aerosols containing NH_4^+, however, being much larger have a slower diffusion rate and pass undisturbed through the denuder. There are various implementations of this method. These range from simple batch denuders, typically a hollow glass tube 0.5 m long and internal diameter 3 mm, pre-coated with acid (e.g. Ferm, 1979), to annular denuders, consisting of two concentric tubes, typically 0.25 m long, sampling

through a 2-3 mm annulus (e.g. Allegrini *et al.*, 1987; Keuken *et al.*, 1988). Annular denuders have the advantage of higher air sampling rates (typically 10-30 $l\ min^{-1}$) compared with simple denuders (typically 3 $l\ min^{-1}$), hence allowing shorter sampling times or improved detection limits. Similarly to the filter packs, these are generally extracted and analysed in the laboratory.

An earlier method of measuring NH_3 was the bubbler technique (passing the air sample through an acidic solution), however this method does not separate the $NH_{3(g)}$ and $NH_4^+{}_{(aerosol)}$ phases and so is more limited in its application.

Automated continuous sampling

A considerable advancement in atmospheric NH_3 measurement was made in the early 1990s with the development of a continuous-flow denuder known as AMANDA (**A**mmonia **M**easurement by **AN**nular **D**enuder sampling with online **A**nalysis) (Wyers *et al.*, 1993b). Full details of this method are given in Section 3.3.1. In brief, the method consists of a rotating annular denuder in which an acidic absorption solution is continuously transported to and from the denuder and analysed for NH_3 concentration online. The instrument is capable of measuring concentrations with a one-minute time resolution and a measurement range of 0.02 $\mu g\ m^{-3}$ – 300 $\mu g\ m^{-3}$. This was the first automated instrument for NH_3 concentration measurement that had such high temporal resolution plus a low detection limit and wide concentration range.

Other automated techniques, which have been developed to measure NH_3, are listed in Table 1.2. Full details of these techniques are given in the literature and will not be presented here. Techniques such as NO_x monitors with NH_3 converters are in principle easy to use, automated, low-maintenance techniques but unfortunately their detection limit is approximately 2 $\mu g\ m^{-3}$. As ambient NH_3 air concentrations away from sources are often < 2 $\mu g\ m^{-3}$ such a technique does not have widespread application for dry deposition measurement.

Table 1.2. Automated measurement techniques for gaseous ammonia.

Measurement technique	References
Continuous-flow denuder: AMANDA (Ammonia Measurement by ANnular Denuder sampling with online Analysis	Wyers *et al.*, 1993b
Chemiluminescence NO_x monitor with NH_3 converter	Breitenbach and Shelef (1973) van Hove *et al.* (1987)
Thermo-denuder	Keuken *et al.* (1989); Langford *et al.* (1989)
Differential optical absorption spectroscopy (DOAS)	Gall *et al.* (1991)
Photoacoustic monitor	Rooth *et al.* (1990); Pushkarsky *et al.* (2002)
Tunable diode laser absorption spectroscopy (TDLAS)	Dias (1998); Warland *et al.* (2001)
Fourier transform infra-red spectrometry (FTIR)	Tuazon *et al.* (1978) Griffith and Galle (2000)
Photofragmentation laser-induced fluorescence	Schendel *et al.* (1990)
Tandem mass spectrometer (TMS)	Shaw *et al.* (1998)
Chemical ionization mass spectrometry (CIMS)	Fehsenfeld *et al.* (2002); Nowak *et al.* (2002)

1.2.2 Intercomparisons of NH_3 measurement techniques

Various inter-comparisons of gaseous ammonia measurement techniques have been carried out both under field conditions and in controlled environments (Gras, 1984; Anlauf *et al.*, 1985; Appel *et al.*, 1988; Ferm *et al.*, 1988; Dasch *et al.*, 1989; Harrison and Kitto, 1990; Wiebe *et al.*, 1990; Pio, 1992; Williams *et al.*, 1992; Mennen *et al.*, 1996; Parrish and Fehsenfeld, 2000; Fehsenfeld *et al.*, 2002). A large number of these studies compared the filter pack and denuder techniques. In particular the studies investigated the potential problems with filter pack sampling, which are: i) adsorption of NH_3 onto any part of the intake system before being captured on the filter (e.g. on the inlet, manifold or prefilter) and ii) volatilisation of NH_3 from particulate ammonium compounds on the pre-filter. These problems can be exacerbated by long sampling periods, high ambient temperatures or heating of filters above ambient temperature and small diameter filter packs (requiring higher filter loadings). Harrison and Kitto (1990) compared filter pack and denuder techniques and discussed the fact that denuder sampling methods are also potentially subject to systematic errors. For example, particle deposition in the denuder can

occur through turbulent or gravitational transfer if the denuder is not vertical. However, the main advantages of denuders are that they are not subject to phase interaction problems (since particle residence times in the denuder are very small). Both filter packs and denuder methods are subject to errors in the measurement accuracy mainly due to variability of blanks. Additionally, inefficient absorption of NH_3 or incomplete extraction of NH_3 collected as NH_4^+, after sampling can occur.

The inter-comparison studies detailed above, typically observed differences of ± 20% between sampling methods (Wiebe *et al.*, 1990). Williams *et al.* (1992) and Harrison and Kitto (1990) concluded that although there are potential problems with the various techniques available, in general the differences observed between the techniques are often due to the specific implementation (site, operator and apparatus) of the techniques rather than to the techniques themselves. Pio (1992), reporting on a major intercomparison of ammonia measurement techniques in Rome, found that for short sampling periods (4 hourly), denuder and filter pack techniques gave on average, the same results for NH_3 and NH_4^+ measurement. Problems of apparent filter pack overestimation of NH_3 and underestimation of NH_4^+, due to an expected volatilisation of NH_4^+ collected on the filter pack pre-filters, only occurred upon extension of the sampling period to collection over 24 hours.

More recent inter-comparisons have compared automated techniques. For example, Mennen *et al.* (1996) compared six automatic ammonia analysers, in the field and in an environmental test chamber, for their suitability for the Netherlands National Air Quality Monitoring Network. They concluded that the continuous flow denuder (AMANDA) was the most suitable choice of instrument for their network due to its low detection limit, high precision, good linear range, high accuracy and fast response time. Although there were some disadvantages to this technique when considering it for a network, such as the need for frequent attention in refilling solutions and checking liquid flows, they suggested technical improvements, which would help solve these issues.

1.2.3 Land-atmosphere exchange measurements of NH_3

As discussed in Section 1.1, it is necessary to obtain an estimate of the deposition or net exchange of NH_3 to an ecosystem in order to assess the potential for ecological effects of NH_3. Methods to measure the exchange of a gas between the atmosphere and the land are described in section 2.2. Various measurements of the land-atmosphere exchange of NH_3 over a wide range of different ecosystems have been conducted during recent years and a review of some of these studies was presented by Sutton *et al.* (1993d). The vast majority of the early micrometeorological measurements of NH_3 exchange were initiated to quantify NH_3 losses from agricultural activities such as land spreading of animal manures, grazing or fertiliser application (Jarvis *et al.*, 1989; Pain *et al.*, 1989; Hatch *et al.*, 1990; Thompson *et al.*, 1990a; 1990b; Jarvis *et al.*, 1991; Whitehead and Raistrick, 1993). It was less common to study ecosystems in a wider sense, not just focusing on the agricultural perspective. Denmead *et al.* (1974) reported the NH_3 exchange over a grazed alfalfa pasture and this was one of the first studies to characterise the patterns of exchange of an ecosystem.

Initial measurements of land-atmosphere exchange of NH_3 (Sutton *et al.*, 1993b; 1993c; Duyzer, 1994; Duyzer *et al.*, 1994) indicated that NH_3 was almost exclusively deposited to semi-natural vegetation such as moorland and forest, whereas it was both emitted from and deposited to agricultural vegetation. However, more recent long-term data (Flechard and Fowler, 1998) demonstrated that emission also occured from moorland, albeit only for 7% of the time. Wyers and Erisman (1998) and Pryor *et al.* (2001) conducted measurements of NH_3 exchange over coniferous and deciduous forest respectively, and observed emission fluxes for part of the period.

Table 1.3 gives details of some of the micrometeorological measurements of land-atmosphere NH_3 exchange conducted in the last 10 years (for previous studies see (Sutton *et al.*, 1993d). It is noticeable that long-term data sets have become more widely available after the development of the continuous denuder technique (AMANDA). These measurements show that most ecosystems experience bi-directional exchange of ammonia and that ecosystems can be a substantial net sink or source of ammonia. For example, deposition rates of -24 g NH_3-N ha^{-1} d^{-1} have been

reported over semi-natural grassland (Sutton *et al.*, 1993b), while emission rates of 80 g NH_3-N ha^{-1} d^{-1} have been measured over oilseed rape after it was cut (Sutton *et al.*, 2000b).

Some studies give an estimate of the annual net exchange. However, as many of the measurements are made over a period of only a few weeks or months, extrapolating these daily average fluxes to an annual value is very uncertain. In addition, most measurements are made during the growing season, which is not likely to be representative of the autumn and winter periods. This highlights the importance and benefit of measuring over a full year.

Most of the measurements listed in Table 1.3 were conducted with the aerodynamic gradient method (see section 2.2). Eddy covariance (EC) measurements of NH_3 flux have been conducted by Shaw *et al.* (1998) using tandem mass spectrometry and by Famulari *et al.* (2004) using tunable diode laser absorption spectrometry. However, the instruments capable of measuring NH_3 concentration at sufficiently high frequency for eddy covariance measurements are costly, technically complex and require significant operator time. The problems of adsorption of NH_3 onto surfaces such as inlet lines also occur with these techniques. For these reasons, eddy covariance measurements of NH_3 are still very much under development and are not yet capable of operating automatically and continuously in the field to obtain long-term measurements of NH_3 exchange. The relaxed eddy accumulation method does not require a fast response analyser (section 2.2.3) and measurements of NH_3 exchange have been made with this technique (Neftel *et al.*, 1999; Zhu *et al.*, 2000; Nemitz *et al.*, 2001a; Hensen *et al.*, 2004). However, similarly to eddy covariance, this technique is still in the development stage for measurement of NH_3 fluxes.

Table 1.3. Micrometeorological measurements of land-atmosphere NH_3 exchange conducted in the last decade.

Authors	Ecosystem Type/Location	Duration of Measurements	Measurement Technique (Time resolution of measurement)	NH_3 Air Concentrations ($\mu g\ m^{-3}$)	Net exchange of NH_3 over the measurement period and range of fluxes observed (Flux measurements are ng $m^{-2}\ s^{-1}$ NH_3 unless otherwise stated. Negative fluxes denote deposition and positive fluxes, emission)
Herrmann *et al.* (2001)	Grass/clover, Switzerland, two adjacent fields: 1) 'low N': 80 kg N $ha^{-1}\ yr^{-1}$ 2) 'high N': 160 kg N $ha^{-1}\ yr^{-1}$	4 months (June-Sept 1999)	[a]Mini Wet Effluent Denuders (Continuous)	Typical conc. 2-4 $\mu g\ m^{-3}$ Except after fertilisation when up to 30 $\mu g\ m^{-3}$	Net exchange: 1) 'low N': -1.23 kg NH_3-N ha^{-1} 2) 'high N': -0.87 kg NH_3-N ha^{-1}
Milford *et al.* (2001)	Wet heathland/ Moorland, Scotland (*Improved grazing land nearby in one wind sector*)	2 weeks (July-Aug 1997)	[b]AMANDA (Continuous)	Mean: 0.26 $\mu g\ m^{-3}$ Strong dependence of concentration on wind direction (240°: 0.07 $\mu g\ m^{-3}$; 150°: 0.75 $\mu g\ m^{-3}$)	After correcting for advection, range of fluxes observed: -107 to 14 ng $m^{-2}\ s^{-1}$ Mean flux: -6 ng $m^{-2}\ s^{-1}$ (-4.2 g NH_3-N $ha^{-1}\ d^{-1}$)*
Mosquera *et al.* (2001)	1) Intensively-managed grassland, The Netherlands 2) Semi-natural grassland, part of a wetland reserve, The Netherlands	1) July 1998 - July 2000 2) June 1994-September 1995	AMANDA (Continuous)	1) Mean ≈ 6 $\mu g\ m^{-3}$ 2) Mean ≈ 4 $\mu g\ m^{-3}$	1) Average diurnal flux ranged from 0–125 ng $m^{-2}\ s^{-1}$ Net exchange: July 98-June 99: +16 kg NH_3-N ha^{-1} ** July 99-June 00: +10 kg NH_3-N ha^{-1} 2) Mean flux ≈ 45 ng $m^{-2}\ s^{-1}$; deposition fluxes observed in the spring, emission in the autumn and winter. Net exchange: June 94-May 95, +16 kg NH_3-N ha^{-1}†
Pryor *et al.* (2001)	Deciduous forest, Indiana, USA	4 field campaigns 1) 19/4/98-5/5/98 2) 8-19/1/99 3) 20/4/99-5/5/99 4) 26/2/00-2/3/00	[c]Wet Effluent Diffusion Denuders (Continuous)	Mean: 1) 1.2 $\mu g\ m^{-3}$ 2) 0.26 $\mu g\ m^{-3}$ 3) 0.65 $\mu g\ m^{-3}$ 1) & 3) measured at 37.7 m, 2) measured at 45.7 m.	Measurements in spring (period 3) showed typical mean daily flux of -21 ng $m^{-2}\ s^{-1}$ (-15 g NH_3-N $ha^{-1}\ d^{-1}$). Observed emission on 3 out of 17 days in period 3) peaking at 55 ng $m^{-2}\ s^{-1}$.

Authors	Ecosystem Type/Location	Duration of Measurements	Measurement Technique (Time resolution)	NH_3 Air Concentrations ($\mu g\ m^{-3}$)	Net exchange of NH_3 over the measurement period and range of fluxes observed
Schjoerring and Mattsson (2001)	1) Winter Wheat 2) Winter Oilseed rape 3) Spring Barley 4) Field Pea (All field sites in Denmark)	2 growing seasons, 1993 and 1994	[d]Passive horizontal flux samplers (weekly batch measurements)	1-4 $\mu g\ m^{-3}$	Net exchange (all emission fluxes): 1) 1993, 20 weeks: 1.5 to 2 kg NH_3-N ha^{-1} 1994, 20 weeks: ≈ 5 kg NH_3-N ha^{-1} 2) 1993, 18 weeks: 3 to 5 kg NH_3-N ha^{-1} ‡ 1994, 20 weeks: 2 to 3 kg NH_3-N ha^{-1} 3) 1993, 17 weeks: ≈ 3 kg NH_3-N ha^{-1} 1994, 16 weeks: ≈ 5 kg NH_3-N ha^{-1} 4) 1993, 8 weeks: ≈ 2 kg NH_3-N ha^{-1} 1994, 14 weeks: ≈ 4 kg NH_3-N ha^{-1}
Spindler *et al.* (2001)	Semi-natural grassland, Germany (*70 kg N ha^{-1} applied, 3 cuts*)	17 days (Sept 1995)	AMANDA (Continuous)	1-5 $\mu g\ m^{-3}$	Mean value not available Range of fluxes observed: -60 to 30 ng $m^{-2}s^{-1}$ Predominantly deposition ≈ *–15 ng $m^{-2}s^{-1}$*
Sutton *et al.* (2000b)	Oilseed rape, Scotland	2 weeks (June 1995)	AMANDA (Continuous)	Pre-cutting mean: 1.03 $\mu g\ m^{-3}$ Post-cutting mean: 2.47 $\mu g\ m^{-3}$	Pre-cutting range of fluxes: –150 to 180 ng $m^{-2}s^{-1}$ Typical daily flux: +28 ng $m^{-2}\ s^{-1}$ (+20 g NH_3-N $ha^{-1}\ d^{-1}$) Post-cutting range of fluxes: –200 to 620 ng $m^{-2}s^{-1}$ Typical daily flux immediately after cutting: (+30 g NH_3-N $ha^{-1}\ d^{-1}$) Typical daily flux at end of the measuring period: +110 ng $m^{-2}\ s^{-1}$ (+80 g NH_3-N $ha^{-1}\ d^{-1}$)

Authors	Ecosystem Type/Location	Duration of Measurements	Measurement Technique (Time resolution)	NH_3 Air Concentrations ($\mu g\ m^{-3}$)	Net exchange of NH_3 over the measurement period and range of fluxes observed
Anderson *et al.* (1999)	Spruce forest, Denmark	7 Field campaigns, ≈ 1 week each (1991-1995)	[e]Annular denuders (3 hr batch measurements)	Mean of all campaigns $\mu g\ m^{-3}$: Stable: 1.11 East winds: 1.47 West winds: 0.49 Overall mean: 0.80	Mean flux of all campaigns ng $NH_3\ m^{-2}\ s^{-1}$ (g NH_3-N $ha^{-1}\ d^{-1}$) Stable: -4.7 (-3.4) East winds: -8.4 (-6.0) West winds: -14.5 (-10.3) Overall mean: -9.1 (-6.5)
Flechard and Fowler (1998)	Moorland, Scotland	13 months (Feb 95-Feb 96)	AMANDA (Continuous)	Median: 0.44 $\mu g\ m^{-3}$	Median over whole period: -5.2 ng $m^{-2}s^{-1}$ (-3.7 g NH_3-N $ha^{-1}\ d^{-1}$)
Hansen *et al.* (1998)	Heathland, Denmark	5 weeks (May – June 95)	[d]Passive f lux samplers (weekly batch measurements)	Weekly mean values: 1.1 - 2.3 $\mu g\ m^{-3}$	Range of weekly mean fluxes: -10.5 to –6 kg NH_3-N $ha^{-1}\ yr^{-1}$
Plantaz (1998)	Grazed pasture, The Netherlands	2 yrs (July 92-July 94)	[f]Thermodenuders & AMANDA for part of the time (Continuous)	Mean ($\mu g\ m^{-3}$): Grazed D: 8.2 Grazed N: 10.3 Nongrazed D: 5.4 Nongrazed N: 6.6	Mean (ng $m^{-2}s^{-1}$) Grazed D: 52; N: –4 Grazed mean: +24 (+17.1 g NH_3-N $ha^{-1}\ d^{-1}$) Nongrazed D: –4; N: –25 Nongrazed mean: -14.5 (-10.3 g NH_3-N $ha^{-1}\ d^{-1}$)
Wyers and Erisman (1998)	Coniferous forest, The Netherlands	2 yrs (Nov 92-Nov 94)	AMANDA (Continuous)	Mean: 5.2 $\mu g\ m^{-3}$ Median: 3.5 $\mu g\ m^{-3}$	-1 to +0.75 $\mu g\ m^{-2}s^{-1}$ Predominantly deposition fluxes
Jambert *et al.* (1997)	Maize, France	≈ 2 weeks (June 1993)	[g]Chemiluminescence (Continuous)	Not reported	Peak flux after fertilisation: +160 g NH_3-N $ha^{-1}\ d^{-1}$ Mean flux: +18 g NH_3-N $ha^{-1}\ d^{-1}$
Sutton *et al.* (1997a)	Grassland, UK	2 weeks (May 1995)	AMANDA (Continuous)	0-30 $\mu g\ m^{-3}$	Range of fluxes: -200 to +400 ng $m^{-2}s^{-1}$ Mean value not available
Sutton *et al.* (1997b)	Upland Moorland, UK	2 weeks (Apr-May 1993)	AMANDA & [h]Batch rotating denuder (Continuous)	0-5 $\mu g\ m^{-3}$	Range of fluxes: -35 to +3 ng $m^{-2}s^{-1}$ Mean value not available

Authors	Ecosystem Type/Location	Duration of Measurements	Measurement Technique (Time resolution)	NH_3 Air Concentrations ($\mu g\ m^{-3}$)	Net exchange of NH_3 over the measurement period and range of fluxes observed
Bussink *et al.* (1996)	Intensively-managed grassland, The Netherlands (*440 kg N ha^{-1} applied*)	17 days (May-Sept 1989)	Acid wash bottles (H_3PO_4) (3 hr batch measurements)	14.7-27.2 $\mu g\ m^{-3}$ only concs reported, not whole period.	Range of fluxes: -1.1 to +0.8 kg NH_3-N $ha^{-1}\ d^{-1}$ Mean value not available
Hesterberg *et al.* (1996)	Extensively-managed Grassland (litter meadow), Switzerland	June 1992-May 1993, weekly and 4 IOP's.	WEDD & passive samplers	0-37 $\mu g\ m^{-3}$ Mean: ≈10 $\mu g\ m^{-3}$	Range of fluxes: -30 to +1.5 kg NH_3-N $ha^{-1}\ yr^{-1}$ Net exchange: -13 kg NH_3-N $ha^{-1}\ yr^{-1}$
Meixner *et al.* (1996)	Cereal crops (wheat, oat, triticale), Germany	1-6 months, 1990, 1994 & 1995	Thermodenuders, AMANDA & batch denuders	0-5 $\mu g\ m^{-3}$	Range of fluxes: -75 to 150 ng $m^{-2}\ s^{-1}$ Mean value not available
Yamulki *et al.* (1996)	Wheat, UK	Mar 1991-April 1992	Annular denuders (35cm long) (batch measurements)	1.5 - 5.04 $\mu g\ m^{-3}$	Seasonal averaged fluxes: -68 to 100 ng $m^{-2}\ s^{-1}$ Net exchange: +1.76 kg NH_3-N $ha^{-1}\ yr^{-1}$
Duyzer (1994)	4 heathland sites, The Netherlands	Weekly campaigns (130 hrs in total) (1984-1987)	Annular denuders (50cm long) (1 hr batch measurements)	Mean: 3.7 $\mu g\ m^{-3}$	-200 to +30 ng $m^{-2}\ s^{-1}$ Net exchange: -13 kg NH_3-N $ha^{-1}\ yr^{-1}$
Duyzer *et al.* (1994)	Douglas fir, The Netherlands	6 Field campaigns (April 1988-March 1990)	Annular denuders (1.5 hr batch measurements)	Mean: 4.8 $\mu g\ m^{-3}$ Median: 4 $\mu g\ m^{-3}$ Range: 0.8-27 $\mu g\ m^{-3}$	Net exchange obtained from daytime measurements: -40 kg N $ha^{-1}\ yr^{-1}$ (-110 g N $ha^{-1}\ d^{-1}$)
Erisman *et al.* (1994)	Heathland, The Netherlands	Apr 89-Apr 90	Thermodenuders, & AMANDA	Not available	Net exchange: -12 kg N $ha^{-1}\ yr^{-1}$

Authors	Ecosystem Type/Location	Duration of Measurements	Measurement Technique (Time resolution)	NH_3 Air Concentrations ($\mu g\ m^{-3}$)	Net exchange of NH_3 over the measurement period and range of fluxes observed
Erisman and Wyers (1993)	2 Heathland sites, The Netherlands	1) 3 weeks (April-May 1991) 2) 3 months (Sept-Nov 1991)	AMANDA	1) 0-25 $\mu g\ m^{-3}$ 2) 0-40 $\mu g\ m^{-3}$	1) -430 to 80 ng $m^{-2}\ s^{-1}$ 2) -480 to 550 ng $m^{-2}\ s^{-1}$ Mean values not available
Sutton *et al.* (1993b)	1) Moorland 2) Semi-natural grassland 3) Semi-natural grassland 4) Coniferous forest, UK (All sites in UK)	Campaigns (days) (1987-1989)	[i]Filter packs (1-3 hr batch measurements)	Mean ($\mu g\ m^{-3}$): 1) 0.67 2) 2.00 3) 1.77 4) 0.20	Mean flux for different sites: ng $NH_3\ m^{-2}\ s^{-1}$ (g NH_3-N $ha^{-1}\ d^{-1}$) 1) –17.3 (-12) 2) –33.9 (-24) 3) –14.3 (-10) 4) –11.0 (-8)
Sutton *et al.* (1993c)	1) Fertilised grassland 2) Barley (Both sites in UK)	Campaigns (days) (1988-1989)	Filter packs (1-3 hr batch measurements)	Mean ($\mu g\ m^{-3}$): 1a) Summer: 0.21 1b) Winter: 1.29 2) 0.99	Mean flux for different sites: ng $NH_3\ m^{-2}\ s^{-1}$ (g NH_3-N $ha^{-1}\ d^{-1}$) 1a) Summer: +7.7 (+5) 1b) Winter: -14.5 (-10) 2) +6.3 (+4)

*1 g NH_3-N $ha^{-1}\ d^{-1}$ = 0.37 kg N $ha^{-1}\ yr^{-1}$

**57% of this emission was estimated to be due to manure spreading; 256 kg N ha^{-1} of slurry and 97 kg N ha^{-1} of mineral fertiliser were spread in 1999.

†Authors suggest presence of ≈ 50,000 geese and 200 horses could help explain these high emissions.

‡Authors have separated fertiliser emissions from plant-derived emissions, plant-derived emissions reported here.

[a]Mini-Wet Effluent Denuders (Neftel et al., 1998)

[b] AMANDA (**A**mmonia **M**easurement by **AN**nular **D**enuder sampling with online **A**nalysis) (Wyers et al., 1993)

[c] WEDD (Wet Effluent Diffusion Denuder) (Vecera and Dasgupta, 1991) (Sorensen *et al.*, 1994)

[d] Passive horizontal flux samplers (Schjoerring, 1995)

[e]Annual denuders sometimes referred to as Ferm denuders (Ferm, 1979)

[f]Thermodenuders

[g]Chemiluminescence, NO monitor with NH_3 converter

[h]Batch rotating denuder (Keuken et al., 1988)

[i]Filter packs

D: daytime, N:nighttime, IOP's: intensive observation period

1.2.4 Land-atmosphere exchange of NH_3 with grassland

Managed grasslands constitute 27% of the land cover of Great Britain (Fuller *et al.*, 1994) and provide the single largest land cover category in GB. Grasslands vary widely in their species composition and management regime from semi-natural unfertilised grassland to high N input intensively managed grassland. These ecosystems display quite different NH_3 exchange characteristics; semi-natural grassland primarily experiences NH_3 deposition and may be adversely affected by that deposition, experiencing species change and/or change in biomass productivity. Intensive grassland experiences both deposition and emission of NH_3, and as such may impact on the atmosphere, for example by increasing emissions or affecting long range transport of pollutants (Sutton *et al.*, 2001a). However, grasslands are currently treated as one vegetation type in UK deposition models (Smith *et al.*, 2000). It is important to improve the parameterisations of NH_3 exchange over different grassland types to increase the accuracy of the UK and European dry deposition budget and assess the effects of NH_3 deposition.

In addition to the interest in contrasting ecosystem types, large rates of NH_3 emission have been observed, following cutting of intensively managed grassland, from the sward itself (Sutton *et al.*, 1997a). It is known that emission of NH_3 occurs from senescing and decomposing vegetation (Whitehead and Lockyer, 1989; Mannheim *et al.*, 1997), but there has been little research investigating NH_3 emissions from a cut sward. Emission of volatile organic compounds (VOC's) has been detected from cut grassland and attributed to a "wounding" of the vegetation (Gouw *et al.*, 1999). Other work has investigated the effect of cutting regimes on the health, yield and species diversity of a sward (Smith *et al.*, 1996a; 1996b; Blum *et al.*, 1997; Evans *et al.*, 1998), but not the effect on NH_3 exchange.

There are several previous micrometeorological flux measurements over grassland (e.g. Denmead *et al.*, 1974; 1976; Sutton *et al.*, 1993b; 1993c; Grünhage *et al.*, 1994; Bussink *et al.*, 1996; Hesterberg *et al.*, 1996; Sutton *et al.*, 1997a; Plantaz, 1998; Herrmann *et al.*, 2001; Mosquera *et al.*, 2001; Spindler *et al.*, 2001). However, only four of these studies reported long-term measurements (> 6 months). Most of these

studies showed NH_3 exchange over grassland to be bi-directional, with both emission and deposition fluxes of NH_3 observed (Table 1.3). The measurements of the net exchange of grassland reported over an annual or seasonal basis range from semi-natural grassland in Switzerland being a net sink of 13 kg N ha^{-1} yr^{-1} (Hesterberg *et al.*, 1996) to intensively-managed grassland in The Netherlands being a net source of between 10-16 kg N ha^{-1} yr^{-1} (Mosquera *et al.*, 2001). However, 57% of the emission in the latter study was estimated to be due to manure spreading (256 kg N ha^{-1} of slurry and 97 kg N ha^{-1} of mineral fertiliser were spread in 1999). Therefore the plant-mediated emissions from the grassland would equate to 6.9 kg N ha^{-1} yr^{-1}. This highlights one of the difficulties in parameterizing NH_3 exchange over different grassland types. It is necessary to separate out the contribution to the NH_3 exchange from the plants themselves and from the fertiliser applied. Plantaz (1998) reported a grazed pasture in The Netherlands to be a net source of NH_3, equivalent to 6.2 kg N ha^{-1} yr^{-1}, while an un-grazed pasture was a sink of –3.8 kg N ha^{-1} yr^{-1}.

In another study, Herrmann *et al.* (2001) measured the NH_3 exchange from two intensively managed grass/clover fields in Switzerland over a single growing season. Mineral fertiliser (NH_4NO_3) was applied at rates of 80 and 160 kg N ha^{-1} yr^{-1}, respectively. Both fields were a net sink for ammonia over the measurement period, with the net exchange over the 4 month measuring period being deposition of -1.23 kg N ha^{-1} and -0.87 kg N ha^{-1}, respectively. Although Herrmann *et al.* (2001) classified these fields as 'low' and 'high' N, it is worth noting that 160 kg N ha^{-1} yr^{-1} is still a relatively low application of N, compared with 350-400 kg N ha^{-1} yr^{-1} typically applied on intensive grassland fields in The Netherlands.

1.3 Pathways of NH_3 exchange

To construct reliable models of dry deposition, it is necessary to develop an understanding of the pathways involved in the exchange process and also of the parameters controlling these pathways. Parameterisations of these processes can then be developed and incorporated into a model (see section 2.4). The pathways involved in land-atmosphere exchange of ammonia are: i) stomatal exchange; ii) leaf surface exchange and iii) ground surface exchange. These processes can occur in parallel and

each process is influenced by a range of factors, varying from the plant specific (e.g. plant species, phenology) to wider ecosystem influences (e.g. soil pH, availability and form of N) to environmental and meteorological influences (e.g. temperature, solar radiation, humidity, wetness, atmospheric turbulence).

1.3.1 Stomatal exchange

Gaseous NH_3 is present in substomatal cavities in thermodynamic equilibrium with the apoplastic (intercellular leaf tissue) NH_4^+ concentration ($[NH_4^+]$). This sub-stomatal NH_3 concentration is known as the stomatal compensation point (χ_s) (Sutton *et al.*, 1995b) and was originally identified by Farquhar *et al.* (1980). If the ambient atmospheric NH_3 concentration is greater than the compensation point, absorption of NH_3 into the leaf by the stomata will occur, whereas emission from the leaf will occur if the reverse is true. The compensation point is therefore a key parameter involved in NH_3 exchange. The switch from absorption of NH_3 to emission of NH_3 by various plant species has been demonstrated by measuring the NH_3 flux in response to changing NH_3 concentration in controlled environment chambers (Farquhar *et al.*, 1980; Husted and Schjoerring, 1995b; Schjoerring *et al.*, 1998; Hill, 1999; Schjoerring *et al.*, 2000; Hill *et al.*, 2001).

A relationship between the stomatal compensation point and the apoplastic $[NH_4^+]$ and pH can be derived from the temperature response of the Henry equilibrium (Eq. 1.4) and the ammonium-ammonia dissociation equilibrium (Eq. 1.5) as described by Nemitz *et al.* (2000b):

$$\chi_s = \frac{161500}{(T_s + 273.15)} \exp\left(\frac{-10380}{T_s + 273.15}\right) \frac{[NH_4^+]_{apo}}{[H^+]_{apo}} \qquad (1.7)$$

where T_s is the temperature of the canopy in °C and all concentrations are in mol l^{-1}. The ammonium/hydronium ratio in the apoplast ($[NH_4^+]_{apo}/[H^+]_{apo}$) has been termed the stomatal emission potential (Γ_s) and has the advantage of being temperature independent, whereas χ_s is a strong function of temperature (doubling with every 5°C increase in temperature). Clearly, the factors which control stomatal opening (solar radiation, water stress) also control this pathway of NH_3 exchange.

Various studies have been conducted to explore influences on the compensation point. Husted and Schjoerring (1995a) developed a vacuum infiltration technique to determine apoplastic $[NH_4^+]$ and $[H^+]$ directly. The value of χ_s can be calculated from $[NH_4^+]_{apo}$ and $[H^+]_{apo}$ as indicated in Eq. 1.7. This bioassay estimate can be compared with estimates from controlled environment studies and micrometeorological measurements.

Schjoerring *et al.* (1998) used the infiltration technique and controlled environment chambers to investigate the physiological parameters controlling plant-atmosphere exchange of ammonia. They found that the form of nitrogen uptake by roots (NH_4^+ or NO_3^-) affects the NH_3 exchange; plants grown in NH_4^+ nutrient solution produced much higher NH_3 emissions than those grown in NO_3^- solutions. They also observed a strong effect of plant developmental stage on χ_s in barley plants, with χ_s decreasing to a minimum around anthesis and then increasing again. Husted *et al.* (2000) investigated the diurnal cycle in apoplastic $[NH_4^+]$ and $[H^+]$ in oilseed rape (*Brassica napus*) and found only a small variation in concentrations. They concluded that the diurnal variations in NH_3 exchange observed in the field are most likely caused by changes in the canopy temperature and stomatal conductance rather than variations in χ_s.

The question of diurnal, seasonal and annual changes in χ_s is of great interest to the modelling community. Currently, a single value for the stomatal emission potential (Γ_s) is used for grassland and arable land throughout the year in the UK deposition model (Smith *et al.*, 2000). Although research has shown that Γ_s does change with plant developmental stage and N supply, until recently, there have not been sufficient measurements from which to derive seasonal parameterisations.

As well as temporal variation within species, there is also strong variation of χ_s between species (Fig. 1.2) (Mattsson *et al.*, 2004). Generally, fertilised croplands or grasslands tend to have higher compensation points than semi-natural unfertilised vegetation (Sutton *et al.*, 1996) which explains the observed increased periods of emission from croplands and intensively-managed grasslands compared with semi-natural vegetation.

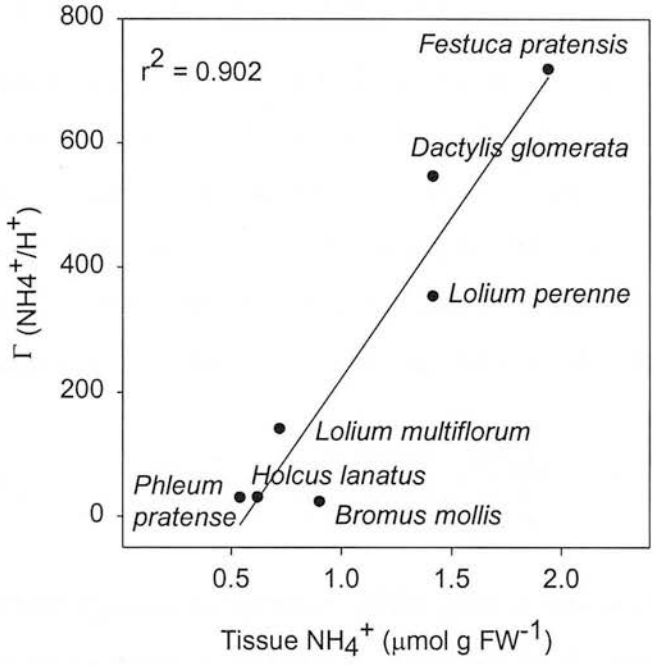

Figure 1.2. Foliar NH_4^+ concentration and Γ_s (apoplastic NH_4^+/H^+) for different plant species (from Mattsson *et al.*, 2004).

1.3.2 Leaf surface exchange

In addition to being absorbed into stomata, NH_3 can also be deposited directly onto the leaf surface or cuticle. This occurs readily when the surface is visibly wet. However, Burkhardt and Eiden (1994) have demonstrated that there are microscopic water 'films' associated with hygroscopic salts on leaf surfaces which allow deposition even when the surface appears dry.

Once NH_3 has been deposited to a leaf surface, it may be washed off by subsequent precipitation, adsorbed into the stomata or it can desorb from the surface and be recycled back into the atmosphere. Periods of desorption of previously deposited NH_3 from evaporating leaf water films have been observed, particularly in the early morning (Sutton *et al.*, 1998; Flechard *et al.*, 1999). Sutton *et al.* (1994) discuss the effect of the chemistry of the leaf surface on cuticular exchange. Initially it was thought that the presence of SO_2 would enhance uptake of NH_3 (co-deposition). However, reaction of NH_3 and SO_2 to form aerosol may actually deplete ambient NH_3 concentrations below the compensation point, leading to emission of NH_3 rather than deposition.

1.3.3 Ground surface exchange

Ammonia can be deposited directly to the ground surface and it can also be emitted or volatilised directly from the surface. Volatilisation is governed by the Henry equilibrium and the ammonium-ammonia dissociation equilibrium in a similar way to exchange within the stomata and an analogous equation to Eq. 1.7 can be used to determine the gaseous ammonia concentration in equilibrium with a ground surface ammonium concentration $[NH_4^+]_g$ and ground surface pH:

$$\chi_g = \frac{161500}{(T_g + 273.15)} \exp\left(\frac{-10380}{T_g + 273.15}\right) \frac{[NH_4^+]_g}{[H^+]_g} \qquad (1.8)$$

where T_g is the temperature of the ground emission source in °C and all concentrations are in mol l^{-1}. Consequently, the rate and amount of volatilisation depends on the amount of ammonium present, the temperature and the pH of the surface. Other parameters affecting volatilisation are soil properties such as the cation exchange capacity, the buffering capacity of the soil, soil texture and moisture and meteorological or environmental factors such as windspeed, precipitation and the ambient atmospheric ammonia concentration (Freney *et al.*, 1981; Sharpe and Harper, 1995).

Each of the pathways of exchange described above will be affected by the degree of turbulence of the atmosphere, the roughness of the surface and the structure of the vegetation. Even if the ground surface layer is a source of NH_3, the emitted NH_3 may be recaptured by the canopy above it, and the consequent NH_3 exchange with the atmosphere may be net deposition. Issues of canopy cycling of NH_3 are discussed by Denmead (1976), Sutton et al. (1995a) and Nemitz *et al.* (2000a).

1.4 N cycling in ecosystems

Nitrogen is an essential nutrient for living organisms, enabling them to produce complex organic molecules such as proteins, amino acids and nucleic acids. Like other nutrients, it is cycled through the biosphere and atmosphere. Ammonia forms only one component of this nitrogen cycle; to fully understand and be able to model NH_3 ecosystem exchange, NH_3 should not be studied in isolation to the rest of the N

cycle. In addition, it is particularly important in the present climate of pollution control measures to look at the nitrogen cycle as a whole, as abatement of one pollutant (such as NH_3) may lead to greater release of another pollutant into the environment (e.g. N_2O emission or nitrate leaching) (Jarvis, 1996; Erisman and Monteny, 1998; Velthof *et al.*, 1998; Brink *et al.*, 2001; Webb *et al.*, 2001).

Many different diagrams and representations of the nitrogen cycle have been published. These differ depending on the particular focus and scope of a study, although the essential processes are the same (e.g. Clark, 1981). The N cycle presented in Fig. 1.3 is for a managed grassland ecosystem. A full global nitrogen cycle (Jenkinson, 1990; Galloway, 1998) includes additional components such as: emissions of NO_x; chemical reactions in the atmosphere; N_2 fixation by the chemical industry (i.e. the production of fertiliser) and the various inputs and outputs from aquatic ecosystems. The grassland N cycle consists of i) inputs to the soil-plant system, ii) transformations within the plant-soil system and iii) outputs. These are described below.

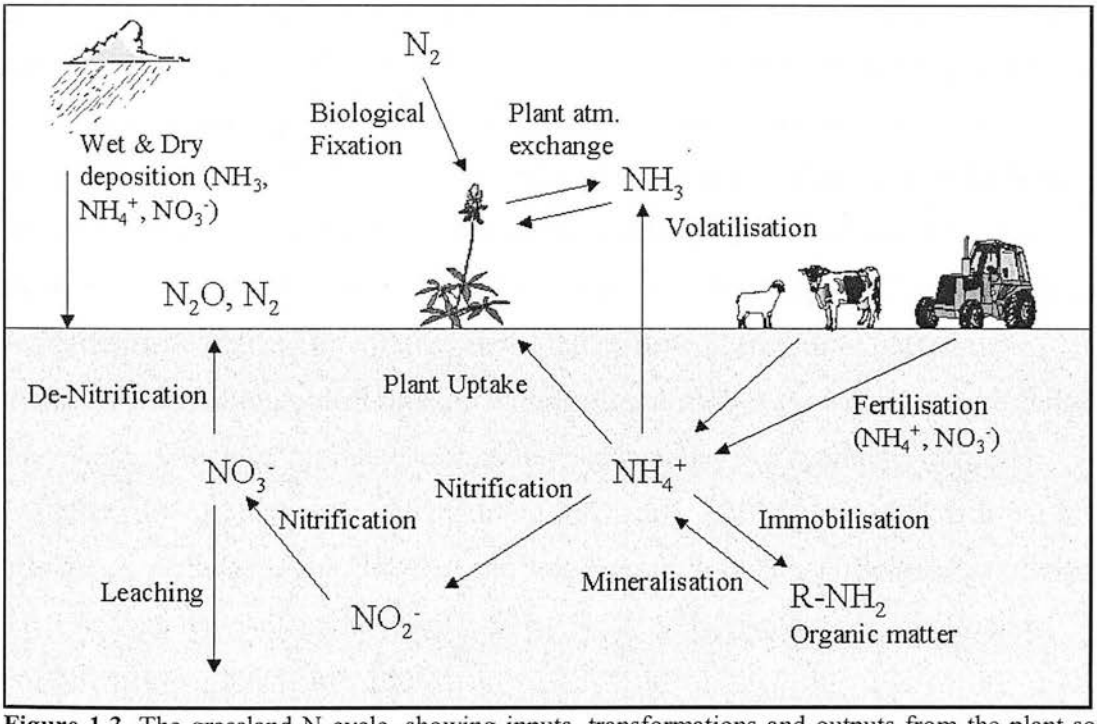

Figure 1.3. The grassland N cycle, showing inputs, transformations and outputs from the plant-soil system.

1.4.1 Inputs to the soil-plant system.

The main N inputs to the soil-plant system are via fertiliser application, biological N_2 fixation, dry and wet deposition of N, decomposition of organic matter and inputs from animals, either directly from excreta deposited while grazing or indirectly from land spreading of animal manures.

The application of fertilisers provides an input of N directly as organic compounds such as urea ($CO(NH_2)_2$) or as inorganic compounds such as ammonium nitrate (NH_4NO_3). Urea is readily hydrolysed into ammonium by the action of the enzyme urease:

$$CO(NH_2)_2 + 2H_2O \rightarrow CO_3^{2-} + 2NH_4^+ . \qquad (1.9)$$

Biological N_2 fixation is a significant source of N to terrestrial ecosystems, currently estimated at 90-130 Mt N yr^{-1} on a global basis (Galloway *et al.*, 1995), the amount fixed varies widely depending on the ecosystem type. Carlsson and Huss-Danell (2003) reviewed a large number of field studies of N fixation and report maximum rates of N fixation of 350, 373 and 545 kg N ha^{-1} yr^{-1} for alfalfa (*Medicago sativa* L.), red clover (*Trifolium pratense* L.) and white clover (*Trifolium repens* L.), respectively. Newbould (1982) reports rates of biological fixation of 5-30 kg N ha^{-1} yr^{-1} for upland pastures in the UK. Fertilisation acts to inhibit biological fixation and therefore in general, biological fixation is a more important input of N in unfertilised ecosystems. Biological fixation is carried out by several species of bacteria, the dominant form of biological fixation in agricultural soils is via bacteria of the genus *Rhizobium*, which fix N_2 in the root nodules of legumes in a symbiotic process. Fixation of N can also occur via lightning (Hill *et al.*, 1980), however, this is not a significant pathway in the UK. Dry and wet deposition of N are discussed in section 1.1.1 and are typically in the range 3-50 kg N ha^{-1} yr^{-1} depending on location and ecosystem type (NEGTAP, 2001).

Inputs of N to the soil-plant system from animals arise predominantly from the urea present in urine and from dung. The urea is rapidly hydrolysed by urease (Eq. 1.9) releasing NH_4^+. The retention of dietary nitrogen is typically only about 23% for

dairy cattle, 10% for beef cattle and 5% for sheep (Whitehead, 1990), so a large quantity of N is excreted. The nitrogen in dung is generally present in resistant organic fractions and so provides less available NH_4^+, but the organic matter is slowly mineralised within the soil (see 1.4.2). As well as providing inputs of N to the soil-plant system, a proportion of the N present in the urine and dung will be lost to the atmosphere via volatilisation of NH_3 (see section 1.4.3).

1.4.2 Transformations within the soil-plant system

The principal processes that occur within the soil system concerning nitrogen cycling are mineralisation, immobilisation, nitrification and assimilation into plants and micoorganisms. Mineralisation is the conversion of organic nitrogen into mineral nitrogen and immobilisation is the opposite process. The amount of mineral nitrogen present in the soil depends on the relative rates of these two processes.

Nitrification is the microbial oxidation of ammonium to nitrite (NO_2^-) and nitrate (NO_3^-). It is carried out by chemoautotrophic and chemoheterotrophic bacteria. The conversion of NH_4^+ to NO_2^- is commonly carried out by *Nitrosomonas europaea* (Eqs. 1.10 and 1.11) whereas *Nitrobacter winogradskyi* oxidises NO_2^- to NO_3^- (Eq. 1.12) (Killham, 1994):

$$NH_4^+ + O_2 + H^+ + 2e^- \rightarrow NH_2OH + H_2O \qquad (1.10)$$

$$NH_2OH + H_2O \rightarrow NO_2^- + 5H^+ + 4e^- \qquad (1.11)$$

$$NO_2^- + H_2O \rightarrow H_2O \cdot NO_2^- \rightarrow NO_3^- + 2H^+ + 2e^- \qquad (1.12)$$

Assimilation of N into plants and microorganisms occurs via the uptake of soluble, low molecular weight N compounds, predominantly ammonium and nitrate. The type of N nutrition (NH_4^+ or NO_3^-) of a plant depends on the availability of the ion, the preference of the species and other factors such as the pH of the soil (Vessey *et al.*, 1990), rooting zone depth and rooting zone temperature (Macduff and Jackson, 1991; Krupa, 2003). Most agricultural crops and fast growing annual species prefer NO_3^-, whilst conifers and other slow growing perennial species prefer NH_4^+ (Malagoli *et al.*, 2000; Krupa, 2003).

Although plant uptake occurs via inorganic forms of N, most of the N in the soil is present in organic form (Killham, 1994). For example the organic N pool for an upland UK pasture soil is estimated to be 6 – 25 t N ha^{-1} (Batey, 1982) whereas the NH_4^+ pool is estimated at 0 to 50 kg N ha^{-1}, 2 - 3 orders of magnitude less than the organic pool. Organic matter content is a slow changing property of a soil; in a sown grassland the total organic matter will progressively increase over a number of years.

1.4.3 Outputs from the soil-plant system

Nitrogen is lost from the soil-plant system via leaching, plant mediated losses of NH_3, volatilisation of NH_3 or other gaseous losses via denitrification. Leaching is the loss of material via water draining down through the soil profile. Nitrate is very susceptible to leaching due to its high solubility and its negative charge, which means that it is not bound to the mostly negative soil colloids. Leached nitrate can constitute a major economic loss of N to farmers, as well as being a health hazard if present in high concentrations in drinking water. Loss of NH_3 from the soil-plant system can also occur via emission from stomata of plants as discussed in section 1.3.1.

Volatilisation of NH_3 is the gaseous loss of NH_3 from the soil-plant surface as described in section 1.3.3. Volatilisation of NH_3 from fertilisers, manure spreading or grazing can also represent a significant loss of N. Volatilisation of NH_3 from urea fertiliser is greater than from ammonium nitrate fertiliser. Van der Weerden and Jarvis (1997) suggest emission factors for NH_3 of 23 % and 1.6% of the N applied for urea and ammonium nitrate fertiliser, respectively. Volatilisation of NH_3 from slurry or manure varies widely depending on the dry matter content of the slurry, the soil and environmental conditions. UK NH_3 emission factors for high dry matter content slurry (> 8%) and farm yard manure (FYM) are 59% and 76% of the total ammoniacal nitrogen (TAN) applied, respectively (Misselbrook *et al.*, 2000). Emissions can be greatly reduced by injecting the fertiliser or slurry below the surface; Misselbrook *et al.* (2000) estimate NH_3 emission reductions of 80% for shallow injection of slurry.

Losses of <5 to 66% of urinary N have been reported (Ball and Ryden, 1984; Lockyer and Whitehead, 1990; Petersen *et al.*, 1998). Ryden *et al.* (1987) and Jarvis *et al.* (1989) suggest emission factors for NH_3 loss from urine of 18% and 11%, respectively. Losses of NH_3 from dung are much less than from urine (< 1%) (Ryden *et al.* (1987).

Denitrification involves the reduction of nitrate into gaseous products of nitrogen: dinitrogen (N_2), nitrous oxide (N_2O) and some nitric oxide (NO).

$$NO_3 \rightarrow NO_2 \rightarrow NO \rightarrow N_2O \rightarrow N_2 \qquad (1.13)$$

Generally the dominant end product of denitrification is N_2, but this varies with soil properties and particularly with soil acidity (Simek and Cooper, 2002). It is carried out mostly by heterotrophic bacteria and occurs in anaerobic conditions when the oxygen present is not sufficient to satisfy the demand from microbial respiration.

1.4.4 Ecosystem modelling

As the above sections show, the N cycle is a complex system involving many processes and interactions. The process of NH_3 exchange is intimately linked to the rest of the N cycle, particularly to the availability of inorganic N in the soil and the movement and transformation of N within the soil-plant system.

Ecosystem modelling seeks to describe the whole ecosystem (plant, soil and atmosphere) and provides a dynamic description of the growth, nutrient and water cycling and gaseous exchange of an ecosystem. This dynamic nature allows models to assess future scenarios of, for example, the effect of climate change, which is not possible with field experiments. Some examples of grassland ecosystem models are: ELM (Innis, 1978); the Hurley Pasture Model (Johnson and Thornley, 1985; Thornley, 1998); GEM (Hunt *et al.*, 1991); CENTURY (Parton *et al.*, 1998); PaSim (Riedo *et al.*, 1998) and SPUR (Foy *et al.*, 1999).

The Hurley Pasture Model (Thornley, 1998) is a grassland ecosystem model with a detailed treatment of ecosystem processes. Riedo *et al.*, (1998) extended the Hurley Pasture Model and developed PaSim (Pasture Simulation Model). Riedo *et al.* (2002)

extended PaSim to include a mechanistic description of bi-directional exchange of NH_3. This is currently the only dynamic ecosystem model to include NH_3 exchange in a mechanistic approach and to account for the bi-directional nature of NH_3 exchange. The CENTURY model does include NH_3 losses as volatilisation but these are assumed to be proportional to gross N-mineralisation. PaSim can simulate the seasonal cycle of NH_3 exchange, linking emissions to the soil N supply and the inputs, outputs and transformations of N and C within the soil-plant system. Such a model is a powerful tool to explore the relationship of NH_3 exchange with external drivers such as management activities and changing climate.

1.5 Objectives and Thesis plan

The objectives of this thesis were:

i) To measure and quantify NH_3 exchange with an intensively managed grassland on a seasonal basis with high temporal resolution,

ii) To investigate the controls on NH_3 exchange, in particular the effects of grassland management, and develop the mechanistic understanding of NH_3 exchange,

iii) To develop the resistance modelling approach for NH_3, in particular, to develop seasonal parameterisations of key variables,

iv) To apply a dynamic grassland ecosystem model and assess its performance for an intensively managed grassland in Scotland. Subsequently to use this model in a predictive capacity to explore the relationship of changing climate and management on NH_3 exchange.

Chapter 1 has provided an introduction to ammonia, its behaviour in the atmosphere, emission sources, ecological effects and pollution control policy. Techniques used to measure NH_3 have been discussed and recent NH_3 land-atmosphere exchange measurements examined. A brief overview of the pathways of NH_3 exchange has been given, along with an introduction to the N cycle and ecosystem modelling.

Chapter 2 gives an introduction to micrometeorology, describes the micrometeorological theory of various techniques of flux measurement and discusses the development of the resistance modelling approach to the interpretation of NH_3 flux measurements.

Chapter 3 provides details of the principal measurement site used in this study and the instrumentation used. It also describes the various measurements undertaken and the methods employed.

Chapter 4 compares key micrometeorological parameters, describes the climatology of the field site, provides the record of field management and grazing activities and presents the results of the vegetation and soil measurements.

Chapter 5 presents the results from the 19 months of measurements of NH_3 exchange at the principal field site. It presents the concentrations and the fluxes and examines the diurnal, seasonal and annual variations in the exchange.

Chapter 6 presents the results of the application of a two-layer resistance model to the NH_3 flux measurements and develops seasonal parameterisations of the key resistances and emission potentials.

Chapter 7 describes the application of the PaSim grassland ecosystem model. The model is compared with NH_3 flux measurements presented in this thesis and used to explore the influence of changing climate and management on NH_3 exchange.

Chapter 8 presents additional NH_3 flux measurements conducted over an intensively managed grassland in Germany. Flux measurements from four different systems are analysed and compared and the resulting best estimate used to investigate the influence of management activities on the exchange. This case study complements the long-term measurements conducted in Scotland.

Chapter 9 summarises and synthesises the research and provides conclusions.

Chapter 2: Micrometeorological Theory

2.1 Introduction

2.1.1 Atmospheric boundary layer

Micrometeorology by definition is concerned with meteorological processes on small temporal and spatial scales; as such, it normally refers to processes occurring in the lower layers of the atmosphere and on space scales of a few mm (e.g. leaf scale) to a few km. The boundary layer of the atmosphere is defined as that part of the troposphere which is directly influenced by the earth's surface and responds to surface forcings (such as friction, heating and cooling), within a timescale of an hour or less (Stull, 1988). Micrometeorological processes occur within this boundary layer. The study of the emission, transport and deposition of atmospheric pollutants is closely linked to micrometeorology. There are many other applications of micrometeorology in areas such as agriculture (protecting crops from drought, flooding and frost and maximising water availability), weather and climate prediction and aeronautics and civil engineering (designing aircraft and structures that can withstand meteorological phenomena).

Three distinct layers can be identified within the atmospheric boundary layer: i) a thin viscous sub-layer where molecular transport dominates over turbulent transport; ii) an inner (or surface) layer constituting about 10% of the boundary layer depth and iii) an outer (or Ekman) layer (Garratt, 1992). The surface layer can be subdivided into two further layers: the roughness sublayer (where surface elements strongly influence the turbulence and mean profiles) and the inertial sublayer (where mean profiles of wind speed are logarithmic in neutral conditions). In the surface layer, in the absence of inhomogenities occurring at the surface, turbulent fluxes vary by less than 10% of their magnitude and so this layer is also known as the "constant flux layer". Micrometeorologists utilise the properties of the constant flux layer to measure the surface-atmosphere exchange of parameters by making measurements at one or a series of heights within the constant flux layer.

2.1.2 *Atmospheric stability*

An important property of the atmosphere affecting vertical transport of entities is the stability of the atmosphere, which can be defined locally by comparing the actual lapse rate of the atmosphere to the dry adiabatic lapse rate (Γ_d). The lapse rate is the change in temperature (T) of an air parcel with height (z). The dry adiabatic lapse rate is the change in temperature with height for a parcel of dry air with no exchange of heat with its surroundings. It is given by $\Gamma_d = dT/dz = -g/c_p = -9.8$ K km^{-1} where g is the acceleration due to gravity and c_p is the specific heat capacity of air (1.01 J g^{-1} K^{-1} at STP) (Monteith and Unsworth, 1990). There are three states of atmospheric stability: neutral, stable and unstable defined as follows:

neutral: $-dT/dz \approx \Gamma_d$

stable: $-dT/dz > \Gamma_d$

unstable: $-dT/dz < \Gamma_d$

In an unstable atmosphere the decrease in temperature with height is greater than Γ_d and ascending air parcels are warmer than their surroundings, thus experiencing net buoyancy which acts to continue their ascent, hence the term unstable. In a stable atmosphere the converse is true; ascending air parcels are cooler than their surroundings and therefore further vertical motion is not enhanced by buoyancy.

Stability can be characterised by the Monin-Obukhov length (L):

$$L = -\frac{\rho_a c_p T u_*^3}{kgH} \qquad (2.1)$$

where ρ_a is the density of dry air (1246 g m^{-3} at STP), T is the absolute temperature in K, u_* is the friction velocity, k is the von Karman constant (= 0.41) and H is the sensible heat flux. The friction velocity is a measure of the turbulent velocity fluctuations in the air and can be found from:

$$u_* = (-\overline{u'w'})^{1/2} \qquad (2.2)$$

where u and w are the horizontal (aligned with mean flow) and vertical components of wind speed and u' and w' are the fluctuations in the horizontal and vertical wind components, respectively (Monteith and Unsworth, 1990).

An alternative measure of stability is the Richardson number (Ri), which is defined as:

$$Ri(z) = \frac{g}{T}\frac{\mathrm{d}T/\mathrm{d}z}{(\mathrm{d}u/\mathrm{d}z)^2}. \qquad (2.3)$$

A convenient property of L is that it is independent of height within the atmospheric boundary layer, whereas Ri is not independent of height and so is a less useful parameter for characterising stability throughout the atmosphere.

2.2 Flux measurement techniques

A flux of a quantity is the transfer of that quantity per unit area per unit time. Micrometeorologists are concerned with fluxes of mass, momentum, heat and moisture to and from Earth's surface; techniques to study these fluxes have been developed over the last 50 years (Monteith and Unsworth, 1990). One method to measure pollutant fluxes is using enclosures to cover the area of interest. The change of concentration over time within the enclosure can be measured or else a dynamic enclosure can be used which actively pumps air through the enclosure and measures the concentration difference between the inlet and outlet (Fowler and Duyzer, 1989). The advantages of enclosures are that they can be used over small areas (of the order of 1 m^2) and so can be used to compare plots with different treatments or in areas, which are otherwise unsuitable for micrometeorological measurements such as steep slopes. The disadvantages are that the enclosures modify the environment (by altering the microclimate and turbulence) and also that many enclosures may be needed to get a representative measurement due to spatial heterogeneity in the sample area. By contrast, micrometeorological techniques make a measurement at the canopy scale integrated over a larger upwind area and the equipment does not disturb the area of measurement. The measurements of NH_3 exchange presented in this thesis were conducted using the micrometeorological aerodynamic gradient

method and this is described below before introducing other micrometeorological methods of flux measurement.

2.2.1 Aerodynamic gradient method

The aerodynamic gradient method measures vertical gradients of windspeed, temperature and trace gas concentration within the constant flux layer of the atmosphere and relates these gradients to the flux using Fick's law of diffusion. Fick's law states that a flux (F), e.g. of a trace gas concentration χ, is a product of its concentration gradient and a diffusivity, which, in the case of turbulent atmospheric transport, is the turbulent diffusion coefficient or eddy diffusivity, K_χ:

$$F_\chi = -K_\chi \frac{\mathrm{d}\chi}{\mathrm{d}z} \tag{2.4}$$

Similar relationships exist for momentum flux (τ) and sensible heat flux (H) as follows (Monteith and Unsworth, 1990):

$$\tau = \rho_a K_M \frac{\mathrm{d}u}{\mathrm{d}z} \tag{2.5}$$

$$H = -\rho_a c_p K_H \frac{\mathrm{d}T}{\mathrm{d}z} \tag{2.6}$$

where K_M and K_H are the eddy diffusivities for momentum and heat, respectively. The eddy diffusivity for momentum is given by:

$$K_M = \frac{k(z-d)u_*}{\Phi_M} \tag{2.7}$$

where Φ_M is the stability correction function for momentum and d is the zero-plane displacement height, the notional height above ground at which the absorption of momentum occurs within a canopy. According to similarity theory (Monin and Obukhov, 1954) the eddy diffusivity for entrained properties is equivalent to that for heat and is given by:

$$K_\chi = K_H = \frac{k(z-d)u_*}{\Phi_H} \tag{2.8}$$

where Φ_H is the stability correction function for heat. The stability correction functions compensate for the non-logarithmic nature of wind, temperature or trace gas profiles in non-neutral conditions. Webb (1970) proposed the following expression for Φ_M and Φ_H for stable conditions:

$$\Phi_M = \Phi_H = (1+5.2\zeta) \tag{2.9}$$

and Dyer and Hicks (1970) proposed the following expression for Φ_M and Φ_H for unstable conditions:

$$\Phi_M{}^2 = \Phi_H = (1-16\zeta)^{-\frac{1}{2}} \tag{2.10}$$

where $\zeta = (z\text{-}d)/L$ is a dimensionless stability parameter.

Alternatively, F_χ may be given by:

$$F_\chi = -u_*\chi_* \tag{2.11}$$

where χ_* is the scaling concentration. The friction velocity and scaling concentration can be found from:

$$u_* = \frac{k(z-d)}{\Phi_M}\frac{\mathrm{d}u}{\mathrm{d}z} \tag{2.12}$$

$$\chi_* = \frac{k(z-d)}{\Phi_H}\frac{\mathrm{d}\chi}{\mathrm{d}z} \tag{2.13}$$

The gradients of concentration and windspeed with height are (approximately) logarithmic and so Eqs. (2.12) and (2.13) can be linearized by integrating. Φ_M and Φ_H are height dependent (see Eqs. 2.9 and 2.10) and so need to be included in the integration. This is achieved using integrated stability functions, Ψ_M and Ψ_H, which are a function of ζ (Panofsky, 1963):

$$u(z-d)=\frac{u_*}{k}\left(\ln\left(\frac{z-d}{z_0}\right)-\Psi_M(\zeta)\right) \tag{2.14}$$

$$\chi(z-d)=\frac{\chi_*}{k}\left(\ln\left(\frac{z-d}{z_0'}\right)-\Psi_H(\zeta)\right) \tag{2.15}$$

where z_0 (roughness length) and z_0' are the notional heights above d at which the windspeed and concentration are predicted to be zero, respectively, if the log profiles were to be extended to the ground.

In stable conditions, the integrated stability functions can be obtained from the straightforward integration of Φ_M and Φ_H as given in Eq. 2.9:

$$\Psi_M=\Psi_H=-5.2\zeta \tag{2.16}$$

whereas in unstable conditions, Paulson (1970) provides the following formulation:

$$\Psi_M=2\ln\left(\frac{1+x}{2}\right)+\ln\left(\frac{1+x^2}{2}\right)-2\tan^{-1}(x)+\frac{\pi}{2} \tag{2.17}$$

$$\Psi_H=2\ln\left(\frac{1+x^2}{2}\right) \tag{2.18}$$

$$\text{where}\quad x=(1-16\zeta)^{\frac{1}{4}} \tag{2.19}$$

Substituting equations 2.14 and 2.15 into equation 2.11 provides an expression for the flux, F_χ, as:

$$F_\chi=k_2\frac{\mathrm{d}u}{\mathrm{d}[\ln(z-d)-\Psi_M(\zeta)]}\frac{\mathrm{d}\chi}{\mathrm{d}[\ln(z-d)-\Psi_H(\zeta)]} \tag{2.20}$$

However, for the flux measurements presented in this thesis, u_* was obtained directly from eddy covariance measurements using a sonic anemometer (see section 2.2.2) rather than from wind speed profiles. Consequently, the flux F_χ was found from the following expression:

$$F_\chi = -ku_* \frac{d\chi}{d[\ln(z-d) - \Psi_H(\zeta)]} \quad (2.21)$$

and Ψ_H was obtained from Eqs. (2.16) or (2.18) using values of L obtained from eddy covariance measurements of u_* and H (Eq. (2.1)).

2.2.2 *Eddy covariance*

The eddy covariance (EC) method is, in principle, preferred to the aerodynamic gradient method as it does not depend upon an empirically derived stability relationship to estimate the flux. The vertical flux of a trace gas is given by the mean, over the sampling interval, of the instantaneous product of its concentration (χ) and the vertical wind speed (w) (e.g. Fowler and Duyzer, 1989; Moncrieff *et al.*, 1997a):

$$F_\chi = \overline{w\chi} \quad (2.22)$$

Using the Reynolds decomposition of w into an average component, $\bar{w}$, plus its instantaneous fluctuation from that average, w', ($w = \bar{w} + w'$) and similarly for χ, ($\chi = \bar{\chi} + \chi'$), Eq. 2.22 can be rewritten as:

$$F_\chi = \overline{w'\chi'} + \overline{\bar{w}\bar{\chi}} \quad (2.23)$$

It is often assumed that over horizontally homogeneous surfaces $\bar{w}$ = zero, and therefore Eq. 2.23 reduces to:

$$F_\chi = \overline{w'\chi'}. \quad (2.24)$$

However, in the presence of sensible and latent heat fluxes, $\bar{w} \neq 0$ and a correction is needed to obtain the flux (see Section 2.3.2).

The fluxes of sensible heat (H), latent heat (λE) and momentum (τ) can also be determined in a similar fashion by eddy covariance:

$$H = \rho_a c_p \overline{w'\theta'} \quad (2.25)$$

$$\lambda E = \frac{\lambda \varepsilon \rho_a}{p_a} \overline{w'e'} \tag{2.26}$$

$$\tau = -\rho_a \overline{w'u'} \tag{2.27}$$

where θ is potential temperature, λ is the latent heat of evaporation, ε is the ratio of the molecular weights of water vapour and dry air, e is the water vapour pressure and p_a is ambient air pressure.

The eddy covariance method requires fast response sampling of the trace gas concentration. The frequency response required depends upon the size of the eddies carrying the flux. The eddy size increases with increasing height above d, surface roughness and decreasing windspeed. Consequently, a different frequency response would be required for measurements above a grassland compared with measurements above a forest. Generally, analysers with a frequency response of between 1 to 10 Hz are adequate for most eddy covariance flux measurements.

2.2.3 Relaxed eddy accumulation

The relaxed eddy accumulation (REA) method operates by sampling air into two reservoirs or two analysers according to whether the sign of the fluctuation of the measured vertical wind component is +ve (updraught) or –ve (downdraught). The concentrations in these two reservoirs, $\overline{\chi^+}$ and $\overline{\chi^-}$ can then be determined with a lower time resolution and the flux is found as:

$$F_\chi = \beta_\chi \sigma_w \left(\overline{\chi^+} - \overline{\chi^-}\right) \tag{2.28}$$

where β_χ is an empirical constant of proportionality and σ_w is the standard deviation of w (Businger and Oncley, 1990; Oncley *et al.*, 1993). Relaxed eddy accumulation is a useful method for those species which do not have a sufficiently fast response analyser to conduct EC measurements. The advantage over the aerodynamic gradient method is that measurements can be made at a single height allowing investigation of flux divergence at different heights. The disadvantage of the REA method is that the concentration difference between the up and down draughts $\left(\overline{\chi^+} - \overline{\chi^-}\right)$ is much

smaller than the $d\chi$ signal for the aerodynamic gradient method and is therefore more difficult to resolve analytically (Sutton *et al.*, 2001a).

2.3 Assessment of flux measurements

2.3.1 Fetch and flux footprint

The validity of the above flux measurement methods relies on the principle of the flux being constant with height in the inertial sub-layer. However, this is only true for the surface layer in equilibrium with a homogeneous surface; changes in the roughness of a surface or in the vegetative properties will lead to changes in the vertical flux. To ensure that the flux measurement is representative of a particular surface, the measurement height must be within the new internal boundary layer which forms after a surface inhomogeneity. The height of this layer (δ) depends on the upwind distance (x_L) or "fetch" to the inhomogenity. Empirical evidence suggests that the ratio of x_L to δ is approximately 100:1.

However, the extent of an upwind area affecting a flux measurement changes with wind direction, wind speed, surface roughness and stability and therefore a more thorough analysis has been developed to assess the contribution to the flux measurement from a particular upwind source area, this is termed "footprint" analysis. Schmid (2002) reviewed the existing footprint modelling approaches and provides a summary of the development of the footprint concept. The footprint is defined as "the upwind area most likely to affect a downwind flux measurement at a given height z" (Schuepp *et al.*, 1990). Schuepp *et al.* (1990) provided analytical solutions of the diffusion equation based on Gash (1986) and defined the cumulative normalized contribution to the flux measurement (CNF) at height z and upwind distance x_L as:

$$\mathrm{CNF}(x_L) = \int_0^{x_L} f(x,z)dx \tag{2.29}$$

$$\mathrm{CNF}(x_L) = \exp\left(\frac{-U(z-d)}{ku_*x_L}\right) \tag{2.30}$$

where U is defined as the average windspeed between the surface and the measurement height z. However, these equations are only defined for neutral stability. Schuepp *et al.* (1990) proposed the multiplication of the U/u_* ratio in Eq. (2.30) by the momentum stability correction function (Φ_M) as an approximation to account for the effect of stability.

Various other studies have developed the footprint analysis (Wilson and Swaters, 1991; Horst and Weil, 1992; 1994; Leclerc *et al.*, 1997; Haenel and Grunhage, 1999; Schmid and Lloyd, 1999). Kormann and Meixner (2001) proposed an analytical model for the footprint, which directly accounts for non-neutral stratification. They calculate the CNF at upwind distance x_L from Eq 2.29 with $f(x, z)$ given by:

$$f = \frac{1}{\Gamma(\frac{1+m}{r})} \frac{\xi^{\frac{1+m}{r}}}{x^{1+(\frac{1+m}{r})}} e^{-\xi/x} \tag{2.31}$$

where Γ is the Gamma function and $\xi(z)$ is the length scale given by:

$$\xi(z) = \frac{U_1 z^r}{r^2 \kappa} \tag{2.32}$$

r is the "shape factor" ($r = 2 + m - n$), U_1 is the constant and m is the exponent in the power-law approximation of the wind velocity profile ($u(z) = U_1 z^m$), κ is the constant and n is the exponent in the power-law approximation of the eddy diffusivity profile ($K(z) = \kappa z^n$), m and n can be found from Eq. 2.33 and Eq. 2.34, respectively.

$$m = \frac{u_*}{k} \frac{\Phi_M}{u(z)} \tag{2.33}$$

$$n = \frac{z}{K} \frac{dK}{dz} = \frac{1}{1+5z/L} \quad \text{for } L > 0 \tag{2.34}$$

$$= \frac{1-24z/L}{1-16z/L} \quad \text{for } L < 0.$$

2.3.2 *Potential errors in flux measurements*

In addition to the measurement requirement of sufficient fetch, the flux methods presented in Section 2.2 also assume stationarity and homogeneity of the atmospheric conditions. In practice, there can be variation in the flux with height, known as flux divergence ($\partial F_z/\partial z$) (Eq. 2.35). Flux divergence can arise from (Fowler and Duyzer, 1989):

$$\frac{\partial F_z}{\partial z} = -\frac{\partial \chi_a}{\partial t} - \frac{\partial F_x}{\partial x} + Q_{chem} \qquad (2.35)$$

i) changes in concentration with time ($\partial\chi_a/\partial t$), leading to changes in the storage of the trace gas in the air column below the measurement level, known as the storage term;

ii) horizontal gradients in concentration leading to a local advection term ($\partial F_x/\partial x$) and

iii) chemical production or consumption of the trace gas between the measurement level and the surface (Q_{chem}).

Storage

The storage term or the resulting difference in the vertical flux due to storage (the storage error, $\Delta F_{z,sto}$) may be found from (Fowler and Duyzer, 1989):

$$\Delta F_{z,sto} = \int_0^{z-d} \frac{\partial \chi_a}{\partial t} dz \qquad (2.36)$$

which is approximately equal to:

$$\Delta F_{z,sto} = (z-d)\frac{\partial \chi_a}{\partial t}. \qquad (2.37)$$

In the case of ammonia, where exchange fluxes are relatively large compared with concentration, the flux divergence due to storage ($\partial\chi_a/\partial t$) is generally small (Sutton *et al.*, 1993a). The magnitude of the storage error is proportional to height and

therefore the error is reduced when making measurements over a smaller height range, such as over grassland.

Advection

The difference in the vertical flux due to advection (the advection error, $\Delta F_{z,adv}$) can be found as (Fowler and Duyzer, 1989; Loubet *et al.*, 2001):

$$\Delta F_{z,adv} = -\int_0^{z-d} u(z)\frac{\partial \chi_a}{\partial x} dz \,. \tag{2.38}$$

If the integrand is assumed to be constant with height then Eq. 2.38 can be simplified to:

$$\Delta F_{z,adv} = -(z-d)u\frac{\partial \chi_a}{\partial x} \,. \tag{2.39}$$

Using Eq. 2.39, an estimate of the advection error can be found from measured wind speeds and horizontal concentration gradients. More thorough assessments of advection have been made by e.g. inversion of a local-scale dispersion-exchange model (Loubet *et al.*, 2001). The flux divergence due to advection can be quite significant for NH_3, particularly where large NH_3 sources exist in the vicinity (Loubet *et al.*, 2001). However, similar to the storage error, the advection error is reduced for rapidly depositing species such as NH_3 and for lower measurement heights (Sutton *et al.*, 1993a).

Chemical production or consumption

The difference in the vertical flux due to chemical production or consumption ($\Delta F_{z,chem}$) can be significant for ammonia where either evaporation of ammonium containing aerosol, or production of aerosol, respectively, occur in the surface layer. Modelling approaches addressing this issue have been developed (e.g. Brost *et al.*, 1988; Kramm and Dlugi, 1994; Nemitz *et al.*, 2000c).

Density corrections

As mentioned in section 2.2.2, eddy covariance measurements need to be corrected due to the presence of sensible and latent heat fluxes. This leads to the following expression for the flux (Webb *et al.*, 1980; Fowler and Duyzer, 1989):

$$F_\chi = \overline{w'\chi'} + (\frac{\chi}{\rho_a})\left[\frac{\mu}{1} + \mu\sigma(1+\mu\sigma)\right]E + (\frac{\chi}{\rho_a})\frac{H}{c_p T} \qquad (2.40)$$

where μ is the ratio of the molecular weight of dry air to that of water vapour, σ is the ratio of the density of water vapour to the density of air.

The measured flux has to be corrected for these sensible and latent heat fluxes to obtain the actual trace gas flux. In practice, the corrections are only significant if the trace gas flux is small compared to its concentration. The need for corrections is eliminated if the trace gas is dried and brought to a reference temperature before measurement (Fowler and Duyzer, 1989). These corrections are also required when measuring with the aerodynamic gradient technique if the air flow is controlled by critical orifices at different heights. Nemitz (1998) derived corrections for flux measurements from such a gradient system and concluded that the corrections were small for NH_3, which exchanges rapidly with the surface.

2.4 Resistance modelling of NH_3 exchange

2.4.1 The resistance modelling approach

Resistance analysis is a technique used by micrometeorologists to identify and parameterise different pathways of exchange. Fluxes of pollutants (or any other quantity) are treated as an analogue of electrical current. Ohm's law ($V = I\,R$) relates the current (I) to the potential difference (V) and resistance (R). In the case of pollutant exchange the flux (F_χ) is equivalent to the electrical current and is equal to the ratio of the concentration difference between two heights and the resistance to transfer between those two heights ($R(z_1, z_2)$):

$$F_\chi = -\frac{\chi(z_2) - \chi(z_1)}{R(z_1, z_2)} \qquad (2.41)$$

The sign convention used is that emission fluxes are positive and deposition fluxes negative.

2.4.2 Canopy resistance model

The first resistance models used to describe pollutant exchange were developed for pollutants, which are only deposited to vegetation, not emitted from vegetation, such as sulphur dioxide (SO_2) and ozone (O_3) (Fowler and Unsworth, 1979) (Fig. 2.1a). In this case the surface concentration is assumed to be zero and the flux can be found as:

$$F_\chi = -\frac{\chi(z-d)-0}{R_t}, \tag{2.42}$$

where R_t is the total resistance to transfer between height (z-d) and the surface, the units of R_t are s m^{-1}.

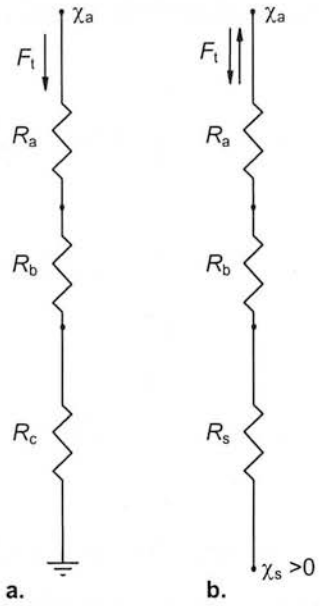

Fig 2.1. Diagram of a) the canopy resistance model and b) the stomatal compensation point model of NH_3 exchange.

The reciprocal of R_t is known as the deposition velocity (V_d). The deposition velocity is a measure of the speed with which a pollutant is deposited to the ground, its units are m s^{-1} and similarly to R_t, it is height dependent. R_t can be separated into component resistances, the aerodynamic resistance (R_a), the boundary layer resistance (R_b) and the canopy resistance (R_c):

$$R_t = R_a + R_b + R_c \tag{2.43}$$

The aerodynamic resistance describes the turbulent transfer through the flux layer between a reference height (z-d) and z_0, the notional height above d at which the windspeed is zero. Trace gases and other entrained properties experience an additional resistance, R_b, due to a quasi-laminar boundary layer at the surface. This leads to the apparent site of exchange of these properties being at $d + z_0'$ where $z_0' < z_0$. R_c is the canopy resistance to pollutant uptake. The maximum deposition velocity (V_{max}) occurs when the canopy resistance is zero and is found from:

$$V_{max} = (R_a + R_b)^{-1}. \tag{2.44}$$

Aerodynamic resistance (R_a)

R_a is determined by integrating the inverse of the eddy diffusivity for momentum (K_M) over the height range between z-d and z_0 (Thom, 1975):

$$R_a(z-d) = \int_{z_0}^{z-d} K_M^{-1}(z)dz \tag{2.45}$$

This leads to the following expression:

$$R_a(z-d) = \frac{\ln\left(\frac{z-d}{z_0}\right) - \Psi_M\left(\frac{z-d}{L}\right)}{ku_*}. \tag{2.46}$$

The transfer of trace gases and other entrained properties is equal to momentum transfer in neutral and stable conditions, therefore Eq. 2.46 can be used for all quantities in these conditions. In unstable conditions, the transfer of trace gases and other entrained properties is not equal to momentum transfer and Garland (1977) derived a relationship which could be used in all stability conditions as follows:

$$R_a(z-d) = \frac{u(z-d)}{u_*^2} - \frac{\Psi_H\left(\frac{z-d}{L}\right) - \Psi_M\left(\frac{z-d}{L}\right)}{ku_*}. \tag{2.47}$$

Laminar boundary layer resistance (R_b)

R_b is usually found from empirical relationships describing the diffusion through the quasi-laminar boundary layer, e.g. as proposed in Garland (1977) for a fibrous surface:

$$R_b = 1.45 Re_*^{0.24} Sc^{0.8} u_*^{-1} \quad (2.48)$$

where Re_* is the turbulent Reynolds number ($Re_*=z_0u_*/\nu$), Sc is the Schmidt number ($Sc=\nu/D_\chi$), ν is the kinematic viscosity of air and D_χ is the molecular diffusivity of the entrained property. Values of $D_\chi = 2.09 \times 10^{-5}$ m^{-2} s^{-1} (Hargreaves and Atkins, 1987) and 2.27×10^{-5} m^{-2} s^{-1} (Monteith and Unsworth, 1990) were used for the diffusivity of NH_3 and water vapour respectively for the measurements presented here, both diffusivities are reported for a temperature of 10 °C. Other parameterisations of R_b exist (e.g. Wesely and Hicks, 1977).

Canopy resistance (R_c)

As described above, R_c is the bulk canopy resistance to pollutant uptake and is given by:

$$R_c = R_t - R_a - R_b \quad (2.49)$$

Replacing R_t in Eq. 2.49 by Eq. 2.42 gives:

$$R_c = -\frac{\chi(z-d)}{F_\chi} - R_a - R_b \quad (2.50)$$

All the terms in Eq. 2.50 can be found from micrometeorological measurements as described in Section 2.2. R_c can also be replaced by component resistances acting in parallel, for example resistances describing uptake through the stomata, to the leaf surfaces and to the soil (Fowler and Unsworth, 1979).

2.4.3 Stomatal compensation point model

The canopy resistance approach is based on the assumption that the concentration at the surface is zero, but this approach is not valid for periods when trace gases are being emitted at the surface. Ammonia is a trace gas, which can be both emitted from and deposited to vegetation. This is because plants contain NH_4^+ in the apoplast and NH_3 is present in substomatal cavities in equilibrium with the apoplastic NH_4^+ concentration (see section 1.3.1). Farquhar *et al.* (1980) proposed that a modelling approach initially developed for carbon dioxide (CO_2) could be adapted for NH_3. The surface concentration, instead of equalling zero, is assumed to be equivalent to the gaseous stomatal concentration or stomatal compensation point (χ_s) (Fig. 2.1b). If all other pathways of exchange than through the stomata are eliminated, the flux is found as:

$$F_\chi = -\frac{\chi(z-d)-\chi_s}{R_a + R_b + R_s} \qquad (2.51)$$

where R_s is the stomatal resistance, the reciprocal of which is the stomatal conductance (g_s). The relative magnitude of χ_s and the ambient NH_3 concentration at a reference height $\chi(z\text{-}d)$ define the direction of the flux: $\chi_s > \chi(z\text{-}d)$ results in emission from the surface; $\chi_s < \chi(z\text{-}d)$ leads to deposition and $\chi_s = \chi(z\text{-}d)$ results in no net flux. The stomatal compensation point can be found from Eq. 1.7 if values for the temperature of the canopy, the apoplastic $[NH_4^+]$ and pH are either known or estimated (see section 1.3.1).

Stomatal resistance (R_s)

The stomatal resistance for NH_3 can be found by equating it to the stomatal resistance for other gases such as ozone, carbon dioxide or water vapour while accounting for differences in the molecular diffusivities of the gases. The stomatal resistance for water vapour transfer (R_{sE}) can be calculated from micrometeorological measurements of latent heat flux (λE) during dry conditions (when all water vapour transfer is assumed to be via stomata) as:

$$R_{sE} = -\frac{e(z_0') - e_{sat}(T(z_0'))}{E} \tag{2.52}$$

where $e(z_0')$ is the water vapour pressure at the leaf surface and $e_{sat}(T(z_0'))$ is the saturated vapour pressure at the temperature of the surface. In addition, there are many parameterisations developed for R_s for CO_2 transfer. One such parameterisation is given in Eq. 2.53 from Jarvis (1976) and Hicks *et al.* (1987). Essentially, stomatal opening depends on light availability but R_s is also modified according to other stress factors:

$$R_s = R_{s,\min} \frac{1 + b / I_p}{f_e f_w f_T f_s} \tag{2.53}$$

$R_{s,min}$ is the minimum value of R_s, b is a constant describing the light response curve, I_p is the photosynthetically active radiation, f_e, f_w, f_T and f_s are correction factors for humidity, water stress, temperature and differences in the molecular diffusivities of the gases, respectively, and take values between 0 and 1.

2.4.4 Single-layer canopy compensation point model

The above two modelling approaches are only valid for NH_3 exchange in particular circumstances, e.g. the stomatal compensation point model is valid for dry daytime conditions or for controlled environment studies when cuticular exchange can be ignored. In the full range of environmental conditions experienced in the field, the two processes of bi-directional exchange with stomata and deposition to leaf surfaces can occur simultaneously. Sutton and Fowler (1993) proposed a model that could account for these two competing processes (Fig. 2.2). The aerodynamic resistance, boundary layer resistance and stomatal resistance are still determined in the same manner.

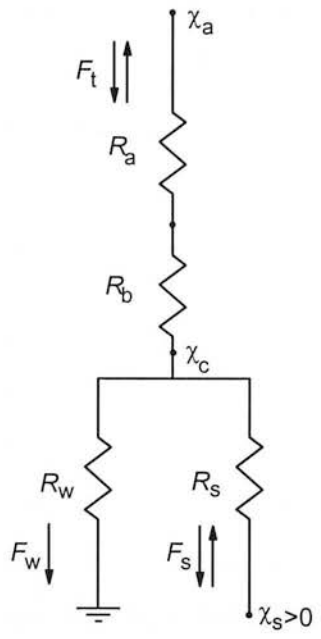

Fig 2.2. Diagram of the single-layer canopy compensation point resistance model of NH_3 exchange (Sutton and Fowler, 1993).

New parameters introduced were the resistance to the leaf cuticles (R_w) and a canopy compensation point (χ_c), which is the notional average concentration in the canopy. It is the relative magnitude of the canopy compensation point and the ambient NH_3 concentration that controls the direction and magnitude of the net flux in this model:

$$F_\chi = -\frac{\chi_a - \chi_c}{R_a + R_b} \tag{2.54}$$

χ_c may be calculated as (Sutton *et al.*, 1995b):

$$\chi_c = \frac{\chi_a (R_a + R_b)^{-1} + \chi_s R_s^{-1}}{(R_a + R_b)^{-1} + R_s^{-1} + R_w^{-1}}. \tag{2.55}$$

Cuticular resistance (R_w)

The cuticular resistance (R_w) governs the deposition of NH_3 to the leaf cuticles. As described in section 1.3.2, NH_3 is readily adsorbed into water films on the leaf surface. Measurements of NH_3 adsorption onto leaves and glass surfaces were conducted by van Hove *et al.* (1989) and Benner *et al.* (1992), respectively. They found increasing adsorption with increasing relative humidity. Sutton *et al.* (1995b)

compared these measurements with nighttime measurements of NH_3 exchange over forest (Wyers *et al.*, 1993a) and proposed the following relationship for the cuticular resistance:

$$R_w = R_{w,min} \exp^{(100 - RH)/a} \quad (2.56)$$

where $R_{w,min}$ is the minimum value of R_w, RH is relative humidity and a is a constant. Duyzer *et al.* (1994) compared canopy resistances from NH_3 exchange over forest against vapour pressure deficit (VPD) and found that the canopy resistance increased at higher VPD, although there was no clear relationship between the two parameters. Nemitz *et al.* (2000b) proposed a relationship for cuticular resistance based on vapour pressure deficit (VPD):

$$R_w = \exp^{(c \times VPD)} \quad (2.57)$$

where c is a constant. However, neither of these parameterisations include the effect of leaf chemistry which also has a strong influence on the cuticular deposition. Sutton *et al.* (1998) extended the single-layer χ_c model and parameterised the leaf surface as an electric capacitor which could be deposited to and also re-emit NH_3. This approach was developed further by Flechard *et al.* (1999) who used the chemical composition of rainfall and dry deposition estimates to simulate the likely chemical composition of the leaf water layers and the corresponding pH. However, as both these models need to be solved dynamically and require increased amount of input data they are not easy to parameterise for many locations, e.g. as required in an atmospheric transport model.

2.4.5 Two-layer canopy compensation point model

The single-layer χ_c model adopts the 'big-leaf' approach to modelling, i.e. it treats the canopy as a single layer and does not accommodate deposition and emission processes from different layers in the canopy, for example when there is a strong ground surface emission source of NH_3 after fertilisation. As an extension to this approach, Nemitz *et al.* (2001b) introduced a two-layer canopy compensation point model (Fig 2.3) which incorporates bi-directional foliar stomatal exchange and

deposition to leaf cuticles, but simultaneously treats NH_3 exchange with the ground surface.

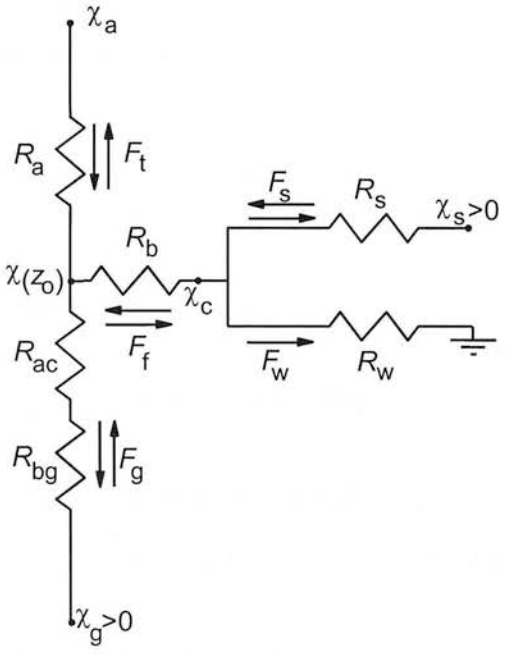

Fig 2.3. Diagram of the two-layer canopy compensation point resistance model of NH_3 exchange (Nemitz *et al.*, 2001b).

There are two emission potentials: one for the foliage, described by χ_s and secondly for a ground source characterised by χ_g. As described in section 1.3.1 (Eq. 1.7) and section 2.4.3, χ_s can be found from the canopy temperature and the ammonium/hydronium ratio in the apoplast ($[NH_4^+]/[H^+]$) which has been termed the stomatal emission potential (Γ_s). χ_g is found from an analogous equation to χ_s (Eq. 1.8) where Γ_g is the ammonium/hydronium ratio of the emission source at the ground surface, be it plant material or soil (see section 1.3.3). There are 6 resistances to transfer: R_a, R_b, R_s, R_w, R_{ac} and R_{bg}. R_{ac} is the in-canopy aerodynamic resistance and R_{bg} is the ground boundary layer resistance. These two resistances act in series and constitute the total ground resistance, R_g, ($R_g = R_{ac} + R_{bg}$).

The net flux is found from:

$$F_\chi = -\frac{\chi_a - \chi(z_0)}{R_a}. \qquad (2.58)$$

The solution for $\chi(z_0)$ is given in Nemitz *et al.* (2001b). As the five component fluxes and χ_c and $\chi(z_0)$ are unknown, any one of the unknown variables can be found by forming 7 linear equations. On substitution and simplification of these linear equations, $\chi(z_0)$ can be calculated as:

$$\chi(z_0) = \frac{\chi_a R_a^{-1} + \chi_g R_g^{-1} + \chi_c R_b^{-1}}{R_a^{-1} + R_b^{-1} + R_g^{-1}} \tag{2.59}$$

and χ_c can be calculated as:

$$\chi_c = \left[\chi_a (R_a R_b)^{-1} + \chi_s \left\{(R_a R_s)^{-1} + (R_b R_s)^{-1} + (R_g R_s)^{-1}\right\} + \chi_g (R_b R_g)^{-1}\right] \times \left[\begin{array}{l}(R_a R_b)^{-1} + (R_a R_s)^{-1} + (R_a R_w)^{-1} + (R_b R_g)^{-1} + (R_b R_s)^{-1} \\ + (R_b R_w)^{-1} + (R_g R_s)^{-1} + (R_g R_w)^{-1}\end{array}\right]^{-1} \tag{2.60}$$

In-canopy aerodynamic resistance (R_{ac})

The in-canopy aerodynamic resistance can be found by integrating the inverse of the eddy diffusivity (K_H) over the height range between the ground surface and the average height of the foliar exchange ($d + z_0$):

$$R_{ac}(d + z_0) = \int_0^{d+z_0} K_H^{-1}(z)dz \tag{2.61}$$

According to Raupach (1989):

$$K_H(z) = \tau_L(z)\sigma_w^2(z) \tag{2.62}$$

where τ_L is the Lagrangian timescale and σ_w is the standard deviation of the vertical wind component. τ_L was parameterised by Raupach (1989) as:

$$\frac{\tau_L(z)u_*}{h_c} = \max\left\{0.3, \frac{k(z-d)}{1.25h_c}\right\} \tag{2.63}$$

where h_c is the canopy height while σ_w is usually assumed to be proportional to u_*.. Hence $K_H \propto u_*$ and $R_{ac} \propto 1/u_*$, as a result of this Nemitz *et al.* (2000b) proposed the following relationship for R_{ac}:

$$R_{ac}(d + z_0) = \alpha(d + z_0)u_*^{-1} \tag{2.64}$$

where α is a constant.

Ground boundary layer resistance (R_{bg})

Little is known about in-canopy or ground boundary layer resistances. However, Schuepp (1977) proposed that the transfer coefficient at the surface is determined by the eddy size near the surface. If it is assumed that a logarithmic wind speed profile exists within the canopy with eddy size proportional to the distance from the surface then a friction velocity within the canopy can be defined and is denoted u_{*g}. The lower boundary of this logarithmic profile is found at a distance δ_0 above the surface where molecular diffusivity become equal to eddy diffusivity. Thus δ_0 can be found approximately as follows:

$$D_\chi = ku_{*g}\delta_0 \tag{2.65}$$

and the ground boundary layer resistance can be parameterised as follows:

$$R_{bg} = \frac{Sc - \ln(\delta_0 / z_g)}{ku_{*g}}. \tag{2.66}$$

where Sc is the Schmidt number and z_g is the height above the surface to which the logarithmic profile extends (Schuepp, 1977).

Chapter 3: Easter Bush: field site and experimental details

3.1 Introduction

The measurements of NH_3 exchange began in May 1998 and were completed in November 1999, a period of 19 months, covering two field seasons. Intensively-managed grassland was chosen as the target ecosystem type due to the seasonal variability of NH_3 exchange expected to be observed and also due to the lack of long-term measurements of NH_3 exchange over this ecosystem type. This chapter provides details of the principal measurement site, the instrumentation used, the measurements undertaken and the methods employed.

3.2 Site description

The principal measurement site was located at a university owned experimental farm (Easter Bush) in southern Scotland (3°12' W, 55° 52' N, elevation 190 m above sea level). The field site consisted of two intensively-managed grassland fields of approximately five ha each. The measurement system was placed on the boundary of the 2 fields (Fig. 3.1) which runs NW to SE. This enabled micrometeorological flux measurements to be conducted over one field in SW wind directions and the other field in NE wind directions, the two prevailing wind directions at this site. These two fields are referred to as 'South' and 'North' field, respectively. The fields received on average between 270 and 320 kg N ha^{-1} yr^{-1} from three fertiliser applications and were cut twice a year for silage (see Section 4.3.1 for full management details). After the second cut, the fields were grazed by cattle and sheep in the late summer and autumn. The surrounding fields are also intensively-managed grassland with similar management. There are two farms in the vicinity: Easter Bush Farm is 400 m due east from the field site; Easter Howgate Farm is 500 m from the field site at a bearing of 250° (Fig. 3.2).

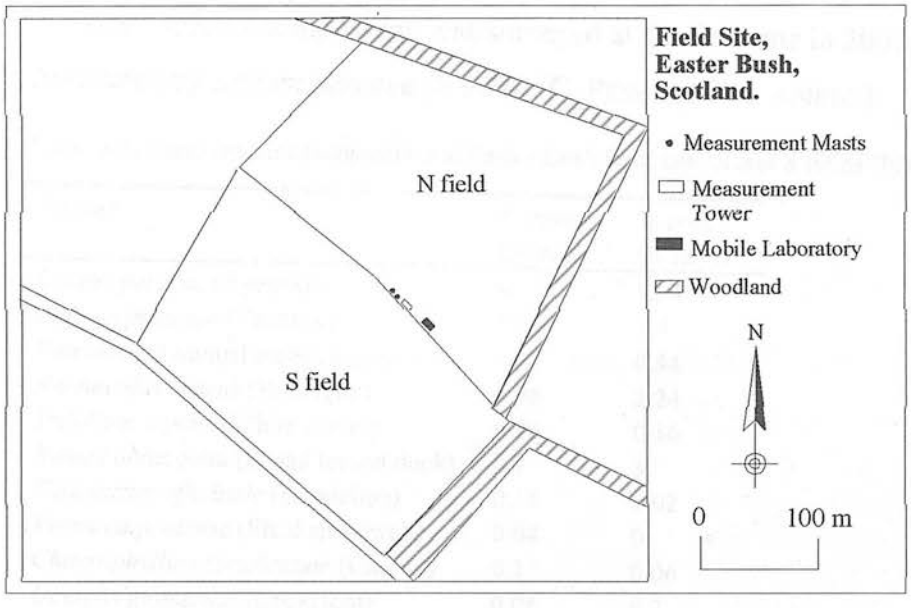

Figure 3.1. Site diagram showing the location of the measurement equipment on the boundary of the two fields.

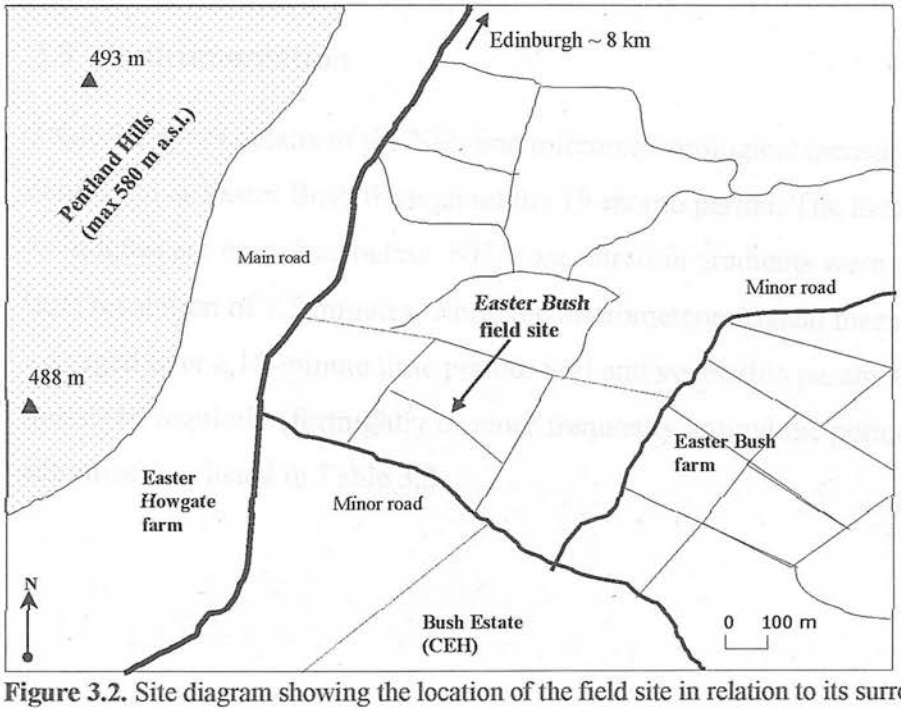

Figure 3.2. Site diagram showing the location of the field site in relation to its surroundings.

The plant species composition was surveyed at the field site in 2002 and is dominated by *Lolium perenne* (> 90%) (C. Pitcairn, Pers. comm.).

Table 3.1. Plant Species composition at Easter Bush field site, N and S fields (Pitcairn, Pers. comm.).

Species	% cover (S field)	% cover (N field)
Lolium perenne (Ryegrass)	96.44	92.46
Phleum pratense (Timothy)	1.66	1.4
Poa annua (Annual meadow grass)	0.20	0.44
Ranunculus repens (Buttercup)	0.98	2.24
Trifolium repens (White clover)	0.26	0.16
Rumex obtusifolia (Broad leaved dock)	0.1	3
Taraxacum officinale (Dandelion)	0.14	0.02
Veronica pratense (Field speedwell)	0.04	0
Chaerophyllum temulentum (Chervil)	0.1	0.06
Dactylis glomerata (Cocksfoot)	0.04	0.2
Holcus lanatus (Yorksire Fog)	0.02	-
Bellis perennis (Daisy)	-	0.02

3.3 Instrumentation

Table 3.2 gives details of the NH_3 and micrometeorological measurements that were conducted at Easter Bush throughout the 19-month period. The instrumentation and techniques are described below. NH_3 concentration gradients were measured with a time resolution of 7.5 minutes, while the micrometeorological measurements were averaged over a 15-minute time period. Soil and vegetation parameters that were measured regularly (fortnightly or more frequently around the period of management activities) are listed in Table 3.3.

Table 3.2. Ammonia and micrometeorological measurements conducted at Easter Bush.

Measurement	Instrumentation	Model and Supplier
NH_3 concentrations (3 heights)	AMANDA[a] (NH_3 analyser)	ECN, The Netherlands
Turbulence parameters (e.g. u_*)	Ultrasonic anemometer	1012RA (Gill Instruments, UK)
Sensible heat flux	Ultrasonic anemometer	1012RA (Gill Instruments, UK)
Windspeed profile (5 heights)	Cup anemometers	(Vector Instruments Ltd, UK)
Air temperature profile (2 heights)	Thermocouples	Fine Gauge Chromel-Constantan, 0.003" (Campbell Scientific, UK)
Water vapour profile (2 heights)	Dew Point Hygrometer	(Campbell Scientific, UK)
Net Radiation	Net radiometer	Q-7 (Campbell Scientific, UK)
Solar radiation	Solar radiometer	SP1110 (Campbell Scientific, UK)
Soil temperature and soil heat flux	Thermocouples and soil heat flux plates	(Campbell Scientific, UK)
Wind direction	Wind vane	W200P (Campbell Scientific, UK)
Precipitation	Tipping bucket rain gauge	(Campbell Scientific, UK)
Leaf wetness	Clip sensors	Burkhardt and Eiden (1994)

[a]AMANDA (Ammonia Measurement by ANnular Denuder sampling with online Analysis)

Table 3.3. Soil and vegetation regular measurements conducted at Easter Bush.

Measurement	Method
Soil available NH_4^+ and NO_3^-	Extraction with 1M KCl followed by colorimetric method
Soil moisture content	% weight loss on drying
Foliage N content	Acid digestion and indophenol blue method
Foliage NH_4^+ content	Grinding followed by centrifugation & NH_4^+ analysis on AMFIA[a]
Apoplastic NH_4^+ content	Vacuum infiltration followed by centrifugation
Leaf Area Index, biomass,	Canopy harvest
Canopy height	Direct measurement

[a]AMFIA (Ammonium Flow Injection Analyser)

3.3.1 Ammonia instrumentation

The NH_3 flux measurements were conducted by the aerodynamic gradient method using the continuous flow denuder referred to as AMANDA, (Ammonia Measurement by ANnular Denuder sampling with online Analysis) (Wyers *et al.*, 1993) to measure the ammonia concentrations at three heights. The advantages of this technique and its comparison with other ammonia measurement techniques have been described in section 1.2.1 and 1.2.2. The AMANDA analyser is ideally suited for micrometeorological measurements because of its low detection limit, high precision and accuracy, good linear range and high time resolution. The high time resolution of this method and the ability to run continuously (e.g. as in the period presented here of 19 months) is a vast improvement on other batch methods and allows a more detailed investigation of the underlying processes and of the diurnal, seasonal and annual variability in the concentrations and exchange of NH_3. Although in principle, the eddy covariance technique might be preferred, instruments capable of rapidly measuring NH_3 concentration are still in the development stage.

The AMANDA analyser uses rotating annular denuders, which consist of two concentric glass tubes of 30 cm length and up to 50 mm diameter, positioned horizontally (Figure 3.3). The walls of the annular space of the denuder are coated with a slightly acidic absorption solution (3.6 mM $NaHSO_4$). Air is pumped through the denuders at a rate of approximately 26 l min^{-1} and any gaseous ammonia present in the air diffuses to the sides of the denuders, where it is captured by the absorption solution. Ammonium aerosol (NH_4^+) passes through un-impeded as rates of sub-micron aerosol diffusion are much smaller than for NH_3.

The absorption solution is continuously pumped through the denuders at a rate of approximately 1 ml min^{-1} and analysed online by a common detector. Once in the detector, the stripping solution containing NH_4^+ is mixed with a solution of 0.5 M NaOH and molecular ammonia is formed. A proportion of this ammonia diffuses through a semi-permeable PTFE membrane and is dissolved in de-ionized water present on the other side of the membrane, where at pH < 7 it is mostly present in the form of NH_4^+. The NH_4^+ concentration in this water flow is determined by conductivity. The analyser is calibrated with aqueous standards of typically 0, 50 and

500 μg l^{-1} NH_4^+. The detection limit is approximately 0.02 μg m^{-3} NH_3 in air. Data-acquisition is through a datalogger present in the analyser.

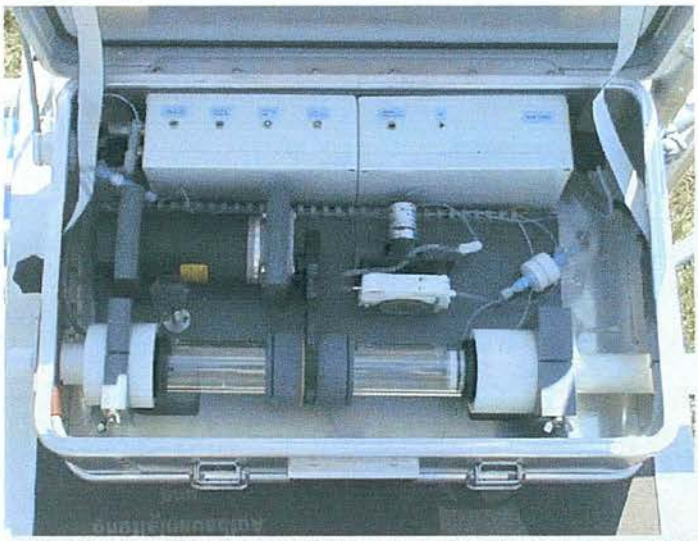

Figure 3.3. One of three rotating annular denuders in the AMANDA analyser.

Concentrations of gaseous ammonia were measured at three heights. The lowest two measurement heights varied with the height of the canopy, but were between 0.35 m to 0.8 m above ground for the lowest height and 0.79 m to 1.21 m above ground for the middle height. The highest measurement level remained at 2.06 m above ground throughout the measurement period. Average concentration values for all three denuders were determined over a 7.5 minute period. The denuders were sampled sequentially with a stabilising time of 120 s and an averaging time of 30 s. Longer lengths of tubing transporting the solution to the detector were attached to denuders 2 and 3 to ensure that the concentrations measured in the analyser for the three heights referred to the same air sampling period. Figures 3.4 and 3.5 show the field set-up and the cutting of the grass on the N field on 31 July 1998.

Figure 3.4. Easter Bush field set up showing from left to right, i) the Bowen Ratio weather station, ii) the NH_3 gradient system, iii) the wind anemometer profile and iv) the sonic anemometer on 28/7/1998. The far field is the S field and is cut, the near field is the N field and is uncut on this date.

Figure 3.5. Easter Bush field set up showing the cut south field and the north field being cut for silage on 31/7/1998.

3.3.2 *Micrometeorological instrumentation*

Ultrasonic anemometer

A Solent Research ultra-sonic anemometer (1012RA, Gill Instruments, Lymington, UK) mounted at 2.1 m provided measurements of horizontal wind speed (U), wind direction, friction velocity ($u*$) and sensible heat flux (H). The anemometer measures the difference in the transit time of sound waves between three pairs of transducers and from this calculates the horizontal and vertical components of the windspeed, as well as the speed of sound, which is related to the air temperature. The virtual sensible heat flux was calculated by eddy covariance (Eq. 2.25) from measurements of fluctuations in vertical wind velocity (w) and fluctuations in the sonic measured air temperature (T). The anemometer was logged at 20.83 Hz using Edisol software (Moncrieff *et al.*, 1997b).

Wind profile

The mean horizontal wind speed, momentum flux and friction velocity were also calculated using the aerodynamic gradient method as an additional and independent method from the eddy covariance measurements. The wind profile was determined from wind speed measurement at five heights using sensitive cup anemometers (Vector Instruments Ltd, Clywd, UK). The measurement heights employed varied with canopy height but ranged between 0.48 m to 2.67 m above ground. The 15-minute average wind speeds were logged using a logger (21x, Campbell Scientific, Loughborough, UK). The use of two independent measurement techniques for windspeed and friction velocity increased the robustness of the final estimate and gave some indication of the uncertainty of the measurement.

Bowen ratio weather station

A Bowen Ratio (BR) system (023A, Campbell Scientific, Loughborough, UK) was installed at the site. This was not used as a BR system, but provided gradients of air temperature and water vapour. Air temperature was measured using fine gauge chromel-constantan (E-type) thermocouples with diameters of 0.003". Water vapour pressure and dew point temperature were measured using a dew point hygrometer.

The height of the lower measurement varied according to canopy height but was in the range 0.4 m to 0.8 m above ground. The top measurement height remained at 2.13 m above ground throughout the measurement period.

In addition, measurements of net radiation, solar radiation and rainfall were made using a Q-7 Net Radiometer, SP1110 Pyranometer sensor and an ARG100 tipping bucket raingauge (all supplied via Campbell Scientific, Loughborough, UK). A potentiometer wind vane (W200P Vector Instruments Ltd, Clywd, UK) was used to record wind direction (threshold 0.6 m s^{-1}). Soil temperature was measured at 2 cm and 10 cm depth at two different locations in the soil using TCAV thermocouples (Campbell Scientific, Loughborough, UK). Soil heat flux was measured at 10 cm depth at two locations using soil heat flux plates (Campbell Scientific, Loughborough, UK). All the above parameters were logged with a 15 min averaging period on a logger (21x, Campbell Scientific, Loughborough, UK).

Leaf wetness

Leaf wetness (LW) has commonly been assessed using a wetness sensing grid as a surrogate for the leaf surface. An example of such a wetness sensor is described by Wie *et al.* (1995) and is provided by Campbell Scientific (Loughborough, UK). This sensor consists of a circuit board with interlaced gold-plated copper fingers. Wetness on the sensor lowers the resistance between the fingers and this change is recorded via a datalogger, the wetness sensing grid is 63 mm by 76 mm.

An alternative type of wetness sensor has been developed by Burkhardt and Gerchau (1994). This wetness sensor consists of gold-plated clip electrodes, which clip directly onto leaves, the conductivity between a pair of electrodes is measured and this increases with leaf wetness. The clip electrodes are 25 mm by 1 mm. There is a clear advantage in this type of sensor in that the measurement is made directly at the leaf surface and not on a surrogate for the leaf surface. By contrast, wetness sensing grids measure the significant events of wetness, such as precipitation, but they are not good at measuring dew or other micro-processes that have been observed using the leaf surface clip sensors, such as recondensation of transpired water vapour to salts on the leaf surface leading to leaf wetness (Burkhardt *et al.*, 1999).

As a consequence of the importance of leaf wetness in ammonia exchange, it was decided to employ the wetness sensing clips at the field site. Six clip sensors as described by Burkhardt and Gerchau (1994) were used in parallel. It is necessary to have replicate clip sensors due to the inhomogeneous nature of leaf wetness (leaves next to each other can experience different levels of wetness due to exposure to rain, sunlight and other meteorological parameters). A 6V (AC, 2 kHz) voltage was applied and the conductivity was continuously logged by a datalogger (21x, Campbell Scientific, Loughborough, UK). The clips were placed near the top of the canopy and moved every week or so to fresh leaves. These measurements of leaf wetness at Easter Bush are reported by Klemm *et al.* (2002) and their relationship with *RH* and precipitation explored, along with three other sites across Europe.

3.4 Vegetation measurements

To aid both interpretation and modelling of the ammonia exchange, an extensive suite of vegetation and soil parameters were measured in addition to the standard meteorological parameters. Measurements were carried out on both south and north fields to assess any differences between the fields and also because the timing of management activities was not always identical on the two fields.

3.4.1 Leaf area index and biomass harvesting

Leaf Area Index (LAI) is a measure of the leaf area of a canopy per unit ground area. It can either by given as single-sided (only the area of one side of the leaf considered) or double-sided (both sides of the leaf considered). The LAI of a plant governs its photosynthetic potential, its interception of light and rain and also the surface available for gas exchange. Consequently, the seasonal variation in LAI is of great interest to modellers of gas exchange and can be incorporated into parameterisations. Measurements of the LAI of the grass canopy at Easter Bush were conducted monthly or more frequently around periods of cutting.

On each sample date, five quadrats of 0.25 m by 0.25 m were harvested and the total fresh weight (f.w.) determined. The leaf area of a sub-sample of known fresh weight was determined using a leaf area meter. The total leaf area was computed from the ratio of the fresh weights of the full sample and sub-sample. In addition, a second

sub-sample with defined fresh weight was taken and dried in an oven at 70 °C for 24 hours until constant weight and reweighed. The amount of biomass harvested (g dry matter m^{-2}) was determined from the ratio of fresh to dry weight and the total fresh weight harvested. The mean and range of canopy height was measured in the two fields approximately every four days using a tape measure. This was a quick measurement to make and is a useful record of canopy growth and productivity.

3.4.2 Total foliar nitrogen and carbon content

Total foliar nitrogen (N) and carbon (C) content were measured at monthly intervals or more frequently close to cutting and fertilising events. Leaf samples were taken either at the same time as the quadrats used for LAI determination or else leaves were sampled from five random locations in each field. A sub-sample of defined fresh weight was taken, the leaves were washed in de-ionised water and dried at 70 °C for 24 hours to determine the water content. A smaller subsample of the dry grass (dry weight approximately 10 g) was ground in a hammer mill (Culatti, Switzerland) to a fine powder. The ground sample was sent to CEH-Merlewood Chemical Analysis Laboratory for analysis of total N and C content. N content was determined by acid digestion and the indophenol blue method (Allen, 1989) and C content was determined by a Carlo Erba type elemental analyser.

3.4.3 Foliar ammonium content

Total foliar NH_4^+ concentration ($[NH_4^+]_{fol}$) was measured fortnightly and more frequently at the time of management events in 1999 and also measured in 1998 by Loubet *et al.* (2002). Although it is strictly the ratio of apoplastic NH_4^+ concentration ($[NH_4^+]_{apo}$) and hydronium concentration $[H^+]_{apo}$ which governs the stomatal compensation point and consequently the emission potential of the vegetation, a close link between $[NH_4^+]_{fol}$ and $[NH_4^+]_{apo}$ has been reported (Hill *et al.*, 2001). As the bioassay for $[NH_4^+]_{fol}$ is less labour intensive than that for $[NH_4^+]_{apo}$, it is of interest to measure this parameter and investigate its dynamics in relation to NH_3 exchange and N supply.

Leaf samples were obtained from five locations selected randomly in both fields. The samples were washed with de-ionised water, frozen with liquid nitrogen and then

ground using a ceramic pestle and mortar. Three replicate sub-samples of the ground leaves were taken and their exact mass recorded (approximately 0.1 g). The ground samples were placed in a 1.5 ml Eppendorf tube and 1 ml of de-ionised water added. The samples were frozen and stored in a freezer at -18°C, prior to analysis at a later date.

On the day of analysis the samples were defrosted and centrifuged for 4 minutes at 15,703 g, 15,300 rpm and 4°C. The supernatant was filtered through a small cotton wool plug in a pipette tip to remove any remaining plant tissues. The NH_4^+ content of this filtered solution ($[NH_4^+]_{sol}$, $\mu g\ NH_4^+\ g^{-1}$) was measured using an AMmonium Flow Injection Analyser (AMFIA, ECN, The Netherlands). The foliar NH_4^+ concentration ($[NH_4^+]_{fol}$, $\mu mol\ NH_4^+\ g(leaf\ f.w.)^{-1}$) was found as:

$$\left[NH_4^+\right]_{fol} = \left[NH_4^+\right]_{sol} \times \frac{m_l + m_{fw}}{m_{fw} + M_{NH4}} \qquad (3.1)$$

where M_{NH4} is the molecular mass of ammonium ($g\ mol^{-1}$), m_l is the mass of de-ionised water added to the plant material (1 g) and m_{fw} is the mass of ground leaves (g), respectively (Hill, 1999; Loubet *et al.*, 2002).

3.4.4 Apoplastic ammonium and pH

The apoplastic NH_4^+ concentration ($[NH_4^+]_{apo}$) and apoplastic pH was measured at Easter Bush from May 1998 to October 1998 by Loubet *et al.* (2002). The full experimental details are given by Loubet *et al.* (2002) and also by Hill (1999), based on the vacuum infiltration technique of Husted and Schjoerring (1995a). The leaves were infiltrated with indigo carmine solution (50 μM) using a 50 ml syringe to repeatedly create vacuum and pressure. After infiltration, the leaves were placed in a centrifuge at 500g for 10 minutes at 4°C and the extracted solution was collected. The NH_4^+ concentration in the extracted solution was measured with the AMFIA and the pH was measured using an InLab 423, semi-micro pH electrode (Mettler Toledo, Udorf, Switzerland).

3.4.5 Root biomass distribution

The amount of plant uptake from different soil layers is determined by the root distribution of an ecosystem. Ecosystem models, which model nutrient uptake from different soil layers, need a measurement or estimation of the root distribution. The vertical root distribution at Easter Bush was measured at the start of the measurement period in four replicate soil columns from each field. The soil column was divided into three depths (0-5 cm, 5-10 cm and 10-15 cm). The roots were separated from the soil, washed and dried at 70 °C for 24 hours and weighed. The fraction of roots in each of these layers compared with the total was calculated.

3.5 Soil measurements

The soil is a crucial component of the biosphere-atmosphere interaction and often gets overlooked when making measurements of NH_3 exchange. However, a full suite of soil measurements was conducted to accompany the measurements of NH_3 exchange presented here. Some soil properties change on long time-scales and so can be characterised by a measurement at one point in time over the duration of the field measurements (e.g. soil type and texture). Other parameters, such as mineral N supply, vary on much shorter timescales as a result of the competing processes of fertilisation, plant uptake, mineralisation, immobilisation, leaching losses and gaseous losses. A programme of regular measurements was introduced to characterise the dynamics of these soil properties.

3.5.1 Soil profile description

A soil pit was dug at Easter Bush on 12/11/02 (Fig. 3.6) and a soil profile description conducted following Hodgson (1974) (R. Rees, Pers. Comm.) (Table 3.4). The soil type at the field site is imperfectly drained Macmerry soil series, Rowanhill soil association.

Table 3.4. Easter Bush soil profile description following Hodgson (1974) (R. Rees, Pers. Comm.).

Horizon	Depth (m)	Description
A1(g)	0-0.18	Brown (5 YR 3/2) occasional mottling; sandy loam, coarse crumb, friable few medium rounded stones; abundant fine roots; gradual change into:
A2(g)	0.18-0.31	Brown (7.5 YR 3/2) mottling, subangular blocky; firm; roots many fine; stones small-medium, common; clear change into:
B1(g)	0.32-0.79	Grey-Brown (10 YR 4/2) abundant mottling (7.5 YR 6/1 – 10 YR 6/8); sandy clay loam, poor blocky; plastic; stones moderate, small-large rounded-subangular; few fine roots; gradual change into:
B2(g)	0.79-1.00	Grey-Brown (7.5 YR 4/3) strongly mottled (7.5 YR 5/8); clay loam; poor blocky; plastic; stones moderate small-large rounded – subangular; very few fine roots; water tables at 85 cm.

Figure 3.6. Soil pit at Easter Bush showing soil profile, 12/11/02.

3.5.2 Soil texture and structure

Soil consists of differently sized particles and the particle size distribution within the soil has a strong influence on both chemical and physical properties of the soil (Rowell, 1994). In particular, hydrological properties of the soil (such as drainage, the ability to hold water and nutrients for plant use) vary considerably with the soil particle size. The classification system, which is most commonly used for soil particle size, is shown in Table 3.5. Soils are classified according to their particle size

distribution into different textural classes, the UK textural classification is given by Rowell (1994).

Table 3.5. Soil particle size classification (from Rowell, 1994).

Description	Size
Stones	> 2 mm
Coarse sand	200 μm – 2 mm
Fine sand	60- 200 μm*
Silt	2- 60 μm*
Clay	< 2 μm

*The European system generally uses 60 μm as the limit between fine sand and silt, although occasionally 20 μm is used.

The particle size distribution was determined for both fields at Easter Bush in two soil layers (0.0 m – 0.15 m and 0.15 m – 0.3 m). The analysis was conducted at CEH-Merlewood Chemical Analysis Laboratory using the sieving and sedimentation method.

3.5.3 Bulk density

The bulk density of the soil is the mass of oven-dried soil present in a given volume (g dry soil cm^{-3}). It is a key parameter describing the physical nature of a soil. Many other physical properties of the soil (in particular those concerning water availability and transport) can be estimated from the soil particle size distribution and bulk density.

A profile of bulk density was determined in both of the Easter Bush fields by using a rectangular sampling device (0.05 m x 0.05 m x 0.05 m) to sample soil of a known volume. The bulk density was determined for 4 layers of 0 m to 0.05 m, 0.05 m to 0.1 m, 0.1 m to 0.15 m and 0.15 m to 0.20 m. The soil was dried for 24 hrs at 105 °C and then weighed.

3.5.4 Soil organic nitrogen and carbon content

Organic matter content is a slow changing property of a soil. Consequently organic C and organic N content were determined once in the duration of the measurements rather than as a repeated measurement. Organic C content was measured by the CEH-Merlewood Chemical Analysis Laboratory using the Tinsley method (Allen, 1989). Total N content was also determined at CEH-Merlewood by H_2O_2 digestion

followed by colorimetry (Allen, 1989). Organic N content was determined from the difference between total N and measured mineral NH_4^+ and NO_3^-.

3.5.5 Soil ammonium and nitrate content

Measurements of available ammonium (NH_4^+) and nitrate (NO_3^-) in the soil and soil moisture content were conducted fortnightly or more frequently before and after cutting and fertilising events. Five replicate soil cores, separated into two layers (0-0.15 m and 0.15-0.30 m), were taken in each of the south and north field along a horizontal transect from the measurement equipment. The samples were bulked and a sub-sample (approximately 100 g) was analysed for moisture content (percentage weight loss on drying for 24 hrs at 105 °C). Another sub-sample was frozen and extracted for available NH_4^+ and NO_3^- at a later date. The extraction process was as follows: 15 g of soil was placed in a 500 ml flask with 50 ml of 1.0 M KCl solution, the flasks were shaken in a mechanical shaker for approximately 30 minutes at 120 rpm, after shaking, the soil solutions were filtered using Whatman 42, 185 mm diameter filters. This process was repeated for reference soil samples and blank KCl solution. The extracted soil solutions were frozen and sent to CEH-Merlewood Chemical Analysis Laboratory where they were analysed for soil available NH_4^+ and NO_3^- by colorimetry (Henriksen and Selmer-Olsen, 1970; Crooke and Simpson, 1971).

3.6 Record of management activities

The Easter Bush grassland is intensively-managed for silage and for grazing. As a result of this there are a variety of agricultural management activities that occur. To fully characterise the site it is necessary to have both detailed data on management activities during the measurement period but also on the preceding 10 years, as the history of a grassland has a strong influence on its present status. A record of management activities was obtained for these timescales from the farm manager. In addition to the record of management activities a record of grazing was kept during grazing periods. This included information on the number and type of animals and the approximate duration they were present in the field.

Chapter 4: Measurements at Easter Bush: site characterisation

4.1 Introduction

Measurements of micrometeorological parameters and site characteristics are required at a site in order to calculate and interpret fluxes and concentrations of a trace gas. For ammonia, it is also beneficial to characterise the foliar and soil N supply and to have information on external influences at a site such as N fertilisation. This chapter provides details of the site features such as fetch, flux footprint and climatology, it also presents results on inter-comparisons that were conducted of key parameters and lists the management activities affecting the site. The chapter also includes results of the accompanying vegetation and soil measurements.

4.2 Climatology and micrometeorology

4.2.1 Inter-comparisons of micrometeorological parameters

Having more than one independent estimate of a measured parameter improves the robustness of the measurements and highlights periods of measurement problems. Inter-comparisons between different techniques or the same technique at different measurement locations, were conducted for the following micrometeorological parameters.

Turbulence and sensible heat flux

The meteorological parameters, u_*, u(1 m), and H were determined by both the eddy covariance and aerodynamic gradient method (Section 2.2) and the two methods were compared to check data quality. Figs. 4.1 and 4.2 show the comparison of the two methods for u_* and H for the period 24-27/7/98. These results show close agreement, which gives confidence in the measurements. Overall, the value of u_* obtained by eddy covariance (u_{*ec}) was slightly larger than the value determined by the aerodynamic gradient method (u_{*ag}). Figure 4.3 shows the comparison for January 1999 ($u_{*ag} = 0.85u_{*ec} - 0.003$, $R^2 = 0.85$, $n = 1786$). The regression for the entire dataset is: $u_{*ag} = 0.78u_{*ec} + 0.052$, $R^2 = 0.69$, $n = 26{,}726$. Figure 4.4 shows

similar results for H. In practice, values of u_*, u(1 m) and H from the eddy covariance method were used for further analysis for the majority of the time with estimates from the aerodynamic method used to fill any periods of missing data in the eddy covariance series.

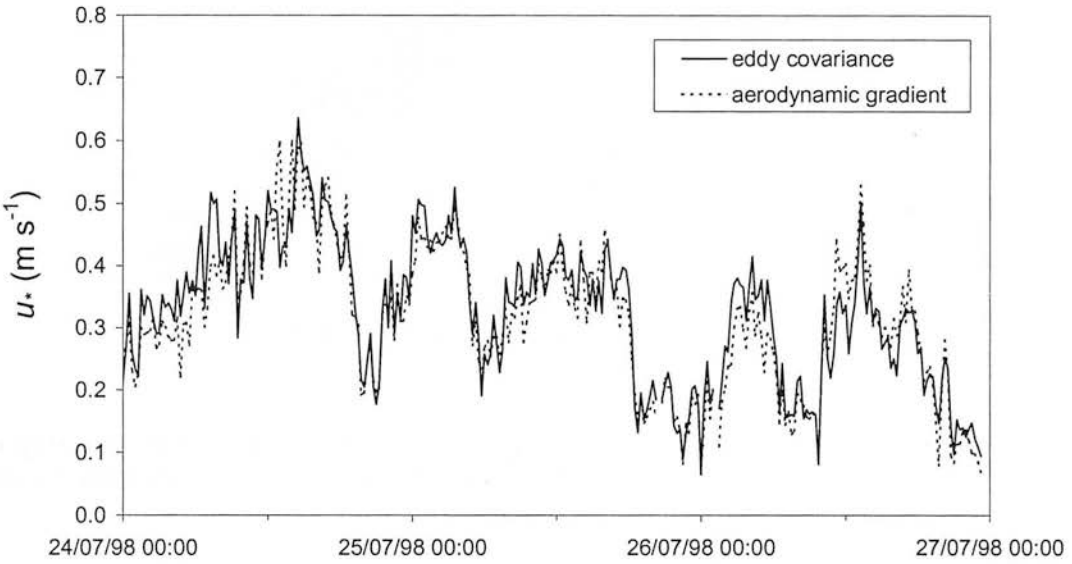

Figure 4.1. Comparison of friction velocity (u_*) measured with the eddy covariance method and the aerodynamic gradient method (see section 3.3.2 for details of instrumentation). Data were filtered according to section 4.2.3.

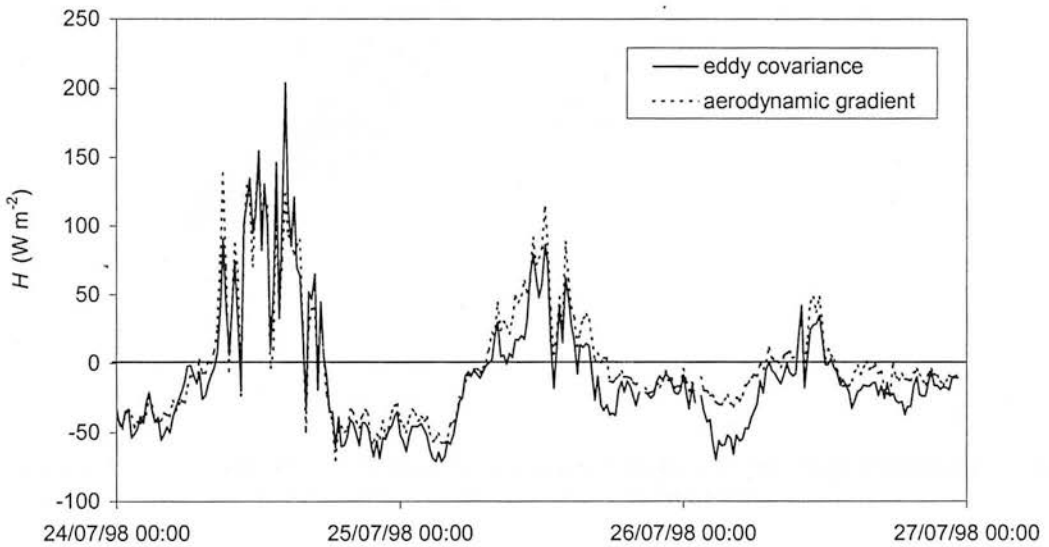

Figure 4.2. Comparison of sensible heat flux (H) measured with the eddy covariance method and the aerodynamic gradient method. Data were filtered according to section 4.2.3.

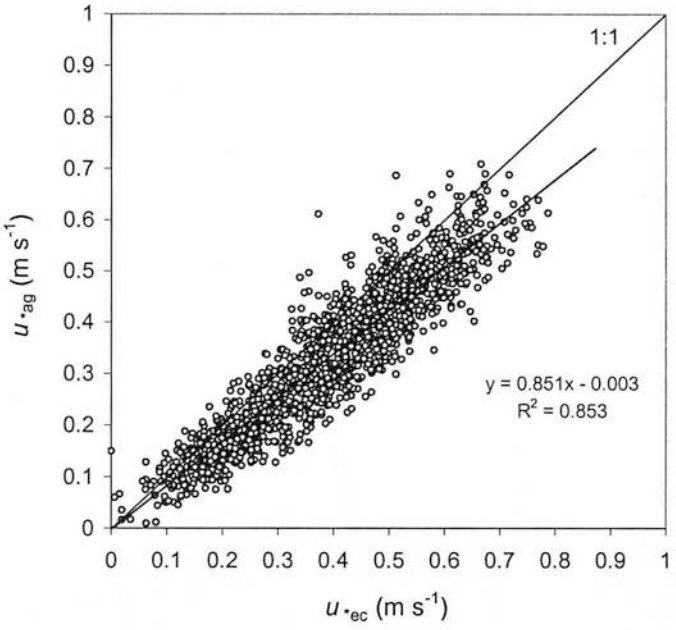

Figure 4.3. Comparison of u_* measured with the eddy covariance method (u_{*ec}) against u_* from the aerodynamic gradient method (u_{*ag}) for the period January 1999.

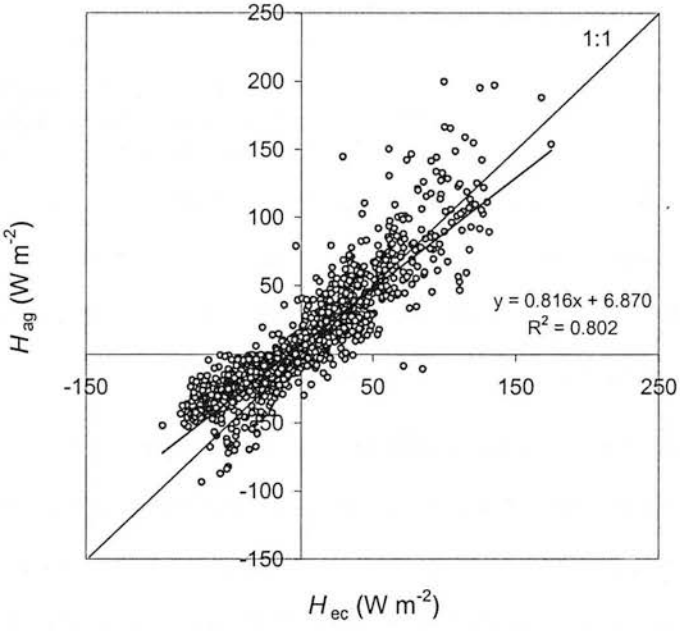

Figure 4.4. Comparison of sensible heat flux measured with the eddy covariance method (H_{ec}) against the aerodynamic gradient method (H_{ag}) for the period September 1998.

Wind direction

Wind direction was recorded at the field site by both the ultrasonic anemometer and by a wind vane located on the wind profile mast. As part of the data assessment, the wind direction from these two sources was compared along with a third estimate from a wind vane at another monitoring cabin located 400 m South from the field site (Fig. 4.5).

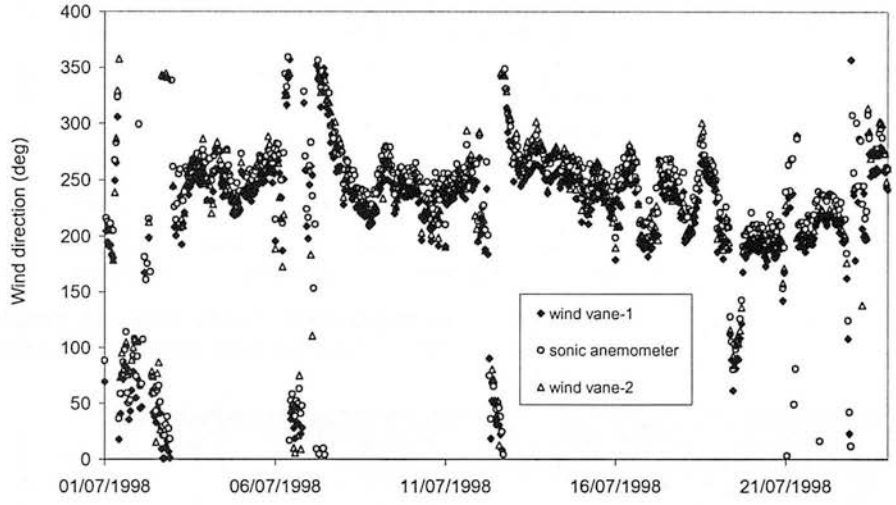

Figure 4.5. Comparison of wind direction measured at the field site with a sonic anemometer against wind direction from wind vanes at the field site (wind vane-1) and from an additional site, 400 m away from the field site in a South direction (wind vane-2). Data only shown for u (2 m) > 0.6 m s^{-1}.

As wind direction is a vector it is not useful to look at a regression of one wind direction against another, instead the "scalar" product of two wind directions can be examined. The scalar product is defined for two vectors X and Y as: $X \cdot Y = |X||Y|\cos\theta$, where θ is the angle between the vectors in radians. Fig. 4.6 shows the cosine of the angle (θ) between the different estimates of wind direction for the same period as shown in Fig. 4.5. For two identical wind directions cos θ = 1, for two perpendicular wind directions, cos θ = 0 and for two anti-parallel wind directions cos θ = -1. For the period shown in Fig. 4.6, cos θ is mostly > 0.95, this corresponds to a difference in wind direction of 18°. The few occurrences where cos θ is not close to 1 indicate periods of disagreement and possible problems with sensors. Analysis of cos θ was conducted for the whole measurement period and for the majority of the time the sonic anemometer estimate was used. The main exception was during the period 9/6/99-30/6/99 when the sonic wind direction

appeared to be shifted by approximately 40° compared with both wind vane estimates (Fig. 4.7). This was possibly as a result of being incorrectly located after being placed back in the field.

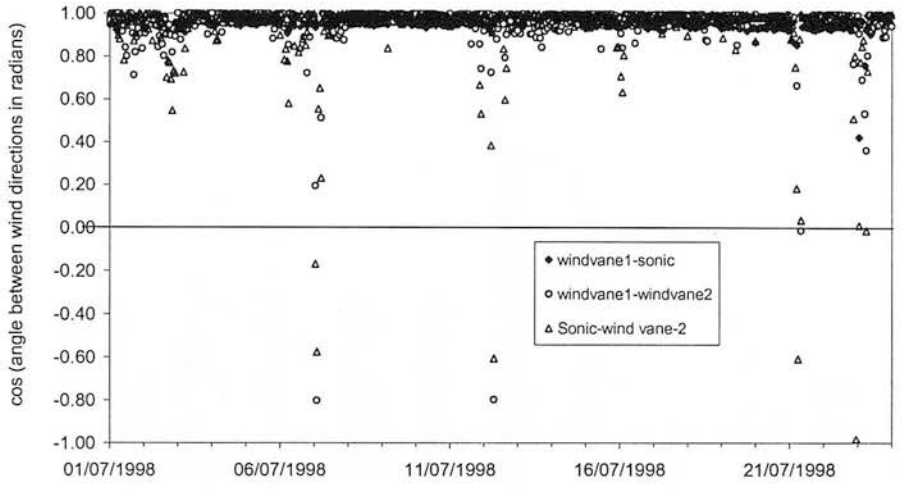

Figure 4.6. Time course of the cosine of the angle (in radians) between different estimates of wind direction for Easter Bush for 1/7-31/7/1998.

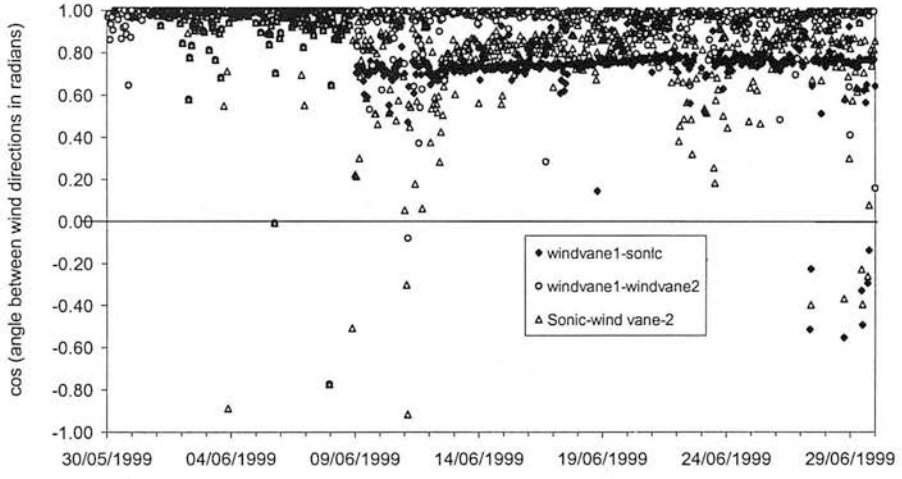

Figure 4.7. Time course of the cosine of the angle (in radians) between different estimates of wind direction for Easter Bush for 1/6-30/6/1998.

Rainfall

The importance of wetness in determining NH_3 exchange has been discussed in Section 1.3. In addition to measuring the wetness directly on the leaves, precipitation was also measured with a tipping bucket rain gauge at the field site. In order to establish the reliability of the rainfall measurement and also to fill in any measurement gaps, the aggregated monthly rainfall from the field site was compared with rainfall data from one of the UK Meteorological Office land surface observation

stations nearby (Fig. 4.8). The observation station was at Bush House, which is located 750 m away from Easter Bush field site in a SSE direction at (3°12' W, 55° 51' N, 184 m a.s.l.).

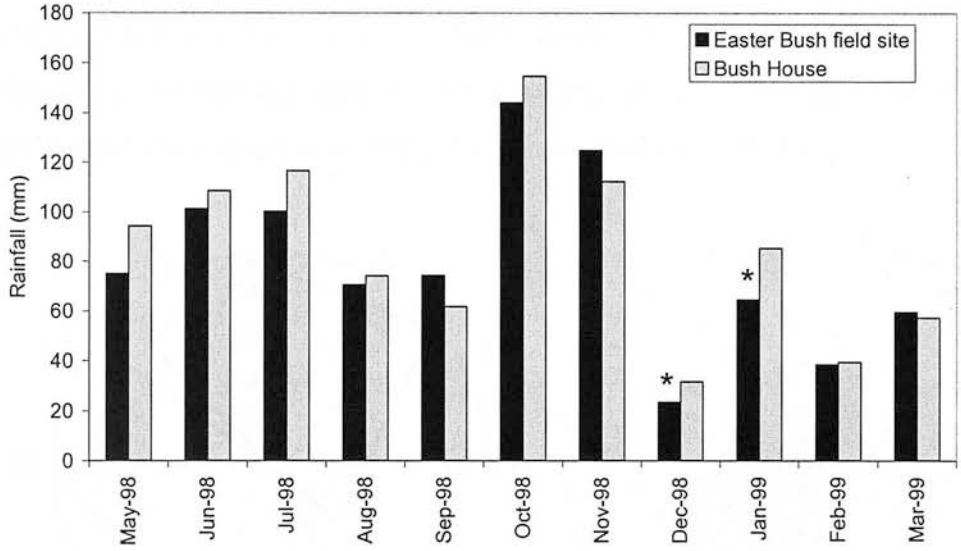

Figure 4.8. Comparison of monthly total rainfall measured at the field site against rainfall data from one of the UK Meteorological Office land surface observation stations (Bush House) for the period May 1998-March 1999. * Data for December 1998 only covers the period 1/12/98-21/12/98 and data for January 1999 only covers the period 13/1/99-31/1/99 due to a power failure over this period at the field site which caused logged data to be lost.

Fig. 4.8. shows close agreement between the field site data and the Met. Office data. The rainfall over the period of comparison (1/5/98-31/3/99, but excluding a large period of no data due to power failures, 21/12/98-13/1/99) was 876 mm (field site) and 937 mm (Met. Office station) a difference of 7%. The Met. Office data was used to complete any data gaps at the field site (in particular 21/12/98-13/1/99) and this resulted in an annual rainfall for 1/5/98-30/4/99 at the field site of 1013 mm.

The above data comparisons demonstrated that the majority of the data collected was consistent and of a sufficient quality to calculate and interpret fluxes. The comparisons and the ability to obtain data from a number of neighbouring sites helped to fill in data on the few occasions when data were either unavailable or of uncertain quality.

4.2.2 Site characterization

Fetch and wind frequency distribution

The dimensions of the field site and the location of the measurement equipment are shown in Fig. 3.1. Fig. 4.9a shows the fetch in more detail as a function of wind direction. This indicates that the fetch was greater than 175 m for wind directions 180°-305° and greater than 200 m for wind directions 315°-55°.

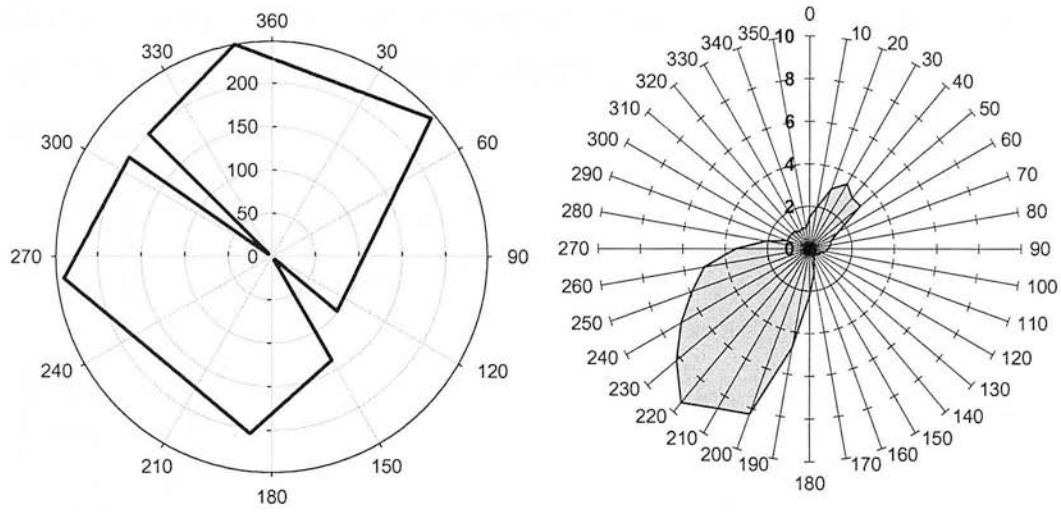

Figure 4.9. a) Fetch (in m) at Easter Bush field site shown as a function of wind direction, b) Wind direction frequency distribution (as % of time) for Easter Bush for the full measurement period 1/5/98-1/12/99.

The fence-line was orientated at 310° to 140°. The fetch was reduced to 5 m along the fence-line due to obstructions either by other measurement equipment placed along the fence-line or due to the mobile laboratory, which was in the direction 140°, 10 m from the ammonia analyser. Fig. 4.9b shows the frequency distribution of wind direction at Easter Bush for the full measurement period (1/5/1998-1/12/1999) and demonstrates that the wind direction was very rarely from along the fence-line (only 1.5 % of the time). Therefore the lack of fetch in these directions did not result in a large loss of data. The wind was from the S field (145°-305°) 69.4 % of the time and from the N field (315°-135°) 27.1 % of the time. The remainder of the time (2.0 %), $u(2.1\text{ m}) < 0.5\text{ m s}^{-1}$. The wind direction cannot be measured accurately with a wind vane at these low windspeeds and so the wind direction from these periods was not included in the wind frequency analysis. Examining Fig. 4.9b shows that not only was the wind from the S field for the majority of the time, it was also from a fairly

narrow sector for most of this time (53% of the time the wind was in the sector 195°-265°).

Flux footprint

Section 2.3.1 discussed the concept of the "footprint" of a flux measurement as the upwind area influencing that flux measurement. A quantitative measure of this footprint is the cumulative normalized footprint (CNF), which is the contribution to the measured flux as a function of the upwind distance or fetch. Fig. 4.10 presents the CNF for three separate measurement periods in neutral, stable and unstable conditions.

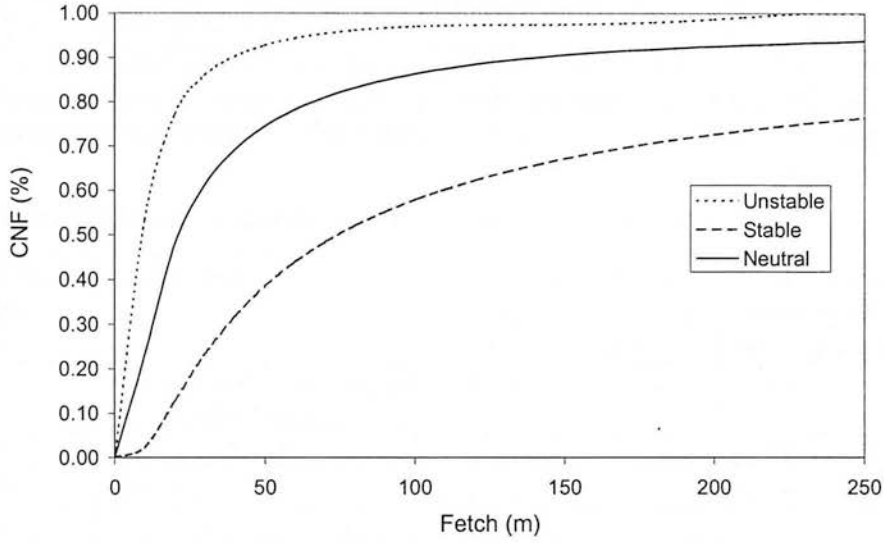

Figure 4.10. Cumulative normalized footprint (CNF) at Easter Bush for three runs: neutral ($L = \infty$), stable ($L = +5$) and unstable ($L = -5$) conditions (all with $u_* = 0.2$ m s^{-1}, $z_0 = 20$ mm, $z\text{-}d = 1$ m).

The average CNF for the whole measurement period (1/5/98-30/11/99) was 86% whilst the median CNF was 91%. For 82% of the time the CNF was > 65%. This provides a check that the available fetch is sufficient for the measurement of flux in any one period. The large proportion of time for which the fetch is sufficient (82%) reflects the generally windy nature of this site.

4.2.3 Filtering procedures

The footprint analysis provides a quantitative assessment of the sufficiency of the available fetch for each individual flux measurement, depending on the wind direction and turbulence conditions at that time. The CNF value was used as part of a

wider set of criteria for filtering the flux measurements. The full meteorological criteria that were used to establish periods when the flux calculations were less certain were as follows: i) CNF< 65%, ii) $|L| < 2$ m and iii) u (1 m) < 0.5 m s^{-1}. The results of applying these meteorological criteria to the measurement data are shown in Table 4.1 and Table 4.2.

Table 4.1. Results of applying filter criteria to the turbulence dataset

Filter No.	Filter criteria	No. of valid u_* data points remaining (15 min averages)	% data coverage of remaining data after applying critera
1	Sensor malfunctioning & power cuts	47,747	91.3%
2	Obstructed wind sector [a]	46,799	89.5%
3	CNF < 65%	43,033	82.3%
4	$\|L\| < 2$ m	42,242	80.8%
5	u(1 m) < 0.5 m s^{-1}	41,605	79.5%

[a]Data removed for wind directions 130°-150° and 305°-315°, this is the direction of the fenceline where flux measurements are obstructed by the mobile laboratory and other equipment.

Table 4.2. Results of applying filter criteria to the NH_3 flux dataset

Filter No.	Filter criteria	no of valid NH_3 flux data points remaining (15 min averages)	% data coverage of remaining data after applying critera
1	Analyser malfunctioning and periods of calibration	37,101	70.9%
2	Obstructed wind sector [a]	36,415	69.6%
3	CNF < 65%	33,710	64.5%
4	$\|L\| < 2$ m	33,092	63.3%
5	u(1 m) < 0.5 m s^{-1}	32,576	62.3%

[a]Data removed for wind directions 130°-150° and 305°-315°, this is the direction of the fenceline where flux measurements are obstructed by the mobile laboratory and other equipment.

The data coverage is reduced from 91.3% to 79.5% for the meteorological data after applying these criteria and from 70.9% to 62.3% for the NH_3 flux data. The reason for the lower data coverage for the NH_3 data is that the AMANDA analyser malfunctioned more frequently than the meteorological measuring equipment. The period 15/12/98 16:30- 13/1/99 10:00 was not included in the calculation of data coverage as the equipment was switched off at this time.

4.2.4 *Climatology of the field site*

The seasonal variability in air temperature, radiation, rainfall and windspeed at Easter Bush field site is shown in Figs. 4.11, 4.12 and 4.13. Mean daily temperatures varied between –1 to 21 °C with a mean annual temperature (1/5/98-30/4/99) of 9.4 °C. Maximum temperatures rarely rose above 25 °C in summer. The minimum temperature falls below freezing on occasions in months October-April.

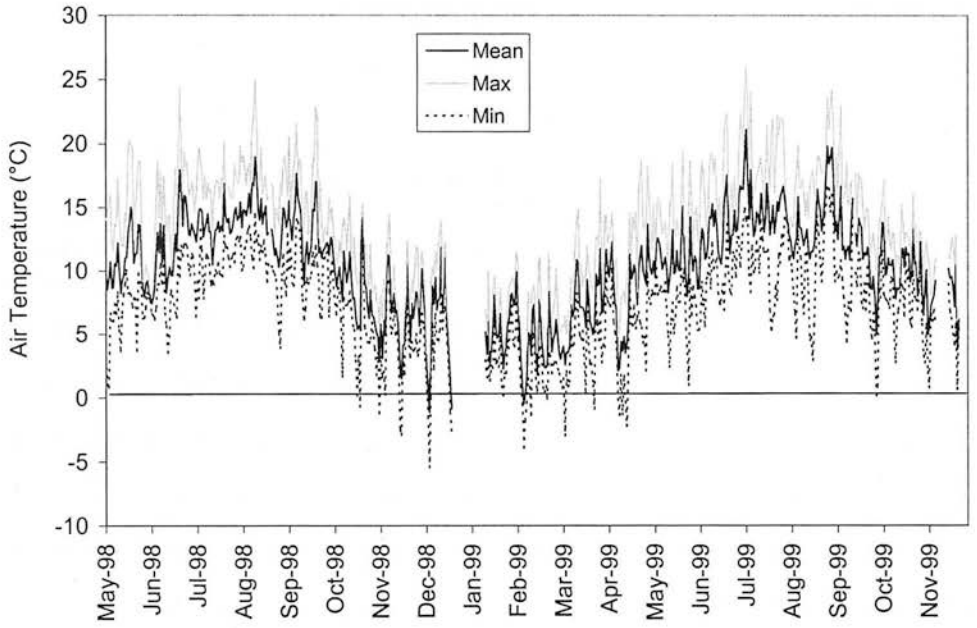

Figure 4.11. Mean, maximum and minimum daily temperatures, measured at 2.13 m at Easter Bush field site.

The pattern of monthly solar and net radiation is shown in Fig. 4.12. This shows maximum values of radiation in May, June and July, while net radiation is negative for November-February. Maximum monthly temperatures are observed in July, August and September.

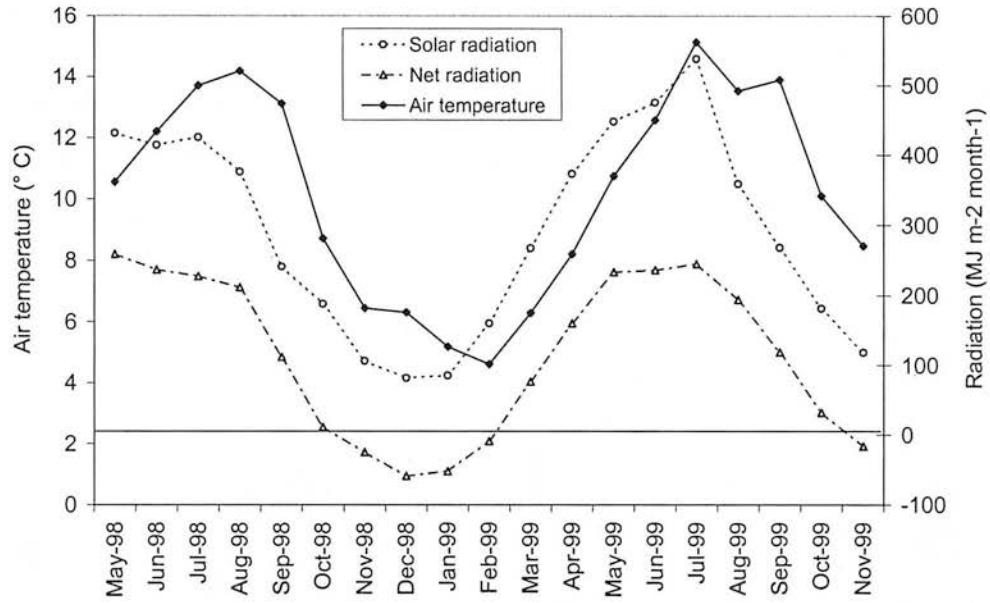

Figure 4.12. Mean monthly air temp (measured at 2.13 m) and monthly sums of solar and net radiation.

Monthly rainfall is shown in Fig. 4.13. This indicates a fairly even distribution of rainfall with only the months August and September 1999 being substantially drier. As stated in Section 4.2.1, the annual rainfall for 1/5/98-30/4/99 at the field site was 1013 mm. The 1961-1990 average rainfall for the Royal Botanic Gardens in the centre of Edinburgh (nearest available certified data source, 26 m a.s.l.) is 638 mm. Mean monthly wind speeds at the field site are generally above 3 m s^{-1} (Fig. 4.13).

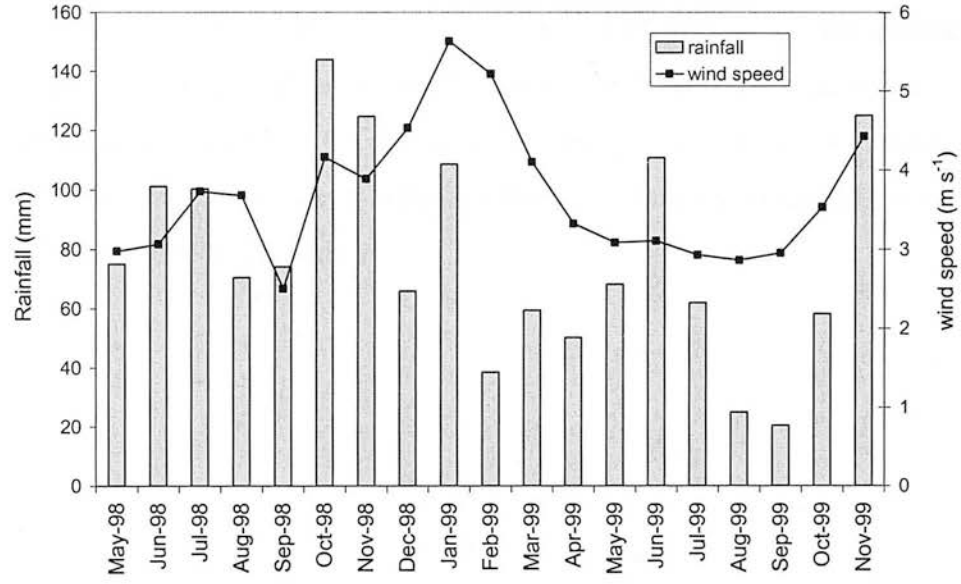

Figure 4.13. Monthly rainfall and mean monthly wind speed. Wind speed was measured with the sonic anemometer at 2.1 m except for May, July, August and September 1999 when the sonic anemometer was unavailable and u(1 m) from the wind profile measurements was used to calculate the monthly mean instead.

Energy Balance

The fluxes of net radiation (R_n), sensible heat (H), latent heat (LE) and soil heat (G) are shown in Fig. 4.14 for an example period (8/7/98-12/7/98). Generally, H and LE are of similar value indicating that Easter Bush is a well watered site at this time.

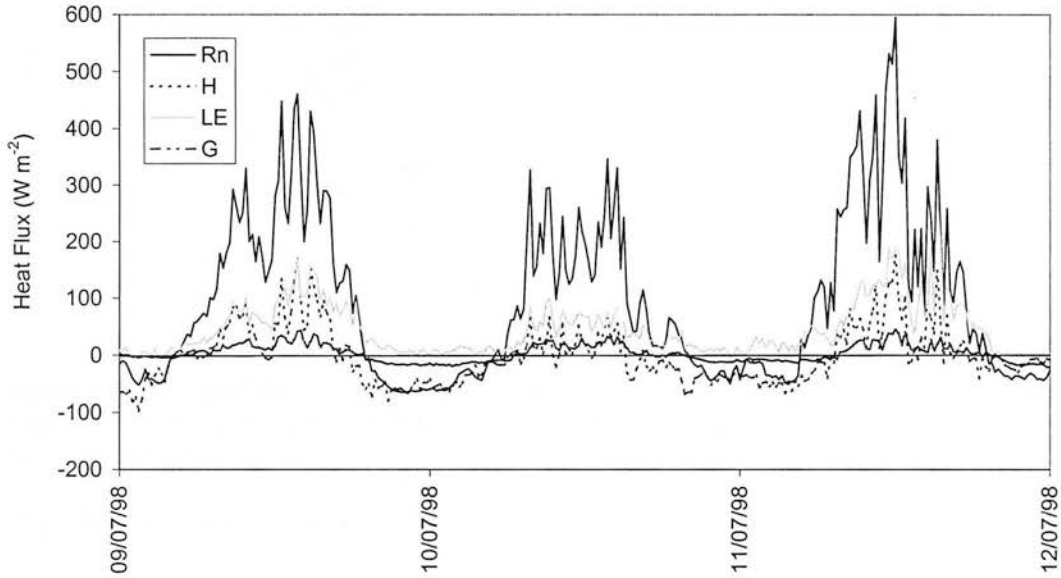

Figure 4.14. Net Radiation (R_n), Sensible Heat Flux (H), Latent Heat Flux (LE) and Soil Heat Flux (G) for the period 9/7/98-12/7/98.

The ability to close the energy balance, i.e. that the available energy reaching the surface ($R_n - G$) is equivalent to the turbulent fluxes of energy leaving the surface ($H + LE$), is a test of the performance of micrometeorological measurements. The degree of energy balance closure for a period in June 1998 is shown in Fig. 4.15. The turbulent fluxes are less than the available energy received at the surface. It is possible that R_n was overestimated or that some flux loss occurred due to the averaging time of 15 minutes.

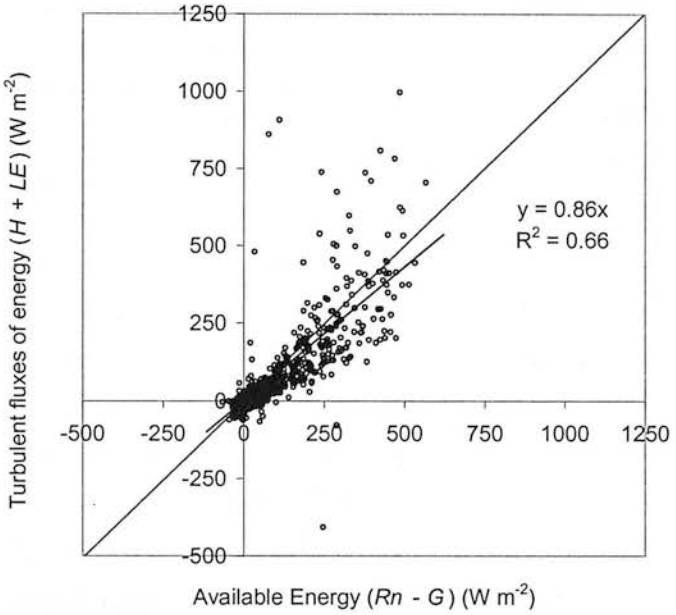

Figure 4.15. Energy Balance Closure: the relationship between available energy (Net Radiation (R_n) – Soil Heat Flux (G)) and turbulent fluxes of energy (Sensible Heat Flux (H) + Latent Heat Flux (LE)) for the period 1/6/98-12/6/98.

4.3 Field management information

4.3.1 Record of field management activities

Details of the management activities, which occurred during the measurement period at Easter Bush, are recorded in Table 4.3 and details of the history of the site over the preceding period are given in Table 4.4. The information was obtained from the farm manager. The fields are usually cut twice for silage and receive between 270-320 kg N ha^{-1} yr^{-1}. In 1998 both fields received 273 kg N ha^{-1} and in 1999 the S field received 312 kg N ha^{-1}, while the N field received 260 kg N ha^{-1}. In July 1999 the grass in the N field was not considered of sufficient quality for silage due to previous wet weather and so it did not receive a second cut, but was grazed by heifers from 28/7/99.

Table 4.3. Management details at Easter Bush field site for the duration of the measurements

Event	N field: Date	N supply kg N ha^{-1}	S field: Date	N supply kg N ha^{-1}
1998				
Fertilising	28/3/98	104[a]	28/3/98	104[a]
Cutting	5/6/98 08:00-11:00		5/6/98 08:00-11:00	
Removing grass	13/6/98 09:00-11:30		8/6/98 09:30-11:00	
Fertilising	13/6/98 15:00-16:00	104[a]	9/6/98 10:20-11:30	104[a]
Cutting	31/7/98 14:35-16:35		28/7/98 18:45-20:15	
Removing grass	2/8/98 15:45-17:15		2/8/98 12:00-13:30	
Fertilising	5/8/9 10:20-11:30	65[a]	5/8/98 15:20-16:30	65[a]
Grazing started	10/8/ 98		10/8/98	
Total N supply		**273**		**273**
1999				
Fertilising	4/4/99 pm	117[a]	4/4/99 pm	117[a]
Cutting	2/6/99		2/6/99	
Removing grass	9/6/99		9/6/99	
Fertilising	11/6/99 16:00	91[a]	11/6/99 16:00	91[a]
Fertilising	18/7/99	52[b]	18/7/99	52[b]
Cutting	N field not cut		28/7/99 13:00-14:10	
Fertilising			2/8/99	52[b]
Grazing started	28/7/99		9/8/99	
Total N supply		**260**		**312**
Urea application for testing REA	Only in S field		12/11/99 10:30-10:45	47[c]

[a]Fertiliser applied: Kemira N-P-K (26-5-10) , total N: 26%
[b]Fertiliser applied: Nitram (NH_4NO_3), total N: 34.5%
[c]Fertiliser applied: Urea ($CO(NH_2)_2$) , total N: 47%

Table 4.4. Management details at Easter Bush over a longer period

	N field and S field
Age of grassland	Approximately 15 years
Details of crops in the 2-3 years before field became grassland	Crop for 1 year and grass before that
Details of grassland management over the years	Similar to measurement years, silage for first part of the year followed by grazing afterwards
Number of cuts, yield per cut or per year.	2 cuts per year 25-30 t ha^{-1} yr^{-1} silage of 25-30% dry matter usually approx. 15 t ha^{-1} yr^{-1} in the 1st cut 10 t ha^{-1} yr^{-1} in the 2nd cut
Fertilisation details over the last 10 years. Total kg N ha^{-1} yr^{-1}	Similar every year 1) Kemira N-P-K compound fertiliser in late March/early April, usually about 100 kg N ha^{-1} 2) Kemira N-P-K compound fertiliser after 1st cut, usually about 100 kg N ha^{-1} 3) Kemira N-P-K compound fertiliser after 2nd cut, usually about 70 kg N ha^{-1} 4) Possibly an extra small boost of NH_4NO_3 in Aug. of approx 50 kg N ha^{-1} (it is thought unnecessary to apply P and K at this point).

4.3.2 Animal numbers

The two fields that form the measurement site are part of a wider network of fields owned by Easter Bush farm (see Fig. 3.2). The measurement fields were grazed, after cutting for silage, in rotation with the other farm fields. Usually dairy cattle are put on the fields soon after the silage cut to get the new-growth, richer grass, and then sheep are grazed later. A record of the grazing was kept and this is shown in Figs. 4.16-4.19 for the two fields and the two field seasons. This record can only give an indication of the grazing numbers and pattern as observations are not available for days when the field site was not visited, e.g. at the weekends. In 1998 the dairy herd (approx. 50 cows) grazed the S field for the latter half of August and then were moved to the N field (Figs. 4.16 - 4.17). The dairy herd were usually on the field between 6:30-14:30 GMT then kept near the farm overnight. Grazing by sheep continued from August 1998-January 1999 and then ceased until after the silage cuts in summer 1999. In 1999, the N field was grazed by heifers from 28th July until the

end of August and the dairy herd grazed the N field in September and the S field in October (Figs. 4.18 - 4.19).

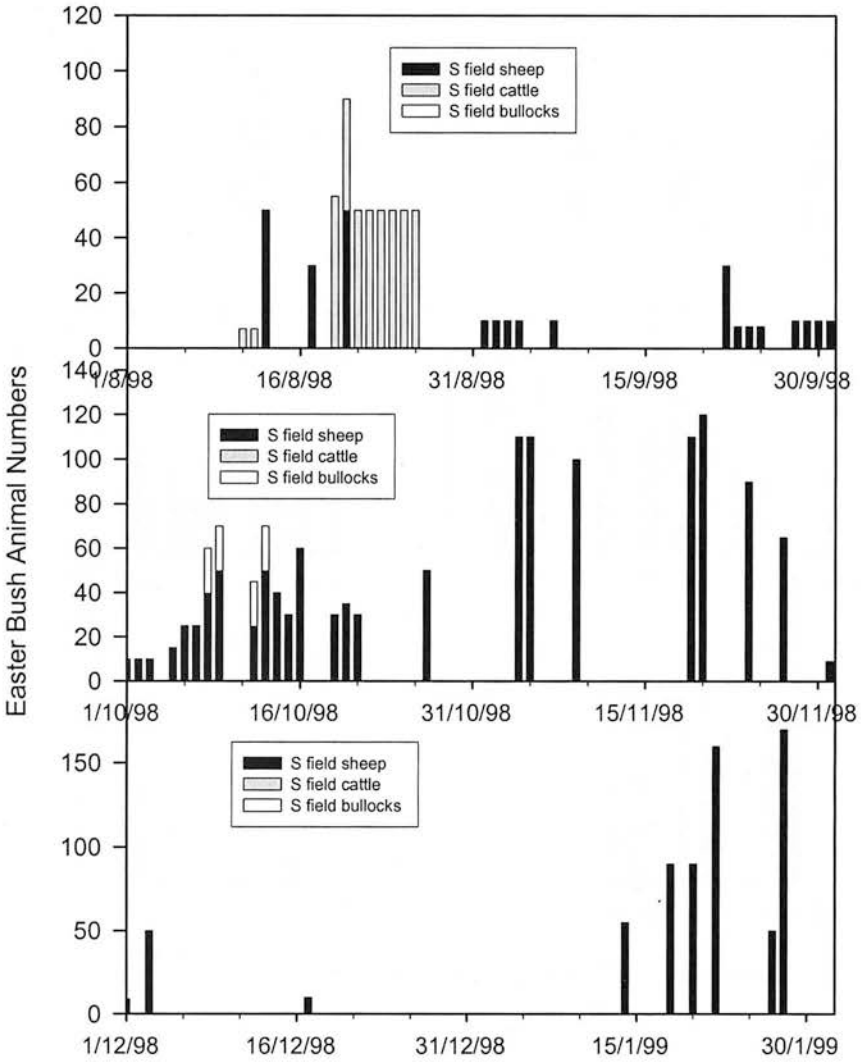

Figure 4.16. Animal numbers for the S field after the 2nd cut in 1998 and Jan 1999. The value given is an average number for each day. The duration of dairy cattle on the field site was usually 07:00-14:00 GMT each day. The duration of sheep was more random due to gates being left open between the N and S field and between other fields. The values given are for positive observations only, observations are not available for days when the field site was not visited. e.g. at the weekends.

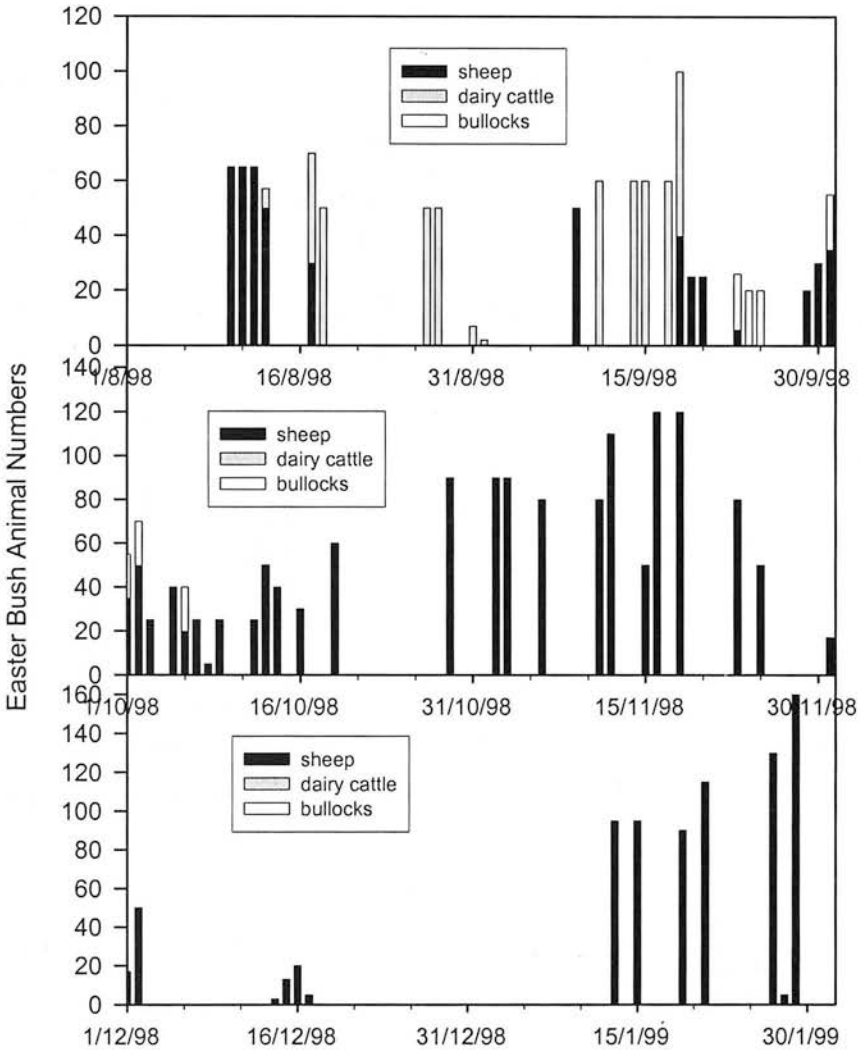

Figure 4.17. Animal numbers for the N field after the 2nd cut in 1998 and Jan 1999.

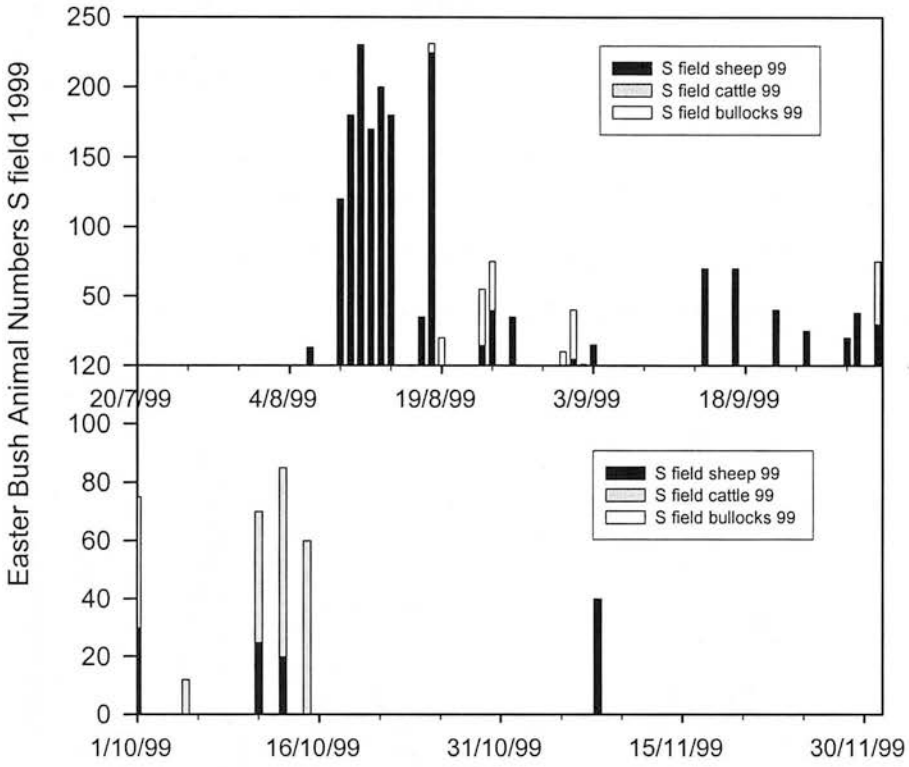

Figure 4.18. Animal numbers for the S field after the 2nd cut in 1999

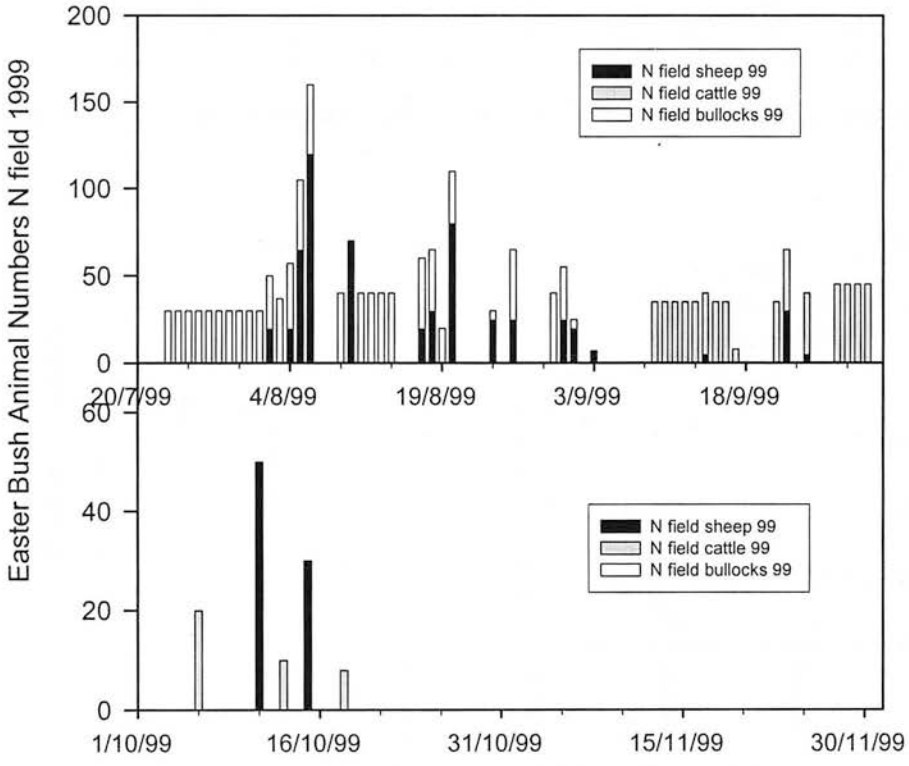

Figure 4.19. Animal numbers for the N field in 1999.

4.4 Vegetation measurements

4.4.1 Sward productivity

Measurements of the mean, minimum and maximum canopy height were taken every few days throughout the measurement period. The mean values for the S field are shown in Fig. 4.20. Leaf Area Index was measured at monthly periods or more frequently at times of cutting. The results for 1999 are given in Fig. 4.21.

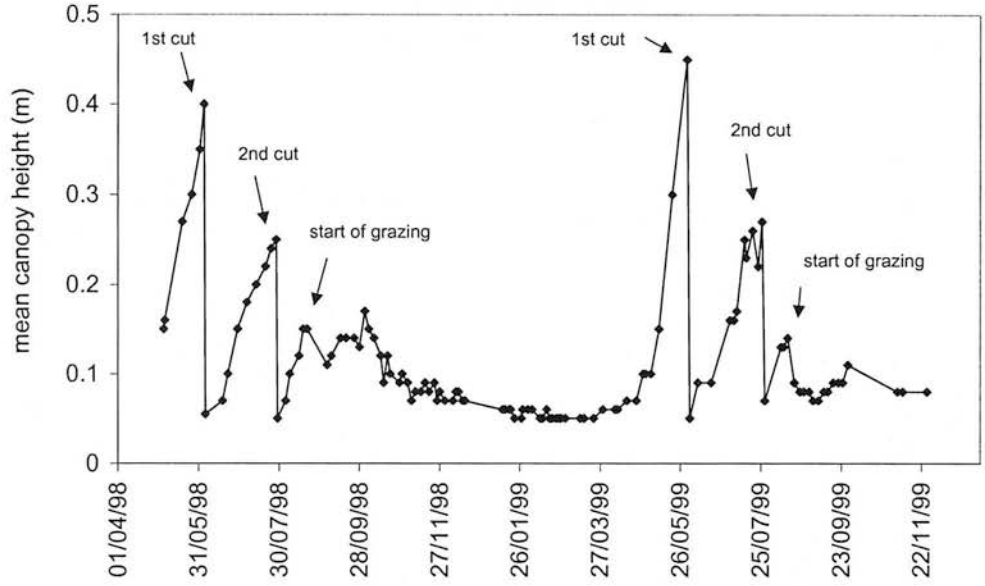

Figure 4.20. Mean canopy height for S field throughout whole measurement period.

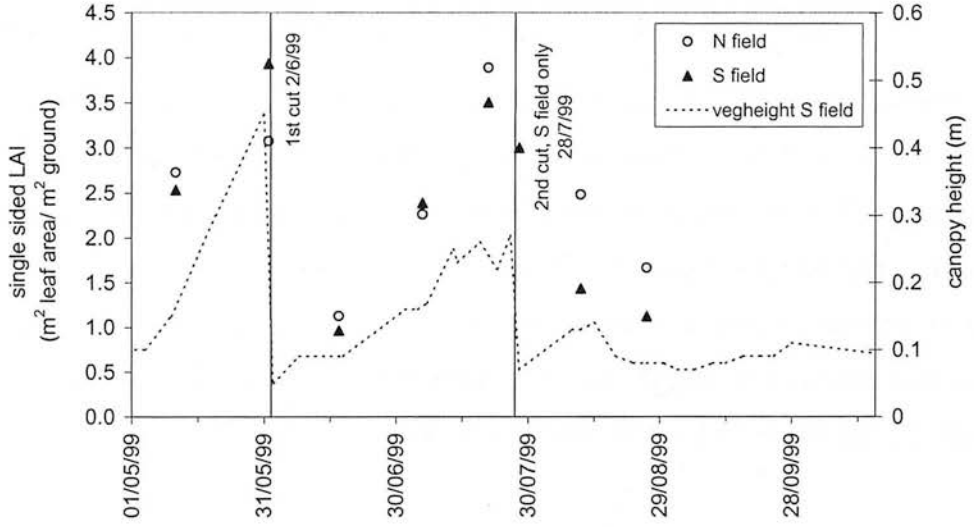

Figure 4.21. Leaf Area Index (LAI) for the two fields shown alongside mean canopy height.

4.4.2 *Total foliar nitrogen and carbon content*

Total foliar nitrogen and carbon content is shown in Fig. 4.22 for the N and S fields for the period 1/4/99-2/9/99. It can be seen that the S field has a consistently higher N content than the N field but that the seasonal variation is similar for both fields. After the second fertilisation on the S field (2/8/99), when the N field is not fertilised, the N content increases by a greater amount on the S field than on the N field, (ratio of N content, S field: N field, changes from 1.23 on 27/7/99 to 1.83 on 11/8/99). The C content of both fields is similar and does not demonstrate a large seasonal pattern.

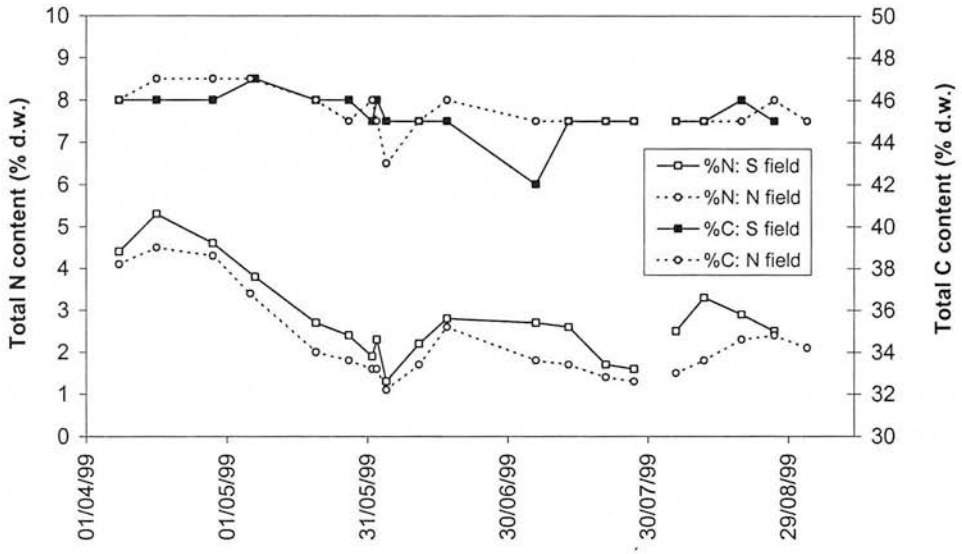

Figure 4.22. Total foliar nitrogen and carbon content for both fields during the period 1/4/99-2/9/99.

4.4.3 *Apoplastic ammonium and pH and foliar ammonium*

The apoplastic NH_4^+ concentration ($[NH_4^+]_{apo}$) and total foliar ammonium concentration ($[NH_4^+]_{fol}$) for *Lolium perenne* at Easter Bush from May 1998 to October 1998 are presented in Figs. 4.23 and 4.24, respectively. These measurements were conducted by Dr. Benjamin Loubet and are reported by Loubet *et al.* (2002) (see Appendix A1). The foliar NH_4^+ measurements include measurements made on the same leaves used to measure apoplastic NH_4^+ (green leaves) and also segments of older leaves (yellow-green leaves), which were not analysed for aploplastic NH_4^+ (see Loubet *et al.*, 2002).

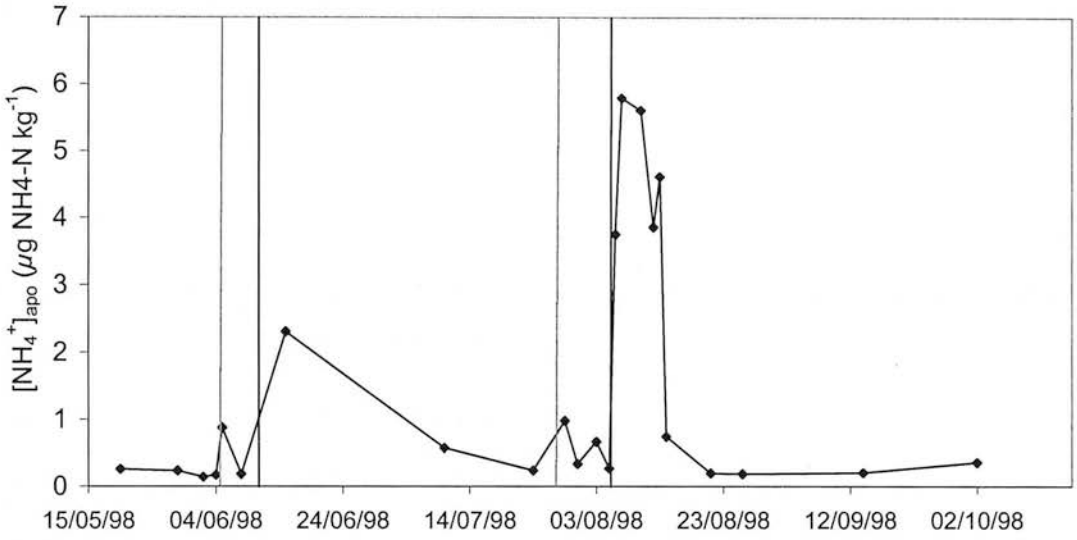

Figure 4.23. Apoplastic ammonium concentration for *Lolium perenne* at Easter Bush S field during the period 25/5/98-2/10/98 (from Loubet *et al.*, 2002). Vertical lines indicate cutting (grey lines) and fertilisation (black lines). For dates and amounts of fertiliser input see Table 4.3.

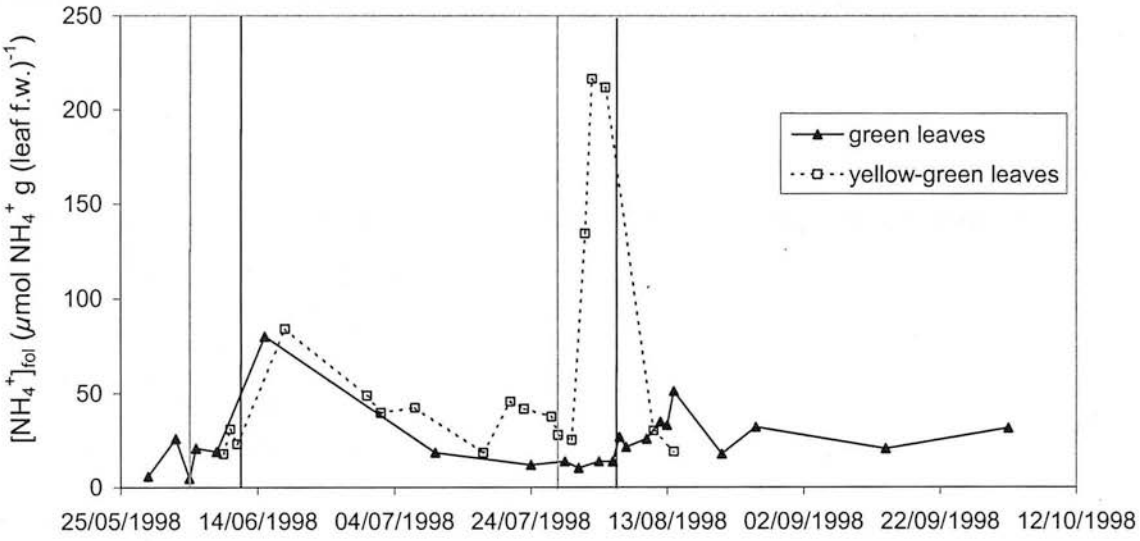

Figure 4.24. Total foliar ammonium content for *Lolium perenne* at Easter Bush S field during the period 25/5/98-2/10/98 (from Loubet *et al.*, 2002). Vertical lines indicate cutting (grey lines) and fertilisation (black lines). For dates and amounts of fertiliser input see Table 4.3.

Significant variation is observed in both apoplastic and foliar NH_4^+ concentration during the season. However, significant changes in apoplastic NH_4^+ are only observed after the fertilisation events, although there may be some evidence of a small increase immediately after cutting. Foliar NH_4^+, does however, increase substantially after the second cut and before the fertilisation. Both apoplastic and foliar NH_4^+ concentration are larger after the second cut and fertilisation than after the first.

4.5 Soil measurements

4.5.1 One-off measurements

Soil texture

The soil particle size distribution was determined at Easter Bush for two soil depths in both the S and N field, the results are given in Table 4.5. The soil is classified as a sandy clay loam according to these results.

Table 4.5. Easter Bush soil particle size distribution

Soil layer depth	Clay (%)	Silt (%)	Sand (fine) (%) 20- 200 μm	Sand (coarse) (%) 200 μm – 2 mm
S field				
0 - 0.15 m	21	17	37	17
0.15 - 0.3 m	23	16	36	17
N field				
0 - 0.15 m	19	20	38	20
0.15 - 0.3 m	20	15	38	20

Bulk density

The bulk density at Easter Bush was determined for the S field at four soil depths. The results are given in Table 4.6.

Table 4.6. Easter Bush soil bulk density

Soil layer depth	Bulk density (g dry soil cm^{-3})
0 - 0.05 m	0.95
0.05 - 0.1 m	1.22
0.1 – 0.15 m	1.13
0.15 –0.2 m	1.03

Soil organic nitrogen and carbon

The soil organic nitrogen and carbon content was determined at Easter Bush for two soil depths in both the S and N field, the results are given in Table 4.7.

Table 4.7. Easter Bush total N and organic C

Soil layer depth	Total N (%)	Organic C (%)
S field		
0 - 0.15 m	0.23	3.3
0.15 - 0.3 m	0.20	3.2
N field		
0 - 0.15 m	0.23	3.1
0.15 - 0.3 m	0.19	3.5

4.5.2 Soil ammonium and nitrate

Measurements of available soil ammonium (NH_4^+) and nitrate (NO_3^-) in the S and N field were conducted fortnightly and more frequently after management events. These data are shown in Figs. 4.25 - 4.28 for the whole measurement period.

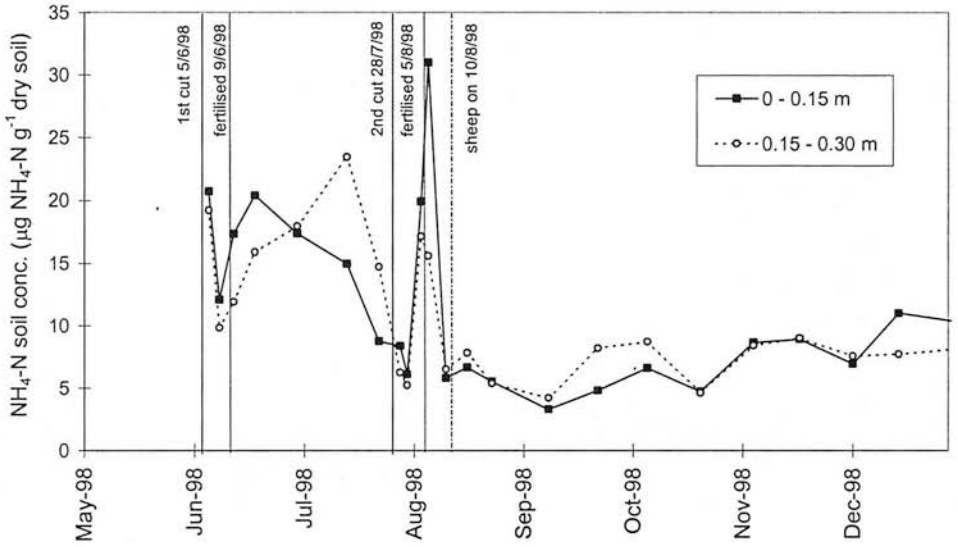

Figure 4.25. Available soil NH_4^+ at two depths for 1998, data is averaged for the N and S field. Timing of cutting, fertilisation and grazing are indicated by vertical lines.

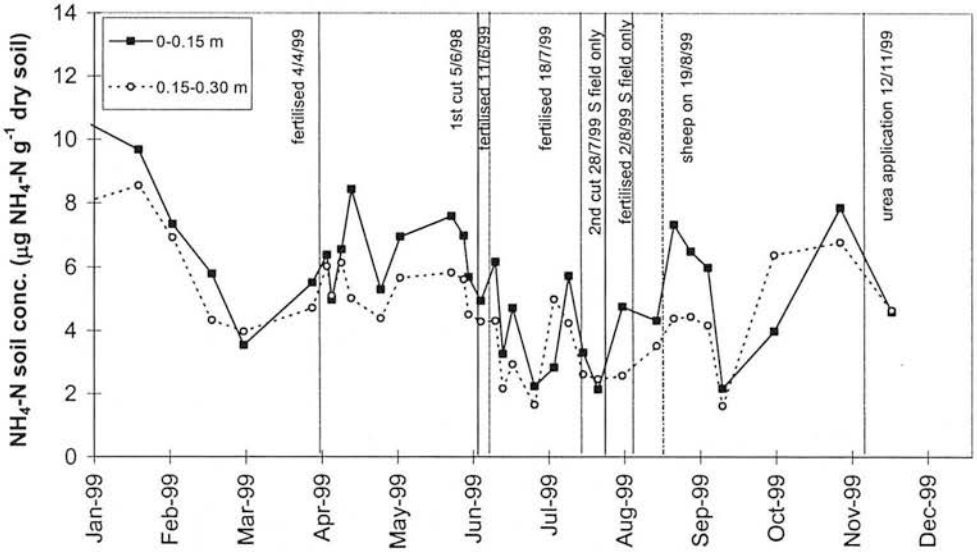

Figure 4.26. Available soil NH_4^+ at two depths for 1999, data is averaged for the N and S field. Timing of cutting, fertilisation and grazing are indicated by vertical lines.

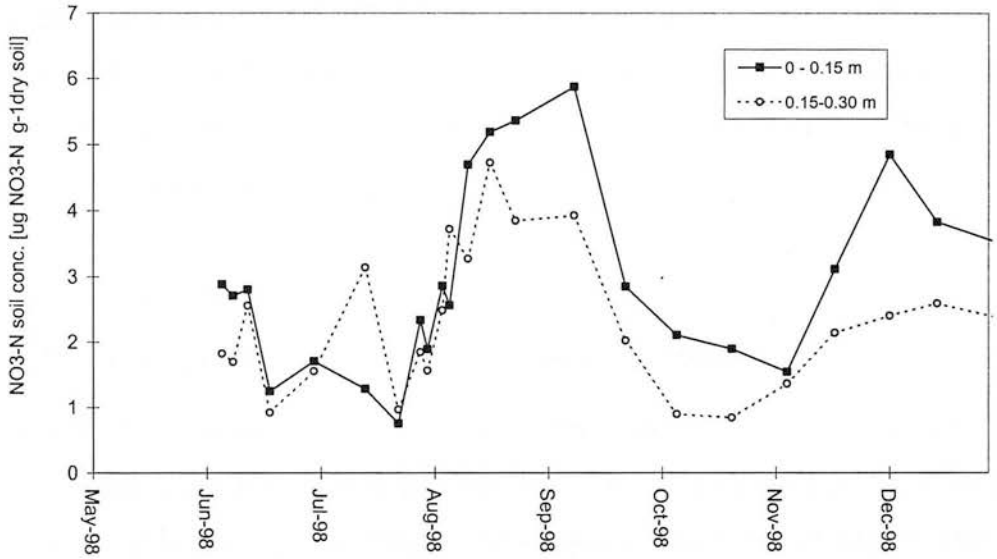

Figure 4.27. Available soil NO_3^- at two depths for 1998, data is averaged for the N and S field.

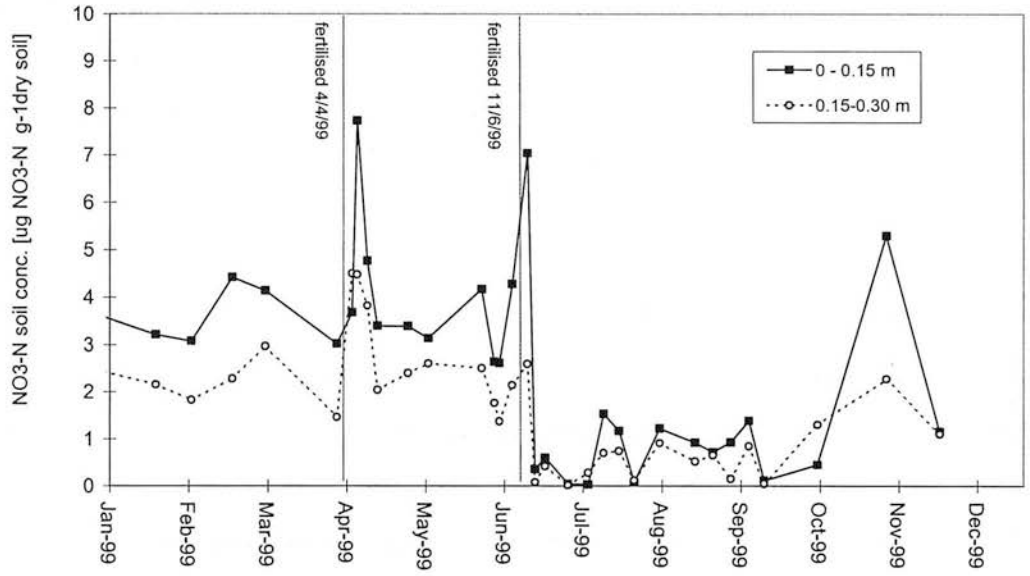

Figure 4.28. Available soil NO_3^- at two depths for 1999, data is averaged for the N and S field.

Seasonal variation is observed in the soil NH_4^+ and NO_3^-. Soil NH_4^+ is greater in the first half of the season and then declines in late August in 1998, while NO_3^- reaches a peak in August and September 1998, this may indicate increased nitrification. Between June-September 1999, soil NO_3^- decreases to very low values, it is not certain what is the cause for this, whether this is real variation in the field or measurement uncertainty.

4.6 Discussion

4.6.1 Inter-comparisons of meteorological parameters

The inter-comparisons of meteorological parameters enabled the quality of the measurements to be assessed and provided a fuller data coverage (91%) as data gaps could be filled. It is particularly useful to have as full a meteorological dataset as possible for modelling purposes. The comparison of u_* and H obtained by the eddy covariance and aerodynamic gradient method was reasonable. It is likely that uncertainty in the wind speed profiles contributed to a large part of these differences.

4.6.2 Site characterisation

The wind frequency distribution demonstrates the wind is predominantly from the SW (69 % of the time) and otherwise is from the NE. Winds along the boundary of the two fields are uncommon, largely due to the channeling effect of the Pentland Hills (see Fig. 3.2). This, along with a generally windy site (mean monthly wind

speeds mostly above 3 m s^{-1}) results in the fetch being sufficient for flux measurements at this site for most of the time. The cumulative normalised footprint (CNF) was > 65% for 82% of the time. This reflects the location and the meteorology of this site.

4.6.3 Vegetation and soil measurements

The vegetation and soil measurements are essential for interpreting NH_3 measurements and also provide either input data for models or data for assessing model performance. Without good quality interpretative data, the NH_3 measurements themselves are less useful as NH_3 exchange varies with many parameters. The foliar N and NH_4^+ and apoplastic NH_4^+ measurements show interesting variation, which will be examined in more detail along with NH_3 exchange measurements in the subsequent chapters. Bioassay measurements of apoplastic and foliar NH_4^+ are still scarce alongside field measurements of NH_3 exchange due to the effort and expertise required. It would be useful to repeat the measurements with a higher frequency before and after cutting and fertilising events to further examine the variation in these plant parameters. The changes in soil mineral N induced by fertilisation were much smaller in 1999 than in 1998, according to the soil analysis, but there is no obvious explanation for this.

Chapter 5: Measurements at Easter Bush: Long-term ammonia concentrations and fluxes

5.1 Ammonia concentrations

Concentrations of gaseous ammonia were measured semi-continuously at Easter Bush for 19 months at three heights above the grass canopy. The two lowest measurement heights varied according to the height of the canopy while the top measurement height remained at 2.06 m above ground. An example of the data collected is given in Fig. 5.1, which presents 15-minute average NH_3 concentrations at the three heights for the month of June 1998.

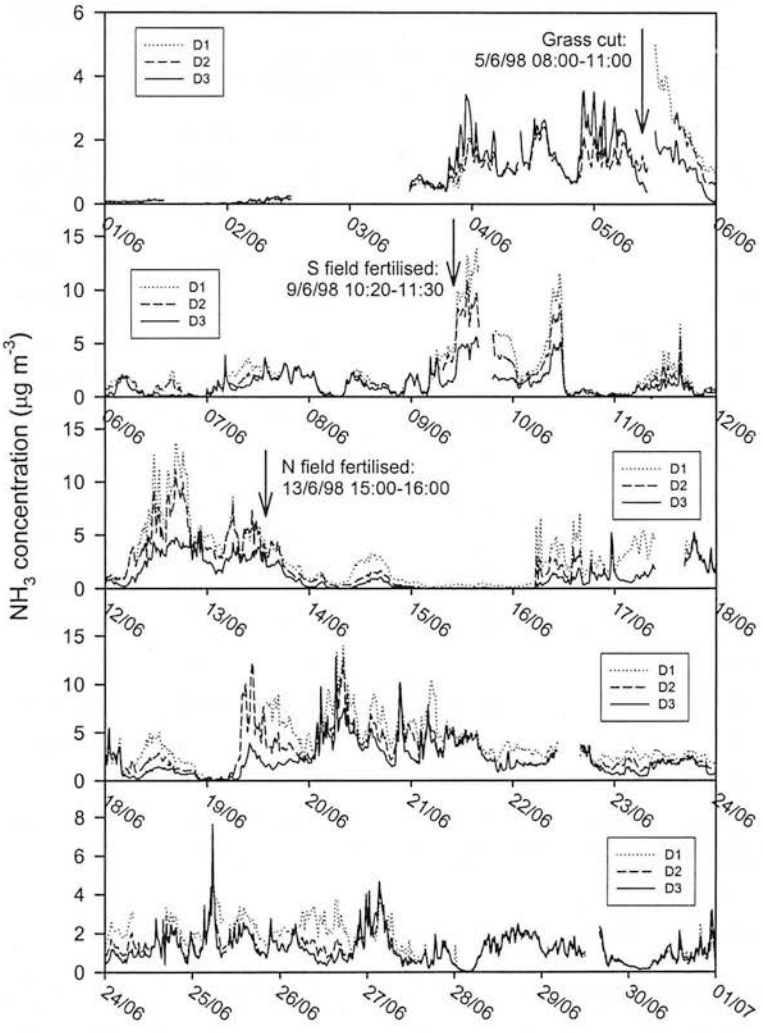

Figure 5.1. NH_3 concentration (15-minute averaging period) at Easter Bush measured at three heights during June 1998. Top height (D3) = 2.06 m, middle height (D2) varied between 0.79-0.94 m and lowest height (D1) varied between 0.45-0.55 m, all heights are above ground.

Fig. 5.1 demonstrates the high temporal resolution of the NH_3 concentration data, which enables the controls on the diurnal and seasonal variations in concentration and flux to be explored. The two measurement fields were both cut on 5/6/98 while the S field and N field were fertilised on 9/6/98 and 13/6/98, respectively (see Table 4.3). The response of the gradient of NH_3 concentration to these management treatments can be seen in Fig. 5.1. For example, prior to 5/6/98, NH_3 concentration was largest at the top measurement height, while during 5/6/98 the gradient switched to larger concentrations close to the canopy. The statistical variations in 15-minute mean NH_3 concentrations at the top height (2.06 m) are given in Table 5.1.

Table 5.1. Statistics of 15-minute mean NH_3 concentrations at Easter Bush, measured at the top height (2.06 m), *n*: number of 15-minute values, μ_A: arithmetic mean, μ_G: geometric mean, σ_G: geometric standard deviation

Month	n	data coverage (%)	Median $\mu g\ m^{-3}$	μ_A $\mu g\ m^{-3}$	μ_G $\mu g\ m^{-3}$	σ_G $\mu g\ m^{-3}$	Min $\mu g\ m^{-3}$	Max $\mu g\ m^{-3}$
May-98	2223	74.7	0.55	1.01	0.57	3.39	0.10	13.67
Jun-98	2595	90.1	1.12	1.43	0.73	4.59	0.00	12.79
Jul-98	2315	77.8	0.78	1.12	0.68	3.78	0.00	9.14
Aug-98	2212	74.3	1.37	1.50	1.10	2.77	0.00	8.34
Sep-98	1620	56.3	0.84	1.16	0.95	3.93	0.00	13.96
Oct-98	1401	47.1	0.65	1.40	0.59	5.25	0.00	32.58
Nov-98	1240	43.1	0.81	1.10	0.43	4.95	0.00	6.28
Dec-98	959	68.1[a]	0.75	1.15	0.67	3.33	0.03	15.35
Jan-99	1656	92.8[a]	0.50	0.89	0.51	3.41	0.00	11.61
Feb-99	1507	56.1	1.37	1.76	1.20	2.86	0.00	17.24
Mar-99	2115	71.1	1.72	2.51	1.56	3.12	0.04	28.54
Apr-99	2252	78.2	0.96	1.51	0.83	3.98	0.00	16.94
May-99	2553	85.8	0.99	1.51	0.94	3.03	0.01	21.19
June-99	2797	97.1	1.30	1.49	0.92	3.20	0.01	15.16
July-99	2459	82.6	0.92	1.22	0.85	2.65	0.01	11.58
Aug-99	2342	78.7	2.26	2.89	2.26	2.17	0.05	23.79
Sept-99	2061	71.6	1.22	1.35	1.51	2.46	0.06	17.47
Oct-99	2294	77.1	1.46	2.10	1.27	3.40	0.00	12.09
Nov-99[b]	948	90.8	0.47	0.81	1.13	3.44	0.01	33.40
Whole Period[c]	37549	73.6	1.07	1.52	0.90	3.63	0.00	33.40
Whole Period[d]	38616	73.8	1.10	1.65	0.94	3.76	0.00	41.16

[a]Data coverage not including switch off period (15/12/98 16:30-13/1/99 10:00)
[b]1/11/99 00:00-12/11/99 00:00 (not including period after urea application on 12/11/99)
[c]1/5/98 00:00-12/11/99 00:00 (not including period after urea application)
[d]1/5/98 00:00-21/11/99 13:00 (including period after urea application)

On 12/11/99, 100 kg ha^{-1} of urea (equivalent to 47 kg N ha^{-1}) was applied on the S field (see Table 4.3 and section 5.3.6). This was a deliberate measure to provide emissions of NH_3 as a field test for a newly developed relaxed eddy accumulation (REA) system for NH_3 (Nemitz *et al.*, 2001a). The application of urea at this time was not part of the normal management of these fields and was arranged with the farm manager as an additional treatment. For this reason the statistical variations in 15-minute mean NH_3 concentrations and other analysis throughout this chapter distinguishes between measurements including and excluding the period after urea application.

The median, arithmetic mean and geometric mean NH_3 concentration for the whole measurement period (1/5/98 00:00-12/11/99 00:00), excluding the period after urea application, were 1.07, 1.52 and 0.90 μg m^{-3}, respectively. The maximum concentration for the whole measurement period, excluding the period after urea application, was 33.4 μg m^{-3}, this occurred on 11/11/99 at 01:15. Concentrations increased after the application of urea on 12/11/99 (see section 5.3.6) and reached a maximum of 59.9 and 41.2 μg m^{-3} at the lowest and highest measurement level, respectively, on 14/11/99 at 18:00.

The monthly arithmetic mean concentration and the monthly maximum concentration for the top measurement level (2.06 m) are presented in Fig. 5.2. These data do not show a clear seasonal cycle. The highest arithmetic mean concentrations are observed in March, August and October 1999. The high value for March 1999 may be related to spreading of fertiliser and other land-spreading of manures in the surrounding area. The high values in August and October 1999 may be related to the high grazing density at the field site in these months, creating a strong local source of NH_3.

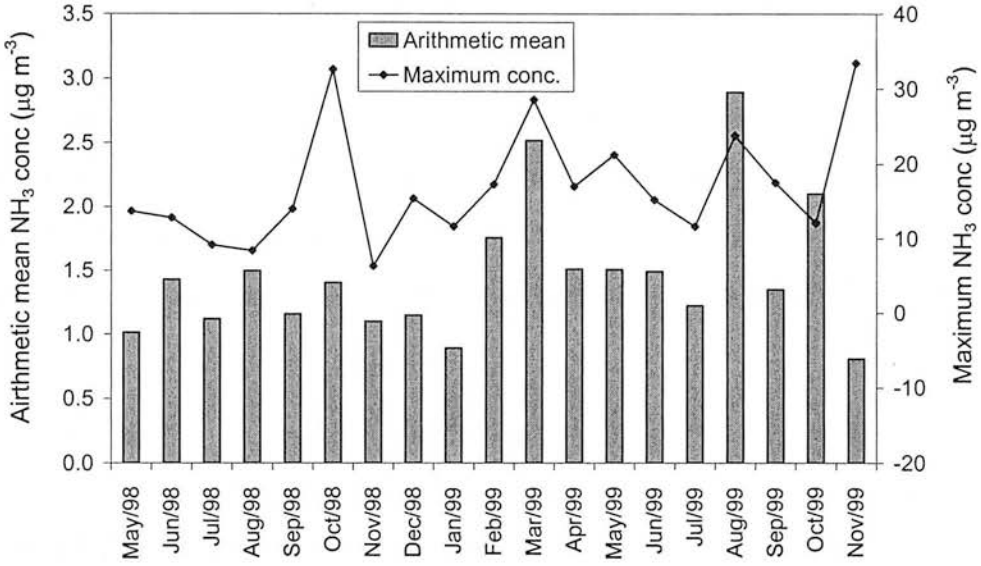

Figure 5.2. Monthly arithmetic mean and monthly maximum of NH_3 concentration at Easter Bush measured at the top height (2.06 m).

There is a slightly stronger seasonal cycle in the geometric mean NH_3 concentration (Fig. 5.3) with peaks occurring in August 98, February, March, August and September 1999. Aside from the months of February and March 99, when concentrations were probably affected by manure spreading on other fields, and the period of grazing (August –Nov 1999), there is a general increase of NH_3 concentration in summer and a decrease in winter months.

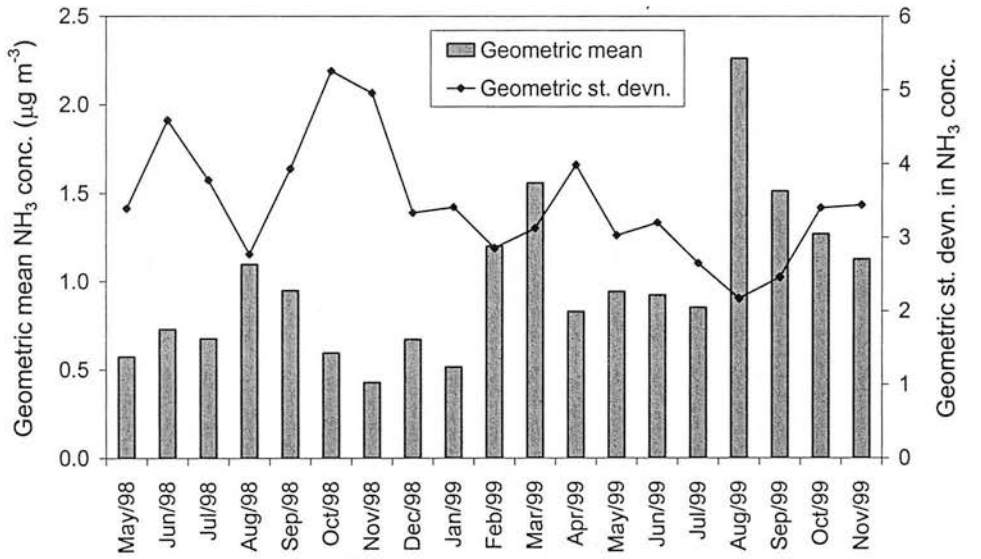

Figure 5.3. Monthly geometric mean and geometric standard deviation in NH_3 concentration at Easter Bush measured at top height (2.06 m).

The geometric mean concentration is less influenced by outlier concentrations than the arithmetic mean and therefore provides a clearer indication of the seasonal

changes in the local background NH_3 concentrations. The geometric standard deviation (σ_G) is a measure of the fluctuation in concentration and is often interpreted as an indication of the nearness to sources (Fowler and Cape, 1982; Burkhardt *et al.*, 1998). The geometric standard deviation in NH_3 concentration at the top height varied between 2.17 and 5.25 $\mu g\ m^{-3}$, peaking in October 1998 (Fig. 5.3) indicating a high variability in concentrations and/or in wind direction for that month.

The statistical variations in concentrations are similar for the middle and lowest measurement heights (data not shown). The frequency distribution of 15-minute mean NH_3 concentration at each height is shown in Figs. 5.4-5.6, all three distributions are slightly skewed towards lower concentration values, compared with a lognormal distribution, which indicates the importance of non-zero background NH_3 concentrations.

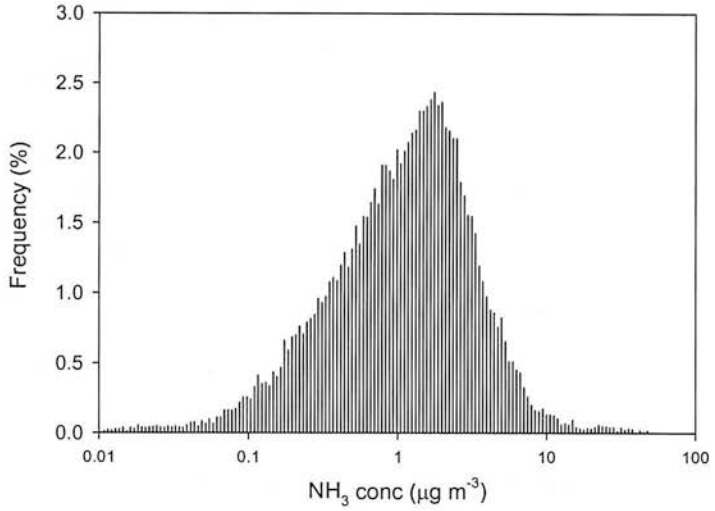

Figure 5.4. Frequency distribution of 15-minute mean NH_3 concentration at the lowest height, which varied between 0.35-0.8 m above ground.

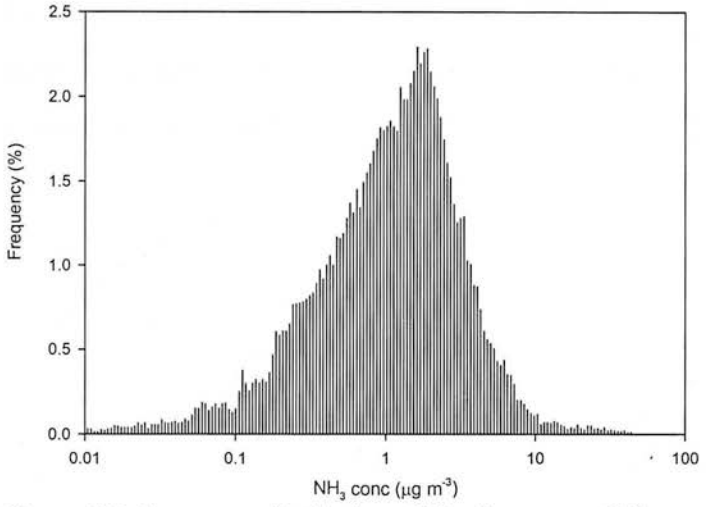

Figure 5.5. Frequency distribution of 15-minute mean NH_3 concentration at the middle height, which varied between 0.79-1.21 m above ground.

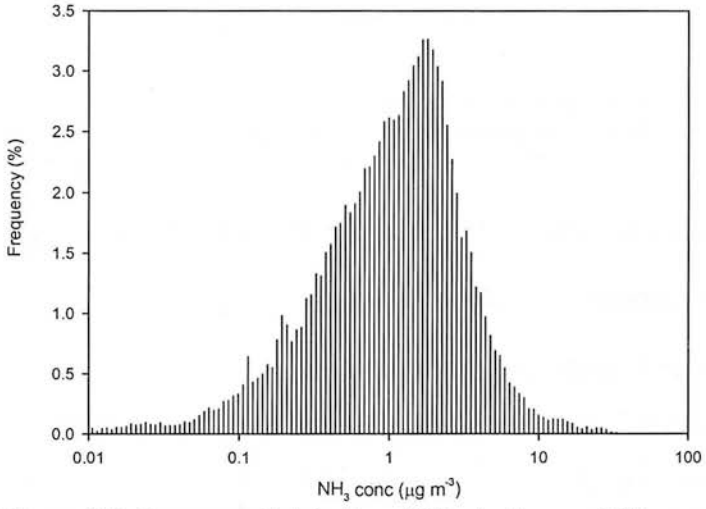

Figure 5.6. Frequency distribution of 15-minute mean NH_3 concentration at the top height (2.06 m).

The variation in NH_3 concentration with wind direction, for each measurement height, is presented in Fig. 5.7 for the whole measurement period, excluding the period after urea application. Data are only shown for 10° sectors with wind frequency > 1.25% to avoid showing unrepresentative conditions; the frequency of wind directions is shown in Fig. 4.9b. Fig. 5.7 clearly demonstrates the influence of Easter Howgate farm (located at 240°, see Fig. 3.2) on the NH_3 concentrations. At 240° the mean concentration at the 3 heights = 2.3 μg m^{-3}, while at 30° the mean concentration at the 3 heights = 1.0 μg m^{-3}, indicating the existence of few NH_3 sources from this direction, as has been observed previously (Burkhardt *et al.*, 1998). Interestingly, the concentration at the lower heights are greater than that at the highest height for wind directions 180°-230°, indicating that the measurement fields themselves are often the main source determining the concentration of ammonia in these wind directions.

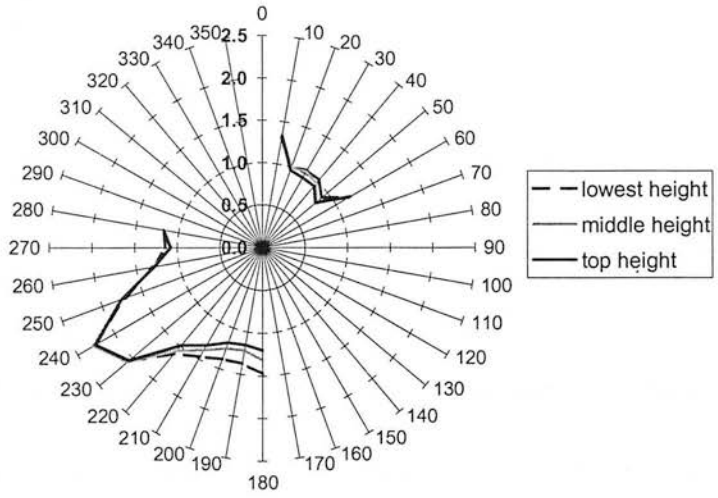

Figure 5.7. Distribution of NH_3 concentration at the three measurement heights with wind direction for windspeeds > 0.5 m s^{-1}, for the whole measurement period (1/5/98 00:00-12/11/99 00:00). Data are only shown for sectors with wind frequency > 1.25%.

5.2 Ammonia exchange: continuous time course

5.2.1 Effect of filtering on ammonia exchange data

Ammonia fluxes were measured at Easter Bush for a semi-continuous period of 19 months using the aerodynamic gradient method as described in section 2.2. Ammonia fluxes were filtered according to the micrometeorological criteria listed in Section 4.2.3 (flux data rejected for: wind directions 130°-150° and 305°-315°,

CNF< 65%, $|L| < 2$ m and $u(1\text{ m}) < 0.5$ m s^{-1}). The flux data, which do not pass the micrometeorological criteria, are more uncertain due to the unreliability of the flux measurement technique in very unstable or stable conditions. However, the flux measurements during extremely stable conditions are usually of small magnitude because values of u_* are small and fluxes are suppressed by the absence of turbulence. Although, the relative error in the flux measurement is large, the absolute error is usually small and it can be argued that removing this data biases the dataset towards daytime flux measurements, which often show larger flux values.

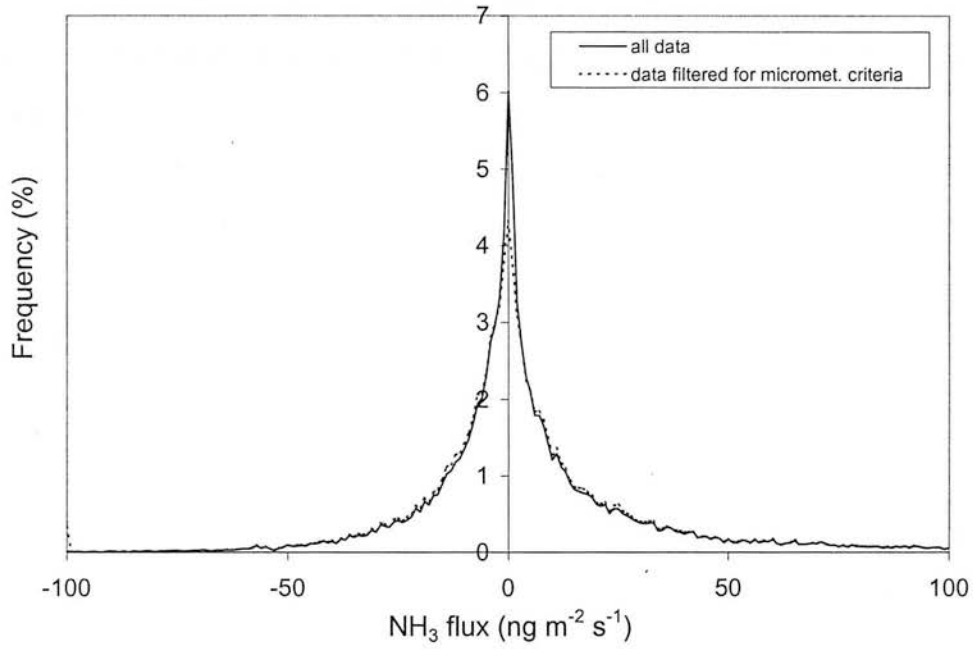

Figure 5.8. Frequency distribution of 15-minute mean NH_3 flux measurements.

The frequency distribution of the 15-minute mean flux values (Fig. 5.8) demonstrates that the data which has been filtered for the micrometeorological criteria does indeed have a decreased proportion of fluxes of smaller magnitude compared with the full dataset, while the frequency distributions for larger flux values are largely similar. Fig. 5.8 demonstrates that there is a fairly equal frequency of emission (+ve) and deposition (-ve) fluxes, although the slightly greater frequency of positive fluxes leads to the median flux of the whole measurement period being +0.50 ng m^{-2} s^{-1} (for filtered data) (Table 5.2).

The statistical variations in 15-minute mean NH_3 flux measurements are given on a monthly basis in Table 5.2 for all available data. Also presented are the results after

filtering the flux data according to the micrometeorological criteria listed above. The median and mean flux over the whole measurement period, excluding the period after urea application, do increase in the filtered dataset compared with the unfiltered dataset, from 0.23 ng m^{-2} s^{-1} (unfiltered) to 0.50 ng m^{-2} s^{-1} (filtered) for the median flux and 13.9 ng m^{-2} s^{-1} (unfiltered) to 14.9 ng m^{-2} s^{-1} (filtered) for the mean flux (Table 5.2), demonstrating that filtering the data does lead to slightly larger flux estimates. The data coverage of NH_3 fluxes for the whole period, including the period after urea application, is reduced from 70.9% to 62.6% by the micrometeorological filtering. The period 15/12/98 16:30 - 13/1/99 10:00 was not included in this calculation of data coverage as the NH_3 analyser was switched off at this time.

Table 5.2. Statistics of 15-minute mean NH_3 flux measurements, before and after filtering for micrometeorological criteria (data rejected for: wind directions 130°-150° and 305°-315°, CNF< 65%, $|L| < 2$ m and $u(1\text{ m}) < 0.5$ m s^{-1}, see section 4.2.3), n: number of 15-minute values.

Period		n	Data coverage (%)	Median ng m^{-2} s^{-1}	Mean ng m^{-2} s^{-1}	Stdev ng m^{-2} s^{-1}	Min ng m^{-2} s^{-1}	Max ng m^{-2} s^{-1}
May-98	All data	2168	72.8	-1.41	-6.91	21.11	-588.2	79.0
	Filtered	1930	64.9	-1.67	-7.16	21.46	-588.2	79.0
Jun-98	All data	2616	90.8	29.54	82.91	160.55	-135.5	2064.3
	Filtered	2305	80.0	34.38	87.42	165.11	-82.2	2064.3
Jul-98	All data	2289	76.9	-5.69	-8.25	21.44	-173.0	261.5
	Filtered	2069	69.5	-6.32	-8.93	21.13	-173.0	261.5
Aug-98	All data	2197	73.8	2.26	7.74	36.52	-848.7	198.3
	Filtered	1991	66.9	2.80	8.55	37.51	-848.7	198.3
Sep-98	All data	1986	69.0	1.49	2.90	20.56	-322.8	112.2
	Filtered	1537	53.4	2.76	4.16	19.82	-322.8	88.6
Oct-98	All data	1376	46.2	0.41	-1.84	26.90	-391.5	84.2
	Filtered	1176	39.5	1.34	-0.58	24.11	-275.7	84.2
Nov-98	All data	1355	47.0	4.62	7.92	16.79	-80.6	109.8
	Filtered	1084	37.6	7.83	9.58	18.21	-80.6	109.8
Dec-98	All data	1002	33.7	4.32	6.96	21.34	-257.9	145.1
	Filtered	847	28.5	6.54	8.31	22.62	-257.9	145.1
Jan-99	All data	1655	55.6	-4.97	-9.32	15.68	-135.1	36.0
	Filtered	1598	53.7	-5.32	-9.58	15.86	-135.1	36.0
Feb-99	All data	1727	64.2	-3.13	-9.19	44.02	-474.7	221.4
	Filtered	1578	58.7	-3.39	-9.79	45.25	-474.7	221.4
Mar-99	All data	2084	70.0	-2.68	-7.09	22.89	-271.6	99.5
	Filtered	1888	63.4	-3.26	-7.40	23.22	-271.6	99.5
Apr-99	All data	2032	70.6	5.38	12.09	47.41	-924.7	331.8
	Filtered	1730	60.1	7.35	14.43	50.14	-924.7	331.8
May-99	All data	2189	73.6	-5.17	-7.32	11.86	-135.4	51.6
	Filtered	2082	70.0	-5.56	-7.54	12.04	-135.4	51.6
June-99	All data	2612	90.7	13.71	77.89	187.10	-132.6	1619.8
	Filtered	2264	78.6	14.99	84.60	198.08	-130.2	1619.8
July-99	All data	1874	63.0	-5.46	-7.71	18.42	-255.1	122.3
	Filtered	1780	59.8	-5.82	-7.99	18.71	-255.1	122.3
Aug-99	All data	1805	60.7	24.86	40.94	48.59	-91.8	361.5
	Filtered	1697	57.0	25.89	42.41	49.17	-91.8	361.5
Sept-99	All data	1697	58.9	14.06	29.84	50.44	-347.3	444.4
	Filtered	1421	49.3	19.03	33.70	51.67	-347.3	303.1
Oct-99	All data	2695	90.6	1.22	5.54	32.91	-498.3	300.4
	Filtered	2264	76.1	1.77	5.51	27.41	-146.3	285.8
Nov-99[a]	All data	828	79.3	-8.62	-9.53	8.53	-42.2	97.7
	Filtered	704	67.4	-10.05	-10.76	8.35	-42.2	97.7
Nov-99[b]	All data	914	70.3	82.32	195.92	279.93	-12.68	1661.27
	Filtered	790	60.8	86.54	206.55	290.78	-12.68	1661.27

Period		*n*	Data coverage (%)	Median ng m^{-2} s^{-1}	Mean ng m^{-2} s^{-1}	Stdev ng m^{-2} s^{-1}	Min ng m^{-2} s^{-1}	Max ng m^{-2} s^{-1}
Whole Period[c]	All data	36187	71.0	0.23	13.93	78.20	-924.65	2064.31
	Filtered	31945	62.6	0.50	14.90	81.27	-924.65	2064.31
Whole Period[d]	All data	37101	70.9	0.41	18.41	93.22	-924.65	2064.31
	Filtered	32735	62.6	0.78	19.52	96.69	-924.65	2064.31

[a]1/11/99 00:00 - 12/11/99 00:00, not including period of urea appliciation.
[b]12/11/99 00:15 - 25/11/99 13:00, period of urea appliciation.
[c]Whole period: 1/5/98 00:00-12/11/99 00:00, not including switch off period (15/12/98 16:30-13/1/99 10:00) and period of urea appliciation (12/11/99 00:00-25/11/99 13:00).
[d]Whole period: 1/5/98 00:00-25/11/99 13:00, not including switch off period (15/12/98 16:30-13/1/99 10:00) but does include period of urea appliciation (12/11/99 00:00-25/11/99 13:00).

The largest monthly mean and median NH_3 flux values occurred in June 1998, June, August and September 1999 (Table 5.2, Fig. 5.9). The largest mean and median monthly deposition NH_3 flux value occurred in November 1999 (prior to application of urea), while the largest 15-minute deposition value occurred in April 1999. Section 5.3 explores these periods in greater detail in relation to management activities and meteorological conditions.

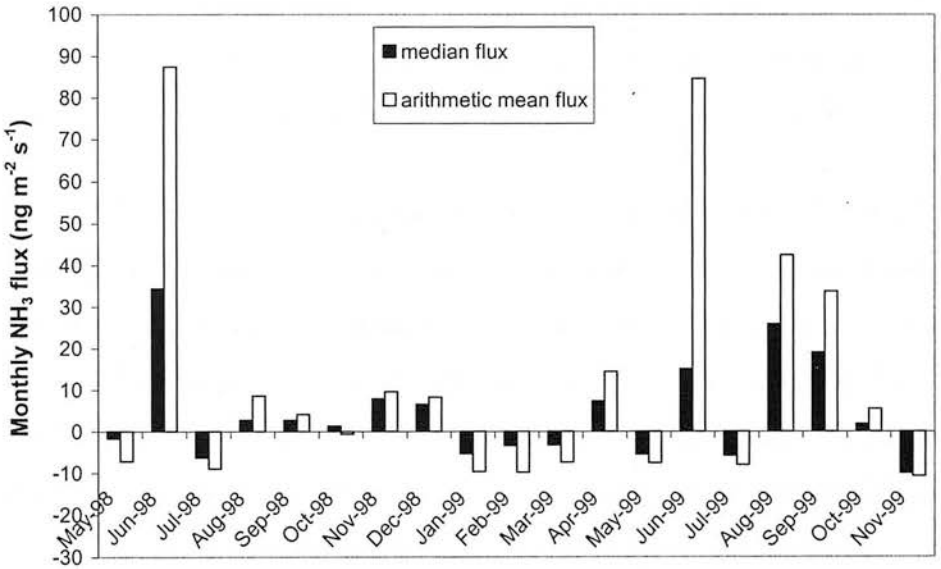

Figure 5.9. Monthly arithmetic mean and median NH_3 fluxes at Easter Bush, November values are for 1-11/11/99 inclusive and therefore do not include the NH_3 emissions from urea.

5.2.2 Effect of corrections on ammonia exchange

In addition to the micrometeorological requirements for flux measurement described in section 5.2.1 and 2.3.1, there are also errors associated in the flux measurement if

the assumptions of stationarity and homogeneity of the atmosphere are not met (see section 2.3.2). The key error terms are known as the storage error, advection error and an error term due to chemical production or consumption. Calculation of storage errors is relatively simple when changes in concentration with time are recorded (see Eq. 2.37). Storage errors for the measurements of NH_3 exchange at Easter Bush were calculated as detailed in Section 2.3.2 and are presented for June 1998 in Fig. 5.10 alongside the measured fluxes.

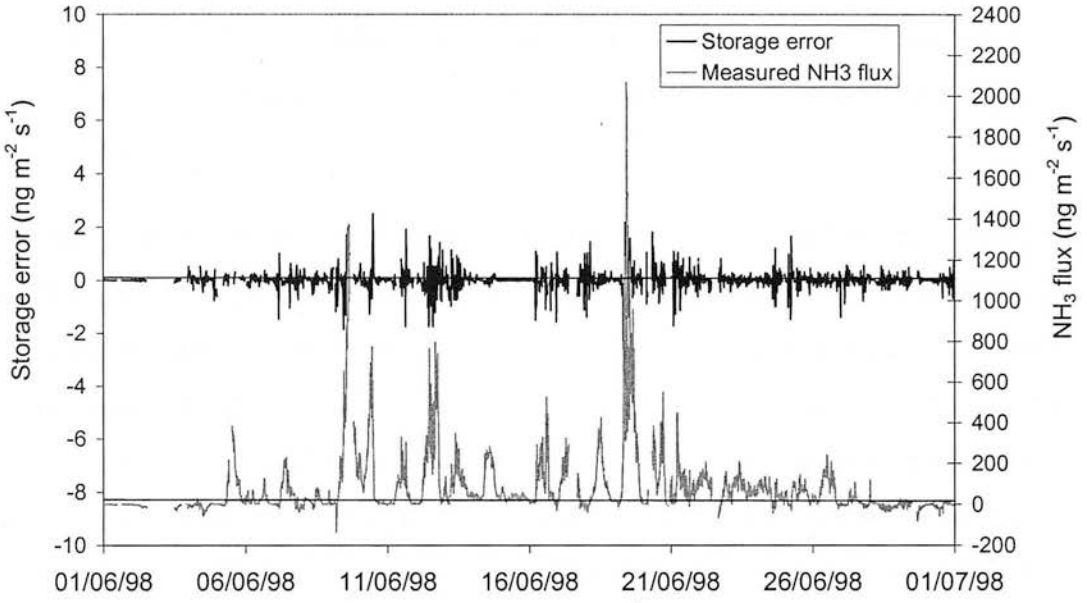

Figure 5.10. Storage errors shown alongside measured NH_3 flux for June 1998.

Fig. 5.10 demonstrates that the storage errors are usually of small magnitude, generally in the range –2 to +2 ng m^{-2} s^{-1}. The median value of the absolute relative error in the measured flux (storage error/measured flux) at $(z\text{-}d)$ = 1 m was < 1% (0.8 %). The change in the mean flux over the whole period was +2.4%, from 13.93 ng m^{-2} s^{-1} uncorrected to 14.26 ng m^{-2} s^{-1} corrected. This minor difference is consistent with the effect of storage on NH_3 usually being small as the fluxes of NH_3 are large compared with the air concentration.

To estimate the advection error, either measured horizontal concentration gradients or a modelling approach is needed (see section 2.3.2). These approaches have been followed for measurements of NH_3 exchange measured in other field studies (Loubet *et al.*, 2001; Milford *et al.*, 2001) but this was not done at Easter Bush due to a lack

of resources. The effects of advection can be large when large sources are close to sites experiencing relatively low values of NH_3 concentration and exchange, such as for the remote moorland adjacent to an intensive pasture considered by Loubet *et al.* (2001) and Milford *et al.* (2001), who found advection errors to vary between 30 to 100% of the measured NH_3 flux with a median value of 38%, compared with the mean measured NH_3 flux of -5 ng m^{-2} s^{-1}. By contrast, the relative errors are much smaller over agricultural fields with larger NH_3 fluxes. As noted by Sutton *et al.* (2002) and discussed in Chapter 8, advection errors may result in both underestimation or overestimation of emissions depending on whether the advection results from near by sources (such as farms) or from the field itself (large field emissions).

To assess the error term due to chemical production of consumption, measurements of HNO_3, HCl and particulate NH_4^+, NO_3^-, Cl^- and SO_4^- need to be measured. This was not done at Easter Bush. However, Nemitz *et al.* (2000c) assessed the chemical interactions with NH_3 exchange over oilseed rape at a coastal site about 20 km from Easter Bush. They found that due to small aerosol concentrations, chemical time-scales for evaporation or formation of NH_4Cl or NH_4NO_3 were much greater than time-scales for diffusive transport above the canopy. Therefore they concluded that gas-particle interactions were unlikely to have affected the measurements of NH_3 exchange above the canopy and would be unlikely to do so in similar areas of low particle concentrations. Particular periods may have occurred where chemical production was more important, but this would have most likely been a result of the perturbation caused during periods of large NH_3 emission. In this case, while the effect on the normally small fluxes of aerosol NH_4^+ may be substantial, the relative effect on NH_3 fluxes would remain small (Nemitz, 1998)

5.2.3 Net daily exchange of ammonia

The net daily fluxes for each month are presented in Figs. 5.10a, b, and c; these figures demonstrate the quantity of data collected. The data presented in these figures have been filtered for obstructed wind sectors but not filtered for the rest of the micrometeorological criteria, in order to see the full pattern of NH_3 exchange. Daily

values are calculated from the mean of available data (values are not shown for data capture < 30%).

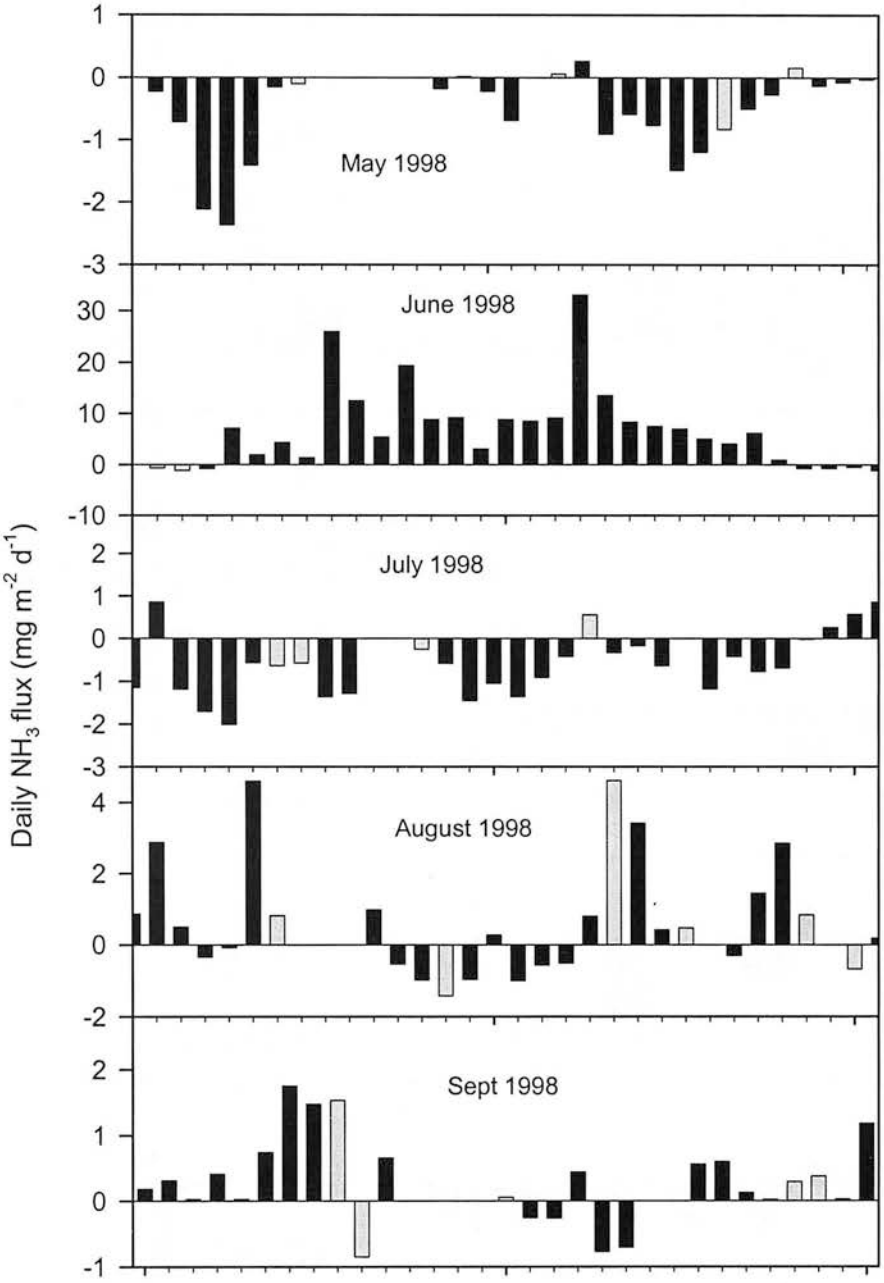

Figure 5.10a. Mean daily NH_3 fluxes at Easter Bush. Black bars are for daily fluxes with data capture > 65%, grey bars are for daily capture between 30%-65%, ticks represent 1 day.

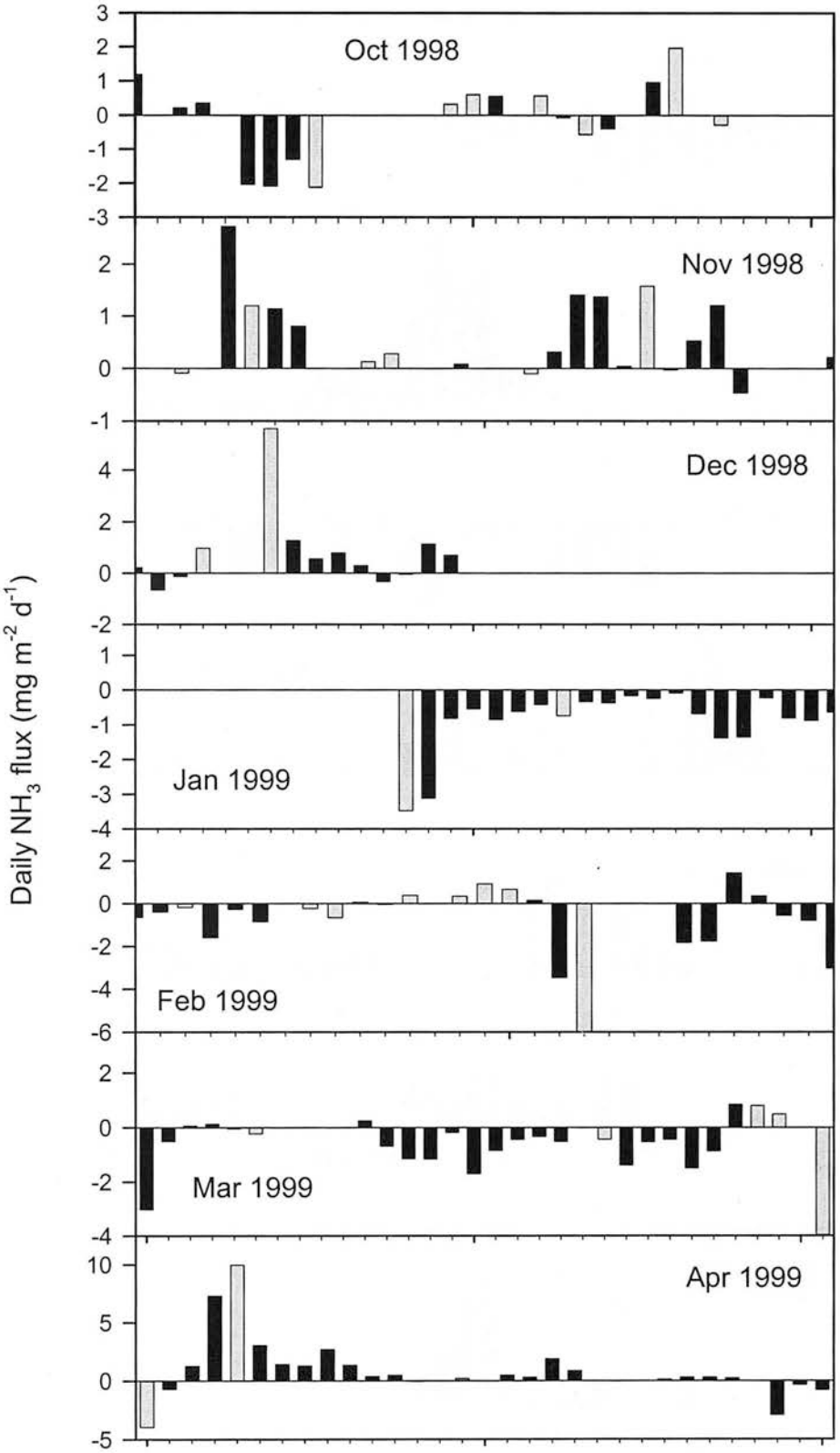

Figure 5.10b. Mean daily NH_3 fluxes at Easter Bush. Black bars are for daily fluxes with data capture > 65%, grey bars are for daily capture between 30%-65%, ticks represent 1 day.

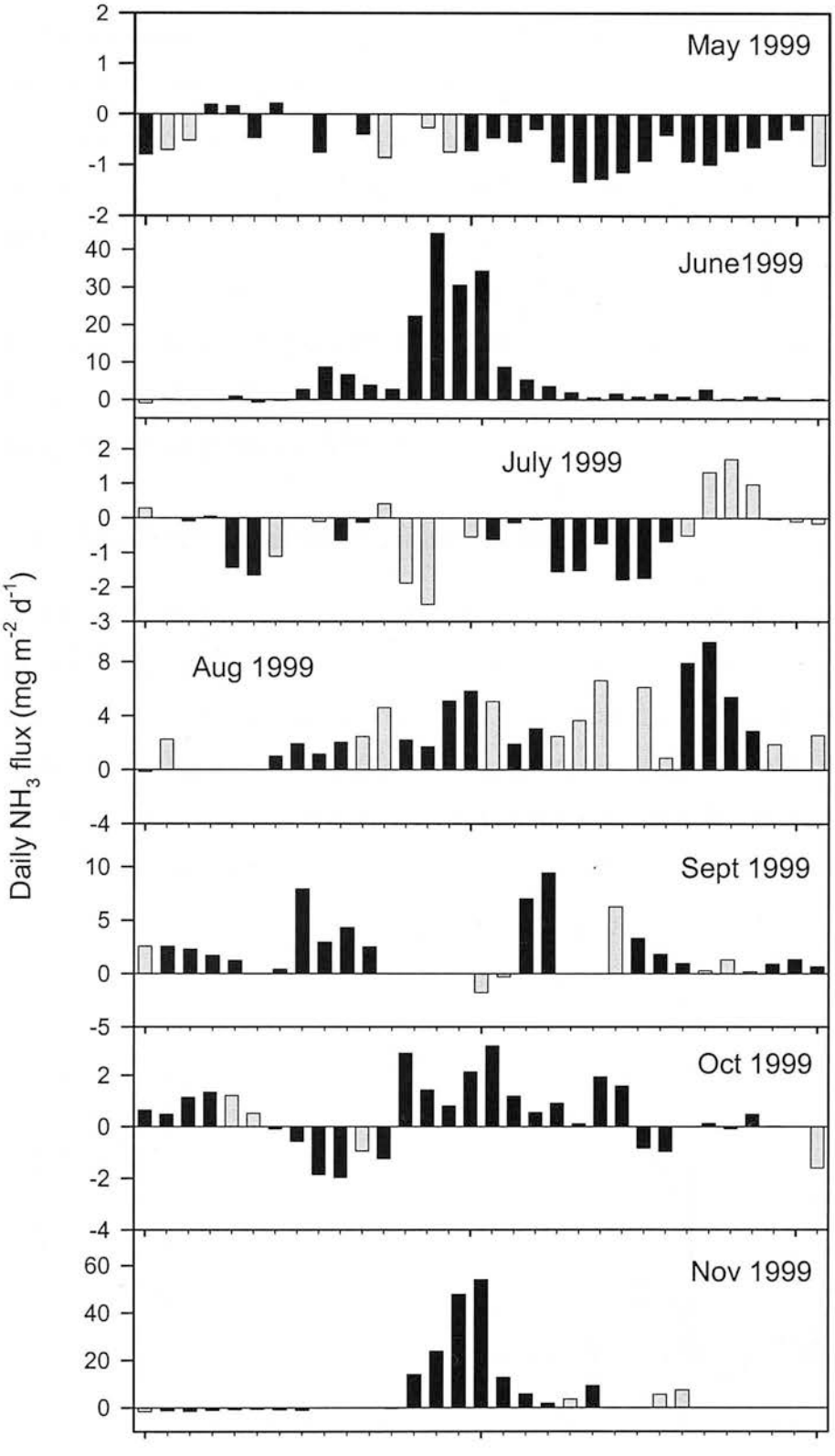

Figure 5.10c. Mean daily NH_3 fluxes at Easter Bush. Black bars are for daily fluxes with data capture > 65%, grey bars are for daily capture between 30%-65%, ticks represent 1 day.

Figs. 5.10a–c demonstrate the bi-directional nature of NH_3 exchange over intensively-managed grassland and the considerable seasonal variation in NH_3 exchange. As noted earlier, the largest monthly mean and median NH_3 flux values occurred in June 1998, June, August and September 1999. These months have an increased proportion of net daily emission fluxes compared with other months. The pattern of NH_3 exchange in June 1998 and June 1999 is characterised by a few large daily emission fluxes, up to 33 and 44 mg m^{-2} d^{-1} for June 1998 and June 1999, respectively, in addition to some small daily deposition fluxes (Fig. 5.10a and c). By contrast, the pattern of NH_3 exchange during the grazing period of August and September 1999 is characterised by less large daily fluxes (up to 10 mg m^{-2} d^{-1}), but a fairly consistent pattern of NH_3 emission.

5.3 Seasonal variation in ammonia exchange

As observed in Section 5.2, the continuous time course of measured NH_3 exchange shows considerable seasonal variation. The relationship of NH_3 exchange with prevailing meteorological conditions and management activities is investigated below for six key periods, each exhibiting a different pattern of NH_3 exchange. These six periods are indicated in Fig. 5.11, which presents daily fluxes for the whole measurement period.

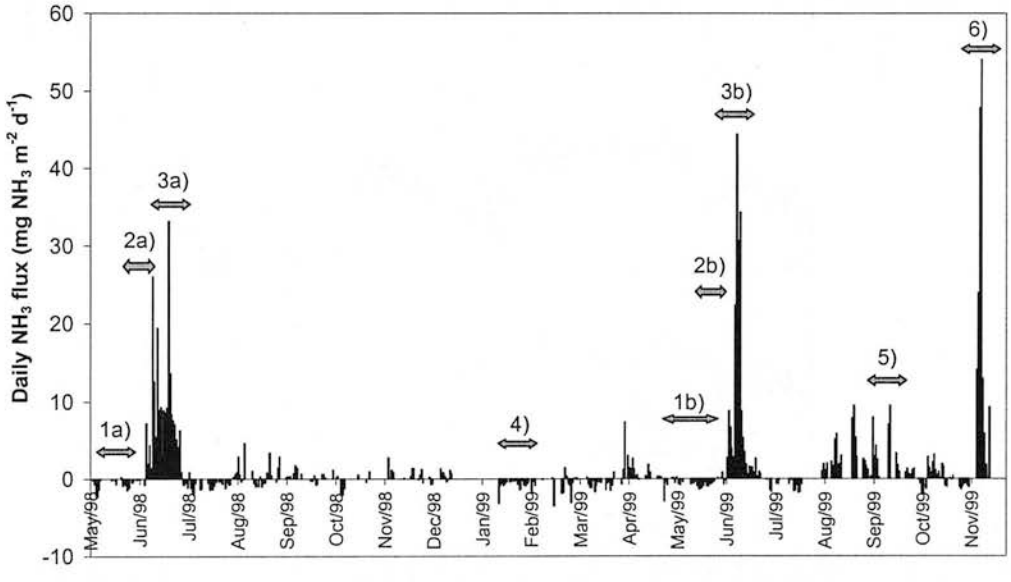

Figure 5.11. Daily fluxes of NH_3 at Easter Bush (only presenting daily fluxes where data capture > 65%). Arrows indicate key periods of NH_3 exchange: 1) Pre-cut, 2) Post-cut, 3) Post-fertilisation, 4) Winter, 5) Grazing and 6) Urea application, a and b indicate periods in 1998 and 1999, respectively.

5.3.1 *Precutting period, spring-early summer*

The period before the 1st cut (1/5/98-5/6/98) shows predominantly deposition fluxes (Fig 5.10a) with the maximum daily deposition flux = -2.37 mg NH_3 m^{-2} d^{-1} (-19.5 g NH_3-N ha^{-1} d^{-1}) and the mean daily flux (mean of daily fluxes with data capture > 65%) = -0.66 mg NH_3 m^{-2} d^{-1} (-5.4 g NH_3-N ha^{-1} d^{-1}). NH_3 concentrations and flux, T(1 m), RH(1 m), wetness, rainfall, u(1 m), V_d and V_{max} are presented in Fig. 5.12 for part of this precutting period (20-27/5/98).

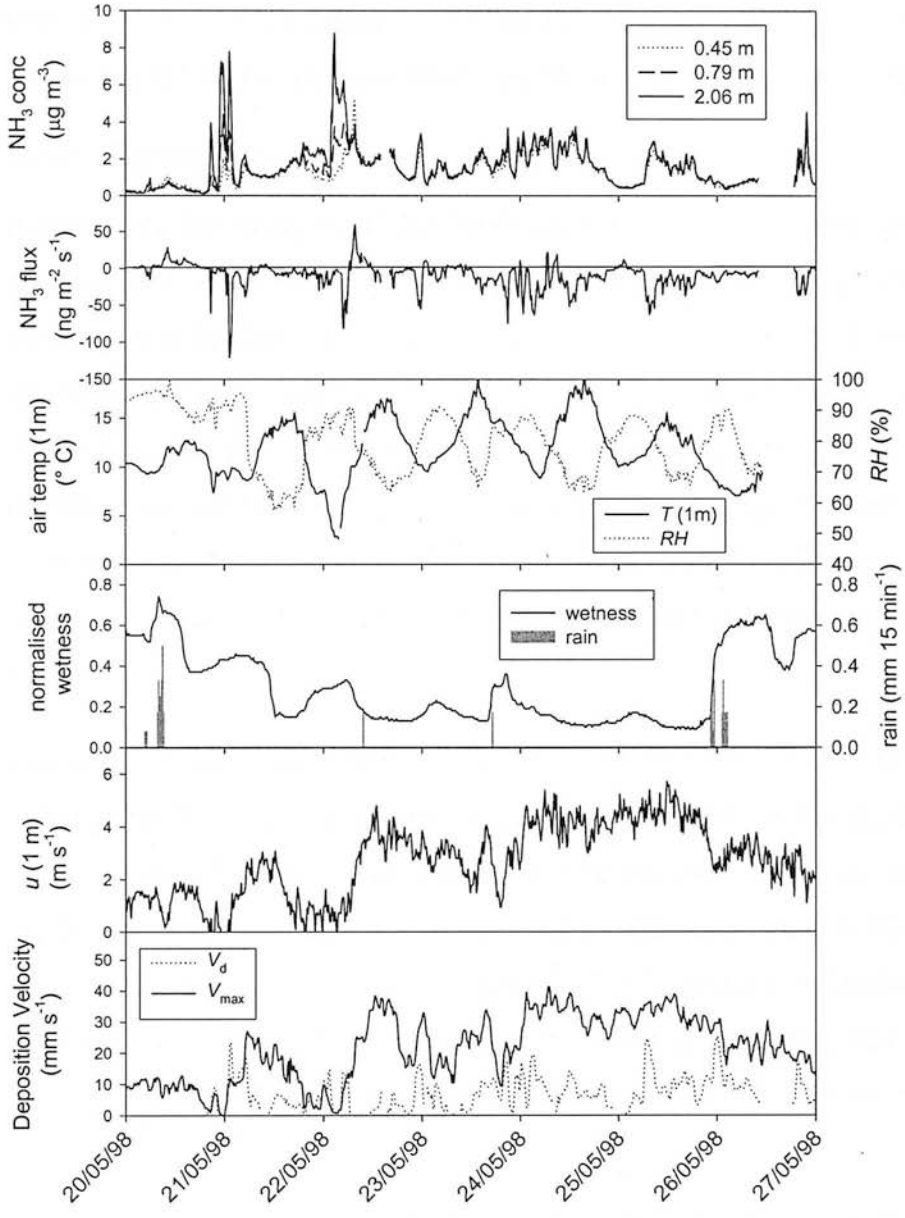

Figure 5.12. NH_3 flux and concentrations at Easter Bush for the period 20-27/5/1998, shown alongside measured values of air temperature (1 m), relative humidity (1 m), canopy wetness and rainfall, windspeed (1 m), V_d and V_{max} (1 hour running median, not plotted for periods of emission).

There are some brief emission periods, which may be due to volatilisation of previously deposited NH_3 on the leaf cuticle, particularly as emission occurs during periods when the canopy is drying out following periods of wetness, e.g. on the 20th and 22nd May 1998. During periods of deposition, the deposition velocity (V_d) can be calculated from Eq. 2.42. The median and mean deposition velocity are 7.2 mm s^{-1} and 8.2 mm s^{-1} for this period (excluding periods of emission). Fig 5.12 demonstrates that the value of V_d is often much less than the maximum deposition velocity permitted by turbulence (V_{max}). The median V_{max} for this period is 22.2 mm s^{-1}, resulting in a ratio of median V_d /median V_{max} of 32%. The median value of R_c for this period is 93 s m^{-1} (again considering the periods of deposition only).

5.3.2 Cutting period

Immediately following the 1st cut for silage at 11:00 on 5/6/98, the grassland starting emitting NH_3, up to 380 ng m^{-2} s^{-1} (Fig. 5.13). Prior to the cutting of the grass, NH_3 exchange was predominantly deposition (section 5.3.1). Although brief emission episodes were observed, the emissions were < 50 ng m^{-2} s^{-1} (Fig. 5.12), nearly an order of magnitude less than the emissions from the cut grassland. In addition, a clear diurnal cycle in NH_3 exchange can be seen with the cutting emissions lasting for most of the daytime rather than for just a brief period during the day. The emission clearly correlates with environmental parameters such as temperature and solar radiation.

Fluxes of similar magnitude were also observed after the 1st cut in 1999 (Fig. 5.17), although the increased emissions seemed to be delayed by a few days, possibly due to heavy rainfall. Smaller NH_3 emissions were observed following the 2nd cut in 1998 (up to 200 ng m^{-2} s^{-1}) and the emissions did not last for as long as after the 1st cut (Fig. 5.18a). In 1999, only the S field received a second cut and unfortunately the wind came from the N field for the days immediately following the cut and so it was not possible to confirm the lower emissions observed after the second cut in 1998 (Fig. 5.18b).

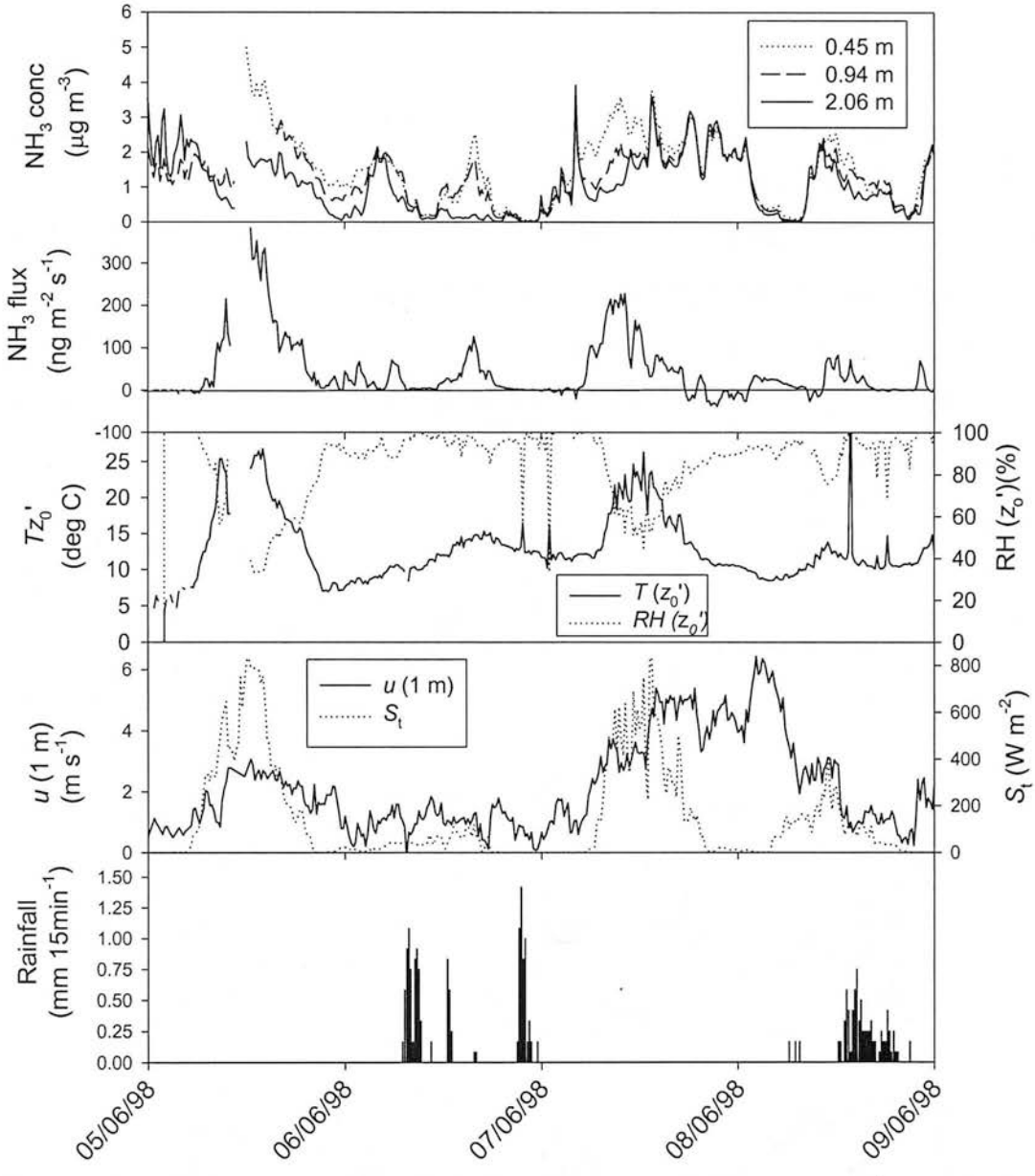

Figure 5.13. NH_3 flux and concentrations at Easter Bush immediately after the 1st cut and prior to fertilisation (5-9/6/1998), shown alongside measured values of air temperature (z_0'), relative humidity (z_0'), windspeed (1 m), solar radiation and rainfall.

5.3.3 *Nitrogen fertilisation*

On 9/6/98 between 10:20-11:30 the S field was fertilised with 104 kg N ha^{-1} of compound fertiliser (Kemira N-P-K, 26-5-10) (see Table 4.3). The field was already emitting NH_3 prior to the fertilisation, about 200 ng m^{-2} s^{-1} between 8:00-10:00 (Fig. 5.14). After fertilisation, the NH_3 fluxes increased up to a peak of 1370 ng m^{-2} s^{-1} at 15:30 and the emission continued overnight (9-10/6/98) indicating direct emission from the fertiliser itself, rather than stomatal emissions (Fig. 5.14). Heavy periods of rainfall on 9/6/98 and 10/6/98 can be seen to have reduced the NH_3 emission.

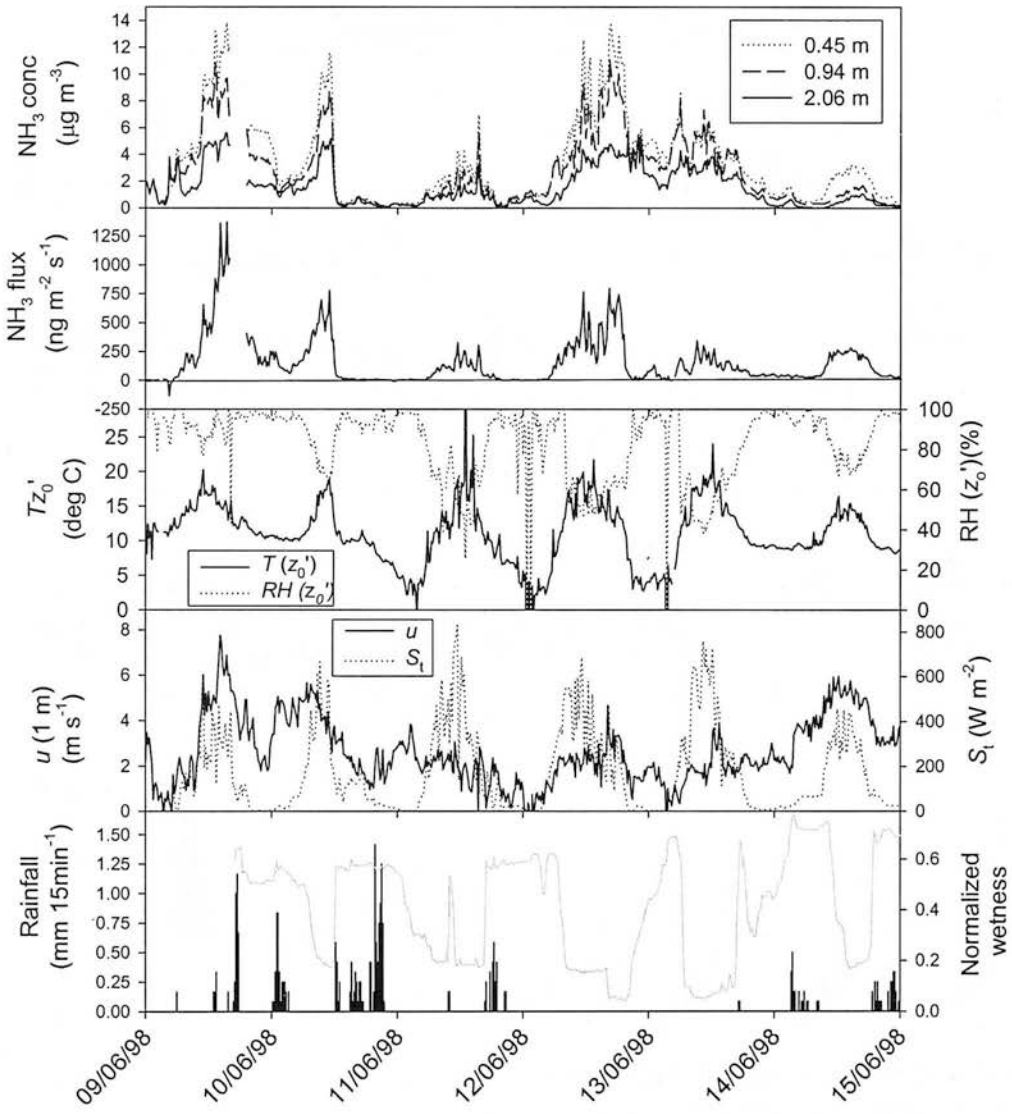

Figure 5.14. NH_3 flux and concentrations at Easter Bush for the period 9-15/6/1998, shown alongside measured values of air temperature (z_0'), relative humidity (z_0'), windspeed (1 m), solar radiation, rainfall and wetness. The field was fertilised with 104 kg N ha^{-1} at 10:20 on 9//61998 (see Table 4.3).

The first day of fertilisation (9/6/98) showed the largest emission and emissions continued for approximately two weeks (Fig. 5.14 and 5.15). It is unlikely that the

direct emission from fertiliser lasted for two weeks as night-time emissions are only observed for the first night following fertilisation. Daytime emissions indicate stomatal control and suggest that the continuation of emission is likely to be from the vegetation itself. The enhanced emissions over this period are a significant contribution to the annual budget (Fig. 5.22).

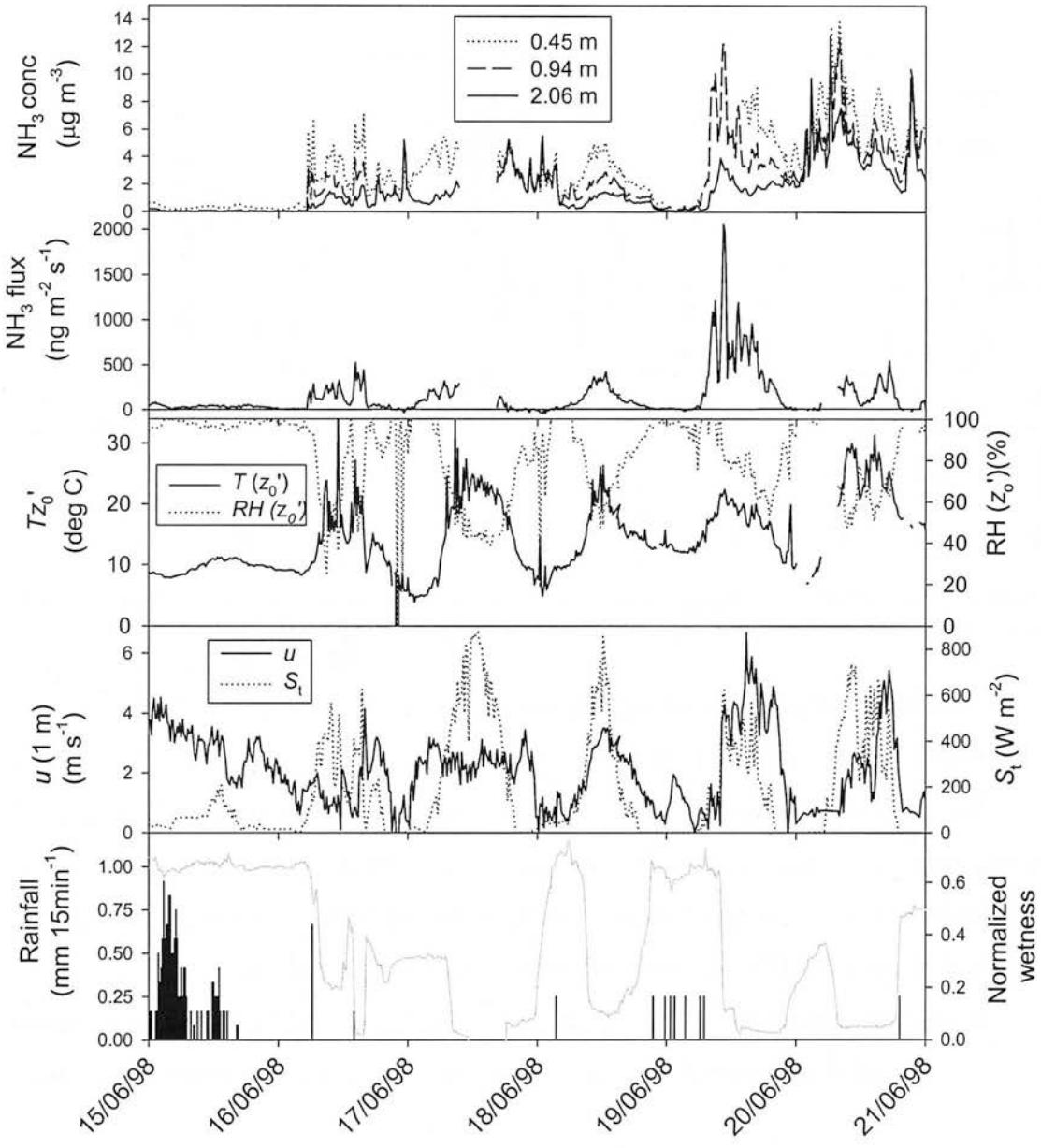

Figure 5.15. NH_3 flux and concentrations at Easter Bush for the period 15-21/6/1998, shown alongside measured values of air temperature (z_0'), relative humidity (z_0'), windspeed (1 m), solar radiation, rainfall and wetness.

The N field was not fertilised until 13/6/98 and this difference of timing of management activities allows the analysis of cutting-induced emissions to continue over a longer period. It is interesting to note that on 11/6/98, when the wind came

from the N field, the measurements still showed enhanced emissions (up to 310 ng m^{-2} s^{-1}) (Fig. 5.16). This is 6 days after the cutting event and provides evidence for the duration of the enhanced emissions from grass cutting without the additional effect from fertilisation. One of the challenges in analysing these fluxes is to separate out the relative contribution of cutting versus fertilisation to the overall exchange after 9/6/98.

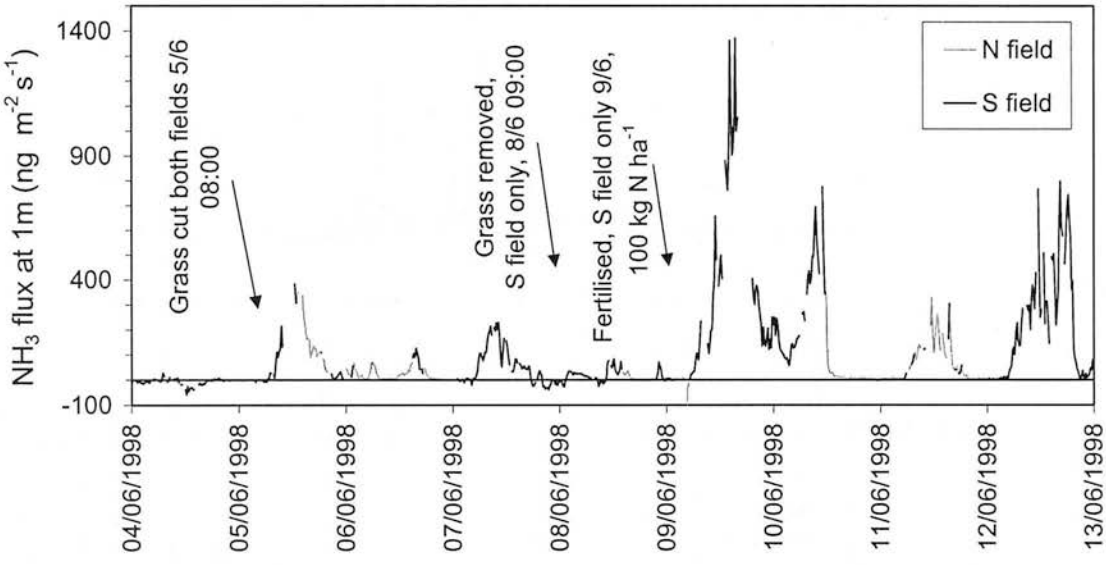

Figure 5.16. NH_3 exchange during the cutting and fertilising period (4-13/6/98), differentiating between NH_3 exchange measured over the S and N field as the timing of the management was different on the two fields (see Table 4.3).

Fluxes of similar magnitude were also observed after the nitrogen fertilisation in June 1999 (Fig. 5.17). Although, interestingly, the peak in emissions was observed three days after the fertiliser was applied. Smaller NH_3 emissions were observed following the fertilisation after the 2nd cut in 1998 (Fig. 5.18). However, a data gap of four days exists from the third day after fertilisation so it is possible that fertilisation emissions did increase but were unrecorded at this time. In 1999, only the S field received a second cut and was fertilised on 2/8/99, but the wind came from the N field during this period and so any emissions from this fertilisation event are unrecorded.

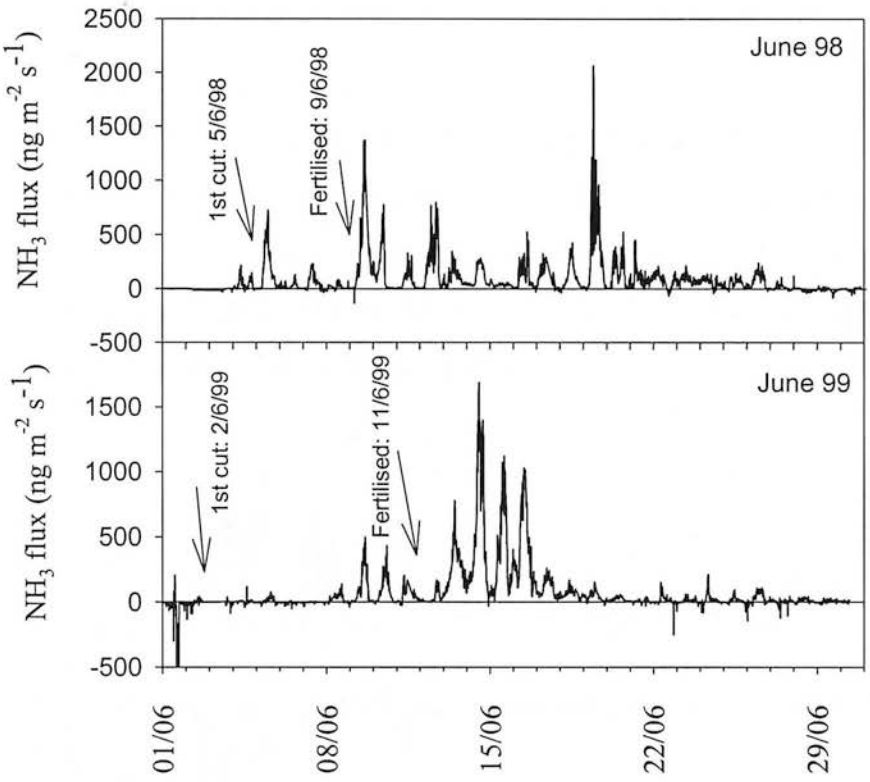

Figure 5.17. NH_3 exchange during the first cutting and fertilising period in 1998 and 1999.

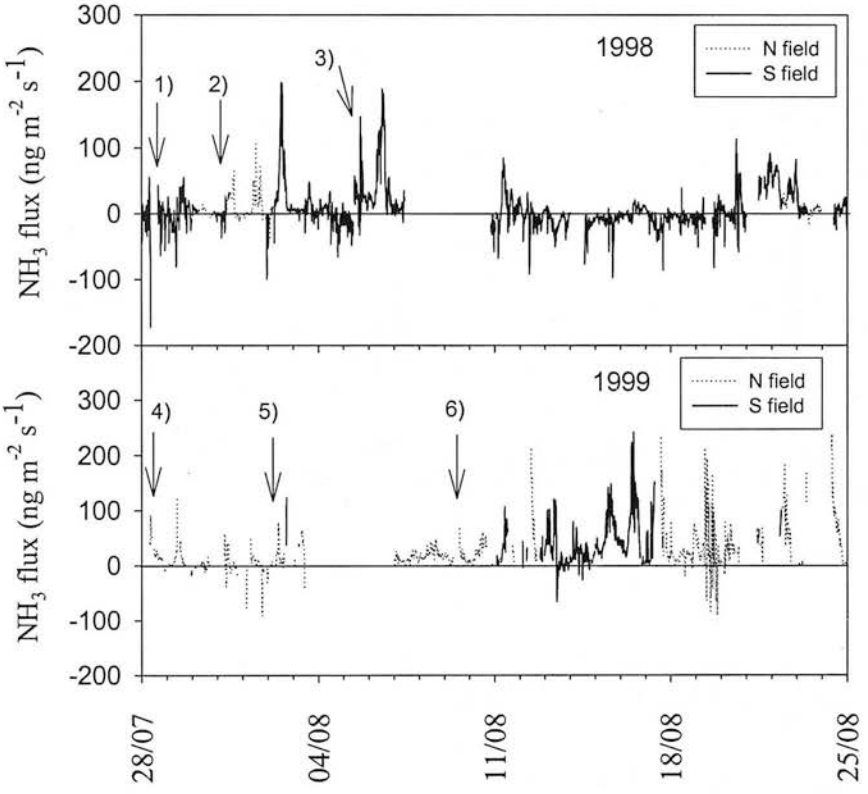

Figure 5.18. NH_3 exchange during the second cutting and fertilising period in 1998 and 1999, differentiating between NH_3 exchange measured over the S and N field. Note the N field did not receive a second cut in 1999. 1) S field cut: 28/7/98, 2) N field cut: 31/7/98, 3) Both fields fertilised: 5/8/98, 4) S field cut & N field grazing starts: 28/7/99, 5) S field fertilised: 2/8/99, 6) S field grazing starts: 9/8/99.

5.3.4 *Winter*

During the winter months and when no animals were present in either field (e.g. January - March 1999), NH_3 exchange was predominantly deposition (Figs. 5.9b and c). The NH_3 concentrations and flux are presented alongside meteorological measurements for 13-20/1/99 in Fig. 5.19. These show fairly large deposition values, the maximum deposition was -135 ng m^{-2} s^{-1} on 13/1/99, reducing to smaller deposition values in the subsequent days.

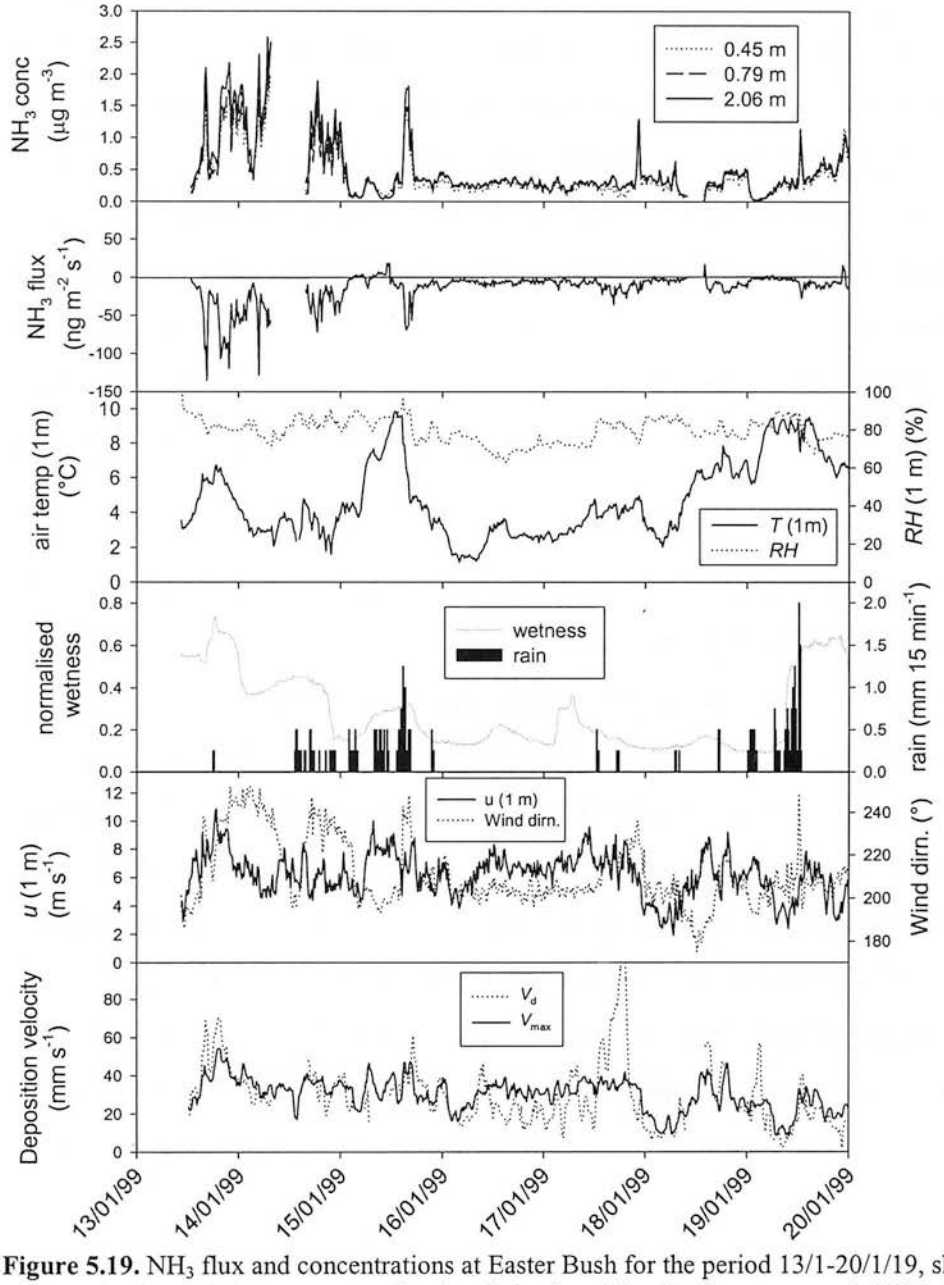

Figure 5.19. NH_3 flux and concentrations at Easter Bush for the period 13/1-20/1/19, shown alongside measured values of air temperature (1 m), relative humidity (1 m), wetness, rainfall, windspeed (1 m), wind direction, V_d and V_{max} (1 hour running median, not plotted for periods of emission).

The windspeed and relative humidity did not vary greatly throughout this period, but the wind direction fluctuated between about 240° and 200° (Fig. 5.19). The changes in concentration, from values of up to 2.6 μg m^{-3} down to background values of about 0.3 μg m^{-3}, are correlated with the changes in wind direction. At a bearing of 240° the wind was coming from Easter Howgate farm (Fig. 3.2) and it is likely that the concentration is enhanced by this local source whereas at a bearing of 200° the wind does not pass over a farm in the near vicinity. These enhanced concentrations lead to a greater deposition flux. The deposition velocity is shown alongside V_{max} and shows that in general the deposition is occurring at the maximum permitted by turbulence indicating minimal canopy resistance. This is in contrast to the values of V_d presented in Section 5.3.1. The occurrence of some V_d values slightly exceeding V_{max} can be attributed to uncertainty in the NH_3 gradient estimates at low NH_3 concentrations. Emission of NH_3 only occurred for a few brief periods, the clearest of which was on 15/1/1999. This was almost certainly the result of desorption of ammonia from leaf surfaces and occurred during a period of increasing temperature and low NH_3 concentration between rain events

5.3.5 Grazing

The period of grazing occurred after the 2nd cut in both years, starting on 10th August in 1998 and on 28th July in 1999. Grazing continued intermittently through the autumn months in 1998 and stopped on 29/1/99. In 1999 grazing also continued throughout the autumn and the last recorded animals were observed on 8/11/99 (see section 4.3.2 for details). In 1999, the N field did not receive a second cut and grazing began earlier than in 1998. NH_3 emissions during a period of grazing in 1999 are presented in Fig. 5.20. A clear diurnal cycle is shown with peak emission generally occurring about midday (up to 300 ng m^{-2} s^{-1} on 8/9/99). During this period the N field was grazed by about 35 dairy cattle and the S field by about 70 sheep. The wind direction was from the S field for the whole of the period shown in Fig. 5.20 (data not shown).

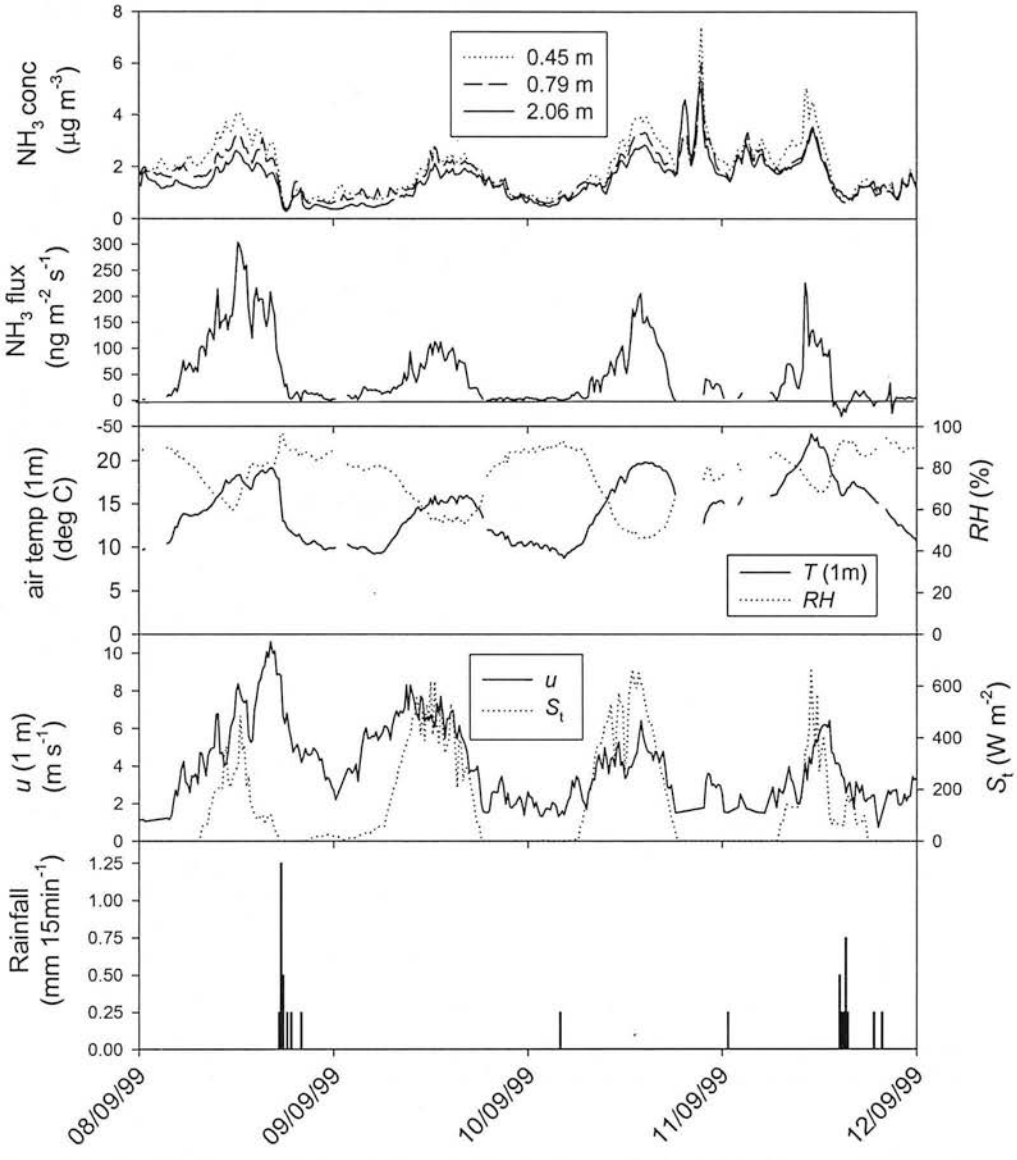

Figure 5.20. NH_3 flux and concentrations at Easter Bush for the period 8-12/9/1999 during a period of grazing, shown alongside measured values of air temperature (1 m), relative humidity (1 m), windspeed (1 m), solar radiation and rainfall.

5.3.6 Urea application

On 12/11/99, 47 kg N ha^{-1} of urea was applied on the S field to provide emissions of NH_3 as a field test for a REA system (Nemitz *et al.*, 2001). The NH_3 exchange up to the 12/11/99 was exclusively deposition, but only of small magnitude (Fig. 5.9d). As explained in section 2.2, the concentration difference between the up and down draughts in an REA system $\left(\overline{\chi^+} - \overline{\chi^-}\right)$ is much smaller than the $d\chi$ signal for the aerodynamic gradient method and is therefore more difficult to resolve analytically.

As a consequence of this difficulty, urea was applied to the field to increase the NH_3 flux to provide a means of testing the system.

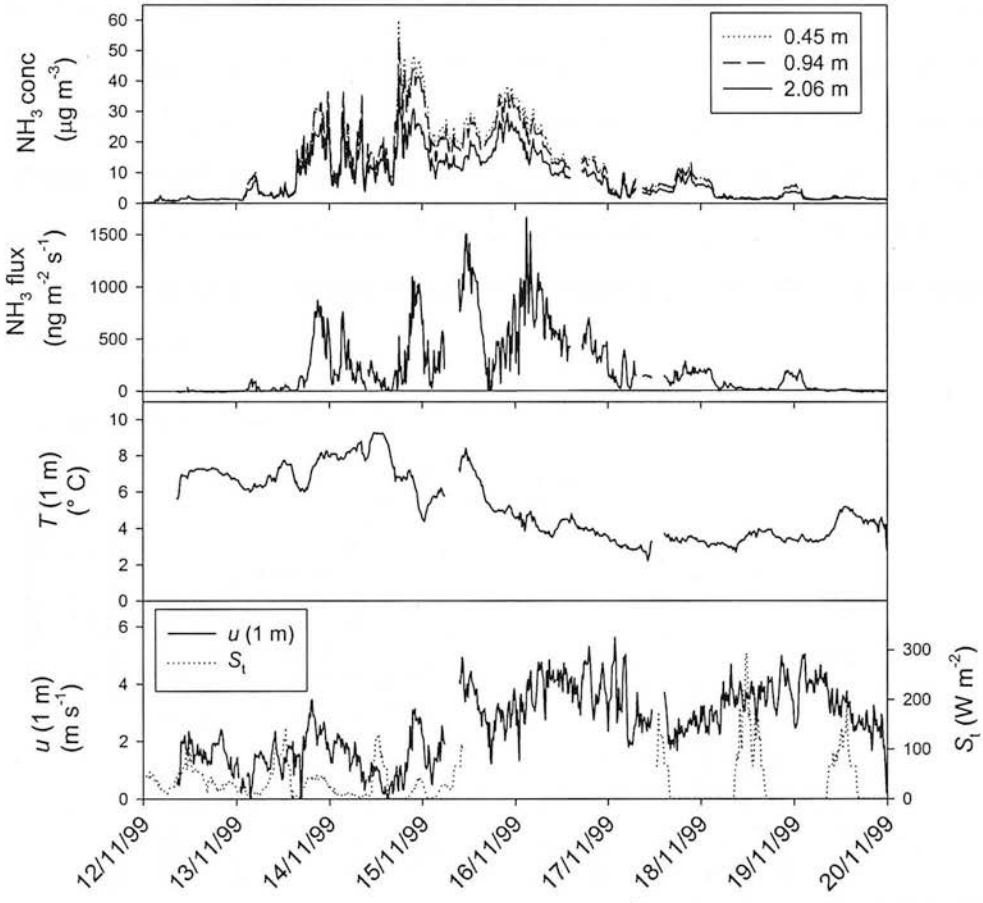

Figure 5.21. NH_3 flux and concentrations at Easter Bush for the period 12-20/11/1999, shown alongside measured values of air temperature measured by the sonic anemometer (2.1 m), windspeed (1 m) and solar radiation.

Emission of NH_3 was negligible on the day of application and started to increase significantly on 13/11/99 at 17:45, the emission continued to increase over the next three days reaching a peak of 1660 ng m^{-2} s^{-1} on 16/11/99 at 03:00. Emissions were large considering the low temperature at this time of year (mean T (2.1 m) over this period = 5.2 °C). There was no rainfall observed during this period (data not shown). NH_3 emission continued during the night, which is indicative of non-stomatal emissions. The total emission during the week following urea application (13/11/99 00:00-20/11/99 00:00) was 1.2 kg N ha^{-1} (from the sum of available 15-minute flux measurements) or 1.3 kg N ha^{-1} (from the mean flux over this period converted to kg ha^{-1}) (for the unfiltered dataset). This NH_3 emission is equivalent to 2.5 or 2.7 % of the N applied, respectively.

5.3.7 *Diurnal cycles of key periods*

Average diurnal cycles in NH_3 concentration and flux for key periods are presented in Figs. 5.20 and 5.21. There is not much variation in the average diurnal cycles in NH_3 concentration for the pre-cut periods, apart from a small increase in concentration at nighttime. This would indicate a larger contribution from local farm sources at night. The grazing period does not show a strong diurnal variation. The post-cut period does, however, show a significant increase in concentration during the day, reflecting increased NH_3 emission from the field itself during daytime (see Section 5.5.3).

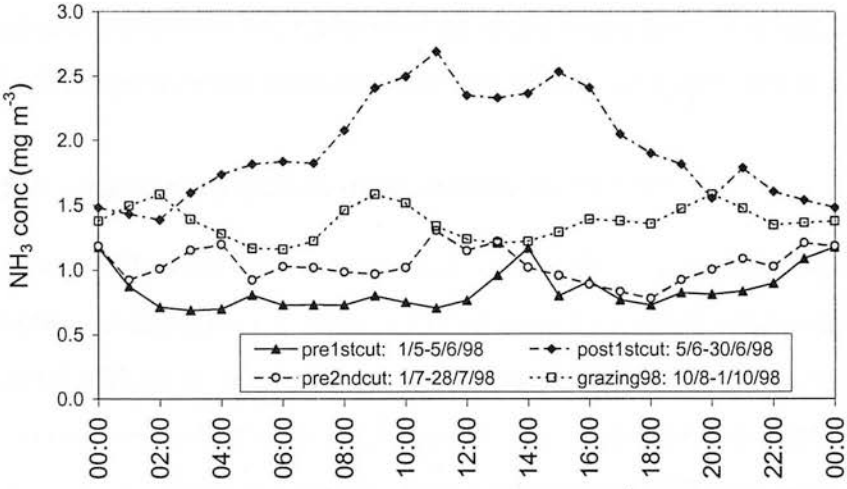

Figure 5.20. Diurnal cycle in NH_3 concentration in different periods.

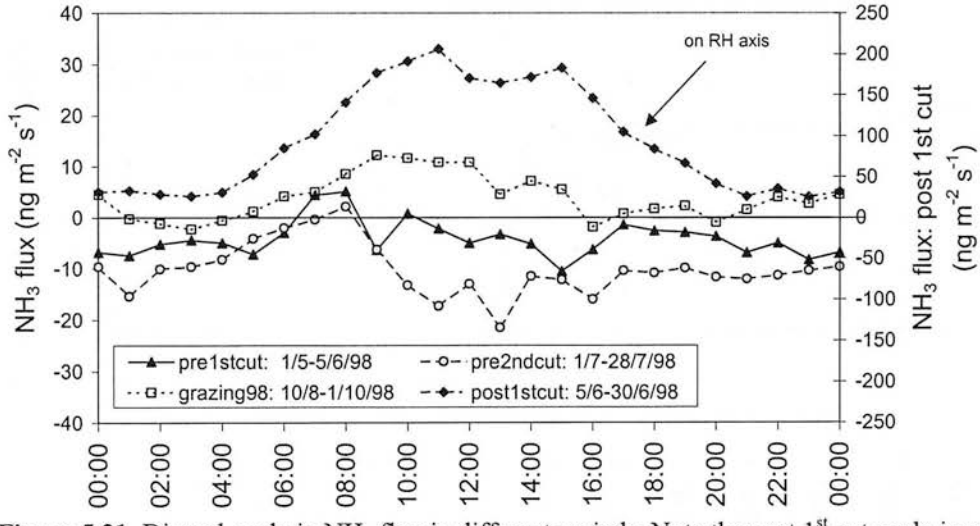

Figure 5.21. Diurnal cycle in NH_3 flux in different periods. Note the post 1st cut cycle is scaled on the right-hand axis, all the other series are scaled on the left-hand axis.

The average diurnal cycles in NH_3 flux show more variation than the concentration. The largest fluxes and largest variation are observed in the post-cut period, when fluxes are larger in the daytime, due to warmer temperatures, stomatal opening and drier leaf surfaces. The grazing period also shows larger concentrations during the daytime, which reflects the effect of temperature and wetness on the emissions. Although there is no stomatal control on emissions of NH_3 from ground sources of NH_4^+, there might be some additional contribution from the plants during this grazing period which would be controlled by stomata. The NH_3 flux in the pre-cut periods is primarily deposition with not much diurnal variation, except for a slight increase in deposition for the 2nd pre-cut period in the middle of the day. The pre-cut periods do show a brief period of emission in the early morning around 0800, indicating emission from cuticular desorption during periods of warming and drying.

5.4 Annual variation in ammonia exchange

Figure 5.22 shows the accumulated NH_3–N flux for the Scottish site in 1998 and 1999 and indicates the large contribution to the overall emission from the first cut and fertilisation. It also demonstrates that the pattern of exchange is similar between the two years although after August, the accumulated flux is greater for 1999. This is most likely due to the greater grazing numbers in 1999 compared with 1998.

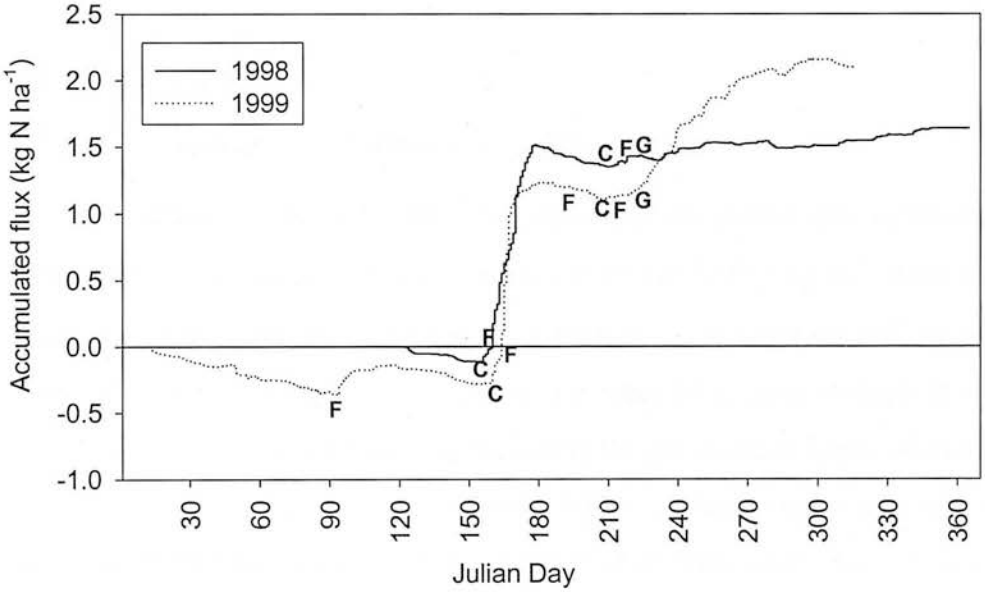

Figure 5.22. Accumulated NH_3-N over the 2 field seasons at Easter Bush, Scotland. 'C' indicates cutting, 'F': $NH_4^+NO_3^-$ fertilisation and 'G': grazing. Timing of management activities given in Table 4.3.

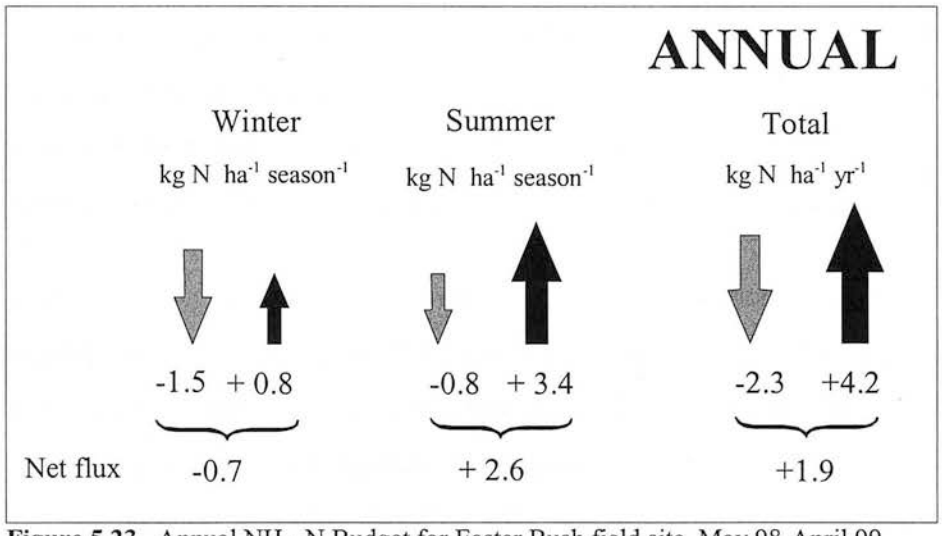

Figure 5.23. Annual NH_3–N Budget for Easter Bush field site, May 98-April 99.

Fluxes obtained over a long period permit the calculation of annual budgets of pollutant exchange. The annual NH_3 budget for the Easter Bush grassland for May 1998-April 1999 is presented in Fig. 5.23. For this period the cut grassland was a net source of NH_3 at a rate of 1.9 kg N ha^{-1} yr^{-1}, although fluxes were bi-directional with deposition dominating in the winter and emission in the summer. The gross emission flux for the year (as the sum of half hourly net emission fluxes) was 4.2 kg N ha^{-1} yr^{-1} equating to 1.6% of the N applied. When taking account of atmospheric deposition (2.3 kg N ha^{-1} yr^{-1}) the net emission flux corresponds to 0.7% of the N applied. Although this is a small net emission flux on a per hectare basis it is significant given the large area of the UK covered by grasslands.

5.5 Discussion

5.5.1 Concentrations of ammonia at Easter Bush

The NH_3 concentrations at Easter Bush, excluding the period after application of urea, varied on a diurnal and seasonal basis between 0-33.4 μg m^{-3}. After application of urea the concentrations increased to 55.9 μg m^{-3}. The median (1.07 μg m^{-3}), arithmetic mean (1.52 μg m^{-3}) and geometric mean NH_3 concentration (0.90 μg m^{-3}) for the whole measurement period, excluding the period after application of urea, are fairly typical long-term average values for NH_3 concentration for this type of mixed rural area. Burkhardt *et al.* (1998) reported an arithmetic mean concentration of 1.4 μg m^{-3} over a two-year period of concentration measurements at a site close to Easter Bush (< 1 km). Flechard *et al.* (1998) reported an arithmetic mean and

geometric mean concentration of 0.89 and 0.43 μg m^{-3} over a 13-month period at a moorland site, approximately 10 km from Easter Bush. Long-term mean NH_3 concentrations measured across the UK in the National Ammonia Monitoring Network (1996-2000) were in the range 0.06 – 11 μg m^{-3} (Sutton *et al.*, 2001).

A clearer seasonal cycle was observed in the monthly geometric mean NH_3 concentration than in the monthly arithmetic mean concentration at Easter Bush, with the geometric mean NH_3 concentration generally displaying an increase in summer and a decrease in winter months. The geometric mean is probably more related to the background concentration signal of NH_3, which will in general increase with temperature due to increased emissions of NH_3 at higher temperatures, while the arithmetic mean is probably more affected by the local sources of NH_3 from the neighbouring farms. The NH_3 concentration enhancement from the farms will depend on the number, type of animal and management of animals (whether they are indoors or outside grazing) and also on the wind direction and atmospheric dispersion (whether plumes from the farm reach the field site).

The geometric standard deviation in NH_3 concentration at the highest measurement level varied between 2.17 and 5.25 μg m^{-3}. These are relatively high values compared with typical values measured for other pollutants. Burkhardt *et al.* (1998) reported a geometric standard deviation in SO_2 concentration of ~2 μg m^{-3} for a mixed rural area over a two year period, the corresponding arithmetic mean in SO_2 concentration was 6.49 μg m^{-3}. These larger values of σ_G indicate that the NH_3 concentrations at Easter Bush are largely influenced by local sources, be they nearby farm sources or emissions from the measurement fields or surrounding fields themselves.

The distribution of concentration with wind direction demonstrates the influence of Easter Howgate farm, located at 240°. Concentrations are enhanced in this wind direction while concentrations from the north-north-east (NNE) sector are a factor of two lower. The NNE sector consists of similarly managed fields in the closest 3 km and changes into residential land as the outskirts of Edinburgh are reached.

5.5.2 *Exchange of ammonia at Easter Bush*

The exchange of ammonia with intensively-managed grassland was measured semi-continuously for 19 months. Filtering for micrometeorological criteria reduced the data capture from 70.9% to 62.6%, which is equivalent to 32,735 15-minute flux measurements. The NH_3 exchange showed large diurnal and seasonal variation, which was strongly linked to external management in addition to meteorological conditions. The mean NH_3 flux for key periods, converted to an equivalent daily flux, is show in Table 5.3. Results are given for the filtered and unfiltered dataset but the values are not substantially different between these two datasets. The largest deposition was in the winter period, equivalent to –6.3 g NH_3-N ha^{-1} d^{-1}, while emissions after cutting in June 1998 and during grazing in August 1999 were similar, equivalent to 30.5 and 34.5 g NH_3-N ha^{-1} d^{-1}, respectively. NH_3 emissions after the June 1998 fertilisation and the urea application in November 1999 were significantly larger, equivalent to 162.7 and 196.6 g NH_3-N ha^{-1} d^{-1}, respectively. These values were determined for the first two days following the fertilisation in June 1998 and the first 7 days following the urea application.

Table 5.3. Equivalent daily ammonia flux for key periods

Measurement Period	Mean NH_3 flux[a] (g NH_3-N ha^{-1} d^{-1})	Mean NH_3 flux[b] (g NH_3-N ha^{-1} d^{-1})
Pre-cut: 1/5/98-4/6/98	-4.9	-5.1
Post-cut: 5/6/98-8/6/98	29.3	30.5
Post-fertilisation: 9/6/98-10/6/98	153.6	162.7
Post-fertilisation: 9/6/98-20/6/98[c]	114.0	122.3
Winter: 13/1/99-31/3/99	-6.0	-6.3
Grazing: 9/8/99-31/8/99	33.0	34.5
Post-urea: 13/11/99-19/11/99	182.3	196.6

[a]Data not filtered for micrometeorological criteria, [b]Data filtered for micrometeorological criteria
[c]Not including 11/6/98 when flux was from unfertilised N field. All dates are inclusive.

Table 1.3 listed net NH_3 exchange values from other measurement studies, Table 5.4 repeats these values again for a selection of the studies and ranks them from the largest deposition to largest emission values. This illustrates that the deposition fluxes measured in the winter and pre-cutting period at Easter Bush are less than some measured values reported over forest ecosystems (Sutton *et al.*, 1993a; Pryor *et al.*, 2001) and semi-natural grassland (Sutton *et al.*, 1993a) while similar to values measured at two moorland sites (Flechard and Fowler, 1998; Milford *et al.*, 2001).

NH_3 emissions after cutting in June 1998 and during grazing in August 1999 are similar to emissions measured over oilseed rape after cutting (Sutton *et al.*, 2000).

Table 5.4. Daily ammonia flux values from other field studies[a]

Ecosystem, location	Mean NH_3 flux over the period (g NH_3-N ha^{-1} d^{-1})	Reference
Semi-natural grassland , UK	-24	Sutton *et al.* (1993a)
Deciduous forest, Indiana, USA	-15	Pryor *et al.* (2001)
Moorland , UK	-12	Sutton *et al.* (1993a)
Grazed pasture, The Netherlands[b]	-10.3	Plantaz (1998)
Semi-natural grassland, UK	-10	Sutton *et al.* (1993a)
Coniferous forest, UK	-8	Sutton *et al.* (1993a)
Spruce forest, Denmark	-6.5	Anderson *et al.* (1999)
Wet heathland/Moorland, Scotland	-4.2	Milford *et al.* (2001)
Moorland, Scotland	-3.7	Flechard and Fowler (1998)
Barley, UK	4	Sutton *et al.* (1993b)
Grazed pasture, The Netherlands[c]	17.1	Plantaz (1998)
Maize, France	18	Jambert *et al.* (1997)
Oilseed rape, Scotland (precut)	20	Sutton *et al.* (2000)
Oilseed rape, Scotland (postcut)	30	Sutton *et al.* (2000)
Oilseed rape, Scotland (postcut, at end of measurement period)	80	Sutton *et al.* (2000)

[a]Note that these values are derived from measurement studies of different durations and using different measurement techniques (see Table 1.3), [b]non-grazed mean, [c]grazed mean.

NH_3 emissions after the June 1998 fertilisation and after the urea application in November 1999 are significantly larger than the NH_3 emissions reported in these studies, but this is to be expected as most of these studies did not report emissions from fertiliser application. The total emission observed in the two days following N fertilisation on 9/6/98 at Easter Bush was 0.3 kg N ha^{-1}, this was equivalent to 0.3 % of the N applied (104 kg ha^{-1}). This percentage increases if the emission on the following days is included but it is difficult to determine what proportion of this emission is direct fertiliser emission and what proportion is plant-mediated emission. Van der Weerden and Jarvis (1997) suggest an NH_3 emission factor for ammonium nitrate fertiliser applied to grassland of 1.6 % of the N applied, and the values recorded here are therefore much smaller than in that study.

The total emission observed in the week following the urea application at Easter Bush was 1.3 kg N ha^{-1}, equivalent to 2.7 % of the N applied. Van der Weerden and

Jarvis (1997) measured ammonia losses of 12 to 46% from urea application in wind tunnels and reviewed other experiments which measured losses of 6 to 49%; they suggest an NH_3 emission factor for urea applied to grassland of 23 % of the N applied. Nathan and Malzer (1994), however, reported losses of only 0.8% of the urea applied. The relatively low emissions at Easter Bush are probably a reflection of the low application rate, the time of year and the prevailing meteorology at this time; for example the mean temperature during this period was only 5.2 °C, which would suppress emissions.

Although the measurements presented here were not designed with the aim of precisely determining emissions from grazing, a quick comparison can be made of the emissions observed during grazing periods with other grazing studies. The mean daily NH_3 flux data for the period 11/8/99 00:00 – 17/8/99 00:00 was 30.8 g NH_3-N ha^{-1} d^{-1}. This reduced period of data is chosen as an example period as the wind direction was from the S field for all this period and a record of animal numbers is available for this period (Fig. 4.18), showing an approximate average of 200 sheep in the S field at this time. The area of the S field is 5.424 ha and therefore if all the emission is presumed to arise from the sheep then this implies daily emissions from the sheep of 0.8 g NH_3-N $sheep^{-1}$ d^{-1}. Jarvis *et al.* (1991) report average losses of 0.9 and 1.2 g NH_3-N $sheep^{-1}$ d^{-1} from non-fertilised pastures and pastures fertilised with 420 kg N ha^{-1}, respectively, which are similar to the estimate obtained from Easter Bush.

The net annual exchange of NH_3 measured at Easter Bush for 1/5/1998 –30/4/1999 was +1.9 kg N ha^{-1} yr^{-1}. Table 1.3 lists values from other measurement studies; Easter Bush net exchange is close to the mid-point of these reported measurements. Duyzer (1994), Erisman *et al.* (1994) and Hesterberg *et al.* (1996) report heathlands and an extensively-managed grassland to be sinks of -12 to -13 kg N ha^{-1} yr^{-1}, while Flechard and Fowler, 1998 report a moorland in southern Scotland to be a net sink of -2.5 kg N ha^{-1} yr^{-1}. Plantaz (1998) reports an un-grazed pasture and a grazed pasture to be a net sink (–3.8 kg N ha^{-1} yr^{-1}) and net source (+6.2 kg N ha^{-1} yr^{-1}), respectively. Mosquera *et al.* (2001) report intensively-managed grassland in The Netherlands as a

net source of between 10 and 16 kg N ha^{-1} yr^{-1} but these measurements include substantial slurry-spreading emissions (see section 1.2.4).

The sum of the NH_3 emissions for the first four days after the cut and prior to the N fertilisation (5/6/98-8/6/98) was 0.122 kg N ha^{-1}. There are 60,500 km^2 of improved grassland in the UK (DETR, 2000), therefore scaling up the cutting emissions across the whole of the UK improved grassland would lead to 0.74 kt NH_3-N. UK NH_3 emissions for 2000 were 319.8 kt NH_3, equivalent to 263.4 kt NH_3-N (Table 1.1) so the cutting emissions would comprise 0.3% of the UK total emissions. If the total gross emissions from the field are summed, this amounts to 4.2 kg N ha^{-1} yr^{-1} x 6,050,000 ha = 25 kt NH_3-N yr^{-1}, equivalent to 9.5% of the UK total emissions. Although this calculation is approximate, it indicates that although direct fertiliser emissions from NH_4NO_3 fertilised grasslands make a small contribution to total NH_3 emission, the gross emission from all processes in fertilised grassland, including stomatal emission and cuticular desorption, make a much larger contribution.

5.5.3 Controls on exchange of ammonia at Easter Bush

It is clear from the full time course of NH_3 exchange (Fig. 5.11) and from exploring different case periods (Section 5.3) that the variation in NH_3 exchange observed at Easter Bush is strongly linked to the external management activities at the field site (cutting, fertilising and grazing). It is interesting to investigate whether these variations in the NH_3 exchange are also detected in the vegetation and soil measurements presented earlier (Section 4.4 and 4.5).

Fig. 5.24 compares the mean daily NH_3 fluxes against the measured values of apoplastic NH_4^+, total foliar NH_4^+ and available soil NH_4^+ and NO_3^- for 15/5/198-10/10/1998. Measurements are shown for the S field only. The foliar NH_4^+ measurements are an amalgamation of two datasets of measurements, one from the same leaves used to measure apoplastic NH_4^+ and the other from older leaves which were not analysed for apoplastic NH_4^+ (see section 4.4.3).

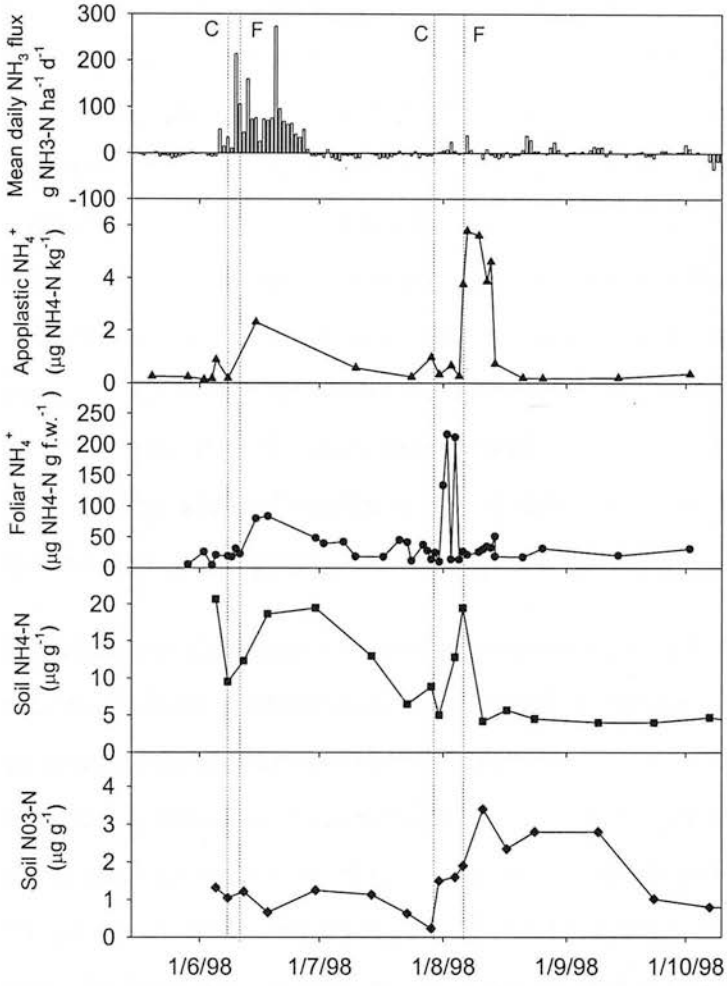

Figure 5.24. Mean daily NH_3 fluxes at Easter Bush plus measured values of apoplastic NH_4^+, total foliar NH_4^+ and soil NH_4^+ and NO_3^-. Vertical lines indicate timing of cutting (C) and fertilisation (F).

Variation is observed in apoplastic NH_4^+, total foliar NH_4^+ and available soil NH_4^+ and NO_3^- after cutting and fertilising events, however there are some interesting differences between the dynamics in these vegetation and soil measurements and the observed NH_3 fluxes. A significant change after cutting and prior to fertilisation is only seen in the foliar NH_4^+ after the second cut. Apoplastic NH_4^+ increases after both fertilisation events but not after cutting. This may be due to a stronger response of apoplastic NH_4^+ to increased available NH_4^+ in the soil, arising from increased NH_4^+ uptake through the xylem to the apoplast. The bioassay measurements are larger after the second cut in contrast to NH_3 emissions which were much greater after the first cut. However, very few bioassay measurements were made after the first cut and fertilisation so these results are less certain and it would be advisable to repeat the bioassay measurements with a higher frequency during both cuts to confirm these differences.

The different dynamics in soil NH_4^+ and NO_3^- are also notable; although both NH_4^+ and NO_3^- increase immediately following the second fertilisation, NH_4^+ then declines while NO_3^- remains at a greater value than before the second cut possibly indicating increased nitrification. If plant uptake of NO_3^- was greater after the second fertilisation then this could explain the reduced NH_3 emissions as plants taking up NO_3^- have been shown to produce smaller emissions than those taking up NH_4^+ (Schjoerring *et al.*, 1998). In summary, these vegetation and soil measurements help explain some of the differences in NH_3 fluxes, but it is still a challenge to link the measurements directly to the observed fluxes. A fully dynamic model which models these various soil and vegetation pools and nitrogen flows allows more detailed examination of the processes (see Chapter 7).

In addition to the strong effect of management, the prevailing meteorological conditions have a substantial effect on NH_3 exchange. Particular meteorological parameters that are known to influence NH_3 exchange are temperature, atmospheric turbulence, solar radiation, humidity and wetness (see section 1.3). Many of these parameters are inter-related (e.g. it is often windier during autumn and winter when temperatures are lower) and so it is difficult to isolate the influences of any one variable. However, as an example, the relationship of NH_3 concentration and NH_3 flux with air temperature are presented in Fig. 5.25 for key periods.

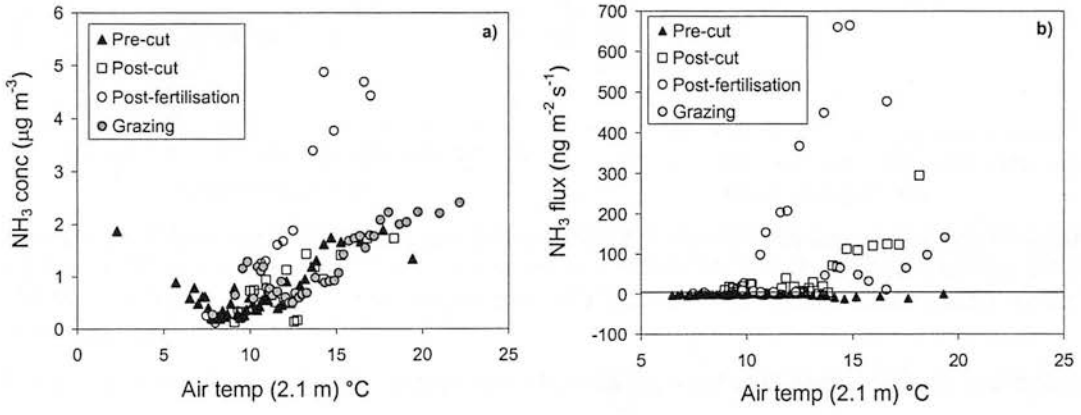

Figure 5.25. a) NH_3 concentration (2.06 m) in relation to air temperature (2.13 m) for different key periods: pre-cutting: 1/5/98–4/6/98, post-cutting: 5/6/98-8/6/98, post-fertilisation: 9/6/98-10/6/98 and grazing: 8/9/99-11/9/99. All dates are inclusive. b) NH_3 flux in relation to air temperature (2.13 m) for same key periods. Data are medians of 10, 25 or 50 15-minute measurements sorted by increasing temperature.

Fig. 5.25a shows that NH_3 concentration in general increases with increasing temperature. An exception is seen for the precut period when temperatures fall below about 7.5 °C, in which case NH_3 concentrations increase with decreasing temperature. The precut period was shown in section 5.3.1 to relate to a period of predominantly NH_3 deposition Low temperatures lead to poorer atmospheric dispersion (as there is less mixing of the atmosphere driven by heating of the surface). If there are local sources of NH_3, e.g. from neighbouring farms, then the plumes from these sources will be less dispersed in colder conditions leading to increased concentrations. The other key periods shown are all periods with predominantly emission of NH_3 and in these cases the NH_3 emission will increase with increasing temperature, either through the NH_3 compensation point increasing with temperature or if it is a soil-surface emission then volatilisation of NH_3 will increase with increasing temperature (see Eqs. 1.7 and 1.8). This increased emission then leads to increased concentration above the field (Fig. 5.26a and b). This interpretation of Figure 5.25a is supported by the observation of increasing NH_3 emission with increasing temperature as shown in Fig. 5.25b.

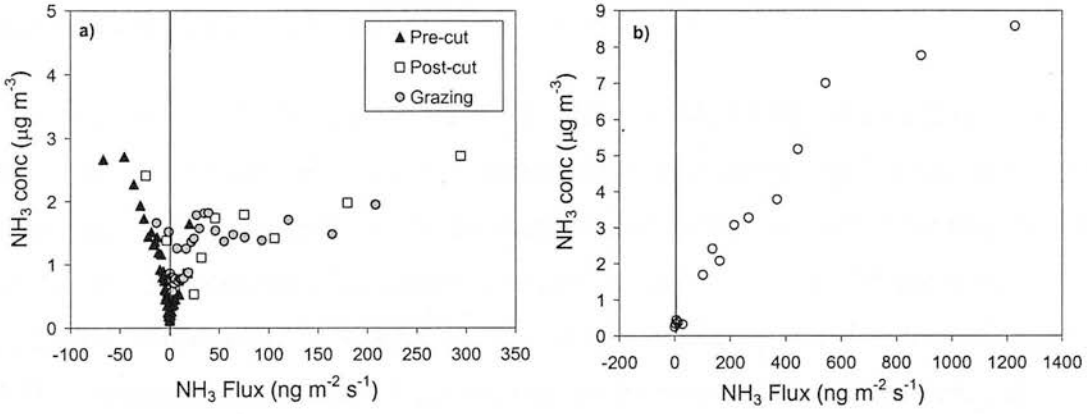

Figure 5.26. NH_3 concentration (1 m) in relation to NH_3 flux for different key periods: a) pre-cutting: 1/5/98–4/6/98, post-cutting: 5/6/98-8/6/98 and grazing: 1/9/99-30/9/99, b) post-fertilisation: 9/6/98-10/6/98. All dates are inclusive. Data are medians of 10, 25 or 50 15-minute measurements sorted by increasing flux.

For pollutants which are only deposited, increasing concentration leads to increasing deposition, as long as the resistances remain similar (see Eq. 2.42). However, for a pollutant such as NH_3, which can experience bi-directional exchange, although the concentration may still determine the flux during deposition periods, during emission periods it may be the NH_3 flux itself, which is controlling the NH_3 concentration at the site. This has also been observed by Sutton *et al.* (2000b) who measured bi-

directional NH_3 exchange over oilseed rape. The relationship of NH_3 concentration with NH_3 flux is presented in Fig. 5.26 for key periods; the data do show NH_3 deposition increases with increasing concentration for deposition periods, while for emission periods, concentration increases with increasing NH_3 flux. This demonstrates that it is the NH_3 flux, which is mostly controlling the NH_3 concentration at the site during these emission periods.

If the concentration was controlling the flux then emissions would increase as the ambient air concentration decreased, which is not observed. This is relevant in relation to the interpretation of bi-directional NH_3 fluxes according to the NH_3 compensation point of the canopy. In a simplified interpretation of this concept, the direction of the flux would depend on how the NH_3 air concentration varied in relation to the compensation point. Hence, if the air concentration was controlling the direction and magnitude of the flux, then emissions would increase as the ambient air concentration decreased. That this is not observed demonstrates that it is the varying magnitude of the surface emission potential (including the compensation point) that determines the magnitude and direction of the flux, rather than the NH_3 air concentrations, the effect of which is secondary.

This is shown most strongly for the fertilisation period, 9/6/98-10/6/98 (Fig 5.26b), while the relationship of increasing concentration with increasing flux seems to reach a plateau at about 50 ng m^{-2} s^{-1} for the post-cut and grazing periods. This may be due to the effect of atmospheric turbulence, which is also correlated with the flux. Increased atmospheric turbulence would increase the flux while also dispersing the NH_3 emissions and therefore dilute the increased concentrations. However, it is interesting that this does not seem to occur during the fertilisation period.

5.5.4 Enhanced ammonia emissions from grass cutting

Increased emissions of NH_3 after fertilisation and during grazing have been observed and quantified through numerous experiments and field studies. However, prior to 1998, increased emissions of NH_3 after grass cutting had been observed in only one other study (Sutton *et al.*, 1997a). The measurements reported in Sutton *et al.* (1997a) were of one day of emissions from cut grassland and were observed while

measuring NH_3 exchange downwind of slurry application. The measurements at Easter Bush provide a more extensive dataset and confirm increased emissions of NH_3 from three separate cutting events with larger emissions seen in the first cut of silage compared with the second. Bioassay measurements of foliar NH_4^+ did show an increase after cutting while apoplastic NH_4^+ showed an increase following fertilisation. Loubet *et al.* (2002) and Sutton *et al.* (2001a) discuss various hypotheses for the increase in foliar and apoplastic NH_4^+ following cutting and fertilising. It may be due to a decrease in net photosynthesis, which is observed following cutting, leading to a reduced utilisation of the available N and hence accumulation of NH_4^+ in the plant tissues. After fertilisation, increased available NH_4^+ in the soil can lead to increased NH_4^+ uptake through the xylem to the apoplast, further increasing NH_3 emissions.

The enhanced NH_3 emissions following cutting could also arise from sources other than the remaining cut sward, for example from the litter and from the soil itself. An integrated experiment on NH_3 exchange was held in Germany in May-June 2000 at an intensively-managed grassland (see Chapter 8). David *et al.* (2004) report cuvette measurements of NH_3 exchange from different compartments (bare soil, cut grass with litter present, cut grass with no litter present), after grass cutting during the integrated experiment. They conclude the origin of the emissions after cutting is difficult to assess, but the emissions are likely to arise from a combination of the remaining sward (including green and senescing leaves) and remaining leaf litter. They conclude that the soil was not a significant contributor to the flux. Further cuvette measurements and physiological measurements would be needed to fully determine the source of the cutting emissions.

Chapter 6: Modelling NH_3 exchange at Easter Bush: resistance modelling

6.1 Introduction

The primary ecological concerns regarding reduced nitrogen are its contribution to acidification and eutrophication of sensitive ecosystems and to aerosol formation in the atmosphere (see Section 1.1.3). The relative contribution of NH_x to acidification of ecosystems is increasing as emissions of sulphur dioxide are decreasing. As a result of these concerns and as a move towards integrated pollution control, NH_x is being incorporated for the first time into European transboundary air pollution abatement strategies (see Section 1.1.4). The assessment of critical load exceedance plays a central role in pollution control strategies and this requires accurate descriptions of the wet and dry deposition of NH_x to ecosystems. Wet deposition of NH_4^+ is more easily measured than NH_3 dry deposition, and there is an extensive monitoring network already in place across Europe. Measurements of dry deposition of NH_3 are complex and costly and as a result there are very few flux monitoring stations. Consequently, estimates of dry deposition of NH_3 across a domain such as the UK or Europe, depend on atmospheric transport models (ATM's), which, in turn, depend on an accurate parameterisation of NH_3 exchange.

A number of models describing dry deposition of NH_3 have been developed using the resistance analogy approach (see Section 2.4). Nemitz *et al.* (2001) introduced a two-layer "canopy compensation point" model, which in addition to describing deposition to the plant cuticle, can account for emission of NH_3 from the canopy and from an additional layer at ground level (Section 2.4.5). However, before this model can be fully adapted within an ATM, progress is required on parameterising the key model variables for the dominant ecosystem types across Europe and also on assessing the seasonal variation of these parameters. Many of the parameterisations for NH_3 exchange currently available were obtained from measurement campaigns of only a few weeks and most parameterisations do not vary seasonally. The measurements presented in Chapter 5 demonstrate the large seasonal variation observed in NH_3 exchange with intensively managed grassland, particularly

following different management activities. The net exchange is seen to change from a source to a sink at different times of the year. This variation is not captured in current parameterisations of NH_3 exchange with grassland (e.g. Smith et al., 2000). This chapter describes the application of the two-layer canopy compensation point model to the Easter Bush field site and develops seasonal parameterisations of NH_3 exchange with the intensively managed grassland.

6.2 Model description

The two-layer canopy compensation point model (Fig. 6.1) was chosen to parameterise the measurements presented here as it balances the requirement of having sufficient complexity to describe the processes involved, while still being simple enough to include in the modelling approach across Europe. A full model description is given in Section 2.4.5.

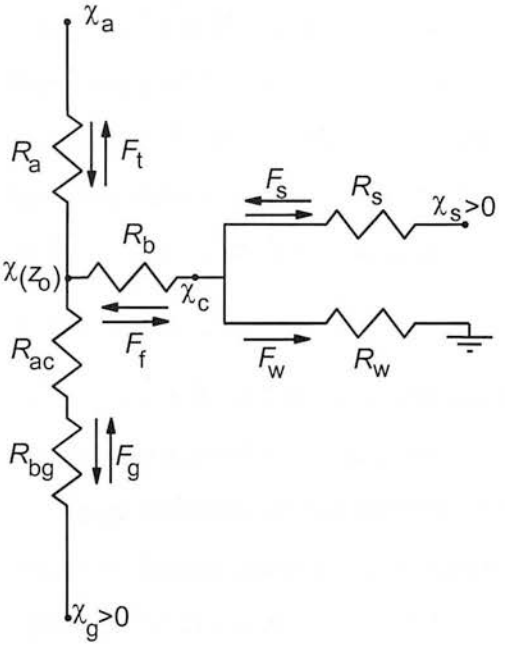

Fig 6.1. Diagram of the two-layer canopy compensation point resistance model of NH_3 exchange (Nemitz *et al.*, 2001). For a description of the symbols see Section 2.4.5.

To recap, the two-layer canopy compensation point model incorporates bi-directional foliar stomatal exchange, deposition to leaf cuticles and NH_3 exchange with the ground surface. There are six resistances to transfer: aerodynamic resistance (R_a), boundary-layer resistance (R_b), stomatal resistance (R_s), cuticular resistance (R_w), in-

canopy aerodynamic resistance (R_{ac}) and ground boundary-layer resistance (R_{bg}) and two emission potentials: the foliar emission potential (Γ_s) and the ground layer emission potential (Γ_g). The ability to parameterise foliar and ground layer emission potentials separately is essential when modelling a system in which fertiliser is applied on a regular basis (three-four times per year) and is a significant improvement on earlier modelling approaches.

6.3 Parameterisations: resistances

A key challenge in developing parameterisations is characterising how the various resistances and emission potentials vary with meteorology, phenology and management activities (such as cutting and fertilising).

6.3.1 Aerodynamic resistance and boundary-layer resistance

Formulations for the aerodynamic resistance and boundary-layer resistance are given in Eq. 2.47 and Eq. 2.48, and relate to meteorological parameters such as u and $u*$. The diurnal and seasonal variation in R_a and R_b arises from the corresponding variation in the meteorological parameters, which can be easily measured. R_a and R_b are independent of plant stage and management activities apart from the interaction with changes in surface roughness.

6.3.2 Stomatal resistance

In contrast to R_a and R_b, stomatal resistance (R_s) and cuticular resistance (R_w) are likely to be dependent on the extent of the canopy. A greater area available for gas exchange should lead to a smaller resistance. Consequently a seasonal parameterisation needs to incorporate some measure of the extent of the canopy. A useful property is the Leaf Area Index (LAI), which is a measure of the leaf area of a canopy per unit ground area (see section 3.4.1). The LAI at Easter Bush was measured monthly or more frequently around periods of cutting. An empirical relationship between canopy height (h_c) in m and LAI in $m^2\ m^{-2}$ was determined for Easter Bush ($LAI = -22.75h_c^2 + 19.2h_c - 0.14$) (Figure 6.2), which enabled the more regularly measured canopy height measurements to be converted to an estimate of LAI. Fig. 6.2 shows that the relationship between canopy height and LAI is not

linear, since as the grassland grows there are more individual tall flower stems that increase the overall mean canopy height, but do not provide a large canopy area.

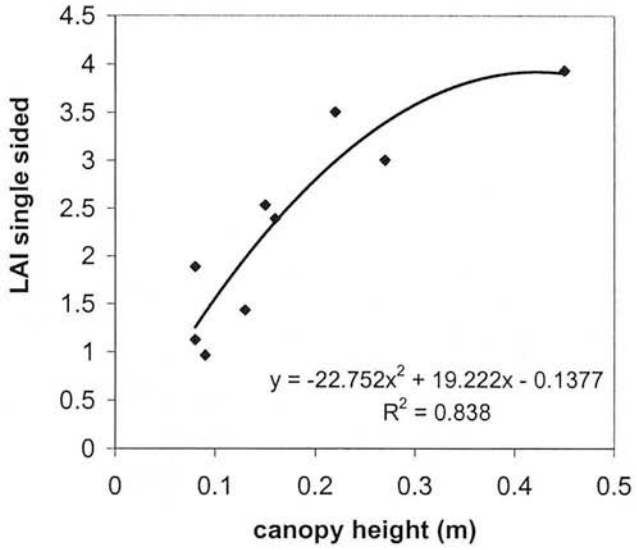

Figure 6.2. Relationship between Leaf Area Index (LAI) and mean canopy height for Easter Bush, 1999 data.

R_s was parameterised from measurements of R_s for water vapour (R_{sE}) (Eq. 2.54) obtained in dry ($RH < 80\%$), daytime ($S_t > 50$ W m^{-2}) conditions for $R_a + R_b < 500$ s m^{-1}. The Hicks *et al.* (1987) formulation was used, adapted by Sutton and Fowler (1993) to use solar radiation (S_t) instead of photosynthetically active radiation (PAR) (Eq. 6.1). Correction factors were not introduced for water stress and humidity as this Scottish site is well watered for all times of the year.

$$R_s = R_{s,min}\left(1+\frac{\beta_s}{S_t}\right)\frac{3.5}{\mathrm{LAI}} \qquad (6.1)$$

$R_{s,min}$ is the minimal stomatal resistance, β_s is a constant. The values of $R_{s,min}$ = 65 s m^{-1} and β_s = 90 W m^{-2} were chosen since they provided close agreement between measured and modelled R_{sE} for a period when the measured LAI was 3.5 m^2 m^{-2} (single-sided). R_s was scaled by LAI for the rest of the measurement period. This gave reasonable agreement between measured and modelled R_{sE} for the whole measurement period. A comparison of measured versus modelled R_{sE} over the period of the 2nd cut in August 1999 is shown in Fig. 6.3. This shows clearly the effect of

the cut, which acts to increase R_{sE} due to the reduction in leaf area, and modelled R_{sE} broadly reproduces these differences.

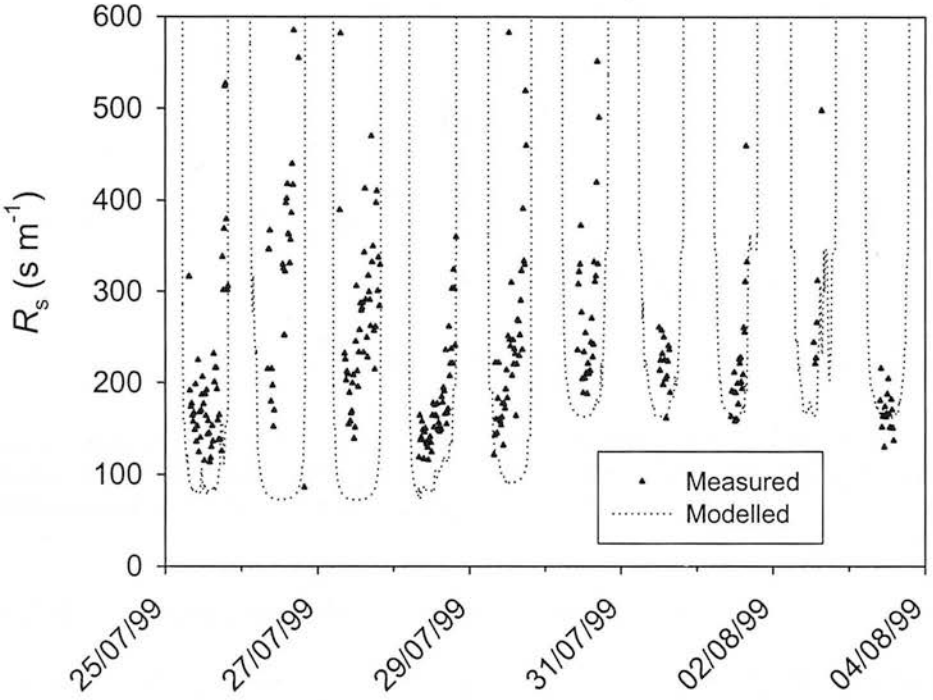

Figure 6.3. Measured and modelled R_{sE} over the period of the 2nd cut, August 1999. Ticks show days at 00:00. Measured data only shown for RH (1 m) < 80%, S_t > 50 W m^{-2} and $R_a + R_b$ < 500 s m^{-1}.

6.3.3 *Cuticular resistance*

Cuticular resistance, R_w, was parameterised following Sutton and Fowler (1993), but incorporating a scaling for LAI:

$$R_w = R_{w,min} \exp\left((100 - RH)/a\right)\frac{3.5}{LAI} \qquad (6.2)$$

where $R_{w,min}$ is the minimum cuticular resistance, RH is relative humidity at 1 m (%) and a is a constant. The parameterised values of R_w were obtained by obtaining the best fit of the model to night-time R_c estimates in a number of key periods, excluding periods of nocturnal soil emissions. During night-time, the stomata are closed and therefore it is assumed that the only major pathway of NH_3 exchange is to the leaf cuticle, so that $R_w \approx R_c$. The parameterised values used were $R_{w,min} = 4$ s m^{-1}, $a = 6.5$; the parameterisation also includes a LAI dependence. Fig. 6.4 shows the relationship between measured night-time R_c (in deposition periods only and while $R_a + R_b$ < 500 s m^{-1}) and RH(1 m) for May 1999, together with the parameterisation for R_w.

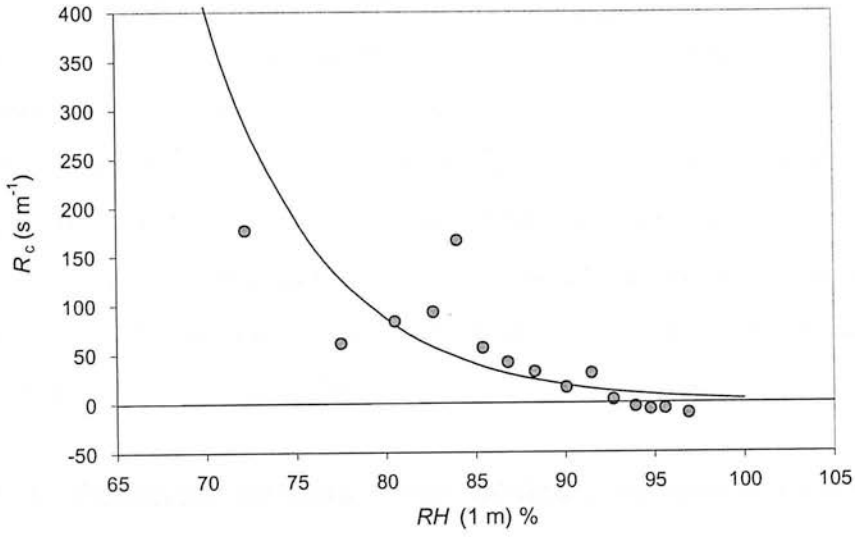

Figure 6.4. Measured values of night-time R_c (for deposition periods only and $R_a + R_b < 500$ s m^{-1}) versus *RH* (1 m) for May 1999, points are medians of 50 values, after sorting for ascending *RH*. The parameterisation for R_w is also shown ($R_{w,min} = 4$ s m^{-1}, $a = 6.5$).

6.3.4 *In-canopy aerodynamic resistance*

Nemitz *et al.* (2001) proposed the following relationship for the in-canopy aerodynamic resistance, $R_{ac}(d + z_0) = \alpha(d + z_0)u_*^{-1}$ (see Section 2.4.5, Eq. 2.64). Measurements of in-canopy turbulence were not conducted at Easter Bush, but in-canopy measurements of σ_w and other parameters were made in a similar grassland canopy (also predominantly *Lolium perenne*) during a field experiment in Braunschweig, Germany, 2000 (Nemitz *et al.*, 2004). These measurements led to an estimate of $\alpha = 40$, for a canopy height of 0.45 m. The same value of α was chosen for the parameterisation of R_{ac} at Easter Bush, but R_{ac} was scaled according to canopy height (h_c) in m:

$$R_{ac}(d + z_0) = \frac{40h_c}{0 \cdot 45} u_*^{-1} \qquad (6.3)$$

6.3.5 Ground boundary layer resistance

The ground boundary layer resistance, R_{bg}, was parameterised following Eq. 2.66.

($R_{bg} = \dfrac{Sc - \ln(\delta_0 / z_g)}{k u_{*g}}$). Schuepp (1977) reports results of in-canopy transfer in a variety of field experiments over different vegetation types. From these

measurements, an empirical relationship can be derived between u_{*g} and wind speed above the canopy ($u_{*g} = u/20$). Schuepp (1977) did not state the height of the wind speed measurements above the canopy but mean wind speed at the sonic height (2.1 m) was used to derive u_{*g} for Easter Bush in the absence of within-canopy turbulence measurements. Schuepp (1977) showed that it is difficult to determine the value of z_g with accuracy, but it is also true that R_{bg} is not that sensitive to changes in z_g. A value of $z_g = h_c/5$ was chosen as a best estimate for z_g, comparing with field measurements reported in Schuepp (1977).

6.4 Parameterisations: stomatal and ground emission potentials

The parameterisation of the emission potentials is more complex as they vary with phenology and management activities and it is also difficult to distinguish between contributions to emission from the two sources (foliar and ground). As an initial step towards providing a fully seasonally varying parameterisation, the emission potentials are parameterised for each of the key periods described in Section 5.3: 1) pre-cut, 2) post-cut, 3) post-fertilisation, 4) grazing and 5) winter). As demonstrated in Section 5.3, these key periods all exhibit a different pattern of NH_3 exchange, some showing net emission while other periods demonstrate net deposition. Based on the other parameters, values of Γ_g were estimated by fitting the model to measured nighttime fluxes, while values of Γ_s were found by fitting the model to measured daytime fluxes.

6.4.1 Pre-cut

The pre-cutting value of the stomatal emission potential (Γ_s) and ground layer emission potential (Γ_g) were estimated at 630 and 110, respectively. The measured and modelled net NH_3 exchange for an example pre-cut period (21-27/5/99) are shown in Fig. 6.5. While this represents a model 'fit', these results show that the model is able to broadly reproduce the temporal structure of the NH_3 exchange fluxes. There are some periods of disagreement, e.g. the model is not able to reproduce the emission period observed on 21/5/99. This emission is probably due to desorption of NH_3 from the cuticle. Such desorption cannot be modelled by this two-

layer model and a dynamic model of the leaf chemistry, such as described by Flechard *et al.* (1999), would be required to reproduce this emission.

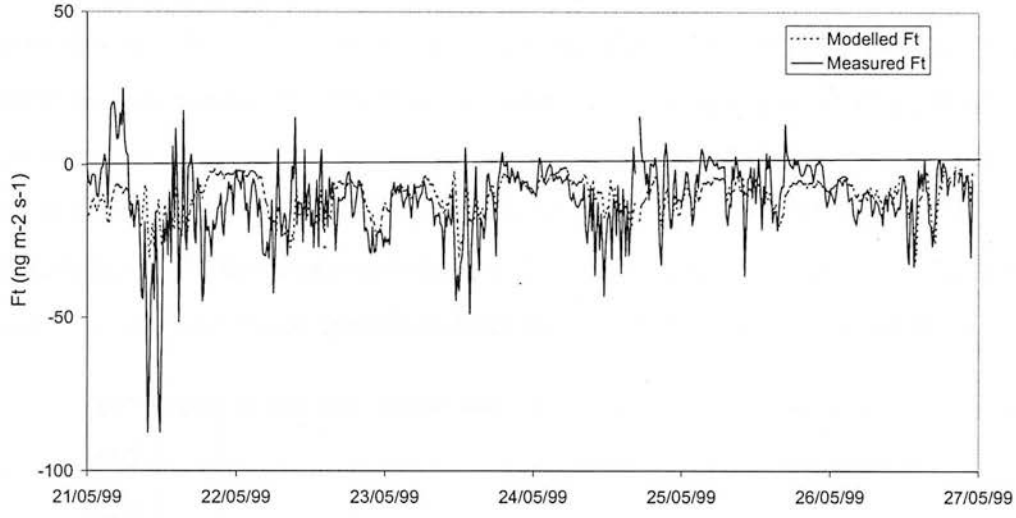

Figure 6.5. Measured and modelled net flux (F_t) for the period 21-27/5/99

6.4.2 Post-cut and fertilisation

The measurements during the 1st cut of silage in 1999 were used to parameterise the emission potentials for the periods of cutting and fertilising. This period was chosen because after this cut on 2nd June 1999, the field was not fertilised until 11th June (Fig. 6.6). Therefore this extended period of nine days enables the foliar emission to be studied separately from the enhanced ground surface emission from fertiliser. In addition, in 1999 the two fields were cut and fertilised at the same time whereas in 1998 the N field was fertilised five days later than the S field and this introduces greater complexity into the modelling process. Enhanced emissions after cutting were not observed until a few days after the cut in 1999 (Fig. 6.6); it is hypothesised that this is due to the large amount of rain that fell immediately after the cut and persisted until seven days after the cut, most likely suppressing any potential emission or recapturing it on wet leaf surfaces.

The fields were fertilised on 11th June in the late afternoon and an increased emission was not observed until 13/6/99 (Fig. 6.6). During 11-12/6/99 there was reduced relative humidity and no rain so it is possible that the pellets of ammonium nitrate fertiliser may not have dissolved immediately, thereby limiting emissions. However, on 13 and 14th June the emissions increased to 750 ng m^{-2} s^{-1} and 1600 ng m^{-2} s^{-1},

respectively; significant nocturnal emissions were also observed. Nocturnal emissions can only arise from non-stomatal emissions and it is concluded that this emission represents direct fertiliser emission at the ground surface. Nocturnal emission continued for 4 more nights. The daytime enhanced emissions continued until approximately 26/6/99. This is unlikely to be continuing direct fertiliser emission as the nocturnal emissions were no longer present and emissions from mineral fertilisers had not been observed to last for two weeks in other field experiments. As discussed in Section 5.5.4, this enhanced emission was likely to be due to a combination of emissions from the sward itself and from leaf litter.

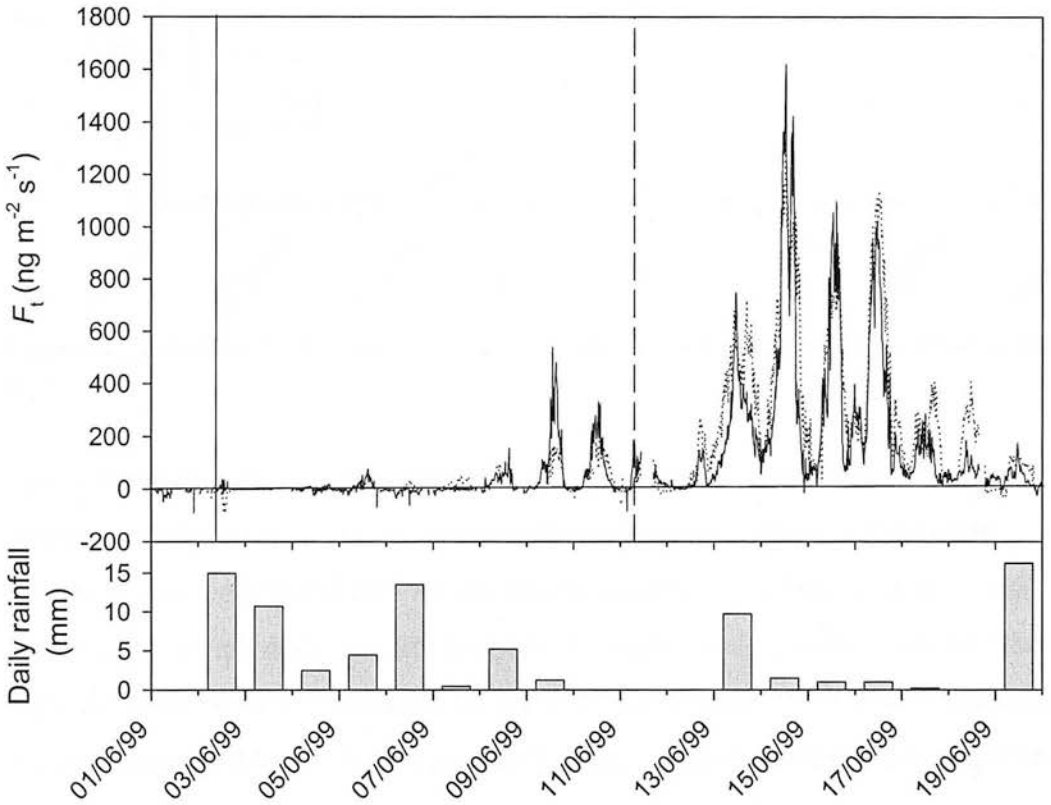

Figure 6.6. Measured and modelled net NH_3 flux (F_t) for 1/6/99-20/6/99, plus the daily rainfall during this period. Vertical lines indicate cutting (solid lines) and fertilisation (dashed lines).

Following these observations, the foliar emission potential, Γ_s, was increased over the cutting period and for the two weeks following fertilisation. An initial parameterisation of Γ_s was obtained by fitting the model on a daily basis to the measurements for the period 2-11th June. A Gaussian curve was fitted to the daily parameterised values of Γ_s to provide a continuous function for the emission potential (Fig. 6.7). The parameterisation of Γ_s reached a maximum of 28,000 at

12:00 on 14/6/99 and then decreased to the background pre-cuttting value of 630 on 27/6/99. To parameterise the increased fertiliser emissions, a ground emission potential, Γ_g, was introduced at the time of fertilisation. Γ_g was decreased from a maximum value of 35,000 and returned to a value of 1100 after 6.5 days (Fig. 6.7). It is not possible to determine precisely the time period of direct fertiliser emissions. The period of 6.5 days was selected as representing the period over which nocturnal emissions were observed.

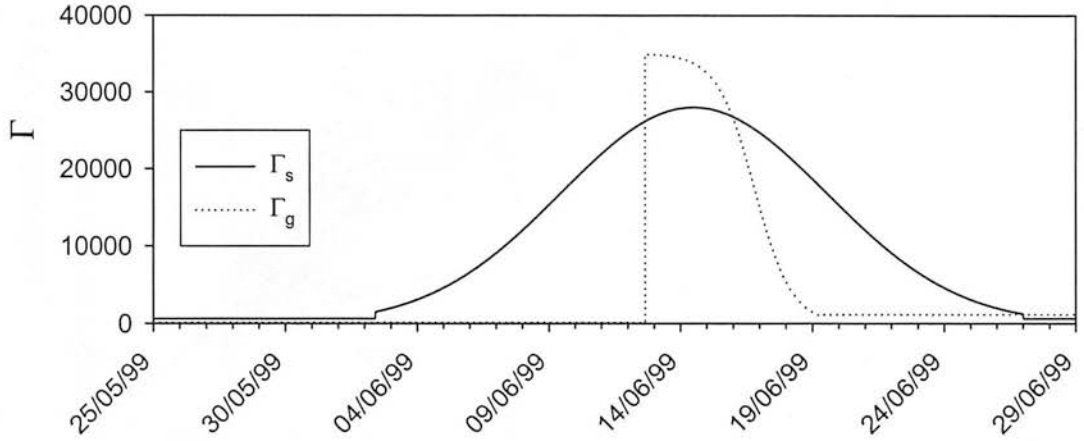

Figure 6.7. Functions for the foliar emission potential (Γ_s) and the ground layer emission potential (Γ_g).

The combination of these two emission potentials in conjunction with the parameterisations for R_s and R_w given earlier gives close agreement between measured and modelled fluxes for the period of cutting and fertilising (Fig. 6.6). However, there are discrepancies between the model and measurements and these indicate areas for improvement in the model. For example, the model overestimates the emissions on 13/6/99 indicating that Γ_g is too large at this time. It is possible that Γ_g (similarly for Γ_s) should increase to a maximum value rather than reaching the maximum immediately after application. In addition, the heavy rainfall on 13/6/99 may have suppressed the emissions. Linking Γ_g mechanistically to precipitation and relative humidity would be an improvement. Emissions are also overestimated on 17 and 18/6/99, this is largely due to stomatal emissions and indicates that Γ_s is possibly overestimated at the end of the cutting and fertilising period.

A comparison of 15-minute measured and modelled NH_3 fluxes for June 1999 is presented in Fig. 6.8. This shows good agreement over the full range of fluxes, with

some underestimation of large emission fluxes and overestimation of fluxes in the lower range. The overall agreement, however is encouraging ($R^2 = 0.83$), given that June 1999 is a period with large variation in NH_3 exchange and considerable changes in canopy area and structure.

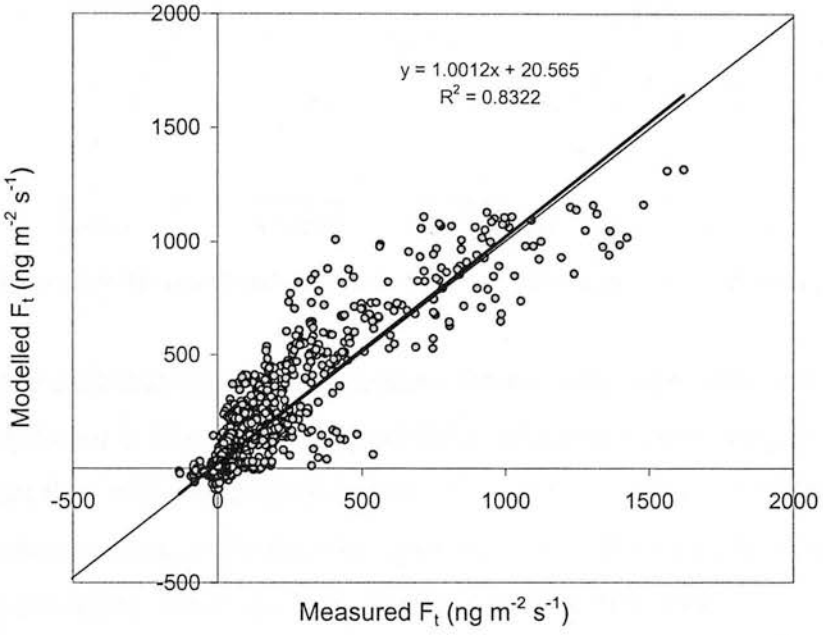

Figure 6.8. Comparison of measured and modelled 15-minute net NH_3 exchange for June 1999.

6.4.3 Grazing

It is also a challenge during the grazing periods to separate the contribution from the foliar and ground level emissions. As an initial estimate, constant parameterisations of Γ_s (= 4000) and Γ_g (= 5000) were chosen during grazing. Fig 6.9 shows the measured and modelled net flux for 8-12/9/99 with these fixed values of Γ_s and Γ_g and all other variables parameterised as described above. The model reproduces the daily structure in the measurements remarkably well given that these fixed emission potentials are used throughout the whole period.

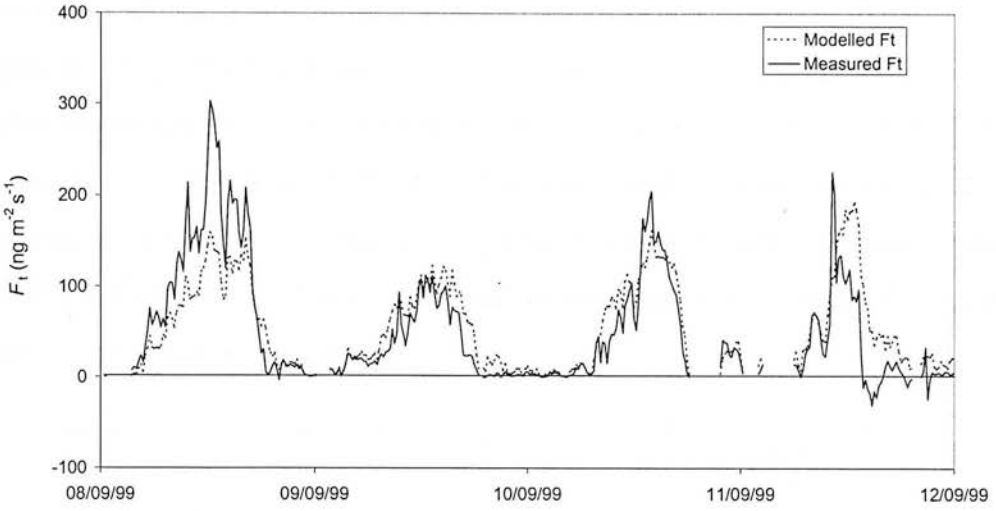

Figure 6.9. Measured and modelled net flux (F_t) for the period 8-12/9/99, $\Gamma_s = 4000$ and $\Gamma_g = 5000$.

The contribution of the component fluxes to the net modelled flux (F_t) for this period is shown in Fig. 6.10. The ground flux (F_g) provides the largest contribution to the net flux, with stomatal emissions (F_s) contributing about 15-30% of the daytime emission flux, while there is significant deposition to the leaf cuticle (F_w), particularly during the late afternoon/evening of 8/9/99.

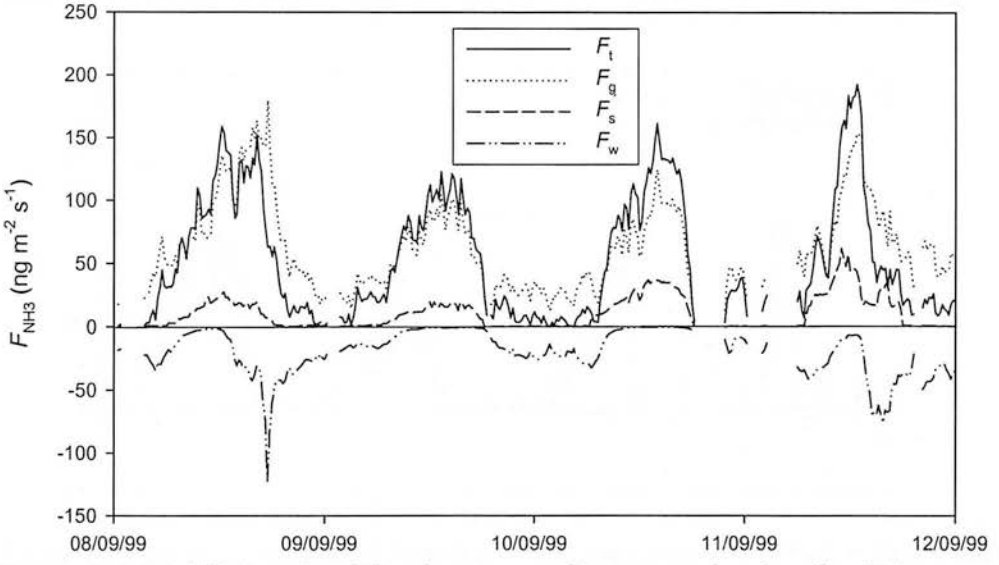

Figure 6.10. Modelled net flux (F_t) and component fluxes, ground surface flux (F_g), stomatal flux (F_s) and cuticular flux (F_w) for the period 8-12/9/99.

Fig. 6.11 shows the modelled flux when the stomatal emission potential is set to near zero. This demonstrates that the model can reproduce the measurements during this grazing period with only emission from the ground layer, with a ground emission potential, Γ_g, of 5500. Fig. 6.12 shows the equivalent modelled flux when the ground

emission potential is set to near zero and demonstrates that a large stomatal emission potential (Γ_g = 20,000) is required to reproduce the measured emission and even with this large emission potential, the magnitude of emissions on 8/9/99 and the nocturnal emissions on 9/9/99 and 11/9/99 are not reproduced. This indicates that the parameterisation of Γ_g for this grazing period is fairly robust. The exact value of Γ_s is difficult to determine, but the modelled net exchange is not too sensitive to the choice of Γ_s in this period.

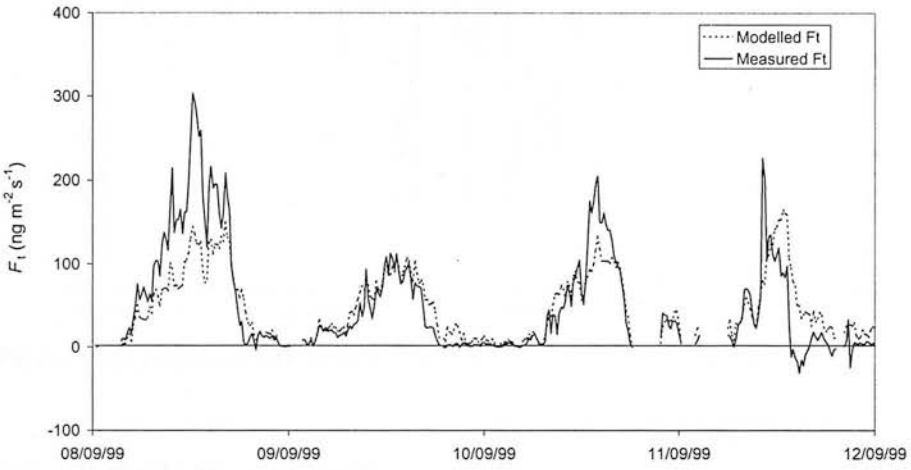

Figure 6.11. Measured and modelled net flux (F_t) for the period 8-12/9/99, Γ_s = 1 and Γ_g = 5500.

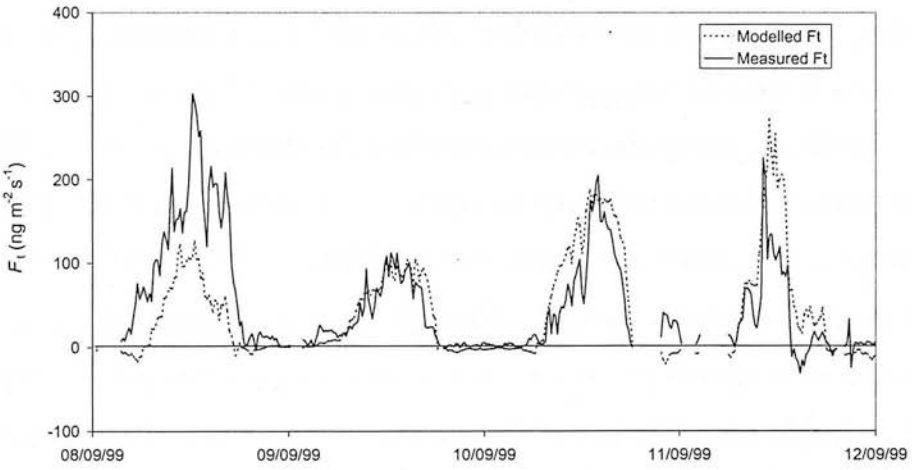

Figure 6.12. Measured and modelled net flux (F_t) for the period 8-12/9/99, Γ_s = 20,000 and Γ_g = 1.

6.4.4 Winter

The performance of the two-layer model for a winter period is shown in Fig. 6.13. The parameterisations of the resistances are identical to those for the previous periods. The foliar emission potential and ground layer emission potential are set at

the same value as for the pre-cut period (630 and 110, respectively). The model generally agrees closely with the measurements apart from underestimating the deposition during the night of 28/1/99 and not reproducing a period of emission on 29/1/99, which was probably a result of cuticular desorption.

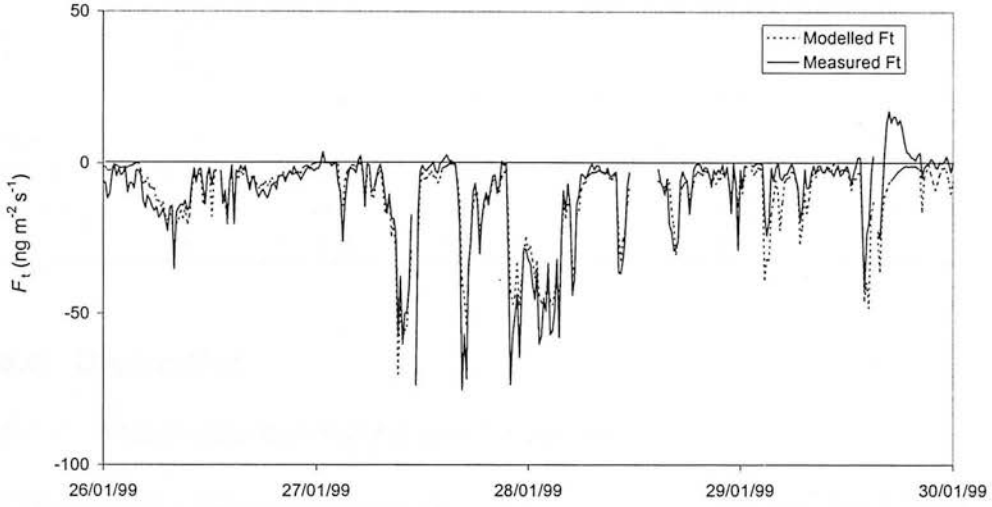

Figure 6.13. Measured and modelled net flux (F_t) for the period 26-30/1/99.

6.5 Sensitivity Analysis

A sensitivity analysis of the modelled mean net NH_3 exchange to changes in key input parameters was conducted for June 1999 and the results are given in Table 6.1. The mean measured values of F_t, $F_{t,\,day}$ and $F_{t,night}$ for June 1999 were 77.9, 99.9 and 29.3 ng m^{-2} s^{-1}, respectively while the corresponding mean modelled values were 99.2, 126.9 and 40.8 ng m^{-2} s^{-1}, respectively. Table 6.1 indicates that in this particular period (June 1999) the model estimate of net NH_3 exchange is most sensitive to Γ_g and the in-canopy resistances R_{ac} and R_{bg}. The sensitivity to Γ_s and $R_a + R_b$ is less (a 25% change in these parameters results in a 8-12% change in the flux). As expected, changes in Γ_s and R_s do not have a significant effect on the nighttime flux, while changes in R_w have a greater effect on the nighttime flux than during the daytime. It must be noted that the sensitivity of the net exchange to these parameters would be different in other key periods, for example during a period of small ground layer emissions, or during a period of predominantly deposition of NH_3. These results are indicative of the model sensitivity during a cutting and fertilising period.

Table 6.1. Sensitivity analysis of the two-layer model. The percentage change in modelled mean net exchange (F_t) for June 1999 is given for a parameter change of ± 25 %. Also shown are the relative changes in modelled daytime ($F_{t,\,day}$) and nighttime ($F_{t,\,night}$) net exchange.

	Percentage change in F_t for the specified parameter change		Percentage change in $F_{t,\,day}$ for the specified parameter change		Percentage change in $F_{t,\,night}$ for the specified parameter change	
Parameter	-25 %	+25 %	-25 %	+25 %	-25 %	+25 %
Γ_s	-11.5	11.5	-13.1	13.1	-1.0	1.0
Γ_g	-18.1	18.1	-15.8	15.8	-32.9	32.9
R_s	9.9	-6.5	11.3	-7.4	1.1	-0.7
R_w	-3.2	2.3	-2.5	1.7	-8.1	6.0
$R_a + R_b$	10.0	-8.2	10.4	-8.5	7.4	-6.4
$R_{ac} + R_{bg}$	13.5	-9.1	10.9	-7.3	30.2	-21.2
χ_a	4.6	-4.6	3.9	-3.9	8.9	-8.9

6.6 Discussion

6.6.1 Seasonally varying parameterisations

The seasonal variation in stomatal, cuticular and in-canopy resistances was parameterised through the seasonal change in measured meteorological parameters such as S_t, RH and u_* and also from changes in LAI or canopy height. Parameterisations of the stomatal and ground layer emission potentials were provided for key periods of the year (Table 6.2). Fixed values of Γ_s and Γ_g were used to parameterise the pre-cut, grazing and winter period, while time-dependent functions were used to model the period of cutting and fertilising, where large variation in measured NH_3 exchange was observed.

Table 6.2. Values of stomatal (Γ_s) and ground layer (Γ_g) emission potentials for key periods.

Period	Γ_s	Γ_g
Pre-cut	630	110
Post-cut and post fertilisation	Max: 28,000	Max: 35,000
Grazing	4000	5000
Winter	630	110

Smith *et al.* (2000) describe a model, which is used to provide dry deposition estimates of pollutants, including NH_3, to the UK. This model only incorporates a single-layer resistance approach for NH_3 exchange, it uses a fixed stomatal emission potential of 3,800 for both grassland and arable land. The results presented here

indicate that an emission potential of 3,800 would be an overestimate in the winter and pre-cut period and a significant underestimate during the cutting and fertilising period. The value is similar to those used in the grazing period, although the two-layer model would give larger emission as it models the two different pathways of exchange, from the soil and from the plant. It would be interesting to examine the consequence of using a seasonally varying emission potential in the UK model. The reduced emission potential in the winter would increase deposition to grassland, therefore possibly reducing deposition to semi-natural areas and result in a decrease in critical load exceedance. Conversely, the increased emission potential in the summer period would lead to more NH_3 being available for deposition to semi-natural areas and a possible increase in critical load exceedance.

6.6.2 Performance of the two-layer model

The two-layer canopy compensation point model provided close agreement with the measured NH_3 fluxes. In particular, the agreement for a range of different periods, exhibiting different NH_3 exchange characteristics is encouraging. The sensitivity analysis demonstrated that the modelled net NH_3 exchange is not too sensitive to changes in the key input parameters. A change of ± 25% in the input parameters resulted in a percentage change in the modelled net NH_3 exchange of between 2.3 to 18.1%. As expected for a fertilising period, the modelled net NH_3 exchange was most sensitive to Γ_g.

One of the advantages of the two-layer model is that it is capable of modelling emission from the plant and from a ground layer source. However, this does increase the complexity of the modelling task and it is a challenge to partition the contribution of the emission from these two sources. Correctly modelling nocturnal emissions provides some confirmation of the choice of Γ_g and this was the method employed in the grazing and fertilising period. Future work could develop fully seasonally varying emission potentials. However, the emission potential estimates are currently empirical and it would clearly be an improvement to model them in a mechanistic approach, in relation to the plant and soil NH_4^+ availability. This is the approach followed in dynamic ecosystem models and the application of such a model to the Easter Bush measurements is described in Chapter 7.

Chapter 7: Modelling NH_3 exchange at Easter Bush: dynamic ecosystem modelling

7.1 Introduction

The previous chapter described results from the application of a two-layer resistance model to the Easter Bush NH_3 exchange measurements. The advantage of the resistance modelling approach is the simplicity of the model, which enables processes of NH_3 exchange to be explored in a relatively straightforward manner. In addition, as the number of input variables required is not too onerous, the model can be incorporated into national or international modelling approaches, allowing generalisation over a larger domain. However, the parameterisation of emission potentials within the resistance modelling approach is currently empirical. The development of bioassays to measure apoplastic NH_4^+ concentration should reduce the empiricism, but there are still uncertainities about the magnitude of the bioassay estimates of apoplastic NH_4^+ concentration (Hill *et al.*, 2001).

Dynamic ecosystem models, however, seek to reduce the level of empiricism and provide a fully mechanistic description of growth, nutrient and water cycling and gaseous exchange of an ecosystem. The advantages of a dynamic ecosystem model compared with a resistance approach are numerous; as an ecosystem model includes the soil, plant and atmosphere in a functional way, the interactions between these compartments can be explored more thoroughly and a more sophisticated treatment of nutrient cycling can be included. In addition, scenarios of change in various input variables can be examined, allowing the effect of climate change or abatement options (for pollutants) to be explored. Various grassland ecosystem models have been developed and some of these are summarised in Section 1.4.4. However, none of these models treat bi-directional exchange of NH_3 with a mechanistic approach; Riedo *et al.* (2002) describe the first approach to provide a functional basis for bi-directional exchange of NH_3 within a grassland ecosystem model named PaSim.

This chapter provides a brief description of the modifications made to PaSim to incorporate NH_3 bi-directional exchange, these modifications were made by Dr.

Marcel Riedo during a fellowship at CEH. Comparisons of model simulations versus 1998 NH_3 exchange measurements at Easter Bush are given by Riedo *et al.*, 2002. This chapter presents comparisons of simulated values against measured vegetation parameters, NH_3 exchange measurements in 1999 and also presents results from some initial scenarios of changing management and climate.

7.2 Model description

A full description of the dynamic ecosystem model, PaSim, is given by Riedo *et al.* (1998) and a description of the modification of PaSim to incorporate bi-directional NH_3 exchange is given by Riedo *et al.* (2002) (also included in Appendix A1). Only a brief description is given here, and the description concentrates on the changes made to include NH_3 exchange.

Earlier versions of PaSim did not include bi-directional exchange of NH_3, instead a fixed amount of NH_3 deposition was included in the model as a driving variable (Riedo *et al.*, 1998). The main modifications to PaSim to enable a better mechanistic description of NH_3 exchange were: i) the incorporation of the two-layer canopy compensation point model (Nemitz *et al.*, 2001) as described in section 2.4.5, ii) the partitioning of plant substrate N into two separate pools, apoplastic substrate N and symplastic substrate N and iii) the separation of the existing single soil layer into multiple soil layers including a soil surface layer, allowing a soil surface NH_3 concentration to be defined.

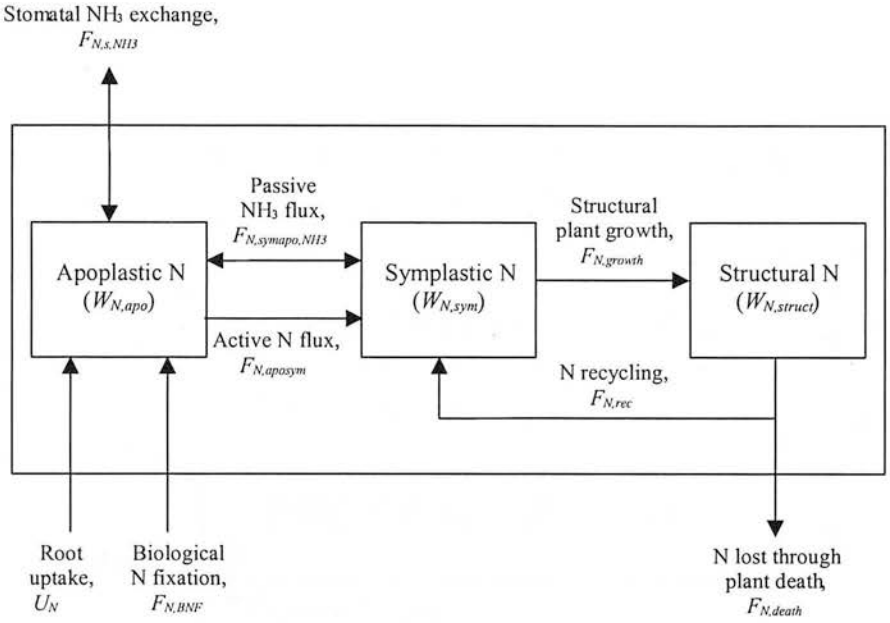

Figure 7.1. Plant N in PaSim is partitioned into structural N, $W_{N,struct}$, apoplastic substrate N, $W_{N,apo}$, and symplastic substrate N, $W_{N,sym}$. All input/output fluxes of the N pools are shown except for the losses from grazing and cutting (from Riedo et al., 2002).

Incorporating the two-layer canopy compensation point model into PaSim involved introducing the two emission potentials, the foliar emission potential, described by χ_s and the ground surface emission potential, characterised by χ_g. All the transfer resistances except R_w, were already present in PaSim for the calculation of evapotranspiration, so a parameterisation for R_w was introduced (Eq. 2.56). The next step was to link the model values of χ_s and χ_g to the N dynamics within the model. Plant substrate N was partitioned into apoplastic and symplastic substrate N (Fig. 7.1), since NH_3 exchange links directly with apoplastic NH_4^+ via stomata. The apoplastic NH_4^+ concentration, $[NH_4^+]_{apo}$, was linked to the apoplastic substrate N concentration, $[N]_{apo}$, and χ_s was linked to $[NH_4^+]_{apo}$ and pH_{apo} via the relationship described in Eq. 1.7. The ground surface emission potential, χ_g, was calculated as the NH_3 concentration in equilbrium with the NH_4^+ concentration in the soil surface solution $[NH_4^+]_{aq,\,surface}$ (similarly to Eq. 1.8). The soil surface solution NH_4^+ concentration was found as a fraction of the total ammoniacal N of the soil surface, $N_{amm,\,surface}$. The parameter $N_{amm,\,surface}$ was determined from the various inputs and outputs of N as described in Fig. 7.2. The soil surface layer thickness was defined as a variable, set to 1 mm for the results presented here.

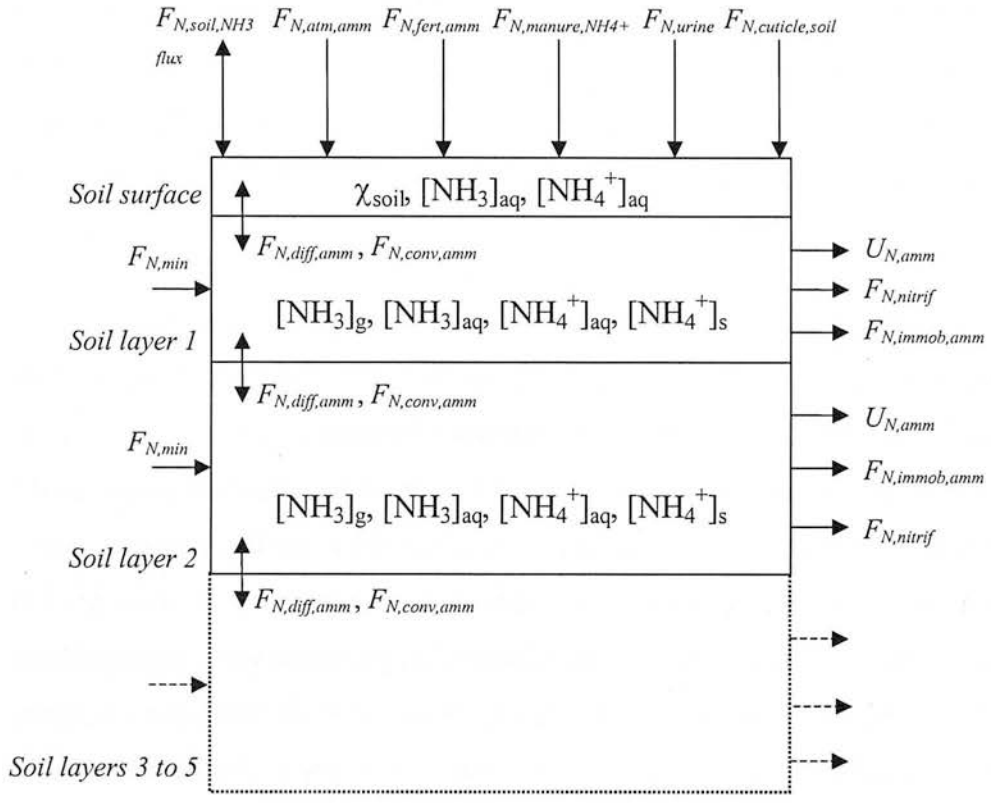

Figure 7.2. Soil ammoniacal N in PaSim is divided among soil surface NH_x, and NH_x in the different soil layers. Soil surface NH_x is partitioned between aqueous NH_4^+, and gaseous and aqueous NH_3. Soil ammoniacal N is partitioned between aqueous and exchangeable solid NH_4^+, and gaseous and aqueous NH_3. All input/output fluxes of the soil N pools are shown, (from Riedo et al., 2002).

7.3 Model application

The main input parameters for PaSim for the Easter Bush simulations were obtained from the measurements described in Chapters 4 and 5. The input parameters include: i) site specific parameters, ii) management activity inputs, iii) meteorological inputs and iv) background CO_2 and NH_3 concentrations. These parameters vary on different time-scales.

There are many site specific parameters required; these include the latitude and longitude, altitude and slope of site and various soil properties such as bulk density, clay, sand and silt fraction, saturated water content and saturated hydraulic conductivity, soil pH and main rooting depth. The soil parameters were obtained from the measurements described in section 4.5. There are, however, some model parameters, which cannot be measured (e.g. the C and N content in specific soil pools such as slow and passive organic matter). These parameters were obtained by PaSim generating equilibrium values during a steady-state simulation run over a

large number of years (≈ 100). Meteorological daily weather data over eight years (1990-1998) were repeated throughout the steady-state simulation so as to get an averaged representation of the climate. This data was obtained from the UK Met Office (Land Surface Observation Stations Data) for the observation station at Bush House.

The management activity inputs required in PaSim are timing of cutting and fertilisation, fertiliser type and amount (separated into ammoniacal and nitrate fractions and organic fertiliser), animal stocking density and duration of grazing. These inputs were obtained from the management record (Table 4.3) and from the record of grazing (Figs. 4.16-4.19). Only grazing by dairy cattle is explicitly included in PaSim and therefore the sheep stocking density was converted to equivalent cattle stocking density by assuming a livestock unit of 0.08 for sheep. Meteorological input parameters required for PaSim are: global radiation (W m^{-2}), precipitation (mm d^{-1}), air temperature (K), water vapour pressure (kPa) and wind speed (m s^{-1}). Hourly values of these parameters were obtained from the measured values given in section 4.2. Background concentrations of CO_2 were assumed to be constant (= 350 ppb), while hourly concentrations of NH_3 were obtained from the top measurement height of the AMANDA analyser.

New model parameters introduced during the incorporation of NH_3 exchange were either derived from literature or parameterised by fitting the model output to measurements of NH_3 exchange at Easter Bush in 1998. Full details of which values were derived from literature and which were parameterised are given by (Riedo *et al.*, 2002). A comparison of measured and simulated parameters for 1998 is also given by (Riedo *et al.*, 2002). It should be noted that the comparison of simulated parameters against 1999 measurements presented here is without any further change to the model.

7.4 Results

7.4.1 Model comparison against measured vegetation parameters

As PaSim provides a dynamic description of the growth and nutrient cycling of the grassland, simulated parameters of growth, biomass and nutrient concentration can

be compared with measurements conducted at Easter Bush throughout the season. Such comparisons are presented in Figs. 7.3-7.6, for the measurements conducted in 1999. The measurements themselves are described in more detail in Chapter 4. As measured values for 1999 were not used to parameterise PaSim, they serve as an indication of how well PaSim is capturing the grassland dynamics.

The seasonal variation in measured and simulated biomass (dry matter m^{-2}) for Easter Bush S field is presented in Fig. 7.3 for 1999; measured data are not presented for the N field as it did not receive a 2nd cut. The simulated change in biomass compares well with the measured values, except for after the second cut when PaSim simulates continued grass growth and a higher value of biomass despite grazing and senescence in the field. This is a feature of PaSim that has previously been recognised (Riedo *et al.*, 1998).

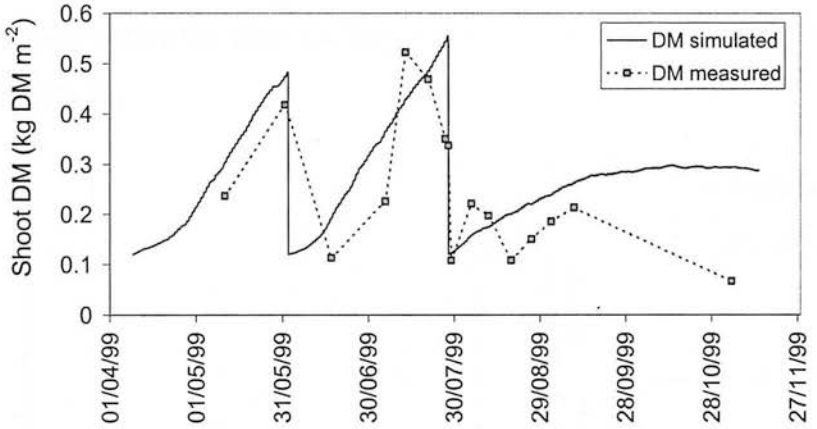

Figure 7.3. Measured shoot dry matter (DM) in S field and simulated shoot dry matter in PaSim for 1999.

The seasonal variation in measured and simulated canopy height is presented in Fig. 7.4 for 1999. This demonstrates that PaSim simulates the initial canopy height in April fairly well, but underestimates the increase in height from mid-May while overestimating the canopy height as the second cut is approached. After the 2nd cut PaSim also overestimates the height; this is consistent with the overestimation in biomass (Fig. 7.3).

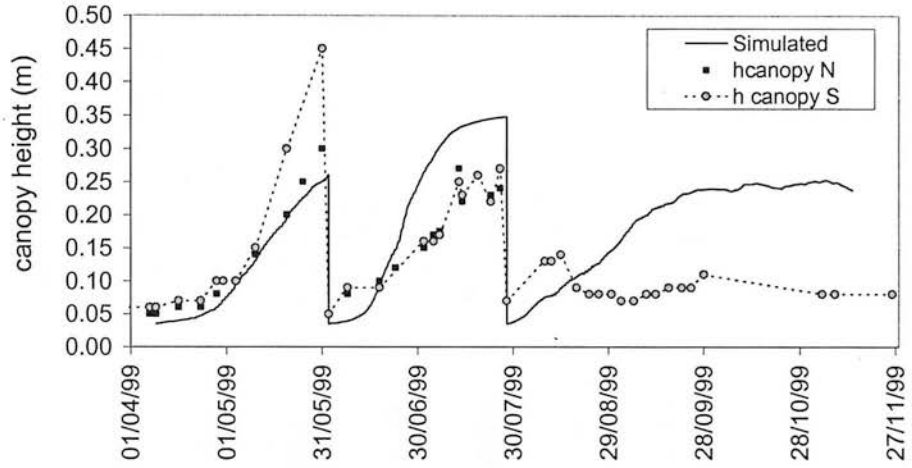

Figure 7.4. Measured canopy height in N and S field and simulated canopy height in PaSim for 1999.

The seasonal dynamics in measured and simulated leaf area index is presented in Fig. 7.5. In a similar manner to the canopy height comparison, PaSim underestimates LAI in May before the first cut, but overestimates LAI after the first cut and at the end of the season.

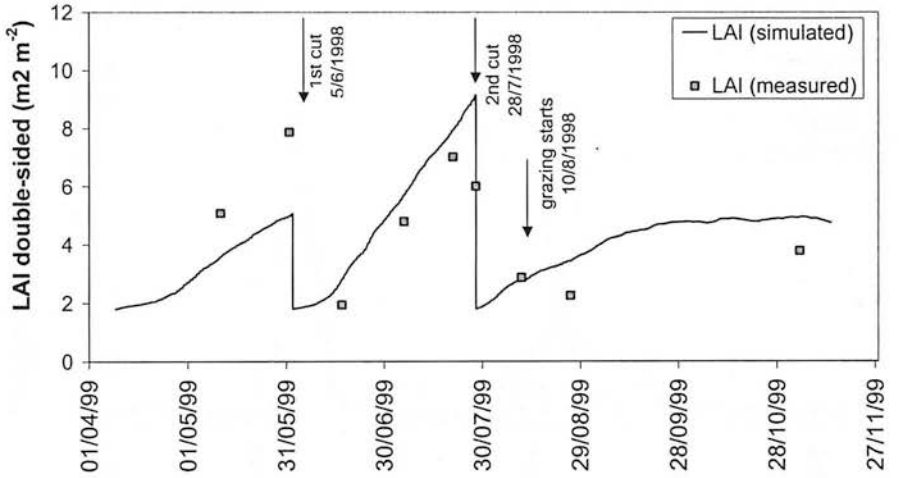

Figure 7.5. Measured LAI in S field and simulated LAI in PaSim for 1999.

The time-course in measured and simulated total foliar N content is presented in Fig. 7.6 for 1999. The timing and general dynamics of the increase and decrease in foliar N are captured by the simulated values, but the magnitude of the changes in measured foliar N content is underestimated.

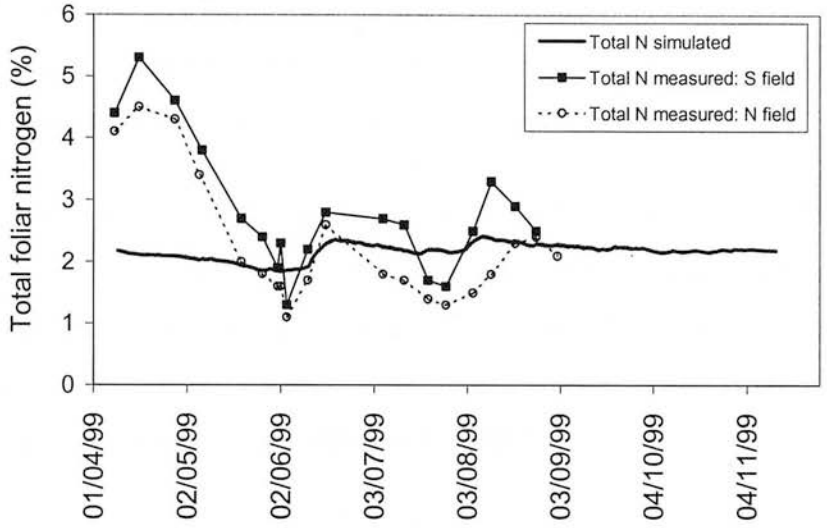

Figure 7.6. Measured total foliar N content in N and S field and simulated total foliar N content in PaSim for 1999.

Measured bioassay and simulated values of apoplastic NH_4^+ content are presented in Fig. 7.7. These values are for 1998 as apoplastic measurements were only conducted in 1998.

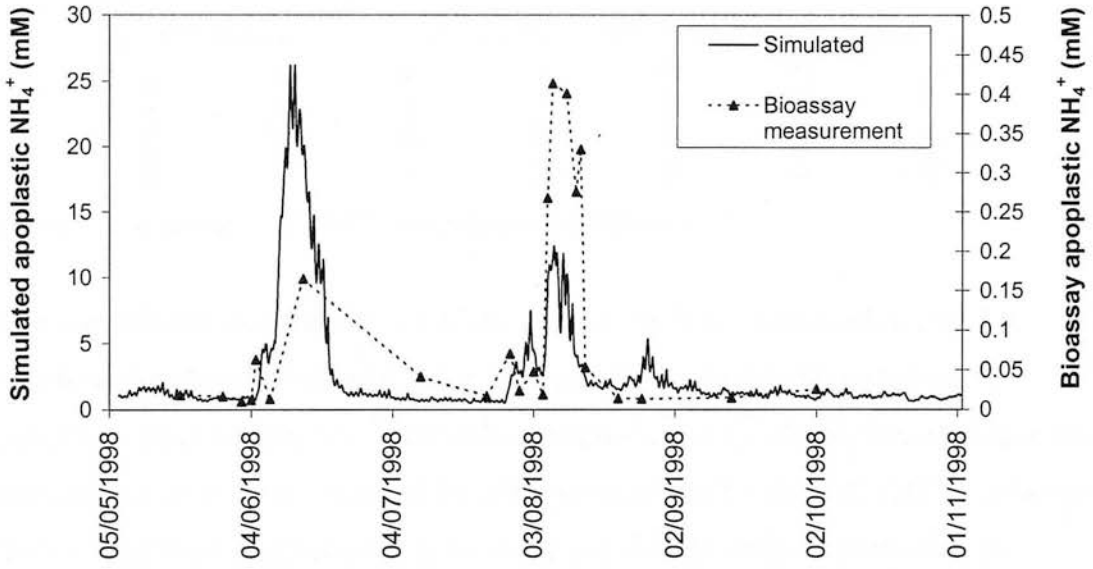

Figure 7.7. Measured apoplastic NH_4^+ content in S field and simulated apoplastic NH_4^+ content in PaSim for 1998.

As discussed in section 5.5.3, the bioassay measurements of $NH_4^+_{apo}$ are larger after the second cut and fertilisation, which is in contrast to NH_3 emissions which were much greater after the first cut. Pasim, however, shows larger values of $NH_4^+_{apo}$ after

the first cut and fertilisation, which is consistent with the NH_3 emissions observed. It is also notable that the bioassay measurements are significantly lower then the simulated values (up to two orders of magnitude lower).

Values of Γ_s (= $[NH_4^+]_{apo}/[H^+]_{apo}$) obtained from the bioassay measurements and simulated values of Γ_s are presented in Fig. 7.8. A similar pattern to $NH_4^+{}_{apo}$ is observed, except that the increase after the first fertilisation is smaller, which is due to a corresponding decrease in bioassay pH_{apo} during this period (data not shown here, but presented by Loubet *et al.*, 2002).

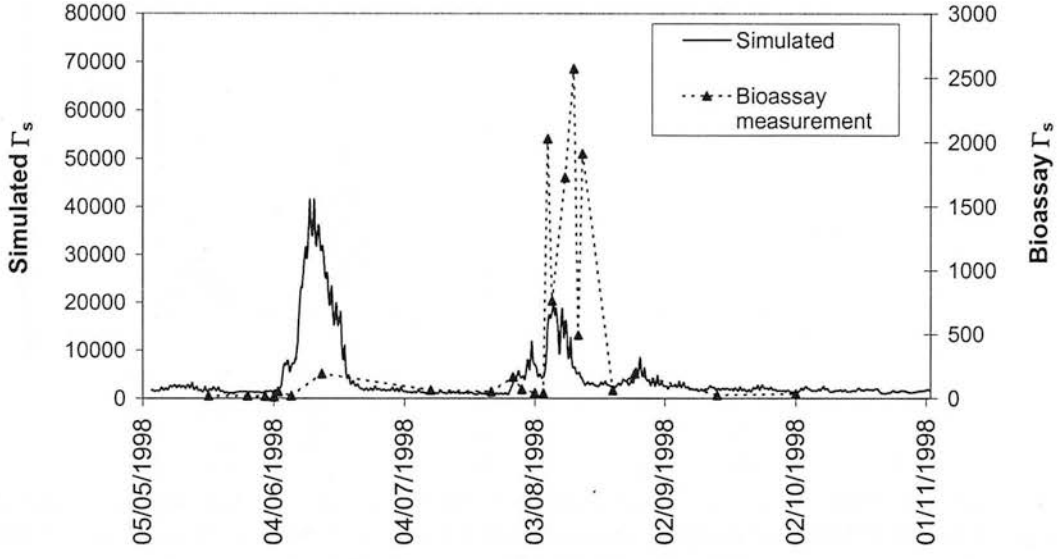

Figure 7.8. Measured Γ_s in S field and simulated Γ_s in PaSim for 1998.

The simulated seasonal dynamics of the plant N pools are presented in Fig. 7.9, which compares values of total foliar nitrogen, total substrate N concentration (apoplastic plus symplastic), apoplastic substrate N and Γ_s. The simulated values are broadly similar to those observed for 1998 as shown by Riedo *et al.* (2002), although there are substantial differences at the daily and weekly scale. In particular, the simulations presented for 1999 include the increase in N concentration following the first fertilisation in spring (4/4/99), which was not shown for 1998. The seasonal variability is greatest for Γ_s and N_{apo}, followed by N_{sub}, with N_{tot} showing the least variation.

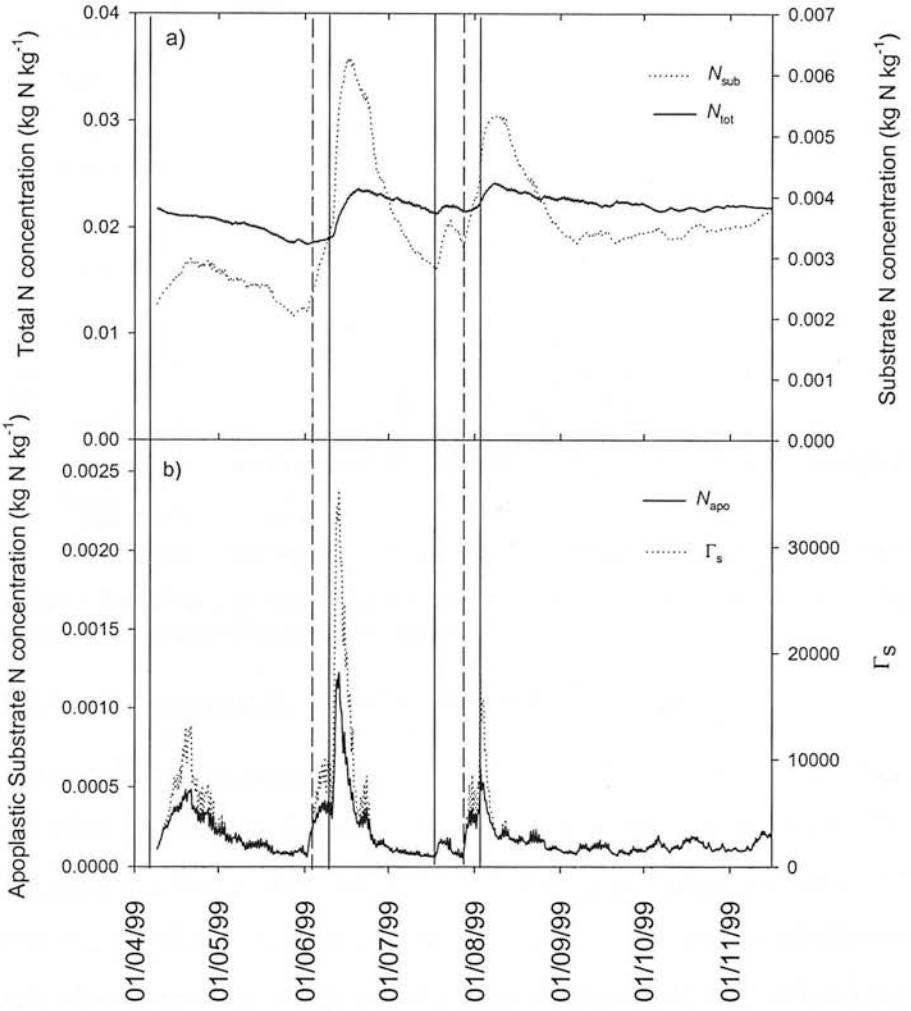

Figure 7.9. Simulated seasonal dynamics of plant N pools and Γ_s for 1999. (a) Plant total N concentration N_{tot}, plant substrate N concentration N_{sub}. (b) Apoplastic substrate N concentration N_{apo}, Γ_s (apoplastic NH_4^+ to H^+ concentration ratio). The N concentrations are given as dry weight. Vertical lines indicate cutting (dashed lines) and fertilisation (solid lines). For dates and amounts of fertiliser input see Table 4.3.

7.4.2 Model comparison against measured ammonia fluxes for 1999

The simulated and measured total NH_3 exchange is presented in Fig. 7.10 for June 1999. The field was cut on 2/6/99 and fertilised on 11/6/99. The simulated values demonstrate a similar temporal variability to the measured NH_3 exchange and the initial cutting emissions are in good agreement. However, simulated cutting emissions are underestimated on 9 and 10/6/98 and the emissions after fertilisation are also underestimated, particularly on 14-16/6/98. The decline in emissions from 17-30/6/98 is captured well by the model.

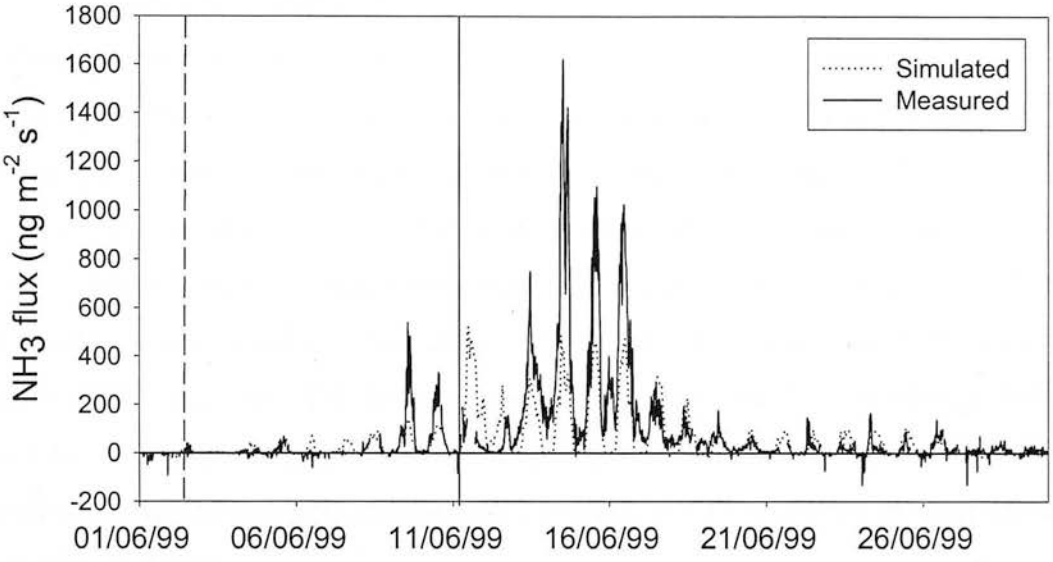

Figure 7.10. Measured and simulated total NH_3 flux for June 1999. Vertical lines indicate cutting (dashed lines) and fertilisation (solid lines).

7.4.3 Component fluxes of modelled NH_3 exchange

The simulated component fluxes of NH_3 exchange (stomatal flux, cuticular flux and soil flux) and the net exchange are presented in Fig. 7.11 for June 1999. The stomatal flux provides the largest contribution to the net exchange for most of this period, with the soil flux only showing emission for the day and a half after fertilisation. The cuticular component is also small except for during 11 and 12/6/98 indicating that most of the stomatal emission flux during this period is emitted to the atmosphere rather than recycled within the canopy.

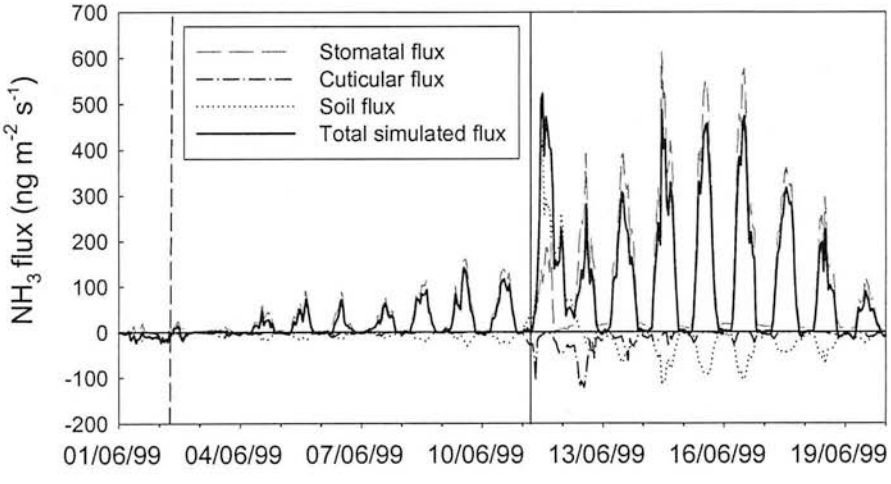

Figure 7.11. Simulated component fluxes of NH_3 exchange (stomatal flux, cuticular flux and soil flux) and the total NH_3 flux for 1-19/6/99. Vertical lines indicate cutting (dashed lines) and fertilisation (solid lines).

7.4.4 Results of management scenarios

Although there are observed differences between the simulated values and measurements, the agreement in the temporal variation and general dynamics of growth indicators, N content and net NH_3 exchange is encouraging. The performance of the model against the measurements provides confidence in the general description of processes within the model. The model can then be run in a predictive capacity to provide values of simulated NH_3 exchange for scenarios of changing mangement or climate. This is the strength of a dynamic model and although only a few key scenarios are presented here, these demonstrate the possibilities of utilising PaSim to explore changing management, climate, pollution climate or other drivers on NH_3 exchange.

Effect of changing N input rates

The first scenario presented in Fig. 7.12 is of changing the amount of fertiliser input. Although, as expected, increasing the fertiliser input does increase emissions of NH_3, there is a non-linearity in the increase in modelled NH_3 emissions. Table 7.1 gives the change in simulated accumulated net flux for 7/5/1998 - 11/12/1998 for the three contrasting fertiliser application rates. There is an increase in accumulated net flux from 1.9 kg N ha^{-1} to 3.32 and 6.20 kg N ha^{-1} for the 2x and 5x increase in fertiliser input, respectively. This is equivalent to 1.7x and 3.3x the original simulated accumulated net flux.

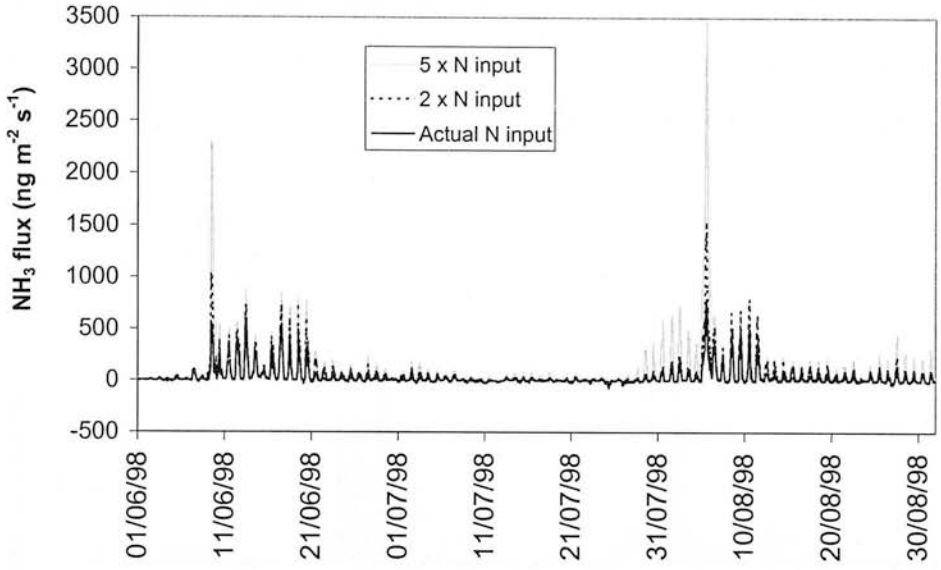

Figure 7.12. Simulated total NH_3 flux for 1/5/1998-11/12/1998 with the original rate of fertiliser N application plus 2x and 5x the original rate of fertiliser N application.

Table 7.1. Changes in simulated accumulated net flux for 7/5/1998 - 11/12/1998 for different rates of fertiliser application.

	Actual N input	2 x N input	3 x N input
Accumulated net flux (kg N ha^{-1})	1.90	3.32	6.20
Percentage Change	-	+74%	+225%
Increase compared with actual input	-	1.7x	3.3x

Effect of changed timing of N fertiliser application

The second scenario presented is the effect of changing the timing of fertiliser application on the NH_3 exchange. Total NH_3 flux is presented in Fig. 7.13 for two simulations, i) with the actual dates of fertiliser applications and ii) with fertiliser applications delayed by two weeks. The same fertiliser N inputs are used in each simulation. The simulated NH_3 emissions are seen to be reduced by this simple measure of delaying the fertiliser application. Table 7.2 gives the change in simulated accumulated net flux for 7/5/1998 - 11/12/1998 for the two different application dates. There is an overall decrease in accumulated net flux from 1.9 kg N ha^{-1} to 1.62 kg N ha^{-1} for the delayed fertiliser application, this is equivalent to a 15%

decrease. The corresponding changes in the component flux values (Table 7.2) demonstrate that this decrease arises from a reduced stomatal emission flux, while in contrast there is a small decrease in net deposition to the cuticle and soil.

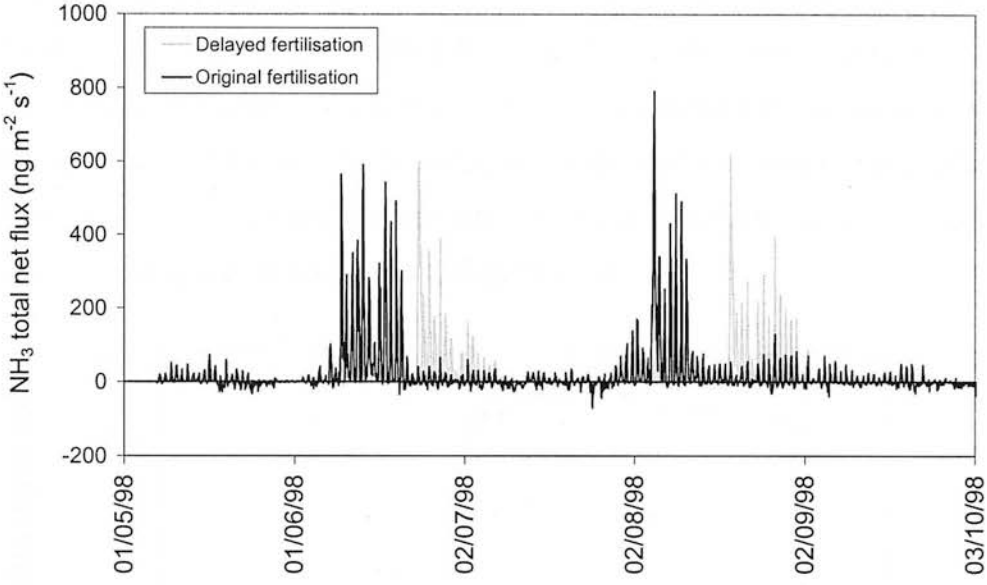

Figure 7.13. Simulated total NH_3 flux for 1/5/1998-11/12/1998 with the original timing of fertiliser applications on 9/6/1998 and 5/8/1998 and with fertiliser applications delayed by two weeks.

Table 7.2. Changes in simulated accumulated net flux for 7/5/1998 - 11/12/1998 for different timing of fertiliser application.

	Accumulated Net Flux (kg N ha^{-1})	Accumulated Stomatal Flux (kg N ha^{-1})	Accumulated Cuticular Flux (kg N ha^{-1})	Accumulated Soil Flux (kg N ha^{-1})
Original date of fertiliser application	1.90	3.24	-0.80	-0.54
Delayed date of fertiliser application by 2 weeks	1.62	2.69	-0.73	-0.34
Percentage Change	-15.2%	-17.0%	+8.6%	+36.2%

7.4.5 Results of climate scenarios

The third scenario presented is the effect of changing air temperature on NH_3 exchange (Fig. 7.14). The NH_3 emissions would be expected to increase with increasing temperature due to the temperature response of the compensation point and other emission processes. The accumulated NH_3 flux does increase with increasing temperature, but it is interesting to note that there is a non-linear response and the response is not as large as the 60% increase expected from an increase of

3 °C purely on the basis of the thermodynamics of ammonia (Eq. 1.7). Decreasing the model input air temperature by 3 °C reduces the accumulated NH_3 flux by a greater amount than the corresponding increase in accumulated NH_3 flux observed when the model input air temperature is increased by 3 °C. In these simulations, absolute humidity was kept constant. To counteract any changes in relative humidity due to rising temperatures, a further simulation was conducted of changed temperatures, but the relative humidity was kept constant. This slightly reduced the effect of the 3 °C increase in temperature on the accumulated NH_3 flux compared with the scenario with constant absolute humidity.

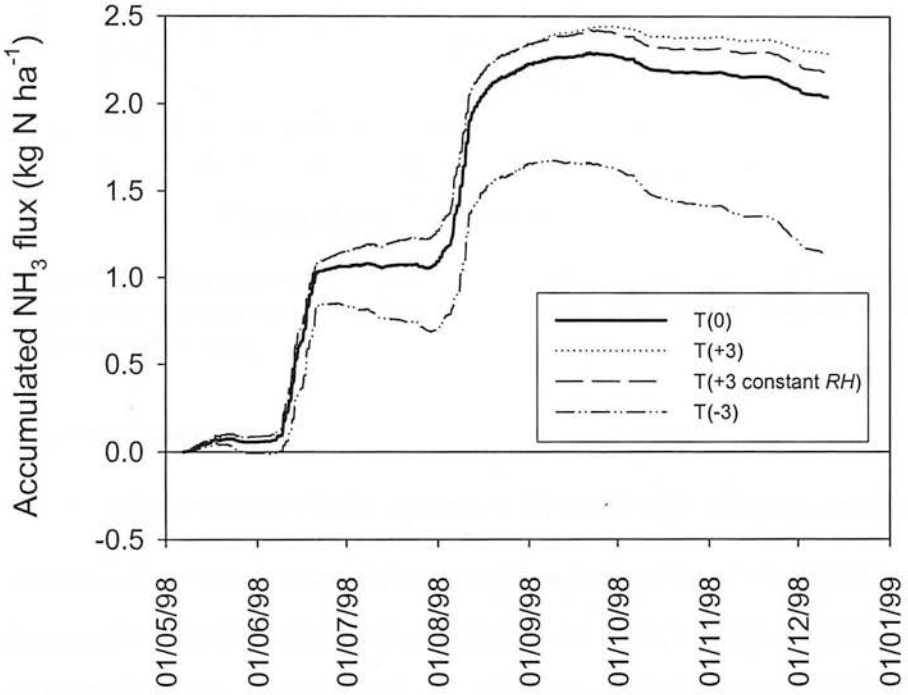

Figure 7.14. Simulated accumulated net NH_3 flux for 1/5/1998-11/12/1998 for different inputs of model air temperature. *T*(0) is the measured air temperature, *T*(+3) and *T*(-3) are measured air temperature plus and minus 3 °C, respectively while T(+3) constant RH is measured air temperature plus 3 °C while keeping the relative humidity constant.

PaSim can also be used to investigate the temperature response of NH_3 emission for a particular case period. Fig. 7.15 presents the increase in mean NH_3 flux for 9/6/1998 (the first day after fertilisation) for various changes in the input of model air temperature. The theoretical increase due purely to the thermodynamics of NH_3 solubility and volatilisation is also shown in Fig. 7.15. This shows clearly how the modelled emissions from PaSim, although they include the thermodynamic effects,

are modified substantially from the thermodynamic response by other interactions within the model.

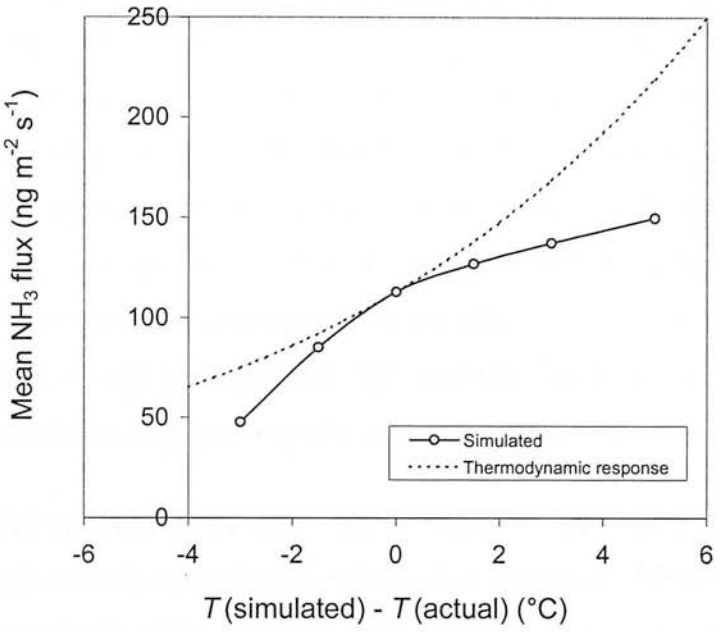

Figure 7.15. Simulated mean NH_3 flux for 9/6/1998 for changing model input air temperature, also shown is the expected increase in NH_3 flux according to the thermodynamic increase in compensation point with temperature.

7.5 Discussion

7.5.1 Model comparison against measured vegetation parameters

The general performance of PaSim against the measured vegetation parameters is reasonable; the biomass, canopy height and LAI are generally similar to the measured values, except for after the 2nd cut when PaSim overestimates the productivity of the grassland (also observed by Riedo *et al.*, 1988). This is an issue, which would need to be addressed in future versions of the model. However, for the analyses presented in this thesis the period of most interest is that around the cutting and fertilising events, so the overestimation of productivity at the end of the season is not considered to have too detrimental an effect on these results.

The comparison of simulated foliar N content with the measurements indicates a possible area for improvement of PaSim. It seems that although the simulated foliar N content has a similar temporal variability to the measured values, the magnitude of the changes is not represented. The decrease in measured foliar N content through

April and May is due to growth dilution, which occurs where plant growth is faster than plant uptake of N. The simulated values also show growth dilution, but the change in foliar N content is smaller than that observed in the measurements. The increase in foliar N after each cutting and fertilising event, observed in the measurements is also observed in the simulated values but again the increase is not as prominent. This difference between the simulated and measured values indicates that the rate of N transfer between the N pools in PaSim (described in Fig. 7.1) is either too large or too small at certain times. For example, if too much N is available for plant uptake in the model as the plant is growing then the effect of growth dilution will be dampened. This therefore suggests the existence of an additional restriction to plant N uptake in the field, which is not parameterised in the model.

The comparison of the simulated values of apoplastic NH_4^+ content and Γ_s again show similar temporal variability, but there are substantial differences in both the magnitude of the values and the fact that the bioassay measured values are larger after the 2nd cut than the 1st. However, as discussed in Section 5.5.3, very few bioassay measurements were made after the first cut and fertilisation, so these results are less certain. The larger simulated values of NH_4^+ content and Γ_s after the 1st cut are consistent with the measured NH_3 emissions being larger after the first cut. Aside from simulated values of NH_4^+ concentration and Γ_s, estimates can also be made via micrometeorological measurements or with controlled cuvette studies (see Section 1.3.1). Lower estimates of apoplastic NH_4^+ concentration and Γ_s from bioassay measurements compared with estimates from cuvette measurements have been observed in numerous studies (e.g. Hill *et al.*, 2001 and Loubet *et al.*, 2002). This inconsistency between bioassay and cuvette estimates has been referred to as the "apoplastic gap". Consequently, it is perhaps no surprise to observe similar differences between the bioassay estimates and the PaSim simulated values. In noting this, it is important to recognise that the bioassay values would be too small to generate any significant stomatal emissions, while the Γ_s values simulated in PaSim are reasonably consistent with the values of Γ_s that were derived directly from the micrometeorological measurements (see Chapter 6).

7.5.2 *Model comparison against measured fluxes*

The agreement of the simulated NH_3 fluxes against measured values (Fig. 7.10) is remarkably close given the large variation in measured fluxes over this period and considering that parameterisation of the model for NH_3 exchange was conducted against 1998 measurements. PaSim does, however, overestimate the NH_3 emission on the first two days after fertilisation and then underestimates the emission for the following four days. The measured NH_3 fluxes show nocturnal emissions occurring three to seven days after the fertilisation application, indicating that soil emissions of NH_3 continue until this time. PaSim, however, only simulates soil emissions of NH_3 for the first one and a half days after fertilisation, this is likely to be largely due to the fertiliser dissolution rate into the soil being currently set at one day in PaSim. This is probably too rapid and it is likely that NH_4^+ is still present in the soil surface layer a number of days later, leading to the observed NH_3 emissions. An improvement to PaSim would be to reduce the fertiliser dissolution rate and link it to precipitation and humidity.

7.5.3 *Scenarios of changing climate and management*

The strength of a fully functional dynamic model is that it can be run in a predictive capacity for changed inputs. However, caution is required when interpreting PaSim results for changing scenarios, as not all processes are necessarily fully understood. This is particularly true for the effect of changing temperature. According to the thermodynamics of ammonia (see section 1.3.1) the stomatal compensation point doubles with every 5 °C increase in temperature and increases by 60% for a 3 °C increase in temperature. However, Fig. 7.14 and 7.15 show that although the simulated NH_3 flux does increase with increasing temperature, the increase is not as large as would be expected purely on the basis of the thermodynamics of ammonia. This shows clearly how the modelled emissions from PaSim, although they include the thermodynamic effects, are modified substantially from the thermodynamic response by other interactions within the model. For example, the increased growth of the plant in warmer conditions may dilute the apoplastic NH_4^+ concentration thereby reducing the compensation point and NH_3 emissions and offset the effect of increasing temperature.

The scenario of changing the timing of the fertiliser application suggests that NH_3 emissions could be reduced by 15% by this measure. As shown in Chapter 5, grass cutting induces NH_3 emissions, possibly through reduced utilisation of the available N and accumulation of NH_4^+ in the plant tissues. It is hypothesised that, if fertiliser N is applied immediately after cutting then the plants are less able to utilise this additional N and this leads to increased emission. Delaying the fertiliser application by a couple of weeks gives the plants a chance to recover and by then they are more able to utilise the increased N. In addition, as the canopy regrows, there is increased potential for any soil emission of NH_3 to be recaptured by the canopy. Delaying timing of fertiliser applications has potential as an NH_3 abatement option, as it involves only minimal additional cost to the farmer. PaSim estimates there to be only a 4% reduction in simulated dry matter production at the time of the next cut.

The scenario of increasing N input rates demonstrates a non-linearity in the corresponding increase in NH_3 emissions. A 2x and 5x increase in fertiliser N input results in 1.7x and 3.3x the original simulated accumulated net NH_3 flux. Most of the net NH_3 emission is due to stomatal emission (e.g. Fig. 7.11), except from the initial days after fertilisation when there are soil emissions. Consequently, the increase in net NH_3 emission is limited by the plant uptake of increased soil N. A limit on the increase in apoplastic NH_4^+ content with increasing fertiliser N input could lead to the observed non-linearity in the simulated NH_3 emissions.

7.5.4 Conclusions

The application of the grassland ecosystem model, PaSim, for the Easter Bush intensive grassland has demonstrated the potential of such an model to extend the understanding of ecosystem level processes of NH_3 exchange and also its potential to explore scenarios of change and potential abatement options for NH_3 emissions. There has been a lack of such ecosystem understanding of NH_3 exchange and the benefits of a model such as PaSim are that for the first time, NH_3 exchange is linked functionally to N cycling within the soil-plant-atmosphere system.

The results here indicate areas for improvement of PaSim, such as examining the processes at the end of the season, which lead to PaSim overestimating the

productivity of the grassland. The difference between measured and simulated foliar N content is also interesting and indicates processes, which occur in the field that are not yet fully parameterised by PaSim. In addition, the simulation of fertiliser dissolution could be improved and linked in a more mechanistic manner to precipitation and humidity. The comparison of simulated parameters against measured parameters is invaluable for development of the model.

Also of interest are the responses of PaSim to changing temperature and changing N inputs. The simulated NH_3 emissions do not follow the expected thermodynamic response to rise in temperature and indicate that there are other ecosystem interactions which offset the effect of increased temperature on NH_3 emissions, such as increased growth. These results indicate that the response of NH_3 exchange to climate change on an ecosystem level is a result of complex interactions, which require further investigation. The results also highlight the need for models such as PaSim, which can investigate the whole ecosystem response to climate change, rather than the response of an individual process.

Chapter 8: Ammonia fluxes over a managed grassland in Germany: The Braunschweig Experiment

8.1 Introduction

In 1998, a European project, GRAMINAE (GRassland AMmonia INteractions Across Europe), was initiated to improve quantification and parameterisation of NH_3 exchange with grasslands across Europe. The focus on grasslands arose since they cover a large land area throughout Europe and also because grasslands exhibit a range of NH_3 exchange characteristics (see section 1.2.4). Prior to this project there were few long-term measurements of NH_3 exchange with grassland from which to derive parameterisations for deposition modelling across Europe. Long-term measurements of NH_3 exchange, with both intensively and extensively managed grassland, were conducted within the GRAMINAE project in six countries (UK, France, The Netherlands, Switzerland, Greece and Hungary) and the measurements presented from Easter Bush in the preceding chapters form the UK contribution. In addition to the long-term measurements in the individual countries there was also an integrated experiment on NH_3 exchange with intensively managed grassland held in Braunschweig, Germany in 2000, involving over 50 scientists (Sutton *et al.*, 2002).

In order to provide a robust dataset of NH_3 exchange with the vegetation, four independent continuous flux gradient systems were operated. Each NH_3 gradient system was provided and operated by a different institute, details of which are given in Table 8.1. I operated the CEH system along with other CEH colleagues. Although there have been many inter-comparisons of ammonia concentration measurements (see Section 1.2.2) there have been few inter-comparisons of ammonia flux measurements. This chapter presents the results of this first major inter-comparison of continuous NH_3 flux measurements. The best estimates of NH_3 flux and concentration from this inter-comparison are then used to explore the pattern of NH_3 exchange with the intensively managed grassland. These results provide a comparison with the results obtained at the Easter Bush site in Scotland. These best estimates of NH_3 concentrations and fluxes were also provided to other participants in the experiment as a basis for further analyses, for example in quantifying

advection fluxes (Loubet *et al.*, 2004), assessing the relaxed eddy accumulation technique for NH_3 (Hensen *et al.*, 2004), modelling the dynamics of ammonia fluxes (Sutton *et al.*, 2004) and quantifying production of particulate ammonium (Nemitz *et al.*, 2004).

8.2 Experimental details

8.2.1 Site description

The field site was intensively managed grassland of approximately 12 ha, located at the experimental farm of the German Federal Agricultural Research Centre, Braunschweig, Germany (52°18'N, 10°26'E; 79 m asl) (Fig. 8.1). The plant species cover was dominated by *Lolium perenne* (62 %) with *Fleum pratense* (16 %), *Festuca pratensis* (11 %) and *Lolium multiflorum* (5 %) also present (Mattson *et al.*, 2004).

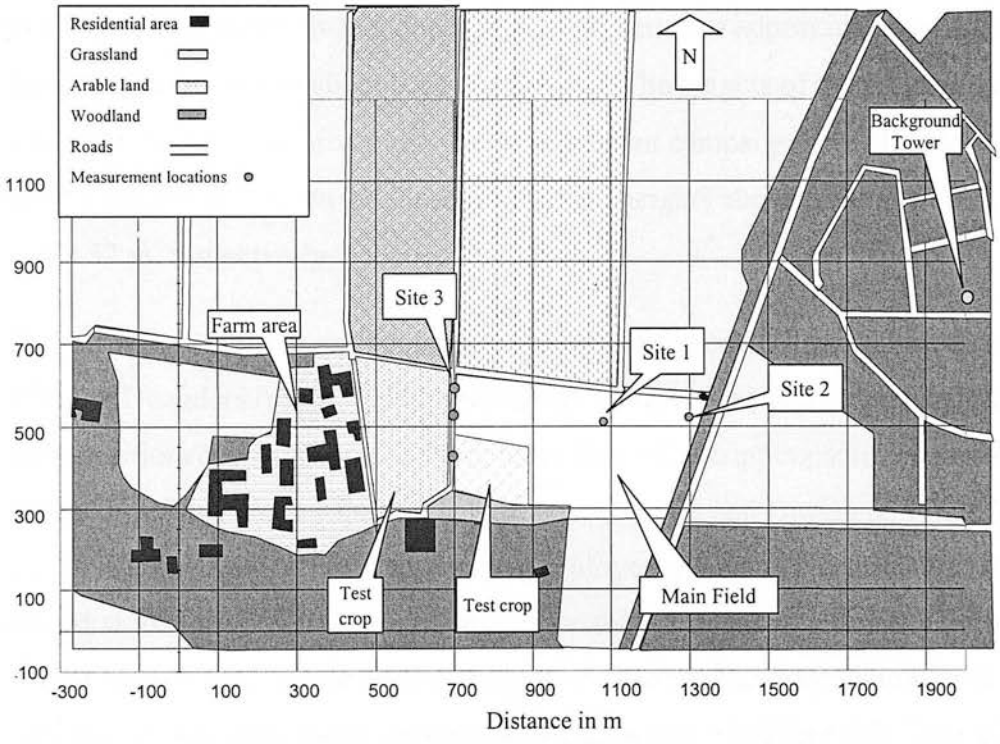

Figure 8.1. Map of the field site in Braunschweig, Germany.

The field was cut for silage on 29/5/2000, the grass removed from the field on 31/5/2000 and the field fertilised on 5/6/2000 with 108 kg N ha^{-1} of calcium ammonium nitrate. The principal micrometeorological measurement location (Site 1) was 380 m from the western edge of the field site (Fig. 8.1). The second

micrometeorological measurement location (Site 2) was 210 m east of Site 1 and 36 m from the eastern edge of the field. Measurements were made at Site 2 in order that any advection of NH_3 from a farm located 610 m west of Site 1 could be identified and quantified.

8.2.2 Measurement techniques and implementation

Ammonia concentrations were determined in gradient configuration using two different measurement techniques (AMANDA and mini-WEDD). The AMANDA continuous flow denuder (Wyers *et al.,* 1993) is described in Section 3.3.1. Two gradient AMANDAs (each consisting of 3 denuder inlets linked to a common ammonium detector) were deployed at Site 1 and one at Site 2. Concentrations were measured sequentially for 2½ minutes at each of three heights, resulting in a 7½ minute profile measurement. These concentrations were averaged to 15 min periods for flux calculation. The air-flow rate of the AMANDAs was approximately 25 *l* min^{-1} and the liquid flow rate through the denuders was approximately 1 m*l* min^{-1}; the detection limit was about 0.02 μg NH_3 m^{-3}. The heights of the concentration measurements varied throughout the measurement campaign according to the canopy height, but the maximum height and minimum heights above ground were 2.37 m and 0.32 m, respectively.

The second continuous ammonia measurement technique utilised miniaturised Wet Effluent Denuders (mini-WEDD), which are silica-coated glass tubes (length 125 mm) positioned vertically, with continuous flow of a stripping solution analysed online by a four-channel fluorescent analyser (Vecera and Dasgupta, 1991; Neftel *et al.*, 1998). The mini-WEDD system was deployed at Site 1. The mini-WEDDs were placed at four heights (0.15 m, 0.3 m, 0.6 m and 1.2 m above ground). However, the lowest mini-WEDD concentration was not used in the flux calculations as it was judged to be too close to the canopy. An air-flow rate of 600 m*l* min^{-1} and a liquid flow rate of 0.12 m*l* min^{-1} were used. The detection limit was 0.1 μg NH_3 m^{-3}. Table 8.1 gives details of the ammonia gradient systems.

Table 8.1: Details of the different continuous ammonia gradient systems used in the Braunschweig experiment.

System acronym	System description	Sampling location
FRI	AMANDA (3 point profile) operated by Forest Research Institute, Hungary	Site 1
FAL-CH	Mini-WEDD (3 point profile) operated by the Swiss Federal Research Station for Agroecology and Agriculture	Site 1
FAL-D	AMANDA (3 point profile) operated by the German Federal Agricultural Research Institute.	Site 1
CEH	AMANDA (3 point profile) operated by the Centre for Ecology and Hydrology, UK	Site 2

Calibration of all systems was with aqueous standards of 0, 50 and 500 mg kg^{-1} NH_4^+, which were prepared centrally and distributed amongst the ammonia analyser operators. In addition, unknown quality control standards were distributed on three occasions to test the accuracy of the analysers. On each occasion, two unknown standards were distributed and the difference in concentration measured by each analyser was compared with the actual concentration difference.

8.2.3 Data processing procedures

The complexities of data processing are increased by the availability of four independent estimates of NH_3 concentration profiles. The following procedure was applied:

i. Any periods of calibration or obvious malfunctioning of each instrument were removed from the dataset of measured concentrations.

ii. Fluxes F_t(1 m) of NH_3 and concentrations at 1 m (χ (1 m)) were calculated using the aerodynamic gradient method according to Section 2.2.1. Flux measurements were rejected during periods when the fetch was obstructed by other equipment or by the edge of the field (see Point a. below for details).

iii. F_t(1 m) and χ (1 m) estimates of the different systems were compared in order to identify any periods where one system had clearly malfunctioned or underperformed which had not yet been identified. These data were then removed.

iv. Given the different estimates of the four systems, gaps in the data create an artificial change in the mean estimate when one system goes offline or comes back online. To avoid this artefact, gaps of < 6 hours in each instrument were filled for F_t(1 m) and χ(1 m) (see Point b. below for details).

v. As the flux measurements were made at two sites, different vertical flux divergence will apply due to horizontal advection where local sources are present. Advection corrections for 1 m above d were calculated by Loubet *et al.* (2004) for the Site 1 and Site 2 measurements and these were applied to the measured fluxes, resulting in an estimate of the fluxes at the canopy surface (F_t (z_o)) (see Section 8.3.3). No corrections to the data for the potential effect of chemical production or consumption are made here, but this effect is assessed by Nemitz *et al.* (2004).

vi. The "mean gradient estimate" (subscript mg) was then calculated for (F_t (z_o)) and χ (1m), as the arithmetic mean of all available individual measurements. At the same stage, corrections for storage errors were also applied.

vii. The data were filtered according to the passing or failing of a set of defined micrometeorological criteria (see Point c. below for details). Data failing these criteria were retained in the dataset, but distinguished as being of lower reliability.

Point a. There was a substantial amount of measurement equipment at Site 1, concentrated on a N-S axis, as well as three mobile laboratories in the N direction. As a result of this, flux measurements from the FAL-D and FRI gradient systems were rejected for wind directions from both the N and S directions (0°- 20° and 180°-190° rejected). Flux measurements from the FAL-CH gradient system were rejected for winds from the NNE direction (10°- 45°), as this system was positioned on a outlying arm to the SW of the main axis and did not have equipment obstructing its fetch in the S direction. Due to the close proximity of the edge of the field to the east of Site 2, flux measurements were rejected at this site for wind directions 0°-170°.

Point b. The gapfilling technique involved calculating the ratio of the individual flux measurement to the mean estimate at the start and end of the gap and then interpolating this ratio. This interpolated ratio was then multiplied by the available mean estimate to fill in missing data. This method propagates the deviations from the mean present at the start and end of the gap and limits the occurrence of step changes in the flux when individual analysers fail or are restored in the dataset. As stated above, only gaps of < 6 hours were filled.

Point c. Finally, the data were filtered according to micrometeorological criteria to identify periods where the fluxes are estimated with less certainty. These micrometeorological criteria were: u (1 m) < 0.8 m s^{-1}, $|L|$ < 5 m and cumulative normalised footprint function (CNF) < 65%. The cumulative normalised footprint function was calculated using the Kormann and Meixner (2001) formulation (see Section 2.3.1).

8.3 Results

8.3.1 Data processing and results of data filtering

The results of the data processing procedures are shown in Table 8.2. These figures indicate that high data coverage at individual sites was achieved even after periods of malfunctioning and obstructed wind sectors were removed. Having four estimates of the flux leads to a "mean gradient estimate" of the flux with an overall data coverage of 97%. This highlights the advantage of having a number of independent systems to achieve a robust estimate of the flux. This data coverage is reduced to 68% if the fluxes, which are calculated with less certainty are removed, showing that meteorological conditions (low windspeed, stable conditions) are the main limitation to obtaining a complete flux dataset. Data on the application of the gapfilling procedure reveal that FAL-CH had the greatest number of gaps filled and that the median gap length varied from 15 mins (FAL-D) to 90 mins (CEH) (Table 8.3).

Table. 8.2. Results of data processing procedures, data covers period 21/5/00 10:00-15/6/00 12:15.

Data-processing Proceedure	No. of valid (15-min) F_t data points after corresponding data-processing proceedure					Data coverage (%)				
	Mean estimate	CEH	FRI	FAL-D	FAL-CH[a]	Mean estimate	CEH[b]	FRI[b]	FAL-D[b]	FAL-CH[c]
i) Removal of periods of calibration or obvious malfunctioning of the instruments	-	1912	1510	1893	1037	-	79	63	79	69
ii) Removal of measurements from obstructed wind sectors	-	1400	1451	1841	1012	-	58	60	76	68
iii) Gaps filled with procedure outlined in Section 8.2.3	-	1557	1531	1968	1372	-	65	64	82	92
iv) Mean gradient estimate	2346	-	-	-	-	97	-	-	-	-
v) Mean gradient estimate filtered for micromet criteria	1633	-	-	-	-	68	-	-	-	-

[a]FAL-CH gradient data starts on 30/5/00 22:15, [b]% data coverage calculated for period 21/5/00 10:00 - 15/6/00 12:15, [c]% data coverage calculated for period 30/5/00 22:15 - 15/6/00 12:15.

Table. 8.3. Results of the application of the gapfilling procedure, data covers the period 21/5/00 10:00-15/6/00 12:15, except for FAL-CH where data covers the period 30/5/00 22:15 - 15/6/00 12:15.

	CEH	FRI	FAL-D	FAL-CH
Number of gaps filled	23	13	31	71
Median gap length (mins)	90	30	15	30
Std. dev. of gap length (mins)	67	107	87	83

8.3.2 Temporal intercomparison of gradient measurements

The range of NH_3 concentrations at 1 m from the four different systems are shown for example days from the pre-cut, post-cut and post-fertilisation periods in Fig. 8.1.

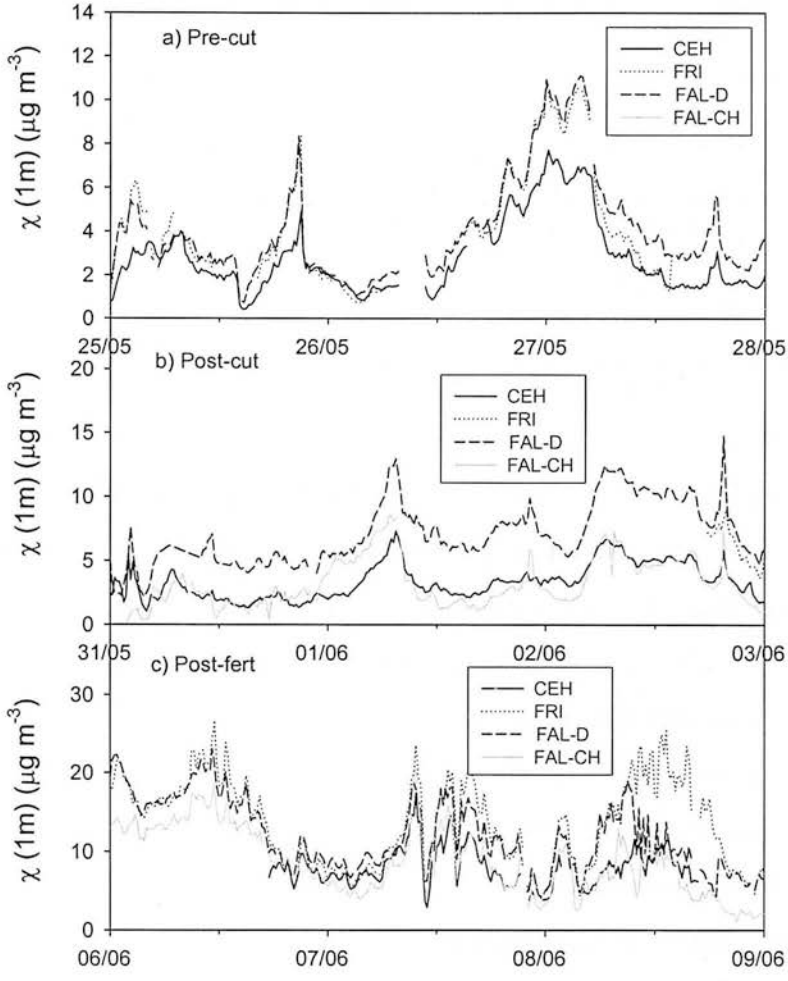

Figure 8.1. Examples of NH_3 concentration (χ (1 m)) for the four different systems for pre-cut, post-cut and post-fertilisation periods, all dates are in 2000.

This figure shows that there are periods of close agreement (e.g. 6th and 7th June 2000) and periods of substantial difference (e.g. 8th June). It can be seen that for certain periods (31/5-2/6/2000) there are consistent concentration differences between the different instruments with FAL-D generally reading higher concentrations than CEH and FAL-CH.

The blind testing of the aqueous ammonium Quality Control standards by the different analysers did indicate periods of significant concentration differences (Table 8.4). In particular, the result of FAL-D over-reading by 41% on 31/5/00 is consistent with Fig. 8.1b. However, the small number of tests meant that it was not possible to adjust the concentrations in an objective manner and so the quality tests were used for interpretation rather than adjustment.

Table 8.4. Results of the blind testing of aqueous ammonium Quality Control standards. The blind standards were prepared by a separate laboratory (ECN, Netherlands). On each occasion two standards were distributed, the difference in concentration measured by each analyser was compared with the actual concentration difference.

Date of test	$[NH_4^+]_{aq}$ of QC standard 1 (mg l^{-1})	$[NH_4^+]_{aq}$ of QC standard 2 (mg l^{-1})	% difference in concentration compared with the unknown standards			
			FRI	FAL-D	FAL-CH	CEH
25/5/00	22	84	44[a]	13	21	16
31/5/00	16	98	16	41	n/a	10
6/6/00	273	38	4	21	n/a	-3

[a]This test was conducted on 22/5/00 for FRI and a contaminated stripping solution container was found to be the cause.

Measurements of NH_3 exchange from the four different systems are presented in Fig. 8.2 for the pre-cut, post-cut and post-fertilisation periods. The flux intercomparison highlights various features. Firstly, it demonstrates the changing pattern of NH_3 exchange during the experiment; before the cutting of the grass, the flux was predominantly deposition to the surface with generally larger deposition at nighttime. After the cutting of the grass, the NH_3 exchange changed to predominantly emission with emission fluxes of up to 550 ng m^{-2} s^{-1}, while after fertilisation the fluxes increased to values of up to 6000 ng m^{-2} s^{-1}. The emission fluxes peaked in the daytime and were generally close to zero during nighttime. As in the comparison of concentration, there were periods of close agreement (e.g. 6th and 7th June 2000) and periods of disagreement (e.g. 1st and 8th June 2000). However generally the fluxes from the different systems showed a similar structure and similar response to the management activities on the field. The larger flux values (e.g. FAL-D on 1st and 2nd June 2000) were generally coupled with larger concentrations at 1 m although this was not always the case (e.g. FAL-D and FRI on 8th June 2000).

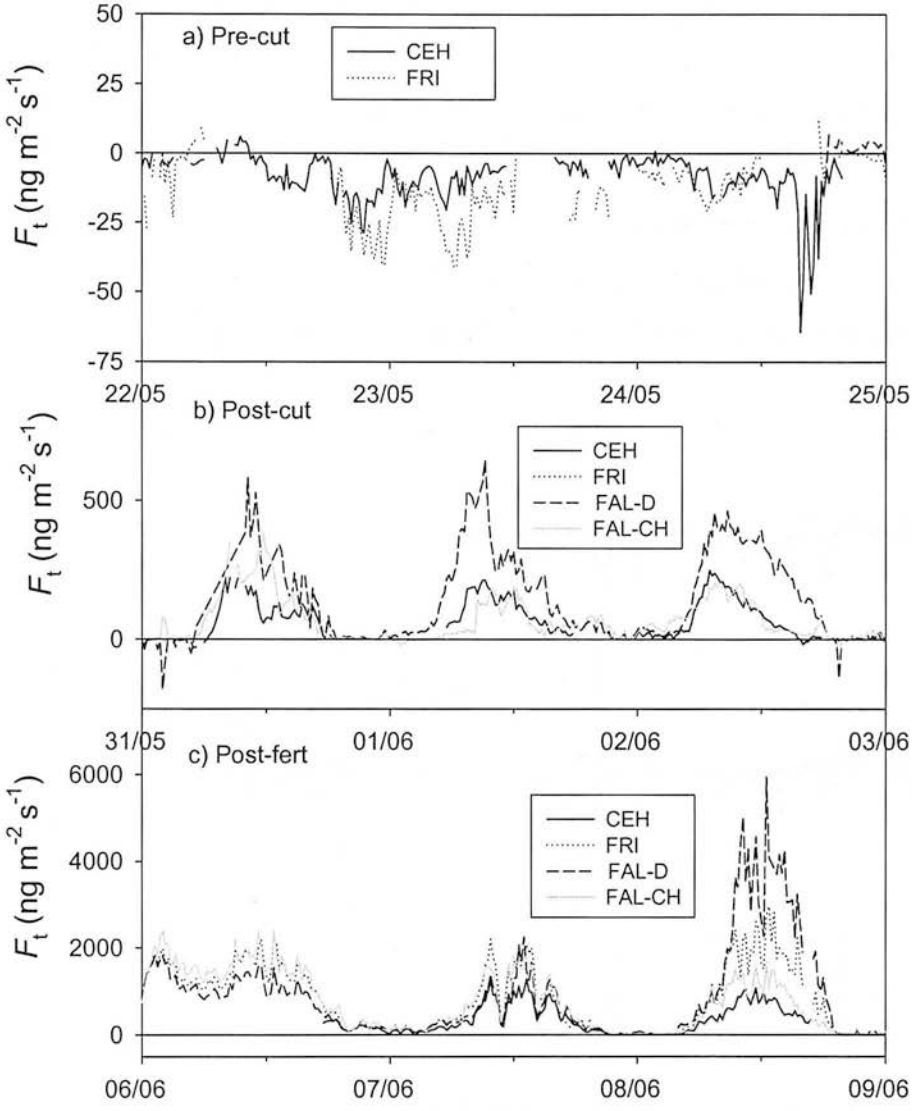

Figure 8.2. Example of NH_3 exchange (F_t) from the 4 different systems for pre-cutting, post-cutting and post-fertilising periods.

8.3.3 Assessment of advection corrections

Estimates of the difference in the vertical flux due to advection (the advection error, $\Delta F_{z,adv}$) were derived from both measurements and modelling by Loubet *et al.* (2004). The modelled estimates of $\Delta F_{t,adv}$ were applied to correct the flux measurements (F_t(1 m)) in order to provide an estimate of the fluxes at the canopy surface (F_t (z_o)). The magnitude of the advection errors at Site 1 and the advection error as a % of (F_t(1 m)) for the whole period are presented in Fig. 8.3. Loubet *et al.* (2004) estimate that the advection corrections at Site 1 due to the farm, 610 m to the west, ranged between 0 and 30 ng m^{-2} s^{-1}. However, few periods of advection from

the farm were observed due to the wind being predominantly from other directions. As well as advection from the farm emissions, advection corrections also occurred due to NH_3 emissions from the field itself and these generally ranged between 0 and 20% of (F_t(1m)). The advection corrections due to the farm were positive and would lead to underestimation of deposition if corrections were not applied. Conversely, the advection corrections due to the field itself after cutting and fertilising were negative and would lead to underestimation of emission if corrections were not applied.

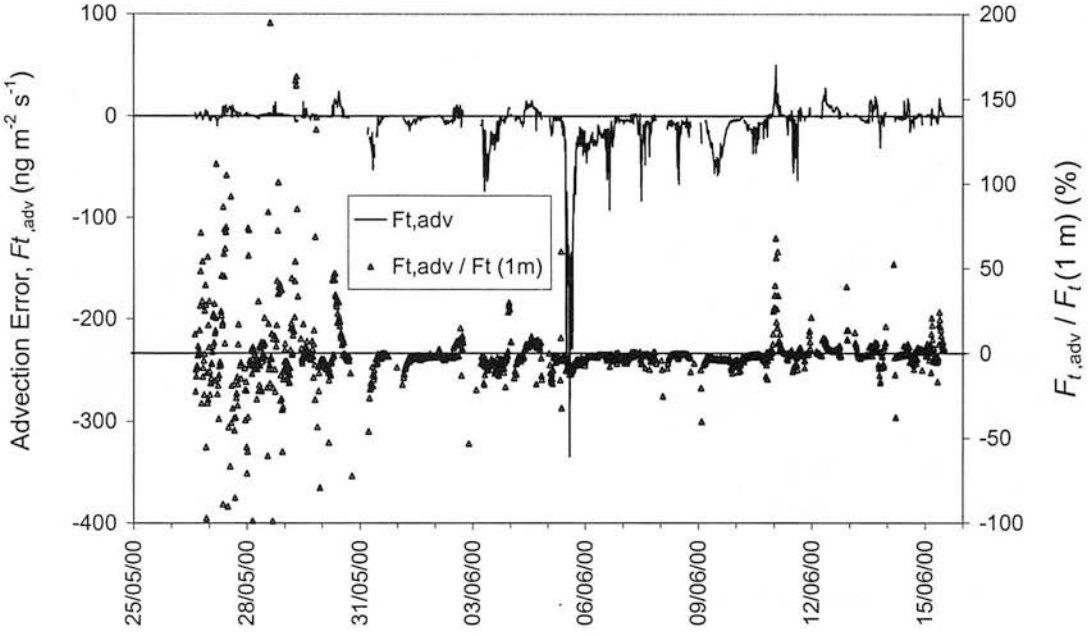

Figure 8.3. Advection error, $F_{t,adv}$ as an absolute value and as a % of the flux (F_t(1 m))

8.3.4 Regression analysis of gradient measurements

Regression of χ (1m) and F_t (z_o) against FAL-CH

Plots of χ(1 m) from FAL-D and CEH versus FAL-CH are shown in Fig. 8.4a and b. FAL-CH was used as the reference in this analysis because it was present at site 1 and also because it helps to illustrate the variation in the response of the FAL-D AMANDA. For FAL-D, χ(1 m) and $F_t(z_o)$ agree well with FAL-CH across the data range for some of the time. However, there are a considerable number of data points that greatly overestimate the concentration and flux compared with FAL-CH. The fact that this is not evident for the whole period suggests that there was some variation in the accuracy of the FAL-D analyser throughout the measurement period,

for example due to variation in the accuracy of the calibration. In addition, temperatures inside the analysers reached 40 °C on some days (data not shown). Although the concentration measurements are corrected for temperature, uncertainties in the temperature correction could lead to inaccurate estimation of concentrations. A similar pattern was seen for FRI, χ(1 m) and $F_t(z_o)$ (data not shown). CEH, χ(1 m) and F_t (z_o), underestimate the FAL-CH values but do not show the variation in agreement demonstrated by FAL-D and FRI.

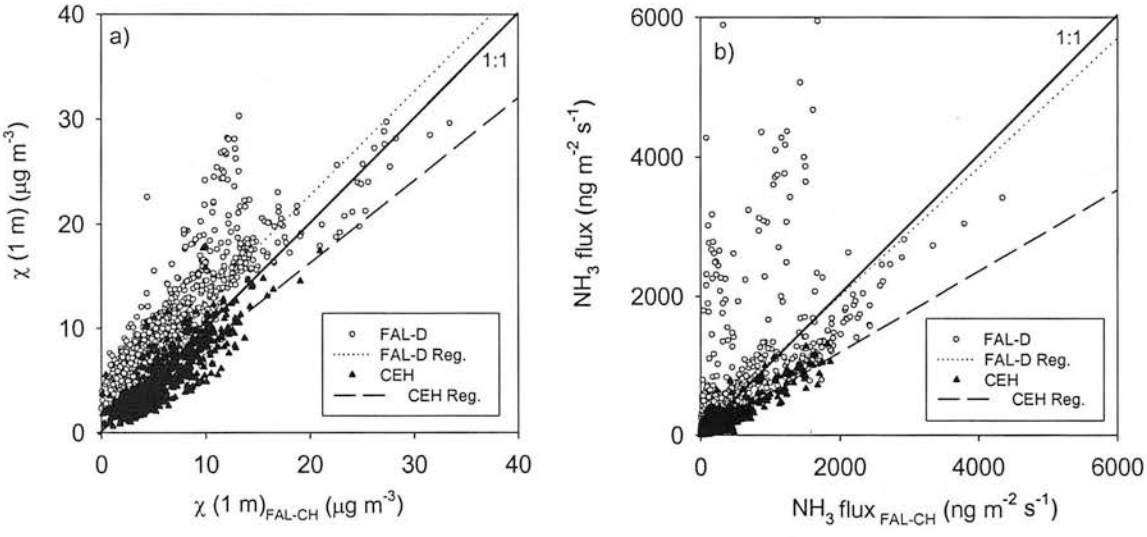

Figure 8.4. Regression of a) χ (1m) and b) NH_3 flux, from FAL-D and CEH against FAL-CH.

Regression of χ (1 m) and F_t (z_o) against mean gradient estimate

After the data processing procedures were conducted as detailed in Section 8.2.3, the "mean gradient estimate" was calculated for F_t and χ(1 m) ($F_{t,mg}$ and $\chi(1\ m)_{mg}$), this is the arithmetic mean of all available individual measurements. The regression of χ $(1\ m)_{mg}$ versus the individual systems is shown in Fig. 8.5a and b and the regression results are given in Table 8.5. These data have been corrected for advection but not for storage errors.

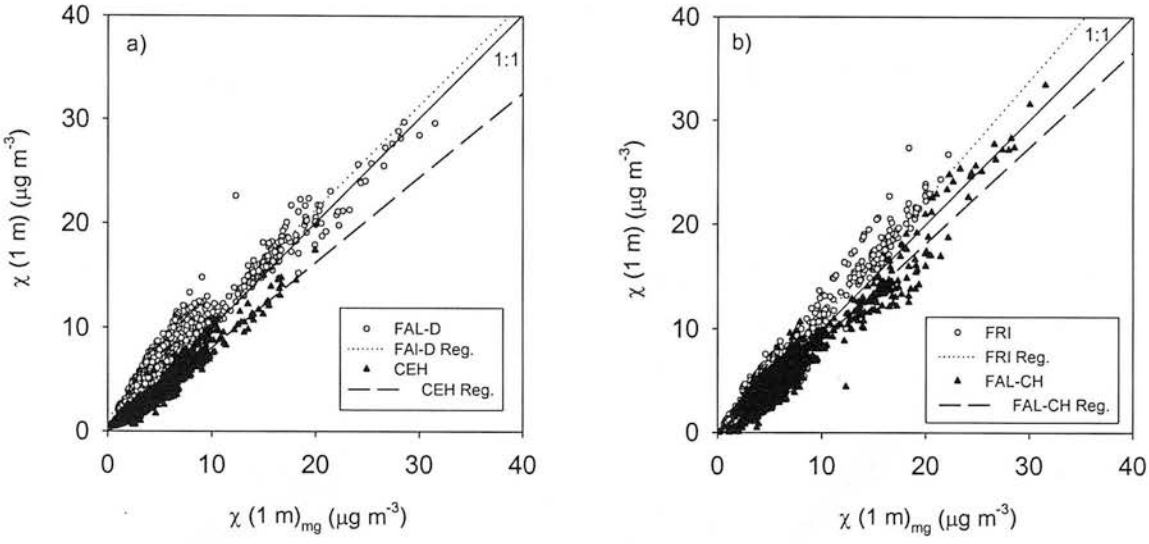

Figure 8.5. Regression of $\chi(1\ m)$ from each system against mean gradient concentration, $\chi(1\ m)_{mg}$, for a) FAL-D, CEH, and b) FRI, and FAL-CH, respectively. Data from 3, 8, 9 and 10/6/00 are not included in the regression.

Data from 3, 8, 9 and 10/6/00 are not included in the regression because on these days there is significant disagreement between the systems with FAL-D and FRI giving higher estimates compared with the CEH and FAL-CH estimates. To include the FAL-D and FRI estimates for these days in the regression would bias the regression towards FAL-D and FRI and may give a false impression of the overall dataset.

Table 8.5. Summary of linear regression results of $\chi(1\ m)$ of the individual systems versus $\chi(1\ m)_{mg}$ expressed in μg m^{-3}, given as $\chi(1\ m)_{individ} = c * \chi(1\ m)_{mg} + b$. The estimates are derived from the data shown in Fig. 8.5. Data from 3, 8, 9 and 10 June are excluded.

	c (slope)	*b* (intercept)	*n*	r^2
$\chi(1\ m)_{FRI}$	1.15	-0.68	1156	0.95
$\chi(1\ m)_{FAL\text{-}D}$	1.00	1.19	1589	0.94
$\chi(1\ m)_{FAL\text{-}CH}$	0.92	-0.31	1015	0.94
$\chi(1\ m)_{CEH}$	0.82	-0.14	1377	0.94

With data from 3, 8, 9 and 10 June removed, Fig. 8.5a and b demonstrate that there is good agreement (see Table 8.5) of $\chi(1\ m)$ between each individual system and the mean estimate and this agreement is encouraging across the concentration range. As indicated by the time series graphs, FAL-D and FRI show slightly higher concentrations than the best estimate, whilst FAL-CH and CEH show slightly lower concentration. The r^2 value for all the regressions is high (all > 0.94) which gives

confidence in the four systems and the overall mean gradient estimate. The regression of $F_{t,mg}$ versus F_t from the individual systems is shown in Fig. 8.6a and b and the regression results are given in Table 8.6.

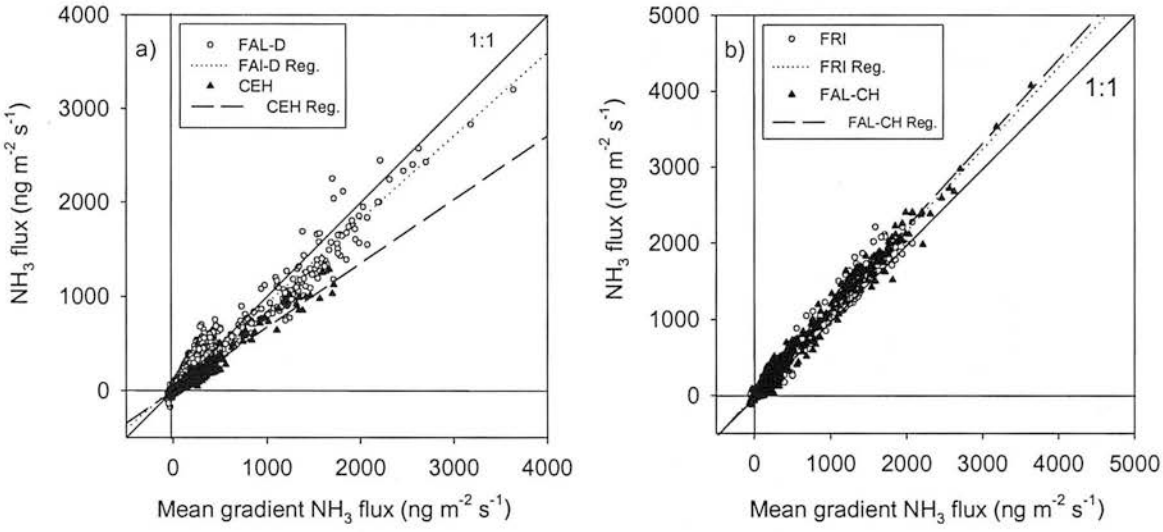

Figure 8.6. Regression of NH_3 flux from each system against mean gradient flux for a) FAL-D, CEH, and b) FRI, and FAL-CH respectively. Data from 3,8,9 and 10/6/00 are not included in the regressions.

Table 8.6. Summary of linear regression results of F_t of the individual systems versus $F_{t,mg}$ expressed in ng m^{-2} s^{-1}, given as $F_{t,individ} = c * F_{t,mg} + b$. The estimates are derived from the data shown in Fig. 8.6.

	c (slope)	b (intercept)	n	r^2
$F_{t,FRI}$	1.08	-4.98	1156	0.98
$F_{t,FAL-D}$	0.89	32.40	1589	0.95
$F_{t,FAL-CH}$	1.11	-4.73	1015	0.98
$F_{t,CEH}$	0.68	-8.79	1377	0.96

As a result of the disagreement between systems on the 3, 8, 9 and 10/6/00 an "alternative gradient estimate" for χ(1 m) and F_t was proposed for these four days. The alternative gradient estimate (subscript ag) consists of the mean of the two remaining systems on these four days. It was not felt that there was sufficient justification to remove the high measurements from the mean dataset. However, it was suspected that on these days the two high systems might not have been operating correctly. This alternative estimate was also provided to other end-users of the data to assess whether there was other supporting evidence for a higher or lower estimate on these days.

8.3.5 *Mean gradient concentration and flux in relation to management activities*

The resulting mean gradient concentrations at 1 m and flux for the whole period are shown in Fig. 8.7. This demonstrates clearly the effect of the management activities (cutting and fertilising) on the flux and concentration. In addition to the mean gradient estimate, Fig. 8.7 also shows the alternative gradient estimate for χ(1 m) and F_t on 3, 8, 9 and 10/6/00.

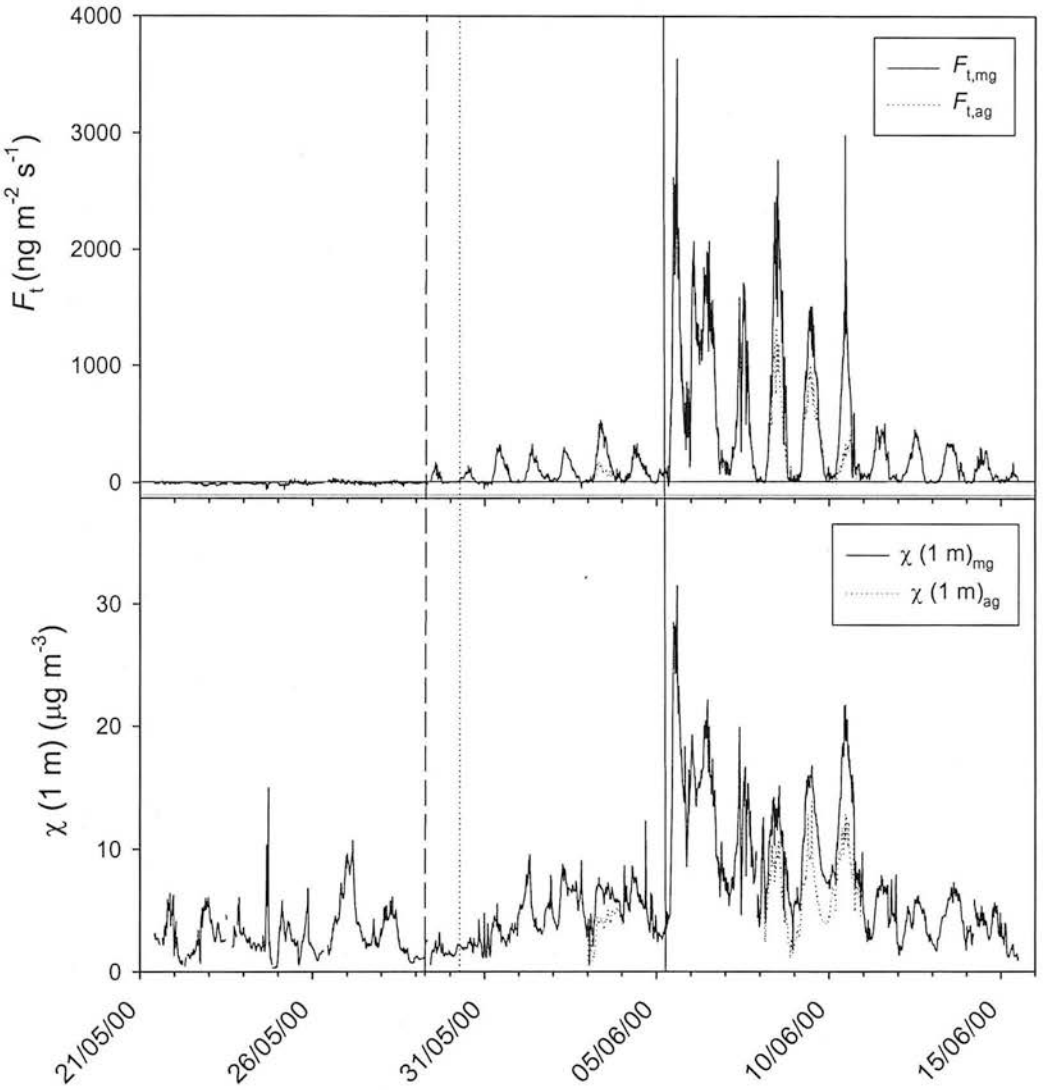

Figure 8.7. Mean gradient estimate of net NH_3 flux ($F_{t,mg}$) and χ(1 m)$_{mg}$ showing response to management activities. The alternative estimate is also shown ($F_{t,ag}$ and χ(1 m)$_{ag}$) on 3, 8, 9 and 10/6/00. Vertical lines indicate cutting (dashed line), removal of the grass from the field (dotted line) and $NH_4^+NO_3^-$ fertilisation (solid line).

Statistics for the mean gradient estimate of χ (1m) and F_t are given in Table 8.7 and 8.8 for the 3 periods: i) pre-cutting; ii) post-cutting/pre-fertilising and iii) post-fertilising. Data have been corrected for advection and storage errors.

Table 8.7. Variations in 15-minute measurements of χ(1 m) throughout different measurement periods, before and after micrometeorological filtering.

Period	Date/Time		Mean $\mu g\ m^{-3}$	Stdev $\mu g\ m^{-3}$	Median $\mu g\ m^{-3}$	Min $\mu g\ m^{-3}$	Max $\mu g\ m^{-3}$	n	Data Coverage (%)
Pre-cut	21/5 10:00 – 29/5 06:00	All data	3.11	1.95	2.61	0.29	15.00	710	94.3
		After filtering	3.14	1.90	2.61	0.35	10.71	596	79.2
Post-cut/ Pre-fertilisation	29/5 06:00 – 5/6 09:00	All data	4.29	2.04	3.97	0.58	12.32	674	98.5
		After filtering	4.39	2.33	3.84	0.58	12.32	393	57.5
Post-fertilisation	5/6 09:00 - 15/6 12:00	All data	8.36	5.47	6.78	0.92	31.52	969	99.6
		After filtering	9.16	5.70	7.38	0.92	31.52	667	68.6

Table 8.8. Variations in 15-minute measurements of net NH_3 flux (F_t) throughout different measurement periods, before and after micrometeorological filtering. Data have been corrected for advection and storage errors.

Period	Date/Time		Mean $ng\ m^{-2}\ s^{-1}$	Stdev $ng\ m^{-2}\ s^{-1}$	Median $ng\ m^{-2}\ s^{-1}$	Min $ng\ m^{-2}\ s^{-1}$	Max $ng\ m^{-2}\ s^{-1}$	n	Data Coverage (%)
Pre-cut	21/5 10:00 – 29/5 06:00	All data	-5.6	11.3	-5.4	-64.9	40.2	710	94.3
		After filtering	-5.8	11.9	-5.8	-64.9	40.2	596	79.2
Post-cut/ Pre-fertilisation	29/5 06:00 – 5/6 09:00	All data	93.7	112.7	54.5	-52.7	590.8	674	98.5
		After filtering	129.3	120.5	97.4	-47.9	590.8	393	57.5
Post - fertilisation	5/6 09:00 - 15/6 12:00	All data	471.5	608.4	194.7	-1.0	3878.2	969	99.6
		After filtering	557.5	603.3	302.9	1.5	3878.2	667	68.6

It can be seen that the median concentrations and fluxes for all periods are slightly smaller than the mean values, reflecting a log normally skewed distribution of both χ(1 m) and F_t. The effect of the data filtering for micrometeorological restrictions (Section 8.2.4, step vii) is illustrated, with slightly larger χ(1 m) and F_t from the filtered dataset. This reflects the fact that more data were excluded from night-time conditions, when χ(1 m) and F_t were smallest.

Pre-cutting

Prior to cutting of the grass, the flux was much less certain (see Fig. 8.9) but was predominantly deposition to the surface (see Fig. 8.2 for typical diurnal course). The mean flux of the pre-cutting period was -5.6 ng m^{-2} s^{-1} if all data are included and -5.8 ng m^{-2} s^{-1} if only data which pass the micrometeorological criteria are included. Any emission, which was observed was generally small, the maximum emission observed over the period was 40 ng m^{-2} s^{-1}. The intensive grassland was generally acting as a sink for NH_3 during this period.

Post-cutting, pre-fertilising

Immediately after cutting (29/5/2000) the NH_3 flux switched to emission. The emission had a diurnal pattern with very small fluxes during night-time and emission fluxes increasing during the daytime; daily peak emission values were 140 to 530 ng m^{-2} s^{-1}. The mean daily flux during the cutting period was 85 ng m^{-2} s^{-1} (all data) or 137 ng m^{-2} s^{-1} (only data which passes the micromet criteria). These values are equivalent to 60 and 97 g N ha^{-1} day^{-1}, respectively.

Post-fertilising

There was a rapid increase in NH_3 flux observed following the N fertilisation (5/6/2000), with values peaking at 3880 ng m^{-2} s^{-1}. During the first two nights after fertilisation (5/6-6/6 and 6/6-7/6) there were mean emissions of 990 ng m^{-2} s^{-1} and 150 ng m^{-2} s^{-1}, respectively. The mean flux over the whole post-fertilising period was 472 ng m^{-2} s^{-1} (all data) or 558 ng m^{-2} s^{-1} (only data which passes the micrometeorological criteria). These values are equivalent to 322 and 380 g N ha^{-1}

day^{-1}, respectively. The emission flux decreased on 11/6/00 but was still up to 500 ng m^{-2} s^{-1}, 13 days after cutting.

The accumulated flux was –0.04, 0.54 and 3.95 kg N ha^{-1} for the pre-cutting, post cutting and post fertilising periods, respectively. The N applied on 5/6/00 was 108 kg N ha^{-1} so the accumulated flux up to 10 days after the fertilisation was 3.7 % of the N applied.

8.3.6 Storage errors

The magnitude of the storage errors in the mean gradient flux estimate and the storage error as a % of ($F_{t,mg}$) for the whole period are presented in Fig. 8.8. Storage errors were calculated according to Section 2.3.2. This figure shows that the storage errors were generally small, the median storage error being 0.004 ng m^{-2} s^{-1}.

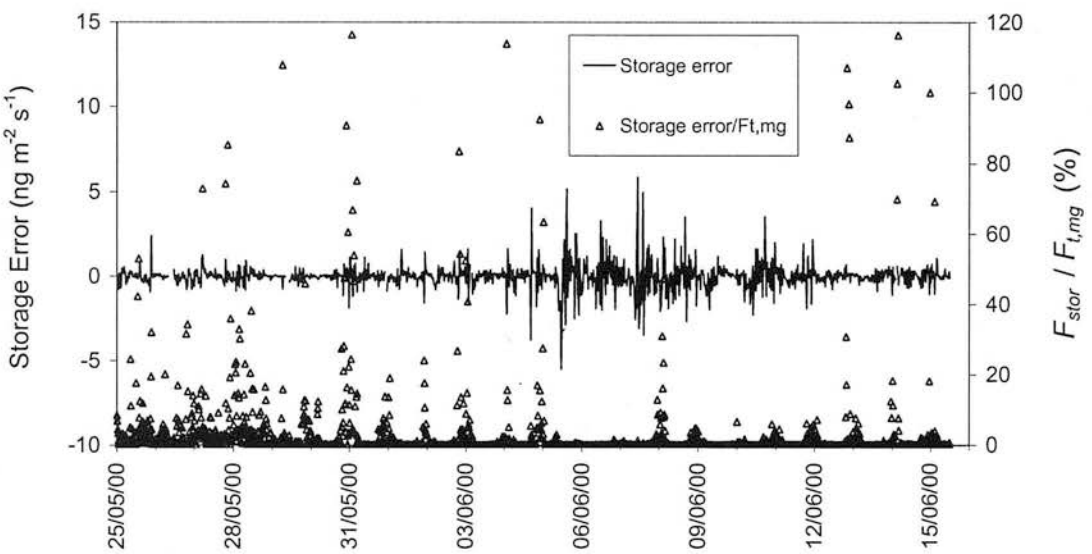

Figure 8.8. Storage error, $F_{t,sto}$ as an absolute value and as a % of the flux ($F_{t,mg}$)

8.3.7 Uncertainties in χ (1 m) and $F_{t,ag}$

The availability of up to four parallel estimates of the ammonia concentrations and fluxes allows the time course of uncertainties in the estimates to be reported as the standard error (SE) of the mean 15-minute values. The SE is calculated as $\sigma_{n-1}/\sqrt{n}$, where σ_{n-1} is the sample standard deviation and n is number of estimates available for a given 15 minute period. Hence the magnitude of the SE depends on both the level of agreement of the denuders and the number of denuders operating at a given time. The time course of the SE is presented in Fig. 8.9 for $F_{t,ag}$ and χ(1 m). Given the

rapid variation in SE on a 15-minute basis, to make the graphs more readable, the values are shown as the 1 hourly running medians of the 15 minute SE values. The values are shown as %SE of the mean, however, in the case of the flux, periods of bi-directional exchange make %SE less meaningful, and therefore the absolute value of SE (in ng m^{-2} s^{-1} is also shown). Fig. 8.9 shows that in the pre-cut period, the SE of the 15-minute values was typically around 60% of $F_{t,ag}$, with absolute SE values of 10-20 ng m^{-2} s^{-1}. Following cutting, the errors differ over the day with daytime SE in the flux typically 40%. The % SE is smallest following fertilisation with daytime values typically 15%, increasing to typically 30% from 10 June. The overall median uncertainty in the 15 minute estimates of χ(1 m) is 18%, with values mostly in the range 5 to 50%.

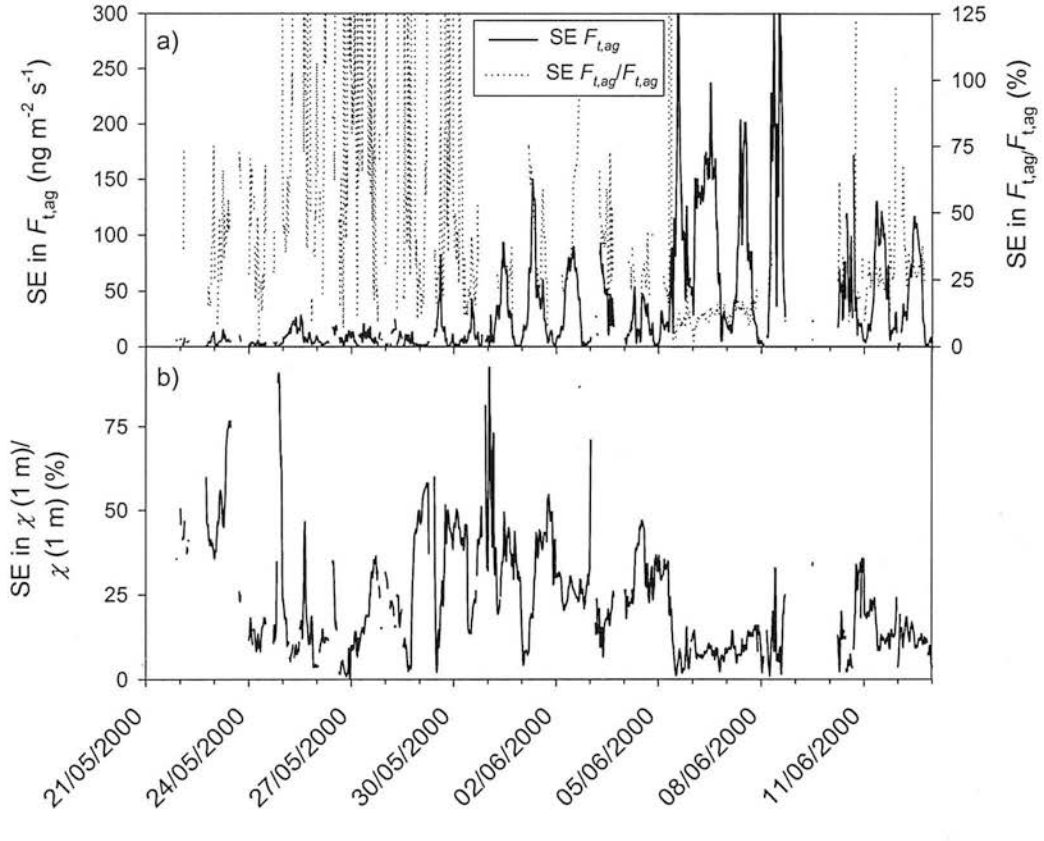

Figure 8.9. Time course of percentage standard errors in a) the measured ammonia flux and b) concentration at (1 m) (from the alternative estimate, using 1 hour medians of 15 minute estimates). Because of the existence of bi-directional exchange for NH_3 flux (giving less meaningful %SE), the absolute value of SE Flux (ng m^{-2} s^{-1}) is also shown.

In addition to giving the uncertainties in the individual 15 minute flux estimates it is possible to consider the statistics of $F_{t,mg}$ and χ (1 m) for the main management

periods and the whole of the experiment. With longer-averaging periods the uncertainties between the different systems reduce, and are shown in Table 8.9.

Table 8.9. Standard errors (SE) and % standard errors in the flux estimates between the 4 ammonia sampling systems according to the different management periods. The mean values for the period are shown in Table 8.7 and 8.8.

	Pre cut	Post cut	Post fert	All campaign
SE in $F_{t,mg}$	4.7	28.8	88.8	57.8
% SE in $F_{t,mg}$	82.8	37.7	22.9	32.1
SE in χ(1 m)	0.49	0.78	1.16	0.87
% SE in χ(1 m)	15.62	19.43	16.01	17.22

8.4 Discussion

8.4.1 Intercomparison of gradient measurements

The inter-comparison of gradient measurements was encouraging, with the regression of F_t from all individual systems versus $F_{t,mg}$ giving $r^2 > 0.95$. There was also good agreement achieved across the concentration range, except for some problem days where overestimation of concentration is suspected to have occurred in some of the systems, possibly due to high operating temperatures and concentrations measured out of the calibration range. The inter-comparison highlighted the need for regular calibration of flux gradient systems and regular quality standard checks. As concluded in Harrison and Kitto (1990), operator differences can induce the same variation in NH_3 measurements as different measuring techniques and although techniques such as AMANDA and the WEDD have been shown to be reliable in measuring NH_3, operators still have to be careful in their running of these systems. A reliable clean deionised water supply, regular changing of pump tubing and regulation of instrument operating temperature are all essential to maintain the reliability of these systems.

Having four independent systems did result in a robust final dataset with data coverage of NH_3 concentrations and fluxes in the mean dataset of 97%. The main restriction on estimates was a filter according to strict micrometeorological criteria, which reduced the flux data coverage to 68% if these filter criteria were applied. It is highly unusual to achieve data coverage of nearly 100% for NH_3 flux measurements and consequently this dataset provides a useful input for end-users of the data such as

modellers. In addition, having four estimates provides an estimate of the uncertainty of the flux measurements. In a typical field experiment it is more likely that there will only be one NH_3 flux measurement system and so it is not possible to get an estimate of the uncertainty other than the scatter in the concentration profiles. In this instance the standard error of the four estimates indicates periods of greater and lesser certainty in the measurement. SEs in 15 minute values were typically between 15-60% of F_t while the value for the whole field campaign was 32%.

8.4.2 Influence of management activities on NH_3 flux

The measurements support the previous finding of enhanced emissions from grass cutting at Easter Bush, with a mean daily flux of 97 g N ha^{-1} day^{-1} after cutting compared with measurements of predominantly deposition before cutting. As expected, emissions were also enhanced following fertilisation, with a mean daily flux of 380 g N ha^{-1} day^{-1}. These values are of a similar magnitude to those observed at Easter Bush (Chapter 5) although the % emission of fertiliser N is higher, amounting to 3.7% of the N applied as calcium ammonium nitrate. The increased percentage emission is possibly a result of the high temperatures, which were observed, particularly in the latter period of the campaign. The mean air temperature at 1 m was 17.6°C during 5/6/00-15/6/00, whilst daily maximums reached 39°C.

Chapter 9: Synthesis and Conclusions

9.1.1 Measurements of ammonia exchange

Measurements of surface-atmosphere ammonia (NH_3) exchange were conducted for a period of 19 months (May 1998-November 1999) over an intensively managed grassland in southern Scotland (Easter Bush) at a 15-minute time resolution. In addition, NH_3 exchange was measured on a campaign basis for just under four weeks over an intensively managed grassland in Germany (Braunschweig). The aerodynamic gradient method was used to calculate NH_3 exchange at both these sites. A comprehensive suite of measurements of micrometeorological, soil and vegetation parameters was also conducted in order to aid interpretation of the measurements and investigation of the controls on NH_3 exchange. In addition, these data were used for the development of models of NH_3 exchange, providing both input data and datasets for assessing model performance. Long-term measurement data with high temporal resolution is essential for the development of models of pollutant exchange, particularly as many current parameterisations within these models were derived from measurement campaign data of short duration.

Comparisons of key micrometeorological parameters, measured by different instruments or at different locations, were conducted to ensure data quality and to fill-in data on the few occasions when data were unavailable. This resulted in high data coverage of 91% for the meteorological data. Data coverage for the NH_3 flux data was 71%, reduced to 62% after applying micrometeorological filtering criteria. This equates to 32,735 individual 15-minute NH_3 flux measurements. Characterisation of the Easter Bush site showed that the cumulative normalized contribution to the flux measurement was was > 65% for 82% of the time. In addition, nearby fields were similarly managed grassland and so could be expected to have a similar NH_3 exchange pattern, thereby not presenting a large discontinuity at the boundary of the field site. The prevailing wind direction was from the south-west (69.4 % of the time) with some north-easterly winds (27.1 % of the time).

The median, arithmetic mean and geometric mean NH_3 concentration for the whole measurement period were 1.07, 1.52 and 0.90 $\mu g\ m^{-3}$, respectively, which are fairly

typical values for a mixed rural area. The monthly geometric standard deviation (σ_G) in NH_3 concentration at the highest measurement level varied between 2.17-5.25. These fairly large values of σ_G indicate that the NH_3 concentrations at Easter Bush are largely influenced by local sources (Burkhardt *et al.*, 1998), and reflect the high spatial and temporal variability of local NH_3 sources and sinks. The median and mean flux over the whole measurement period were emission of 0.23 and 13.9 ng m^{-2} s^{-1}, respectively. These values are for the unfiltered dataset, the values increase slightly if data are filtered for strict micrometeorological criteria, but the values are not substantially different (0.50 and 14.9 ng m^{-2} s^{-1}, respectively).

The NH_3 exchange was bi-directional with large diurnal and seasonal variation. This variation was shown to be strongly linked to grassland management (cutting, fertilisingand grazing) and phenology in addition to meteorology (temperature, solar radiation, humidity, wetness and atmospheric turbulence). The grassland at Easter Bush varied from being a net sink for NH_3 during winter months (-6.0 g NH_3-N ha^{-1} d^{-1}) and prior to cutting of the grass (-4.9 g NH_3-N ha^{-1} d^{-1}) to being a net source after the grass was cut (29.3 g NH_3-N ha^{-1} d^{-1}) and after nitrogen fertilisation (153.6 g NH_3-N ha^{-1} d^{-1}). Net emission was also observed during grazing periods (33.0 g NH_3-N ha^{-1} d^{-1}). The pattern of NH_3 exchange was similar for 1998 and 1999.

The temporal pattern of NH_3 exchange at Braunschweig was similar to Easter Bush, with a similar magnitude of deposition prior to cutting of the grass (-4.0 g NH_3-N ha^{-1} d^{-1}). However, the emissions following cutting of the grass (66.7 g NH_3-N ha^{-1} d^{-1}) and following fertilisation (335.5 g NH_3-N ha^{-1} d^{-1}) at Braunschweig were about twice as large as those at Easter Bush. This is reflected in the substantial difference between accumulated NH_3 flux at Braunschweig during 21st May-5th June compared with the same period at Easter Bush in 1998 and 1999 (Fig. 9.1). It is likely that the higher temperatures (up to 40 °C) and dry conditions during the Braunschweig experiment favoured higher emissions and decreased deposition. In addition, more fertiliser N was applied at Braunschweig than at Easter Bush (Table 9.1), although the difference in application rate is not large enough to explain the full difference in emission. There is the possibility that some of the NH_3 analysers at Braunschweig were over-reading concentrations and fluxes (discussed in Chapter 8).

However, the 'alternative' gradient accumulated flux is also presented in Fig. 9.1 and this is still considerably larger than the Easter Bush estimates.

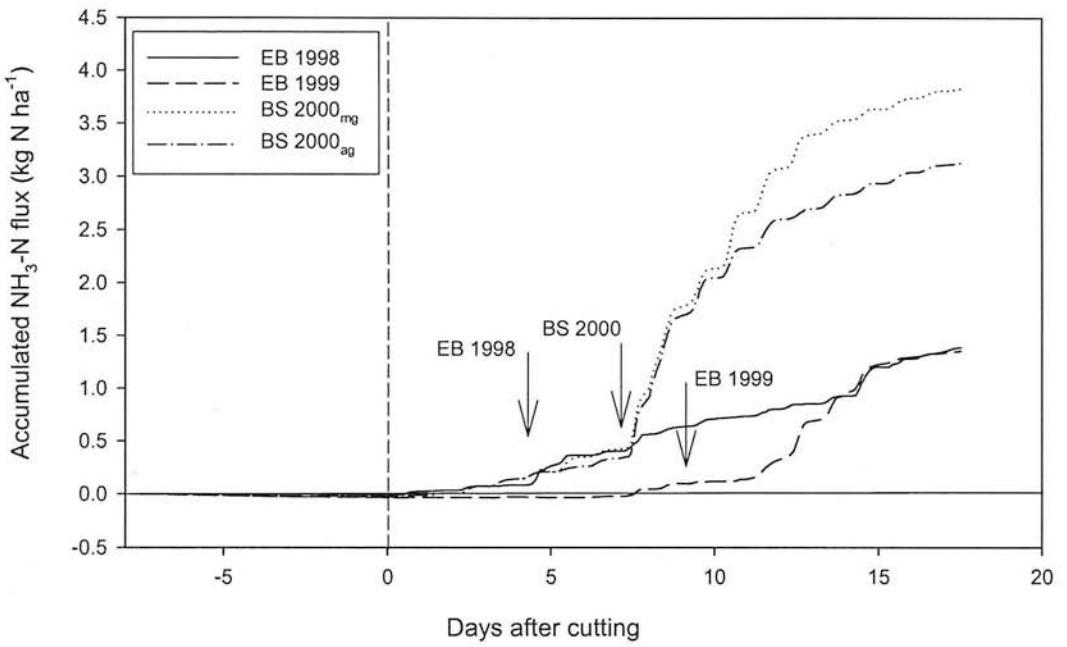

Figure 9.1. Accumulated NH_3 flux for 21st May to 5th June for Easter Bush 1998 and 1999 and Braunschweig 2000. The two different estimates for Braunschweig are for the mean (mg) and alternative (ag) gradient estimate (see Chapter 8 for details). The vertical dashed line indicates the time of cut and the arrows indicate the different N fertilisation dates (see Table 9.1 for details).

Table 9.1. Field management details and accumulated flux over period of 1st cut (7.5 days prior to cut and 17.5 days after cut) for Easter Bush and Braunschweig (data from Table 4.3 and Section 8.2.1).

Field Site	Date of cut	Date of fertilisation	Amount of fertiliser N applied (kg N ha^{-1})	Type of fertiliser applied	Accumulated flux
Easter Bush 1998	5/6/98	9/6/98	104	Compound (N:P:K) (26-5-10)	1.39
Easter Bush 1999	2/6/99	11/6/99	91	Compound (N:P:K) (26-5-10)	1.36
Braunschweig 2000	29/5/00	5/6/00	108	Calcium ammonium nitrate	3.82 (3.12*)

*Accumulated flux for alternative gradient estimate

Enhanced emissions of NH_3 were observed following four separate grass cutting events (June 1998, August 1998 and June 1999 at Easter Bush and June 2000 at Braunschweig) with peak emissions of 380, 200, 539 and 508 ng m^{-2} s^{-1}, respectively. The magnitude of these emissions was up to an order of magnitude greater than the emissions observed from the grassland prior to cutting. Enhanced

NH_3 emissions from cut grassland have been observed, but not quantified prior to this study (Sutton *et al.*, 1997a). The similarity of the NH_3 response to grass cutting between the two years at Easter Bush and between locations in two different countries provides corroboration for this emission source. The origin of the emission was less easily identified; an increase in foliar NH_4^+ after cutting supports the hypothesis that the increased emissions are at least partially from the remaining cut sward. However, there could also be a contribution from litter and senescing leaves. The relative contribution of the different sources remain to be quantified.

The net annual budget of NH_3 exchange for the Easter Bush grassland for May 1998-April 1999 was emission of NH_3 of 1.9 kg N ha^{-1} yr^{-1}, equating to 1.6% of the fertiliser N applied. The gross emission flux for the year (sum of all emission events) was 4.2 kg N ha^{-1} yr^{-1}. Scaling up these gross emissions across the whole of the UK improved grassland (60,500 km^2) would lead to 25 kt NH_3-N, equivalent to 9.5% of the UK total emissions. These results indicate that the gross emission from all processes in fertilised grassland, including emissions from fertilisation, grazing and from cutting, make a significant contribution to the NH_3 emission budget of the UK.

The net annual NH_3 exchange can be compared with other N species to obtain a full N budget. As other N species were not measured at the Easter Bush site, measurements from a nearby moorland site Flechard (1998) are used to construct the N budget (Table 9.2). This results in the net annual N budget for Easter Bush being deposition of 3.8 kg N ha^{-1}.

Table 9.2. Estimate of net annual N budget at Easter Bush (all values except NH_3 from Flechard, 1998)

N species	Net annual N exchange kg N ha^{-1} yr^{-1}*
NH_3: Dry	+1.9
NH_4^+: Dry	-0.3
NH_4^+: Wet	-2.4
NO_3^-: Dry	-0.4
NO_3^-: Wet	-1.9
HNO_2: Dry	-0.1
NO_X: Dry	-0.6
Total Dry	+0.5
Total Wet	-4.3
Total Dry + Wet	-3.8

*Positive values indicate emission and negative values indicate deposition

These values can be compared with more recent measurements of wet NH_4^+ (3.2 kg N ha^{-1}) and wet NO_3^- (2.4 kg N ha^{-1}) from a second nearby moorland site for the period 1/5/02-28/4/03 (L. Shepard, Pers. Comm.), which would give a slightly larger net annual N budget for Easter Bush of 5.1 kg N ha^{-1} deposition.

In addition to emissions following cutting and fertilising with ammonium nitrate, emissions were also observed during grazing periods and after application of urea. Urea was applied to Easter Bush to provide sufficient emissions of NH_3 to test a newly developed REA system. Emissions from the application of urea (2.7% of N applied) were at the low end of published values (6-49% of N applied), but probably reflect the low application rate, the time of year and the prevailing meteorology at this time (e.g. low temperatures, high *RH* and wetness). Results from a period of sheep grazing at Easter Bush indicated an upper limit of emissions of 0.8 g NH_3-N $sheep^{-1}$ d^{-1}. This value is of a similar magnitude to other published values (0.9-1.2 g NH_3-N $sheep^{-1}$ d^{-1}) (Jarvis *et al.*, 1991).

The net NH_3 exchange over intensively managed grassland at Easter Bush was a small source (1.9 N ha^{-1} yr^{-1}). Semi-natural and forested ecosystems tend to be net sinks for ammonia, while studies over arable crops and intensively managed grassland receiving higher fertiliser N input (e.g. in The Netherlands) have reported larger net annual sources of NH_3.

The influence of meteorological conditions on the NH_3 concentrations and exchange was examined; NH_3 concentration increased with increasing temperature except for temperatures below about 7.5 °C, in which case NH_3 concentration increased with decreasing temperature (observed for a period of predominantly deposition fluxes). NH_3 emission fluxes also increased with increasing temperature, although not as strongly as the thermodynamic response. Evidence of NH_3 flux controlling the NH_3 concentration at the site was also observed during emission periods, this is contrary to the standard inferential approach for estimating NH_3 flux, which presumes that increased concentration leads to increased deposition.

9.1.2 Modelling of ammonia exchange

NH_3 exchange is particularly challenging to model due to its bi-directional nature and its high spatial and temporal variability. It is also strongly dependent on ecosystem type, phenology, management and meteorological conditions as shown in Chapter 5. The incorporation of NH_3 for the first time in European transboundary air pollution abatement strategies increases the need for accurate parameterisations of the dry deposition of NH_3 to ecosystems. A two-layer canopy compensation point resistance model, incorporating bi-directional foliar stomatal exchange, deposition to leaf cuticles and NH_3 exchange with the ground surface, was applied to the NH_3 measurements at Easter Bush. Close agreement between measured and modelled fluxes was obtained by introducing seasonally varying foliar and ground layer emission potentials (Γ_s, Γ_g) for key periods. This is a significant improvement on the current use of a constant emission potential within national deposition models and leads to a more accurate prediction of net NH_3 exchange. Indeed, the results presented here indicate that the constant stomatal emission potential of 3,800 currently used in the UK deposition model (Smith *et al.*, 2000) would be an overestimate in the winter and pre-cut period and a significant underestimate during the cutting and fertilising period. Incorporating the seasonally varying emission potentials presented here in the UK deposition model may lead to a decrease in critical load exceedance in the winter and a corresponding increase in the summer.

In addition to the resistance modelling approach, a dynamic grassland ecosystem model (PaSim) was applied to the NH_3 measurements. In PaSim, the emission potentials and NH_3 exchange are linked functionally to plant and soil N cycling so the ecosystem processes and interactions of NH_3 exchange can be explored in detail. Initialisation and input data required for PaSim were obtained from the measurements at Easter Bush. Other measurement data was used to assess the performance of PaSim. Fig. 9.2 presents the time varying stomatal emission potential (Γ_s) simulated by PaSim and compares it against the parameterisations of Γ_s and Γ_g obtained from the two-layer canopy compensation point modelling. It can be seen that the maximum values of Γ_s are similar (35,000 in PaSim and 28,000 in the two-layer model) and the initial increase in Γ_s is very similar. However, PaSim simulates

a sharper peak in Γ_s over the period of fertilisation. The comparison of simulated Γ_s with bioassay estimates (Fig. 7.8) shows that the bioassay estimates are up to two orders of magnitude lower than the simulated values. Discrepancies between bioassay and other estimates of Γ_s, such as from cuvette studies, has been observed in other studies (e.g. Hill *et al.*, 2001). The reasons for these discrepancies are not yet fully understood, although pH gradients in the apoplast with localised hotspots, which are not measured by the bioassay technique, may explain some of the variation.

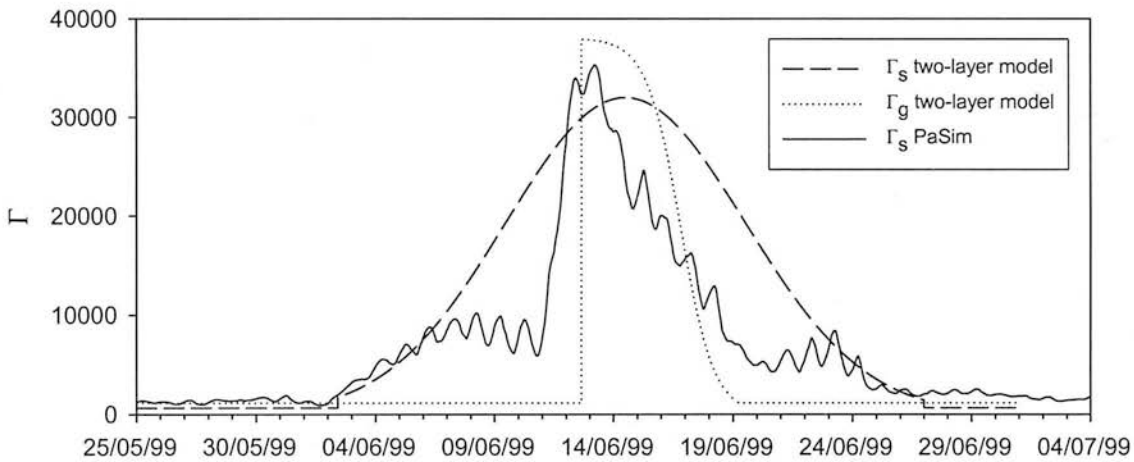

Figure 9.2. Parameterisations of Γ_s and Γ_g derived for the cutting and fertilising period at Easter Bush during June 1999 with the two-layer canaopy compensation point model compared against simulated Γ_s from PaSim for the same period in 1999.

Various simulated parameters in PaSim were compared with measured values and these comparisons indicate areas where the mechanisms are well described in the model and areas for improvement. For example, the simulated foliar N content has a similar temporal variability to the measured values, but the magnitude of the changes is not represented (Fig. 7.6). This difference between the simulated and measured values indicates that there may be an additional restriction to plant N uptake in the field, which is not parameterised in the model.

Scenarios of changing climate and management were explored with PaSim. The simulated NH_3 emissions did not follow the expected thermodynamic response to a rise in temperature and demonstrated the complexity of the ecosystem level response of NH_3 exchange to climate change, indicating that there are other ecosystem

interactions, which offset the effect of increased temperature on NH_3 emissions, such as increased growth. Simulated NH_3 emissions were reduced by 15% by delaying the timing of fertiliser applications by two weeks, indicating the potential of this measure as an NH_3 abatement option.

9.1.3 Recommendations for future work

Measurement of ammonia exchange:

- Enhanced emissions of NH_3 from grass cutting have been observed and quantified, but further work is needed to investigate the relative contribution of the possible sources (the remaining sward, litter and soil). It would be valuable to conduct cuvette measurements alongside micrometeorological measurements of NH_3 exchange and also conduct more frequent bioassay analyses of apoplastic and foliar NH_4^+ concentration.

- One of the challenges in quantifying the enhanced emissions of NH_3 from grass cutting is to partition the net exchange into enhanced NH_3 emission from the effect of cutting and from the effect of N fertilisation. Experiments to investigate cutting emissions at a field level without the additional fertilisation effect should be initiated. This would help quantify the magnitude and timecourse of enhanced emissions from cutting without the secondary effect of fertilisation.

- The partitioning of soil and foliar emission during grazing and after fertilising is also not fully quantified. Cuvette measurements should be conducted to isolate the different pathways of NH_3 exchange.

- Long-term measurements are invaluable for developing the understanding of the controls on NH_3 exchange and also for model development. Further long-term measurements of NH_3 exchange are needed over other key ecosystem types in Europe to characterise the seasonal exchange. In particular more measurements are required over forests and crops as there are few long-term studies of NH_3 exchange over these ecosystems.

Modelling of ammonia exchange:

- The two-layer canopy compensation point model has been shown to provide close agreement between measured and modelled net NH_3 exchange of intensively managed grassland. A significant development has been the introduction of seasonal parameterisations of emission potentials. This approach should be extended for other periods and for other key ecosystems, to enable the two-layer model to be fully incorporated into national and European atmospheric transport models.

- Further work is required on incorporating the current state of knowledge of NH_3 exchange into atmospheric transport models. In particular, the consequence of introducing seasonal parameterisations of emission potentials should be explored.

- The cuticular resistance (R_w) is still one of the least well characterised resistances for NH_3 exchange, more investigations are required of the relationship of R_w with pollution climate and wetness to improve the generalisation of R_w across Europe.

- More measurements of within canopy turbulence are required to extend the knowledge of in-canopy resistances and futher develop their seasonal parameterisation.

- The application of a dynamic grassland ecosystem (PaSim) demonstrated the potential of such a model to investigate the ecosystem level processes of NH_3 exchange. There is scope for improvement of the model, particularly the description of fertiliser dissolution and the rates of N transfer between the various plant N pools. The response of simulated NH_3 exchange to climate change should also be explored more thoroughly as initial scenarios demonstrated the response of NH_3 emission to increased temperature may not be as strong as expected purely on a thermodynamic basis. In addition, PaSim should be used to explore other NH_3 emission abatement options.

- This thesis largely concentrated on conducting long-term measurements of NH_3 exchange at a high time resolution along with detailed soil and vegetation measurements, this required a significant measurement effort. This dataset is now a valuable resource and should be utilised further in investigating the controls on NH_3 exchange, in model development and in validation of UK and European atmospheric transport models.

References

Achermann, B., Bobbink, R. (2003) Workshop summary. In: Achermann, B., Bobbink, R. (Eds.), Empirical critical loads for nitrogen, UNECE Expert Workshop, 11-13 November 2002, pp. 11-18. SAEFL, Berne, Switzerland.

Aerts, R., Berendse, F., Decaluwe, H., Schmitz, M. (1990) Competition in heathland along an experimental gradient of nutrient availability. *Oikos,* **57**, 310-318.

Allegrini, I., Desantis, F., Dipalo, V., Febo, A., Perrino, C., Possanzini, M., Liberti, A. (1987) Annular denuder method for sampling reactive gases and aerosols in the atmosphere. *Sci. total Environ.,* **67**, 1-16.

Allen, A.G., Harrison, R.M., Wake, M.T. (1988) A meso-scale study of the behaviour of atmospheric ammonia and ammonium. *Atmos. Environ.,* **22**, 1347-1353.

Allen, S.E. (1989) Analysis of vegetation and other organic materials. In: Allen, S.E. (Ed.), *Chemical analysis of ecological materials*, pp. 46-61.

Andersen, H.V., Hovmand, M.F., Hummelshoj, P., Jensen, N.O. (1999) Measurements of ammonia concentrations, fluxes and dry deposition velocities to a spruce forest 1991-1995. *Atmos. Environ.,* **33**, 1367-1383.

Anlauf, K.G., Fellin, P., Wiebe, H.A., Schiff, H.I., Mackay, G.I., Braman, R.S., Gilbert, R. (1985) A comparison of 3 methods for measurement of atmospheric nitric-acid and aerosol nitrate and ammonium. *Atmos. Environ.,* **19**, 325-333.

Appel, B.R., Tokiwa, Y., Kothny, E.L., Wu, R., Povard, V. (1988) Evaluation of procedures for measuring atmospheric nitric-acid and ammonia. *Atmos. Environ.,* **22**, 1565-1573.

Ball, P.R., Ryden, J.C. (1984) Nitrogen relationships in intensively managed temperate grasslands. *Plant and Soil,* **76**, 23-33.

Barthelmie, R.J., Pryor, S.C. (1998) Implication of ammonia emissions for fine aerosol formation and visibility impairment - a case study from the Lower Fraser Valley, British Columbia. *Atmos. Environ.,* **32**, 345-352.

Batey, T. (1982) Nitrogen cycling in upland pastures of the UK. *Phil. Trans. R. Soc. Lond. Ser. B Biol. Sci.,* **296**, 551-556.

Benner, W.H., Ogorevc, B., Novakov, T. (1992) Oxidation of SO_2 in thin water films containing NH_3. *Atmos. Environ.,* **26**, 1713-1723.

Blum, H., Hendrey, G., Nosberger, J. (1997) Effects of elevated CO_2, N fertilization, and cutting regime on the production and quality of *Lolium perenne* L. shoot necromass. *Acta Oecologica-International Journal Of Ecology,* **18**, 291-295.

Bobbink, R. (1991) Effects of nutrient enrichment in dutch chalk grassland. *J. appl. Ecol.,* **28**, 28-41.

Bobbink, R., Heil, G.W., Raessen, M. (1992) Atmospheric deposition and canopy exchange processes in heathland ecosystems. *Environ. Pollut.,* **75**, 29-37.

Bobbink, R., Ashmore, M.R., Braun, S., Fluckiger, W., van den Wyngaert, I.J.J. (2003) Empirical nitrogen critical loads for natural and semi-natural ecosystems: 2002 update, Empirical critical loads for nitrogen, UNECE Expert Workshop, 11-13 November 2002, pp. 43-170. SAEFL, Berne, Switzerland.

Breitenbach, L.P., Shelef, M. (1973) Development of a method for the analysis of NO_2 and NH_3 by NO-measuring instruments. *J. Air Pollut. Control Assoc.,* **23**, 128-131.

Brink, C., Kroeze, C., Klimont, Z. (2001) Ammonia abatement and its impact on emissions of nitrous oxide and methane in Europe - Part 1: method. *Atmos. Environ.,* **35**, 6299-6312.

Brost, R.A., Delany, A.C., Huebert, B.J. (1988) Numerical modeling of concentrations and fluxes of HNO_3, NH_3, and NH_4NO_3 near the surface. *J. geophys. Res.,* **93**, 7137-7152.

Burkhardt, J., Eiden, R. (1994) Thin water films on coniferous needles. *Atmos. Environ.,* **28**, 2001-2011.

Burkhardt, J., Gerchau, J. (1994) A new device for the study of water-vapor condensation and gaseous deposition to plant-surfaces and particle samples. *Atmos. Environ.,* **28**, 2012-2017.

Burkhardt, J., Sutton, M.A., Milford, C., Storeton-West, R.L., Fowler, D. (1998) Ammonia concentrations at a site in southern Scotland from 2 yrs of continuous measurements. *Atmos. Environ.,* **32**, 325-331.

Burkhardt, J., Kaiser, H., Goldbach, H., Kappen, L. (1999) Measurements of electrical leaf surface conductance reveal recondensation of transpired water vapour on leaf surfaces. *Plant Cell Environ.*, **22**, 189-196.

Businger, J.A., Oncley, S.P. (1990) Flux measurement with conditional sampling. *J. atmos. ocean. Technol.*, **7**, 349-352.

Bussink, D.W., Harper, L.A., Corre, W.J. (1996) Ammonia transport in a temperate grassland .2. Diurnal fluctuations in response to weather and management conditions. *Agron. J.*, **88**, 621-626.

Carlsson, G., Huss-Danell, K. (2003) Nitrogen fixation in perennial forage legumes in the field. *Plant and Soil,* **253**, 353-372.

Choularton, T.W., Gay, M.J., Jones, A., Fowler, D., Cape, J.N., Leith, I.D. (1988) The influence of altitude on wet deposition comparison between field-measurements at Great Dun Fell and the predictions of a seeder feeder model. *Atmos. Environ.*, **22**, 1363-1371.

Clark, F.E. (1981) The nitrogen cycle, viewed with poetic licence. In: Clark, F.E., Rosswall, T. (Eds.), *Terrestrial Nitrogen Cycles*, Swedish Natural Science Research Council, Stockholm, Sweden, pp. 13-24.

Crooke, W.M., Simpson, W.E. (1971) Determination of ammonium in kjeldahl digests of crops by an automated procedure. *J. Sci. Fd. Agric.*, **22**, 9-10.

Dasch, J.M., Cadle, S.H., Kennedy, K.G., Mulawa, P.A. (1989) Comparison of annular denuders and filter packs for atmospheric sampling. *Atmos. Environ.*, **23**, 2775-2782.

David, M., Cellier, P., Roche, R., Daemmgen, U., Sutton, M.A. (2004) Analysis of ammonia fluxes with intensively managed grassland using dynamic chambers. II The effects of management options. *Manuscript for special issue of Braunschweig experiment, In prep.*

DEFRA (2002) Ammonia in the UK, Department for Environment, Food and Rural Affairs, London, UK.

Denmead, O.T., Simpson, J.R., Freney, J.R. (1974) Ammonia flux into the atmosphere from a grazed pasture. *Science,* **185**, 609-610.

Denmead, O.T., Freney, J.R., Simpson, J.R. (1976) A closed ammonia cycle within a plant canopy. *Soil Sci. Biochem.*, **8**, 161-164.

DETR (2000) Accounting for nature: assessing habitats in the UK countryside (Countryside survey 2000), Department of the Environment, Transport and the Regions, London, UK.

Dias, G.M. (1998) Development of an ammonia measurement and sampling system based on tunable diode laser spectroscopy. PhD Thesis. University of Guelph.

Dragosits, U., Sutton, M.A., Place, C.J., Bayley, A.A. (1998) Modelling the spatial distribution of agricultural ammonia emissions in the UK. *Environ. Pollut.*, **102**, 195-204.

Duyzer, J. (1994) Dry deposition of ammonia and ammonium aerosols over heathland. *J. geophys. Res.*, **99**, 18757-18763.

Duyzer, J.H., Verhagen, H.L.M., Weststrate, J.H., Bosveld, F.C., Vermetten, A.W.M. (1994) The dry deposition of ammonia onto a Douglas-fir forest in the Netherlands. *Atmos. Environ.*, **28**, 1241-1253.

Dyer, A.J., Hicks, B.B. (1970) Flux gradient relationships in the constant flux layer. *Q. J. R. met. Soc.*, **96**, 715-721.

Erisman, J.W., Wyers, G.P. (1993) Continuous measurements of surface exchange of SO_2 and NH_3: Implications for their possible interaction in the deposition process. *Atmos. Environ.*, **27**, 1937-1949.

Erisman, J.W., Vanelzakker, B.G., Mennen, M.G., Hogenkamp, J., Zwart, E., Vandenbeld, L., Romer, F.G., Bobbink, R., Heil, G., Raessen, M., Duyzer, J.H., Verhage, H., Wyers, G.P., Otjes, R.P., Mols, J.J. (1994) The Elspeetsche Veld experiment on surface exchange of trace gases - summary of results. *Atmos. Environ.*, **28**, 487-496.

Erisman, J.W., Monteny, G.J. (1998) Consequences of new scientific findings for future abatement of ammonia emissions. *Environ. Pollut.*, **102**, 275-282.

Evans, D.R., Williams, T.A., Jones, S., Evans, S.A. (1998) The effect of cutting and intensive grazing managements on sward components of contrasting ryegrass and white clover types when grown in mixtures. *J. agric. Sci. Camb.*, **130**, 317-322.

Famulari, D., Fowler, D., Hargreaves, K.J., Nemitz, E., Weston, K. (2004) Eddy covariance measurements of ammonia fluxes from grassland. *Water Soil and Air Pollution-In prep.*

Fangmeier, A., Hadwigerfangmeier, A., Vandereerden, L., Jager, H.J. (1994) Effects of atmospheric ammonia on vegetation - a review. *Environ. Pollut.*, **86**, 43-82.

Farquhar, G.D., Firth, P.M., Wetselaar, R., Weir, B. (1980) On the gaseous exchange of ammonia between leaves and the environment: determination of the ammonia compensation point. *Plant Physiol.*, **66**, 710-714.

Fehsenfeld, F. (1995) Measurement of chemically reactive trace gases at ambient concentrations. In: Matson, P.A., Harriss, R.C. (Eds.), *Biogenic trace gases: measuring emissions from soil and water*, Blackwell Science Ltd, Oxford, UK, pp. 206-258.

Fehsenfeld, F.C., Huey, L.G., Leibrock, E., Dissly, R., Williams, E., Ryerson, T.B., Norton, R., Sueper, D.T., Hartsell, B. (2002) Results from an informal intercomparison of ammonia measurement techniques. *J. geophys. Res.*, **107**, art. no.-4812.

Ferm, M. (1979) Method for determination of atmospheric ammonia. *Atmos. Environ.*, **13**, 1385-1393.

Ferm, M., Areskoug, H., Hanssen, J.E., Hilbert, G., Lattila, H. (1988) Field intercomparison of measurement techniques for total NH_4^+ and total NO_3^- in ambient air. *Atmos. Environ.*, **22**, 2275-2281.

Fisk, M.C., Schmidt, S.K. (1996) Microbial responses to nitrogen additions in alpine tundra soil. *Soil Biol. Biochem.*, **28**, 751-755.

Flechard, C.R. (1998) Turbulent exchange of ammonia above vegetation. Ph.D. Thesis. University of Nottingham, UK, 231 pp.

Flechard, C.R., Fowler, D. (1998) Atmospheric ammonia at a moorland site. II: Long-term surface-atmosphere micrometeorological flux measurements. *Q. J. R. met. Soc.*, **124**, 759-791.

Flechard, C.R., Fowler, D., Sutton, M.A., Cape, J.N. (1999) A dynamic chemical model of bi-directional ammonia exchange between semi-natural vegetation and the atmosphere. *Q. J. R. met. Soc.*, **125**, 2611-2642.

Fournier, N., Pais, V.A., Sutton, M.A., Weston, K.J., Dragosits, U., Tang, S.Y., Aherne, J. (2002) Parallelisation and application of a multi-layer atmospheric transport model to quantify dispersion and deposition of ammonia over the British Isles. *Environ. Pollut.*, **116**, 95-107.

Fowler, D., Unsworth, M.H. (1979) Turbulent transfer of sulphur dioxide to a wheat crop. *Q. J. R. met. Soc.*, **105**, 767-783.

Fowler, D., Cape, J.N., Leith, I.D., Choularton, T.W., Gay, M.J., Jones, A. (1988) The influence of altitude on rainfall composition at Great Dun Fell. *Atmos. Environ.*, **22**, 1355-1362.

Fowler, D., Duyzer, J.H. (1989) Micrometeorological techniques for the measurement of trace gas exchange. In: Andreae, M.O., Schimel, D.S. (Eds.), *Exchange of trace gases between terrestrial ecosystems and the atmosphere*, John Wiley & Sons Ltd., pp. 189-207.

Fowler, M.C., Cape, J.N. (1982) Air pollutants in agriculture and horticulture. In: Unsworth, M.H., Orwood, D.P. (Eds.), *Effecs of gaseous air pollution in agriculture and horticulture*, Butterworth, London, pp. 3-26.

Foy, J.K., Teague, W.R., Hanson, J.D. (1999) Evaluation of the upgraded SPUR model (SPUR2.4). *Ecol. Model.*, **118**, 149-165.

Freney, J.R., Simpson, J.R., Denmead, O.T. (1981) Ammonia volatilization. In: Clark, F.E., Rosswall, T. (Eds.), *Terrestrial Nitrogen Cycles*, Swedish Natural Science Research Council, Stockholm, Sweden, pp. 291-302.

Fuller, R.M., Groom, G.B., Jones, A.R. (1994) The land cover map of Great Britain: an automated classification of landsat thematic mapper data. *Photogram. Engng rem. Sensing*, **60**, 553-562.

Gall, R., Perner, D., Ladstatter-Weissenmayer, A. (1991) Simultaneous determination of NH_3, SO_2, NO and NO_2 by direct UV-absorption in ambient air. *Fresenius Journal of Analytical Chemistry*, **340**, 646-649.

Galloway, J.N., Schlesinger, W.H., Levy, H., Michaels, A., Schnoor, J.L. (1995) Nitrogen-fixation - anthropogenic enhancement-environmental response. *Global biogeochem. Cycles*, **9**, 235-252.

Galloway, J.N. (1998) The global nitrogen cycle: changes and consequences. *Environ. Pollut.*, **102**, 15-24.

Garland, J.A. (1977) The dry deposition of sulphur dioxide to land and water surfaces. *Proc. R. Soc. Lond., A*, 245-268.

Garratt, J.R. (1992) The atmospheric boundary layer. Cambridge University Press, Cambridge, UK 316 pp.

Gash, J.H.C. (1986) A note on estimating the effect of a limited fetch on micrometeorological evaporation measurements. *Boundary-layer Met.*, **35**, 409-413.

Goodwin, J.W.L., Salway, A.G., Murrells, T.P., Dore, C.J., Passant, N.R., Eggleston, H.S. (2000) UK emissions of air pollutants 1970-1998. AEAT/R/EN/0270, AEA Technology.

Gouw, J.A., Carleton, J.H., Custer, T.G., Fall, R. (1999) Emissions of volatile organic compounds from cut grass and clover are enhanced by the drying process. *Geophys. Res. Lett.*, **26**, 811-814.

Gras, J.L. (1984) A field comparison of 2 atmospheric ammonia sampling techniques. *Tellus*, **36**, 38-43.

Griffith, D.W.T., Galle, B. (2000) Flux measurements of NH_3, N_2O and CO_2 using dual beam FTIR spectroscopy and the flux-gradient technique. *Atmos. Environ.*, **34**, 1087-1098.

Grünhage, L., Dämmgen, U., Haenel, H.D., Jäger, H.J. (1994) Response of a grassland ecosytem to air-pollutants. 3 The chemical climate - vertical flux densities of gaseous species in the atmosphere near the ground. *Environ. Pollut.*, **85**, 43-49.

Haenel, H.D., Grunhage, L. (1999) Footprint analysis: A closed analytical solution based on height-dependent profiles of wind speed and eddy viscosity. *Boundary-layer Met.*, **93**, 395-409.

Hansen, B., Nornberg, P., Rasmussen, K.R. (1998) Atmospheric ammonia exchange on a heathland in Denmark. *Atmos. Environ.*, **32**, 461-464.

Hargreaves, K.J., Atkins, D.H.F. (1987) The measurement of ammonia in the outdoor environment using passive diffusion tube samplers. AERE-R-12568, Harwell Laboratory, Didcot, UK.

Harrison, R.M., Kitto, A.M.N. (1990) Field intercomparison of filter pack and denuder sampling methods for reactive gaseous and particulate pollutants. *Atmos. Environ.*, **24**, 2633-2640.

Hatch, D.J., Jarvis, S.C., Dollard, G.J. (1990) Measurements of ammonia emission from grazed grassland. *Environ. Pollut.*, **65**, 333-346.

Heil, G.W., Diemont, W.H. (1983) Raised nutrient levels change heathland into grassland. *Vegetatio*, **53**, 113-120.

Henriksen, A., Selmer-Olsen, A.R. (1970) Automatic methods for determining nitrate and nitrite in water and soil extracts. *Analyst, Lond.*, **95**, 514-518.

Hensen, A., Nemitz, E., Flynn, M., Blatter, A., Jones, S.K., Hensen, B., Otjes, R.P., Corbusen, J., Erisman, J.W., Sutton, M.A., Gallagher, M.W., Geern, L.L., Neftel, A. (2004) Comparison of REA methods for NH_3 during the Braunschweig joint field experiment. *Manuscript for special issue of Braunschweig experiment, in prep.*

Herrmann, B., Jones, S.K., Fuhrer, J., Feller, U., Neftel, A. (2001) N budget and NH_3 exchange of a grass/clover crop at two levels of N application. *Plant and Soil*, **235**, 243-252.

Hesterberg, R., Blatter, A., Fahrni, M., Rosset, M., Neftel, A., Eugster, W., Wanner, H. (1996) Deposition of nitrogen-containing compounds to an extensively managed grassland in central Switzerland. *Environ. Pollut.*, **91**, 21-34.

Hettelingh, J.P., Posch, M., De Smet, P.A.M. (2001) Multi-effect critical loads used in multi-pollutant reduction agreements in Europe. *Water, Air Soil Pollut.*, **130**, 1133-1138.

Hicks, B.B., Baldocchi, D.D., Meyers, T.P., Hosker, R.P., Matt, D.R. (1987) A preliminary multiple resistance routine for deriving dry deposition velocities from measured quantities. *Water, Air Soil Pollut.*, **36**, 311-330.

Hill, P.W. (1999) Physiological aspects of the exchange of gaseous ammonia between *Luzula sylvatica* (Huds.) Gaud. and the atmosphere. Ph.D. Thesis. University of Dundee, 216 pp.

Hill, P.W., Raven, J.A., Loubet, B., Fowler, D., Sutton, M.A. (2001) Comparison of gas exchange and bioassay determinations of the ammonia compensation point in *Luzula sylvatica* (Huds.) Gaud. *Plant Physiol.*, **125**, 476-487.

Hill, R.D., Rinker, R.G., Wilson, H.D. (1980) Atmospheric nitrogen fixation by lightning. *J. Atmos. Sci.*, **37**, 179-192.

Hodgson, J.M. (1974) Soil survey field handbook technical monograph No. 5. Bartholemew.

Horst, T.W., Weil, J.C. (1992) Footprint estimation for scalar flux measurements in the atmospheric surface-layer. *Boundary-layer Met.*, **59**, 279-296.

Horst, T.W., Weil, J.C. (1994) How far is far enough - the fetch requirements for micrometeorological measurement of surface fluxes. *J. atmos. ocean. Technol.*, **11**, 1018-1025.

Hunt, H.W., Trlica, M.J., Redente, E.F., Moore, J.C., Detling, J.K., Kittel, T.G.F., Walter, D.E., Fowler, M.C., Klein, D.A., Elliott, E.T. (1991) Simulation model for the effects of climate change on temperate grassland ecosystems. *Ecol. Model.*, **53**, 205-246.

Husted, S., Schjoerring, J.K. (1995a) Apoplastic pH and ammonium concentration in leaves of *Brassica-Napus* L. *Plant Physiol.*, **109**, 1453-1460.

Husted, S., Schjoerring, J.K. (1995b) A computer-controlled system for studying ammonia exchange, photosynthesis and transpiration of plant canopies growing under controlled environmental-conditions. *Plant Cell Environ.*, **18**, 1070-1077.

Husted, S., Schjoerring, J.K., Nielsen, K.H., Nemitz, E., Sutton, M.A. (2000) Stomatal compensation points for ammonia in oilseed rape plants under field conditions. *Agric. For. Met.*, **105**, 371-383.

Innis, G.S. (1978) Grassland simulation model, Ecological Studies. Springer-Verlag, New York pp.

IPCC (1996) Climate Change 1995. The science of climate change. University Press, Cambridge, UK pp.

Jambert, C., Serca, D., Delmas, R. (1997) Quantification of N-losses as NH_3, NO, and N_2O and N_2 from fertilized maize fields in southwestern France. *Nutrient Cycling in Agroecosystems,* **48**, 91-104.

Jarvis, P.G. (1976) The interpretation of the variations in leaf water potential and stomatal conductance found in canopies in the field. *Phil. Trans. R. Soc. Lond. Ser. B Biol. Sci.*, **273**, 593-610.

Jarvis, S.C., Hatch, D.J., Lockyer, D.R. (1989) Ammonia fluxes from grazed grassland - annual losses from cattle production systems and their relation to nitrogen inputs. *J. agric. Sci. Camb.*, **113**, 99-108.

Jarvis, S.C., Hatch, D.J., Orr, R.J., Reynolds, S.E. (1991) Micrometeorological studies of ammonia emission from sheep grazed swards. *J. agric. Sci. Camb.*, **117**, 101-109.

Jarvis, S.C. (1996) Future trends in nitrogen research. *Plant and Soil,* **181**, 47-56.

Jenkinson, D.S. (1990) An introduction to the global nitrogen-cycle. *Soil Use Mgmt,* **6**, 56-61.

Johnson, I.R., Thornley, J.H.M. (1985) Dynamic model of the response of a vegetative grass crop to light, temperature and nitrogen. *Plant Cell Environ.*, **8**, 485-499.

Keuken, M.P., Schoonebeek, C.A.M., Vanwensveenlouter, A., Slanina, J. (1988) Simultaneous sampling of NH_3, HNO_3, HCl, SO_2 and H_2O_2 in ambient air by a wet annular denuder system. *Atmos. Environ.*, **22**, 2541-2548.

Keuken, M.P., Wayersijpelaan, A., Mols, J.J., Otjes, R.P., Slanina, J. (1989) The determination of ammonia in ambient air by an automated thermodenuder system. *Atmos. Environ.*, **23**, 2177-2185.

Killham, K. (1994) Soil ecology. Cambridge University Press, Cambridge, UK 242 pp.

Klemm, O., Milford, C., Sutton, M.A., Spindler, G., van Putten, E. (2002) A climatology of leaf surface wetness. *Theoretical and Applied Climatology,* **71**, 107-117.

Kormann, R., Meixner, F.X. (2001) An analytical footprint model for non-neutral stratification. *Boundary-layer Met.*, **99**, 207-224.

Kramm, G., Dlugi, R. (1994) Modeling of the vertical fluxes of nitric-acid, ammonia, and ammonium-nitrate. *J. atmos. Chem.*, **18**, 319-357.

Krupa, S.V. (2003) Effects of atmospheric ammonia (NH_3) on terrestrial vegetation: a review. *Environ. Pollut.*, **124**, 179-221.

Langford, A.O., Goldan, P.D., Fehsenfeld, F.C. (1989) A molybdenum oxide annular denuder system for gas phase ambient ammonia measurements. *J. atmos. Chem.*, **8**, 359-376.

Leclerc, M.Y., Shen, S.H., Lamb, B. (1997) Observations and large-eddy simulation modeling of footprints in the lower convective boundary layer. *J. geophys. Res.*, **102**, 9323-9334.

Lee, J.A., Caporn, S.J.M. (1998) Ecological effects of atmospheric reactive nitrogen deposition on semi-natural terrestrial ecosystems. *New Phytol.*, **139**, 127-134.

Lockyer, D.R., Whitehead, D.C. (1990) Volatilization of ammonia from cattle urine applied to grassland. *Soil Biol. Biochem.*, **22**, 1137-1142.

Loubet, B., Milford, C., Sutton, M.A., Cellier, P. (2001) Investigation of the interaction between sources and sinks of atmospheric ammonia in an upland landscape using a simplified dispersion-exchange model. *J. geophys. Res.*, **106**, 24,183-124,196.

Loubet, B., Milford, C., Hill, P.W., Tang, Y.S., Cellier, P., Sutton, M.A. (2002) Seasonal variability of apoplastic NH_4^+ and pH in an intensively managed grassland. *Plant and Soil,* **238**, 97-110.

Loubet, B., Milford, C., Hensen, A., Dammgen, U., Erisman, J.W., Cellier, P., Sutton, M.A. (2004) Advection of NH_3 over a pasture field and its effect on gradient flux measurements. *Manuscript for special issue of Braunschweig experiment, in prep.*

Macduff, J.H., Jackson, S.B. (1991) Growth and preferences for ammonium or nitrate uptake by barley in relation to root temperature. *J. expl Bot.,* **42**, 521-530.

Malagoli, M., Dal Canal, A., Quaggiotti, S., Pegoraro, P., Bottacin, A. (2000) Differences in nitrate and ammonium uptake between Scots pine and European larch. *Plant and Soil,* **221**, 1-3.

Mannheim, T., Braschkat, J., Marschner, H. (1997) Ammonia emissions from senescing plants and during decomposition of crop residues. *Zeitschrift Fur Pflanzenernahrung Und Bodenkunde,* **160**, 125-132.

Mattsson, M., Herrmann, B., Jones, S., Borrella, S., Mäck, G., Dorsey, J., Schjoerring, J.K. (2004) Contribution of different grass species to NH_3 exchange between plants and the atmosphere in an intensively managed grassland. *Manuscript for special issue of Braunschweig experiment, in prep.*

Meixner, F., Wyers, G.P., Neftel, A. (1996) Bi-directional exchange of ammonia over cereals. In: Borrell, P.M., Borrell, P. (Eds.), Proc. EUROTRAC'96, pp. 129-135. Computational Mechanics Publications, Southampton, UK.

Mennen, M.G., VanElzakker, B.G., VanPutten, E.M., Uiterwijk, J.W., Regts, T.A., VanHellemond, J., Wyers, G.P., Otjes, R.P., Verhage, A.J.L., Wouters, L.W., Heffels, C.J.G., Romer, F.G., VandenBeld, L., Tetteroo, J.E.H. (1996) Evaluation of automatic ammonia monitors for application in an air quality monitoring network. *Atmos. Environ.,* **30**, 3239-3256.

Michaels, R.A. (1999) Emergency planning and the acute toxic potency of inhaled ammonia. *Envir. Hlth Perspectives,* **107**, 617-627.

Milford, C., Hargreaves, K.J., Sutton, M.A., Loubet, B., Cellier, P. (2001) Fluxes of NH_3 and CO_2 over upland moorland in the vicinity of agricultural land. *J. geophys. Res.,* **106**, 24169-24181.

Misselbrook, T.H., Van der Weerden, T.J., Pain, B.F., Jarvis, S.C., Chambers, B.J., Smith, K.A., Phillips, V.R., Demmers, T.G.M. (2000) Ammonia emission factors for UK agriculture. *Atmos. Environ.,* **34**, 871-880.

Moller, D., Schieferdecker, H. (1985) A relationship between agricultural NH_3 emissions and the atmospheric SO_2 content over industrial-areas. *Atmos. Environ.,* **19**, 695-700.

Moncrieff, J., Valentini, R., Greco, S., Seufert, G., Ciccioli, P. (1997a) Trace gas exchange over terrestrial ecosystems: methods and perspectives in micrometeorology. *J. expl Bot.,* **48**, 1133-1142.

Moncrieff, J.B., Massheder, J.M., deBruin, H., Elbers, J., Friborg, T., Heusinkveld, B., Kabat, P., Scott, S., Soegaard, H., Verhoef, A. (1997b) A system to measure surface fluxes of momentum, sensible heat, water vapour and carbon dioxide. *J. Hydrol.,* **189**, 589-611.

Monin, A.S., Obukhov, A.M. (1954) Basic laws of turbulent mixing in the ground layer of the atmosphere. *Trans. Geophys. Inst. Akad. Nauk USSR,* **151**, 163-187.

Monteith, J.L., Unsworth, M.H. (1990) Principles of environmental physics. Edward Arnold, London 291 pp.

Mosquera, J., Hensen, A., van den Bulk, W.C.M., Vermeulen, A.T., Erisman, J.W. (2001) Long term NH_3 flux measurements at two locations in the Netherlands. *Water, Air Soil Pollut. Focus,* **1**, 203-212.

Mozurkewich, M. (1993) The dissociation-constant of ammonium-nitrate and its dependence on temperature, relative-humidity and particle-size. *Atmos. Environ.,* **27**, 261-270.

Nathan, M.V., Malzer, G.L. (1994) Dynamics of ammonia volatilization from turkey manure and urea applied to soil. *Soil Sci. Soc. Am. J.,* **58**, 985-990.

Neftel, A., Blatter, A., Gut, A., Hogger, D., Meixner, F., Ammann, C., Nathaus, F.J. (1998) NH_3 soil and soil surface gas measurements in a triticale wheat field. *Atmos. Environ.,* **32**, 499-505.

Neftel, A., Blatter, A., Otjes, R., Erisman, J.W., Hansen, A. (1999) State of the art REA NH_3 flux measurements, 10th Nitrogen Workshop, pp. 49. RVAU, Copenhagen, Copenhagen.

NEGTAP (2001) Transboundary air pollution: acidification, eutrophication and ground-level ozone in the UK, National Expert Group on Transboundary Air Pollution, Department of Environment, Food and Rural Affairs, London, UK.

Nemitz, E. (1998) Surface-atmosphere exchange of ammonia and chemically interacting species. Ph.D. Thesis. UMIST, UK, 302 pp.

Nemitz, E., Sutton, M.A., Gut, A., San Jose, R., Husted, S., Schjoerring, J.K. (2000a) Sources and sinks of ammonia within an oilseed rape canopy. *Agric. For. Met.*, **105**, 385-404.

Nemitz, E., Sutton, M.A., Schjoerring, J.K., Husted, S., Paul Wyers, G. (2000b) Resistance modelling of ammonia exchange over oilseed rape. *Agric. For. Met.*, **105**, 405-425.

Nemitz, E., Sutton, M.A., Wyers, G.P., Otjes, R.P., Schjoerring, J.K., Gallagher, M.W., Parrington, J., Fowler, D., Choularton, T.W. (2000c) Surface/atmosphere exchange and chemical interaction of gases and aerosols over oilseed rape. *Agric. For. Met.*, **105**, 427-445.

Nemitz, E., Flynn, M., Williams, P.I., Milford, C., Theobald, M.R., Blatter, A., Gallagher, M.W., Sutton, M.A. (2001a) A relaxed eddy accumulation system for the automated measurement of atmospheric ammonia fluxes. *Water, Air Soil Pollut. Focus*, **1**, 189-202.

Nemitz, E., Milford, C., Sutton, M.A. (2001b) A two-layer canopy compensation point model for describing bi-directional biosphere-atmosphere exchange of ammonia. *Q. J. R. met. Soc.*, **127**, 815-834.

Nemitz, E., McFiggins, G., Dorsey, J., Gallagher, M.W., Erisman, J.W., Otjes, R.P., Jongejan, P., Sutton, M.A. (2004) Gas-to-particle conversion above grassland, following the application of NH_4NO_3 fertilisers. *Manuscript for special issue of Braunschweig experiment, in prep.*

Newbould, P. (1982) Biological nitrogen-fixation in upland and marginal areas of the UK. *Phil. Trans. R. Soc. Lond. Ser. B Biol. Sci.*, **296**, 405-417.

Nihlgård, B. (1985) The ammonium hypothesis - an additional explantation to the forest die-back in Europe. *Ambio*, **14**, 2-8.

Nilsson, J., Grennfelt, P. (1988) Critical loads for sulphur and nitrogen. UNECE/Nordic Council workshop report, Skokloster, Sweden, March 1988. Nordic Council of Ministers, Copenhagen.

Nowak, J.B., Huey, L.G., Eisele, F.L., Tanner, D.J., Mauldin, R.L., Cantrell, C., Kosciuch, E., Davis, D.D. (2002) Chemical ionization mass spectrometry technique for detection of dimethylsulfoxide and ammonia. *J. geophys. Res.*, **107**, art. no.-4363.

Oncley, S.P., Delany, A.C., Horst, T.W., Tans, P.P. (1993) Verification of flux measurement using Relaxed Eddy Accumulation. *Atmos. Environ.*, **27**, 2417-2426.

Pain, B.F., Phillips, V.R., Clarkson, C.R., Klarenbeek, J.V. (1989) Loss of nitrogen through ammonia volatilization during and following the application of pig or cattle slurry to grassland. *J. Sci. Fd Agric.*, **47**, 1-12.

Panofsky, H.A. (1963) Determination of stress from wind and temperature measurements. *Q. J. R. met. Soc.*, **89**, 85-94.

Parrish, D.D., Fehsenfeld, F.C. (2000) Methods for gas-phase measurements of ozone, ozone precursors and aerosol precursors. *Atmos. Environ.*, **34**, 1921-1957.

Parton, W.J., Stewart, J.W.B., Cole, C.V. (1998) Dynamics of C, N, P and S in grassland soils - a model. *Biogeochemistry*, **5**, 109-131.

Paulson, C.A. (1970) The mathematical representation of wind speed and temperature profiles in the unstable atmospheric surface layer. *J. appl. Meteorol.*, **9**, 857-861.

Petersen, S.O., Sommer, S.G., Aaes, O., Soegaard, K. (1998) Ammonia losses from urine and dung of grazing cattle: Effect of N intake. *Atmos. Environ.*, **32**, 295-300.

Pio, C.A., Harrison, R.M. (1987) Vapor-pressure of ammonium-chloride aerosol - effect of temperature and humidity. *Atmos. Environ.*, **21**, 2711-2715.

Pio, C.A. (1992) Measurement of ammonia and ammonium in the atmosphere by denuder and filter pack methods. Evaluation of the Rome field intercomparison exercise. In: Allegrini, I. (Ed.), *Development of analytical techniques for atmospheric pollutants, Air Pollution Research Report 41,*, CEC Brussels, pp. 239-252.

Pitcairn, C.E.R., Fowler, D., Grace, J. (1991) Changes in species composition of semi-natural vegetation associated with the increase in atmosperic inputs of nitrogen, Report to Nature Conservancy Council. Institute of Terrestrial Ecology, Edinburgh.

Plantaz, M.A.H.G. (1998) Surface-atmosphere exchange of ammonia over grazed pasture. Landbouwuniversiteit Wageningen, The Netherlands, 197 pp.

Portejoie, S., Martinez, J., Landmann, G. (2002) Ammonia of farm origin: impact on human and animal health and on the natural habitat. *Productions Animales*, **15**, 151-160.

Posch, M., Hettelingh, J.P., De Smet, P.A.M. (2001) Characterization of critical load exceedances in Europe. *Water, Air Soil Pollut.*, **130**, 1139-1144.

Pryor, S.C., Barthelmie, R.J., Sorensen, L.L., Jensen, B. (2001) Ammonia concentrations and fluxes over a forest in the midwestern USA. *Atmos. Environ.*, **35**, 5645-5656.

Pushkarsky, M.B., Webber, M.E., Baghdassarian, O., Narasimhan, L.R., Patel, C.K.N. (2002) Laser-based photoacoustic ammonia sensor for industrial applications. *Applied Physics B special issue: Trends in Laser Sources, Spectroscopic Techniques and Their Applications to Trace Gas Detection,* **75**, 391-396.

Raupach, M.R. (1989) Applying lagrangian fluid-mechanics to infer scalar source distributions from concentration profiles in plant canopies. *Agric. For. Met.*, **47**, 85-108.

Riedo, M., Grub, A., Rosset, M., Fuhrer, J. (1998) A pasture simulation model for dry matter production, and fluxes of carbon, nitrogen, water and energy. *Ecol. Model.*, **105**, 141-183.

Riedo, M., Milford, C., Schmid, M., Sutton, M.A. (2002) Coupling soil-plant-atmosphere exchange of ammonia with ecosystem functioning in grasslands. *Ecol. Model.*, **158**, 83-110.

Rooth, R.A., Verhage, A.J.L., Wouters, L.W. (1990) Photoacoustic measurement of ammonia in the atmosphere - influence of water-vapor and carbon-dioxide. *Appl. Optics,* **29**, 3643-3653.

Rowell, D.L. (1994) Soil science: methods and applications. Harlow, Longman 350 pp.

Ryden, J.C., Whitehead, D.C., Lockyer, D.R., Thompson, R.B., Skinner, J.H., Garwood, E.A. (1987) Ammonia emission from grassland and livestock production systems in the UK. *Environ. Pollut.,* **48**, 173-184.

Schendel, J.S., Stickel, R.E., Vandijk, C.A., Sandholm, S.T., Davis, D.D., Bradshaw, J.D. (1990) Atmospheric ammonia measurement using a VUV/photo-fragmentation laser-induced fluorescence technique. *Appl. Optics,* **29**, 4924-4937.

Schjoerring, J.K., Husted, S., Mattsson, M. (1998) Physiological parameters controlling plant-atmosphere ammonia exchange. *Atmos. Environ.*, **32**, 491-498.

Schjoerring, J.K., Husted, S., Mack, G., Nielsen, K.H., Finnemann, J., Mattsson, M. (2000) Physiological regulation of plant-atmosphere ammonia exchange. *Plant and Soil,* **221**, 95-102.

Schjoerring, J.K., Mattsson, M. (2001) Quantification of ammonia exchange between agricultural cropland and the atmosphere: Measurements over two complete growth cycles of oilseed rape, wheat, barley and pea. *Plant and Soil,* **228**, 105-115.

Schmid, H.P., Lloyd, C.R. (1999) Spatial representativeness and the location bias of flux footprints over inhomogeneous areas. *Agric. For. Met.*, **93**, 195-209.

Schmid, H.P. (2002) Footprint modeling for vegetation atmosphere exchange studies: a review and perspective. *Agric. For. Met.*, **113**, 159-183.

Schuepp, P.H. (1977) Turbulent transfer at the ground: on verification of a simple predictive model. *Boundary-layer Met.*, **12**, 171-186.

Schuepp, P.H., Leclerc, M.Y., Macpherson, J.I., Desjardins, R.L. (1990) Footprint prediction of scalar fluxes from analytical solutions of the diffusion equation. *Boundary-layer Met.*, **50**, 353-373.

Seinfeld, J.H., Pandis, S.N. (1998) Atmospheric chemistry and physics. From air pollution to climate change. John Wiley, New York 1326 pp.

Sharpe, R.R., Harper, L.A. (1995) Soil, plant and atmospheric conditions as they relate to ammonia volatilization. *Fertilizer Research,* **42**, 149-158.

Shaw, W.J., Spicer, C.W., Kenny, D.V. (1998) Eddy correlation fluxes of trace gases using a tandem mass spectrometer. *Atmos. Environ.*, **32**, 2887-2898.

Simek, M., Cooper, J.E. (2002) The influence of soil pH on denitrification: progress towards the understanding of this interaction over the last 50 years. *Eur. J. Soil Sci.*, **53**, 345-354.

Singles, R., Sutton, M.A., Weston, K.J. (1998) A multi-layer model to describe the atmospheric transport and deposition of ammonia in Great Britain. *Atmos. Environ.*, **32**, 393-399.

Smith, R.I., Fowler, D., Sutton, M.A., Flechard, C., Coyle, M. (2000) Regional estimation of pollutant gas dry deposition in the UK: model description, sensitivity analyses and outputs. *Atmos. Environ.,* **34**, 3757-3777.

Smith, R.S., Buckingham, H., Bullard, M.J., Shiel, R.S., Younger, A. (1996a) The conservation management of mesotrophic (meadow) grassland in northern England. 1. Effects of grazing, cutting

date and fertiliser on the vegetation of a traditionally managed sward. *Grass Forage Sci.*, **51**, 292-305.

Smith, R.S., Corkhill, P., Shiel, R.S., Millward, D. (1996b) The conservation management of mesotrophic (meadow) grassland in northern England. 2. Effects of grazing, cutting date, fertiliser and seed application on the vegetation of a agriculturally improved sward. *Grass Forage Sci.*, **51**, 576-588.

Soderlund, R., Svensson, B.H. (1976) The global nitrogen cycle. In: Soderlund, R., Svensson, B.H. (Eds.), *N, P, S: Global cycles*

Spindler, G., Teichmann, U., Sutton, M.A. (2001) Ammonia dry deposition over grassland-micrometeorological flux-gradient measurements and bidirectional flux calculations using an inferential model. *Q. J. R. met. Soc.*, **127**, 795-814.

Stull, R.B. (1988) Introduction to boundary layer meteorology. Kluwer Acad. Publ., London 666 pp.

Sutton, M.A. (1990) The surface atmosphere exchange of ammonia. Ph.D. Thesis. University of Edinburgh, UK, 194 pp.

Sutton, M.A., Fowler, D. (1993) A model for inferring bi-directional fluxes of ammonia over plant canopies. In: *The measurement and modelling of atmospheric composition changes including pollution transport*, pp. 179-182. World Meteorological Organization, Sofia.

Sutton, M.A., Fowler, D., Hargreaves, K., Storeton-West, R. (1993a) Interactions of NH_3 and SO_2 exchange inferred from simultaneous flux measurements over a wheat canopy. In: Slanina, J., Angeletti, G., Beilke, S. (Eds.), *General Assessment of biogenic emissions and deposition of nitrogen compounds, sulphur compounds and oxidants in Europe, Proceedings of the joint CEC/BIATEX workshop, Aveiro*, CEC, Brussels, pp. 165-182.

Sutton, M.A., Fowler, D., Moncrieff, J.B. (1993b) The exchange of atmospheric ammonia with vegetated surfaces. I: Unfertilized vegetation. *Q. J. R. met. Soc.*, **119**, 1023.

Sutton, M.A., Fowler, D., Moncrieff, J.B., Storeton-West, R.L. (1993c) The exchange of atmospheric ammonia with vegetated surfaces. II: Fertilized vegetation. *Q. J. R. met. Soc.*, **119**, 1047.

Sutton, M.A., Pitcairn, C.E.R., Fowler, D. (1993d) The exchange of ammonia between the atmosphere and plant-communities. *Adv. ecol. Res.*, **24**, 301-393.

Sutton, M.A., Asman, W.A.H., Schjoerring, J.K. (1994) Dry deposition of reduced nitrogen. *Tellus*, **46B**, 255-273.

Sutton, M.A., Fowler, D., Burkhardt, J.K., Milford, C. (1995a) Vegetation atmosphere exchange of ammonia: Canopy cycling and the impacts of elevated nitrogen inputs. *Water, Air Soil Pollut.*, **85**, 2057-2063.

Sutton, M.A., Schjorring, J.K., Wyers, G.P. (1995b) Plant atmosphere exchange of ammonia. *Philos. Trans. R. Soc. Lond. Ser. A*, **351**, 261-276.

Sutton, M.A., Nemitz, E., Fowler, D., Wyers, G.P., Otjes, R.P., San José, R., Moreno, J., Schjoerring, J.K., Husted, S., Meixner, F.X., Ammann, C., Neftel, A., Gut, A. (1996) Exchange of atmospheric ammonia with European ecosystems (EXAMINE): Final report to the European Commission., Institute of Terrestrial Ecology, Edinburgh.

Sutton, M.A., Milford, C., Dragosits, U., Singles, R., Fowler, D., Ross, C., Hill, R., Jarvis, S.C., Pain, B.F., Harrison, R., Moss, D., Webb, J., Espenhahn, S., Halliwell, C., Lee, D.S., Wyers, G.P., Hill, J., ApSimon, H.M. (1997a) Gradients of atmospheric ammonia concentrations and deposition downwind of ammonia emissions: first results of the ADEPT Burrington Moor experiment. In: Jarvis, S.C., Pain, B.F. (Eds.), *Gaseous nitrogen emissions from grasslands*, Cab International, pp. 131-139.

Sutton, M.A., Perthue, E., Fowler, D., StoretonWest, R.L., Cape, J.N., Arends, B.G., Mols, J.J. (1997b) Vertical distribution and fluxes of ammonia at Great Dun Fell. *Atmos. Environ.*, **31**, 2615-2624.

Sutton, M.A., Burkhardt, J.K., Guerin, D., Nemitz, E., Fowler, D. (1998) Development of resistance models to describe measurements of bi-directional ammonia surface-atmosphere exchange. *Atmos. Environ.*, **32**, 473-480.

Sutton, M.A., Dragosits, U., Tang, Y.S., Fowler, D. (2000a) Ammonia emissions from non-agricultural sources in the UK. *Atmos. Environ.*, **34**, 855-869.

Sutton, M.A., Nemitz, E., Milford, C., Fowler, D., Moreno, J., San Jose, R., Wyers, G.P., Otjes, R.P., Harrison, R., Husted, S. (2000b) Micrometeorological measurements of net ammonia fluxes over oilseed rape during two vegetation periods. *Agric. For. Met.*, **105**, 351-369.

Sutton, M.A., Milford, C., Nemitz, E., Theobald, M.R., Hill, P.W., Fowler, D., Schjoerring, J.K., Mattsson, M.E., Nielsen, K.H., Husted, S., Erisman, J.W., Otjes, R., Hensen, A., Mosquera, J., Cellier, P., Loubet, B., David, M., Genermont, S., Neftel, A., Blatter, A., Herrmann, B., Jones, S.K., Horvath, L., Fuhrer, E.C., Mantzanas, K., Koukoura, Z., Gallagher, M., Williams, P., Flynn, M., Riedo, M. (2001a) Biosphere-atmosphere interactions of ammonia with grasslands: Experimental strategy and results from a new European initiative. *Plant and Soil,* **228**, 131-145.

Sutton, M.A., Tang, Y.S., Dragosits, U., Fournier, N., Dore, A.J., Smith, R.I., Weston, K.J., Fowler, D. (2001b) A spatial analysis of atmospheric ammonia and ammonium in the U.K. *Scientific World,* **1 (S2)**, 275-286.

Sutton, M.A., Milford, C., Nemitz, E., Theobald, M.R., Riedo, M., Hargreaves, K.J., Hill, P.W., Dragosits, U., Fowler, D., Schjoerring, J.K., Mattsson, M.E., Husted, S., Erisman, J.W., Hensen, A., Mosquera, J., Otjes, R., Cellier, P., Loubet, B., David, M., Neftel, A., Hermann, B., Jones, S.K., Blatter, A., Horvath, L., Weidinger, T., Meszaros, R., Raso, J., Mantzanas, K., Koukoura, Z., Gallagher, M., Dorsey, J., Flynn, M., Lehman, B., Burkhardt, J., Dammgen, U., (2002) Ammonia exchange with vegetation: measurement, modelling & application. In: Reuther, P., Midgely, P..M., (Ed.), *Transport and chemical transformation in the troposphere. (Proceedings from the EUROTRAC Symposium 2002)*, Margraf Verlag, Weikersheim, pp. 49-60.

Tang, Y.S., Cape, J.N., Sutton, M.A. (2001) Development and types of passive samplers for monitoring atmospheric NO_2 and NH_3 concentrations. *Scientific World,* 513-529.

Thom, A.S. (1975) Momentum, mass and heat exchange of plant communities. In: Monteith, J.L. (Ed.), *Vegetation and the atmosphere*, Academic Press, Chichester, UK, pp. 57-109.

Thompson, R.B., Pain, B.F., Lockyer, D.R. (1990a) Ammonia volatilization from cattle slurry following surface application to grassland. 1. Influence of mechanical separation, changes in chemical-composition during volatilization and the presence of the grass sward. *Plant and Soil,* **125**, 109-117.

Thompson, R.B., Pain, B.F., Rees, Y.J. (1990b) Ammonia volatilization from cattle slurry following surface application to grassland. 2. Influence of application rate, wind-speed and applying slurry in narrow bands. *Plant and Soil,* **125**, 119-128.

Thornley, J.H.M. (1998) Grassland dynamics. An ecosystem simulation model., CAB International, Oxon. pp.

Tilman, D., Wedin, D. (1991) Dynamics of nitrogen competition between successional grasses. *Ecology,* **72**, 1038-1049.

Tuazon, E.C., Graham, R.A., Winer, A.M., Easton, R.R., Pitts, J.N., Hanst, P.L. (1978) A kilometer path-length Fourier-transform infrared system for the study of trace pollutants in ambient and synthetic atmospheres. *Atmos. Environ.*, **12**, 865-875.

UNECE (1988) Proc. ECE Critical levels workshop, Bad Harzburg, 14-18 March 1988.

Van Breemen, N., Burrough, P.A., Velthorst, E.J., Vandobben, H.F., Dewit, T., Ridder, T.B., Reijnders, H.F.R. (1982) Soil acidification from atmospheric ammonium-sulfate in forest canopy throughfall. *Nature,* **299**, 548-550.

Van Breemen, N., Driscoll, C.T., Mulder, J. (1984) Acidic deposition and internal proton sources in acidification of soils and water. *Nature,* **307**, 599-604.

van der Eerden, L.J., Dueck, T.A., Berdowski, J.J.M., Greven, H., Vandobben, H.F. (1991) Influence of NH_3 and $(NH_4)_2SO_4$ on heathland vegetation. *Acta Botanica Neerlandica,* **40**, 281-296.

van der Eerden, L.J.M., Dueck, T.A., Posthumus, A.C., Tonneijck, A.E.G. (1994) Assessment of critical levels for air pollutant effects on vegetation: some considerations and a case study on NH_3. In: Ashmore, M.R., Wilson, R.B. (Eds.), *Critical levels of air pollutants for Europe. Proceedings of the UNECE Workshop on Critical Levels*, Air Quality Division, Department of the Environment, London, pp. 55-63.

van der Weerden, T.J., Jarvis, S.C. (1997) Ammonia emission factors for N fertilizers applied to two contrasting grassland soils. *Environ. Pollut.*, **95**, 205-211.

van Hove, L.W.A., Koops, A.J., Adema, E.H., Vredenberg, W.J., Pieters, G.A. (1987) Analysis of the uptake of atmospheric ammonia by leaves of *Phaseolus-vulgaris* L. *Atmos. Environ.*, **21**, 1759-1763.

van Hove, L.W.A., Adema, E.H., Vredenberg, W.J., Pieters, G.A. (1989) A study of the adsorption of NH_3 and SO_2 on leaf surfaces. *Atmos. Environ.*, **23**, 1479-1486.

Vecera, Z., Dasgupta, P.K. (1991) Measurement of atmospheric nitric and nitrous acids with a wet effluent diffusion denuder and low-pressure ion chromatography postcolumn reaction detection. *Anal. Chem.*, **63**, 2210-2216.

Velthof, G.L., van Beusichem, M.L., Oenema, O. (1998) Mitigation of nitrous oxide emission from dairy farming systems. *Environ. Pollut.*, **102**, 173-178.

Vessey, J.K., Henry, L.T., Chaillou, S., Raper, C.D. (1990) Root-zone acidity affects relative uptake of nitrate and ammonium from mixed nitrogen-sources. *J. Plant Nutr.*, **13**, 95-116.

Warland, J.S., Dias, G.M., Thurtell, G.W. (2001) A tunable diode laser system for ammonia flux measurements over multiple plots. *Environ. Pollut.*, **114**, 215-221.

Webb, E.K. (1970) Profile relationships: The log-linear range and extension to strong stability. *Q. J. R. met. Soc.*, **96**, 67-90.

Webb, E.K., Pearman, G.I., Leuning, R. (1980) Correction of flux measurements for density effects due to heat and water vapour transfer. *Q. J. R. met. Soc.*, **106**, 85-100.

Webb, J., Henderson, D., Anthony, S.G. (2001) Optimizing livestock manure applications to reduce nitrate and ammonia pollution: scenario analysis using the MANNER model. *Soil Use Mgmt*, **17**, 188-194.

Wesely, M.L., Hicks, B.B. (1977) Some factors that affect the deposition rates of sulfur dioxide and similar gases on vegetation. *J. Air Pollut. Control Assoc.*, **27**, 1110-1116.

Whitehead, D.C., Lockyer, D.R. (1989) Decomposing grass herbage as a source of ammonia in the atmosphere. *Atmos. Environ.*, **23**, 1867-1869.

Whitehead, D.C. (1990) Atmospheric ammonia in relation to grassland agriculture and livestock production. *Soil Use Mgmt*, **6**, 63-65.

Whitehead, D.C., Raistrick, N. (1993) The volatilization of ammonia from cattle urine applied to soils as influenced by soil properties. *Plant and Soil*, **148**, 43-51.

Wie, Y.Q., Bailey, B.J., Stenning, B.C. (1995) A wetness sensor for detecting condensation on tomato plants in greenhouses. *J. Agric. Engineering Research*, **61**, 197-204.

Wiebe, H.A., Anlauf, K.G., Tuazon, E.C., Winer, A.M., Biermann, H.W., Appel, B.R., Solomon, P.A., Cass, G.R., Ellestad, T.G., Knapp, K.T., Peake, E., Spicer, C.W., Lawson, D.R. (1990) A comparison of measurements of atmospheric ammonia by filter packs, transition-flow reactors, simple and annular denuders and fourier-transform infrared-spectroscopy. *Atmos. Environ.*, **24**, 1019-1028.

Williams, E.J., Sandholm, S.T., Bradshaw, J.D., Schendel, J.S., Langford, A.O., Quinn, P.K., Lebel, P.J., Vay, S.A., Roberts, P.D., Norton, R.B., Watkins, B.A., Buhr, M.P., Parrish, D.D., Calvert, J.G., Fehsenfeld, F.C. (1992) An intercomparison of 5 ammonia measurement techniques. *J. geophys. Res.*, **97**, 11591-11611.

Wilson, J.D., Swaters, G.E. (1991) The source area influencing a measurement in the planetary boundary-layer - the footprint and the distribution of contact distance. *Boundary-layer Met.*, **55**, 25-46.

Wyers, G.P., Oties, R.P., Erisman, J.W. (1993a) Dry deposition of ammonia onto a coniferous forest. In: Slanina, J., Angeletti, G., Beilke, S. (Eds.), *General Assessment of biogenic emissions and deposition of nitrogen compounds, sulphur compounds and oxidants in Europe*, CEC, Brussels, pp. 139-145.

Wyers, G.P., Oties, R.P., Slanina, J. (1993b) A continuous-flow denuder for the measurement of ambient concentrations and surface-exchange fluxes of ammonia. *Atmos. Environ.*, **27**, 2085-2090.

Wyers, G.P., Erisman, J.W. (1998) Ammonia exchange over coniferous forest. *Atmos. Environ.*, **32**, 441-451.

Yamulki, S., Harrison, R.M., Goulding, K.W.T. (1996) Ammonia surface-exchange above an agricultural field in southeast England. *Atmos. Environ.*, **30**, 109-118.

Zhu, T., Pattey, E., Desjardins, R.L. (2000) Relaxed eddy-accumulation technique for measuring ammonia volatilization. *Envir. Sci. Technol.*, **34**, 199-203.

DYNAMICS OF AMMONIA EXCHANGE IN RESPONSE TO CUTTING AND FERTILISING IN AN INTENSIVELY-MANAGED GRASSLAND

C. MILFORD*, M. R. THEOBALD, E. NEMITZ and M. A. SUTTON
Centre for Ecology and Hydrology (CEH), Edinburgh Research Station, Bush Estate, Penicuik, Midlothian, Scotland, U.K.
(author for correspondence, e-mail: cmil@ceh.ac.uk, fax: +44 (0) 131 445 3943)*

(Received 7 July 2000; accepted 31 January 2001)

Abstract. Continuous micrometorological measurements of ammonia (NH_3) exchange were made for a period of 19 months (May 1998–November 1999) over intensively managed grassland in southern Scotland. This study focused on the influence of management activities, such as cutting and fertilising, on vegetation-atmosphere exchange of NH_3. Measurements were conducted within the European project GRAMINAE (GRassland AMmonia INteractions Across Europe) within which the Scottish site forms one of 6 sites in an E–W transect across Europe. NH_3 emissions were enhanced (up to 300 ng m^{-2} s^{-1}) after cutting followed by larger emissions after fertilising (up to 1400 ng m^{-2} s^{-1}). Annual budget calculations show the intensive grassland acted as a net source (1.8 kg N ha^{-1} yr^{1}) although fluxes were bi-directional with deposition dominating in the winter and emission in the summer. Initial modelling of the NH_3 exchange using a 'canopy compensation point' model has been conducted for key periods. The dynamics of the fluxes during these key periods, such as before and after cutting and fertilising, may be reproduced by introducing different values of the apoplastic ratio, $\Gamma = [NH_4^+]/[H^+]$.

Keywords: ammonia, biosphere-atmosphere exchange, grasslands, resistance modelling

1. Introduction

Excess nitrogen (N) deposition is known to lead to acidification and eutrophication (van Breemen and van Dijk, 1988; Fangmeier *et al.*, 1994), and the contribution of NH_3 to these issues is increasingly recognised as implementation of abatement measures has reduced emissions of sulphur (Bull and Sutton, 1998). Ammonia (NH_3) and ammonium (NH_4^+) (collectively NH_x) have been identified as contributing approximately 60% of the total nitrogen input and 44% of the acidifying input to the U.K. (CLAG, 1997). Detrimental effects to vegetation as a result of NH_3 have been shown to be almost exclusively a response to NH_3 deposition rather than due to elevated concentration levels of NH_3 (Bobbink, 1998). Consequently, to assess the impact of NH_x, it is necessary to quantify the deposition of NH_3 to vegetation.

Long-term measurements of trace gas exchange yield valuable information on diurnal and seasonal patterns of exchange, which cannot be gained from measurement 'campaigns' of a few weeks. In the case of NH_3, long-term, high temporal resolution measurements have been made possible by the development of

the continuous denuder technique in the early 1990s (Wyers *et al.*, 1993). A recent European project GRAMINAE (GRassland AMmonia INteractions Across Europe) was instigated to quantify exchange of NH_3 with grasslands across an East-West transect across Europe. The measurements presented here are from a site in southern Scotland, one of six sites in the transect. The measurements focus on grassland as an ecosystem for a number of reasons. Firstly, grasslands constitute one of the major ecosystems in terms of land cover throughout Europe. For example, in Great Britain (G.B.), grassland constitutes the single largest land cover category with 27% of land cover from managed grasslands alone (Fuller *et al.*, 1994). However, grasslands vary widely in their species composition and management regime from semi-natural unfertilised grassland to high N input intensively managed grassland. These two ecosystems express different NH_3 exchange characteristics; semi-natural grassland primarily receives NH_3 deposition and may be impacted by that deposition, experiencing species change or change in biomass productivity. Conversely, intensive grassland displays both deposition and emission of NH_3 and as such may impact the atmosphere, for example by increasing emissions or affecting long-range transport of pollutants.

In addition to the interest in contrasting ecosystem types, large rates of NH_3 emission have been observed following cutting of intensively managed grassland, from the sward itself (Sutton *et al.*, 1997). There has been little research investigating precisely this emission source although previous work has addressed the emission of NH_3 from senescing and decomposing vegetation (Whitehead and Lockyer, 1989; Mannheim *et al.*, 1997). Emission of volatile organic compounds (VOCs) has also been detected from cut grassland and attributed to a 'wounding' of the vegetation (Gouw *et al.*, 1999).

This article provides an introduction to the long-term measurements of NH_3 exchange at the intensively managed grassland in southern Scotland and also shows initial results from parameterisation of the NH_3 exchange using a resistance model developed for bi-directional exchange of ammonia.

2. Materials and Methods

2.1. Micrometeorological approaches

The NH_3 fluxes were determined using the aerodynamic gradient method, which couples vertical concentration profiles of NH_3 with turbulence information. The flux of NH_3 (F_χ) is calculated as:

$$F_\chi = -ku_* \frac{\partial \chi}{\partial \left[\ln (z-d) - \Psi_H \left(\frac{z-d}{L}\right)\right]}, \tag{1}$$

where k is the von Karman constant (0.41), u_* is the friction velocity, χ is concentration of gaseous ammonia, z is height above ground, d is the zero-plane

displacement, L is the Monin-Obukhov length and $\Psi_H((z-d)/L)$ is the integrated stability correction function for entrained properties (Sutton *et al.*, 1993). A negative value of F_χ denotes deposition.

A resistance analogy of trace gas transfer is often applied to interpret measured fluxes (Fowler and Unsworth, 1979). There are various implementations of this approach; the simplest assumes that the concentration at the absorbing surface is zero, allowing only for deposition. The resistance model used to interpret the measurements presented here is a 'canopy compensation point' model, which allows bi-directional exchange with stomata in parallel with deposition to leaf cuticles (Sutton *et al.*, 1995). This model includes four resistances to transfer: R_a, aerodynamic resistance; R_b, boundary layer resistance; R_w, resistance to leaf cuticles and R_s the stomatal resistance. F_t denotes net flux and is calculated from:

$$F_t = \frac{\chi_c - \chi_a\,(z-d)}{R_a\,(z-d) + R_b}\,, \tag{2}$$

where χ_a is ambient NH_3 concentration at a reference height, e.g. 1 m, χ_c is the 'canopy compensation point', to be distinguished from χ_s, the 'stomatal compensation point'. If the ambient concentration is equivalent to the canopy compensation point then the net flux is zero. The stomatal compensation point is the gaseous NH_3 concentration in thermodynamic equilibrium with dissolved NH_4^+ in the apoplast (intercellular fluid), it can be estimated from direct measurements or interpreted from exchange measurements (Farquhar *et al.*, 1980; Schjoerring *et al.*, 1998). The value of χ_c is estimated as (Sutton *et al.*, 1995):

$$\chi_c = \frac{(\chi_s/R_s) + \chi_a/(R_a + R_b)}{(R_a + R_b)^{-1} + R_s^{-1} + R_w^{-1}}\,. \tag{3}$$

2.2. Site description

The measurement site was located in southern Scotland (3°2′W, 55°52′N, elevation 190 m above sea level) on the boundary of two intensively managed grassland fields (>90% *Lolium perenne*) of approximately 5 ha each (Figure 1). The fields receive on average 270 kg N ha^{-1} yr^{-1} between three applications and are cut twice a year for silage (5 June and 28 July, 1998). From August 1998–January 1999 the fields were used for grazing, dairy cattle first and sheep later. The measurements began in May 1998 and were completed in November 1999, a period of 19 months covering two field seasons. This article presents results from the first year of measurements, May 1998–April 1999.

2.3. Instrumentation

Ammonia concentrations were determined using an automated high-resolution ammonia analyzer denoted AMANDA (Ammonia Measurement by ANnular Denuder sampling with online Analysis) (Wyers *et al.*, 1993). This technique captures gaseous ammonia in a continuous flow annular denuder using a stripping solution of 3.6 mM sodium hydrogen sulphate ($NaHSO_4$) and determines the concentration online by conductivity. Calibrations were conducted weekly with aqueous standards of NH_4^+. The detection limit is approximately 0.02 μg m^{-3} NH_3 in air. The annular denuders were placed at three heights above ground to determine the vertical concentration profile. The time resolution of this method (7.5 min sampling cycle in these measurements) is a vast improvement on other methods, such as filter packs (2–3 hr sampling), and allows a more detailed investigation of the underlying processes.

Meteorological measurements of momentum flux, sensible heat flux (H) and u_* were made with an ultra-sonic anemometer (Gill Instruments, Lymington, U.K.) compared against measurements obtained from a profile of wind speed at 5 heights using sensitive cup anemometers (Vector Instruments Ltd, Clywd, U.K.) and temperature and humidity profiles supplied by a Campbell Bowen ratio system (Campbell Scientific, Loughborough, U.K.). Net radiation, solar radiation, soil temperature, soil heat fluxes, rainfall and wind direction were also measured. The flux dataset was screened for equipment failure, calibration periods and for wind directions along the line of the dividing fence (130–150 and 310–330°). Fluxes calculated for periods with low turbulence ($u_* < 0.1$ m s^{-1}) were not used for model parameterisation purposes. Average data coverage of NH_3 concentration for the period May 1998–April 1999, after excluding periods of calibration and equipment maintenance, was 62%.

3. Results and Discussion

3.1. Meteorological

The comparison of u_* and H measured by the eddy correlation and aerodynamic method showed good agreement (data not shown). Having two independent estimates improves the robustness of the measurements and highlights periods of measurement problems. In practice, values of u_* and H from the eddy correlation method were used for the majority of the time with the estimates from the aerodynamic method used to fill any periods of missing data.

The wind direction frequency distribution is shown with the site map in Figure 1. This figure shows that the dominant wind direction was SW and there were few occurrences of wind direction along the boundary of the field. The average contribution to the flux measurement from the upwind fetch area was 87% using the formulation of Schuepp *et al.*, (1990). The fields adjacent to the measurement

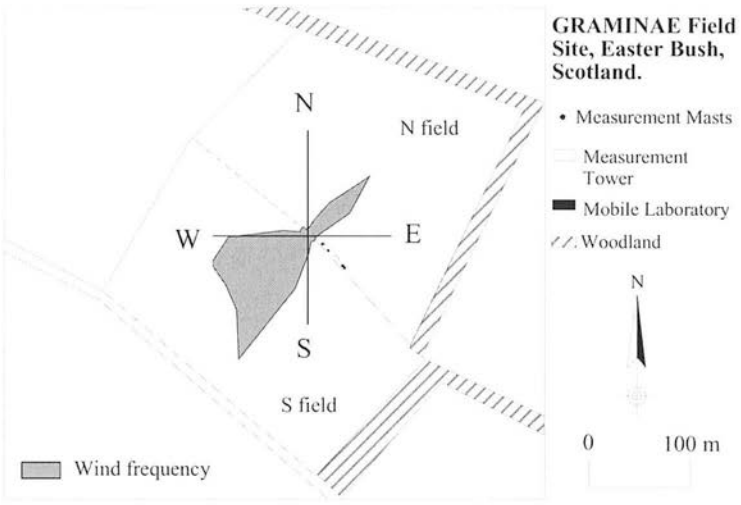

Figure 1. Site map showing the location of the measurement equipment on the boundary of the two fields plus the wind direction frequency distribution.

fields in the SW, NW and NE direction were also intensively managed grassland. For the purposes of the following analysis the fields to the NE and SW of the measurement equipment are referred to as the N field and S field, respectively.

3.2. NH_3 CONCENTRATIONS AND FLUXES

Ambient NH_3 concentration at the top height ranged between 0–33μg m^3 (15 min averages) with an arithmetic mean of 1.4 μg m^3 and a median of 0.94 μg m^3 for the period May 1998–April 1999. Figure 2 shows NH_3 concentration at three heights and the corresponding flux for (a) 27 May 1998, a typical day before the cut and (b) 11 June 1998, 6 days after the first cut with wind direction from the N field. Before the cut (Figure 2a), the dominant pattern of NH_3 exchange over the grassland was deposition with only small periods of emission. Immediately following cutting the grassland starting emitting NH_3 (see Figure 3). Figure 2b shows the typical magnitude of emission fluxes after the cut, displaying a clear increase in emission starting at 06:00 and reverting to near zero emission at 20:00. It is only such high temporal resolution data that can show these fine changes in NH_3 flux and allow investigation into the controlling processes responsible for the changes.

Examining the NH_3 flux on a weekly scale (Figure 3) shows the diurnal variability in the NH_3 exchange and the effects of short-term meteorological conditions and management activities. These results clearly demonstrate the enhanced NH_3 emissions following cutting, of up to 300 ng m^{-2} s^{-1}. These emissions are an order of magnitude greater than the typical emission observed over the grassland previous to cutting, and confirm the earlier observations of emission from cut grassland

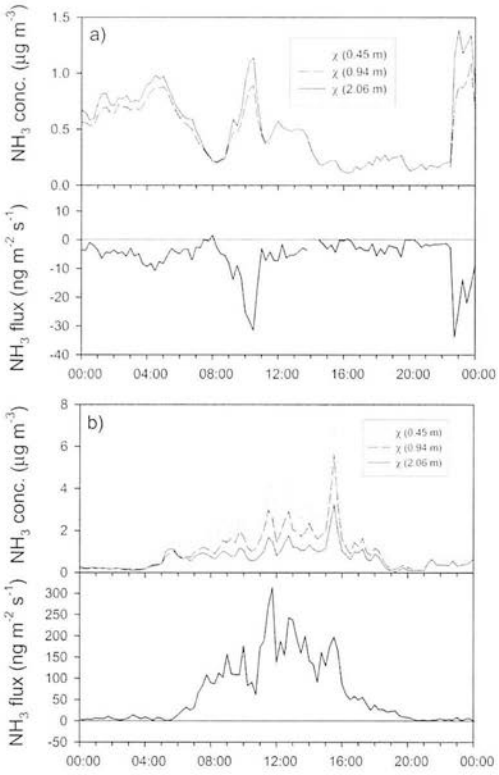

Figure 2. NH_3 concentrations at three heights and calculated flux for (a) 27 May 1998, a typical day before the cut and (b) 11 June 1998, 6 days after the cut with wind direction from the N field.

(Sutton *et al.*, 1997). However, it is still uncertain what the mechanism for the ammonia release is.

On 9 June 1998 the S field was fertilised with 100 kg N ha^{-1}. The fluxes immediately increased up to 1400 ng m^{-2} s^{-1} and the emission continued overnight indicating direct emission from the fertiliser itself, rather than stomatal emissions. The N field was not fertilised until 13 June 1998 and this difference of timing of management activities allows the analysis of cutting induced emissions to continue over a longer period. It is interesting to note that on 11 June 1998, when the wind came from the N field, the measurements still showed enhanced emissions (up to 310 ng m^{-2} s^{-1}). This is 6 days after the cutting event and provides evidence for the duration of the enhanced emissions from grass cutting without the additional effect from fertilisation. One of the challenges in analysing fluxes for the S field is to separate out the relative contribution of cutting versus fertilisation to the overall exchange after 9 June 1998.

Increasing the temporal scale and examining the seasonal variation in daily NH_3 flux (Figure 4) highlights the longer-term influence of the management activities on the seasonal NH_3 exchange. The enhanced emissions following the first cut

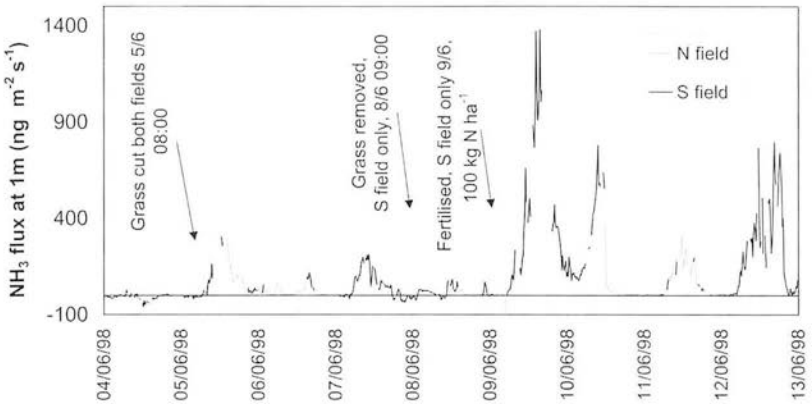

Figure 3. NH_3 Concentrations and flux at 1 m, 4–13 June 1998, arrows show timing of management activities. The fluxes are separated into 2 classes: (i) wind direction from the N field and (ii) wind direction from the S field.

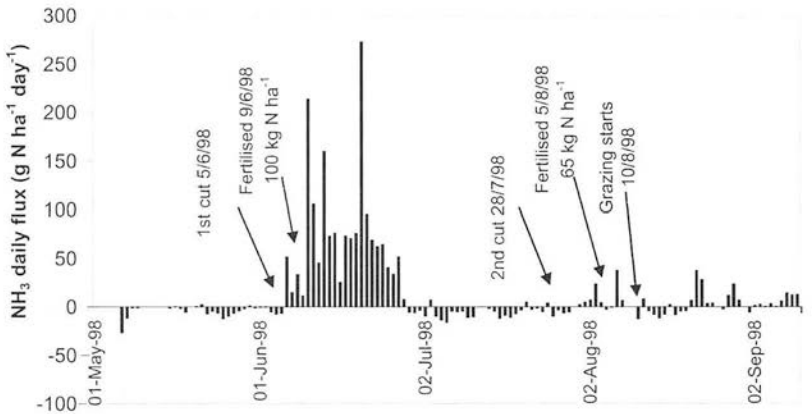

Figure 4. Mean daily flux of NH_3 as g N ha^{-1} day^{-1}, arrows show timing of 1st and 2nd cut of silage, and subsequent application of fertiliser and start of grazing.

of silage are seen to continue for approximately three weeks. Interestingly, the response following the second cut on 28 July 1998 is much smaller. Explanations for the differences between cuts are being explored, such as variations in meteorological conditions (temperature, rainfall, turbulence) or variations in soil and foliar nitrogen supply. Currently there is no simple explanation for the differences observed and it is likely to be due to a combination of the above factors.

The long-term nature of the fluxes provides data to calculate annual budgets of NH_3 exchange. In 1998/1999 the cut grassland was a net source of NH_3 at a rate of 1.8 kg N ha^{-1} yr^{-1}, although fluxes were bi-directional with deposition dominating in the winter and emission in the summer. The gross emission flux for the year (as the sum of half hourly net emission fluxes) was 4.1 kg N ha^{-1} yr^{-1} equating to 1.6% of the N applied (a figure of interest for emission factor calculations). When

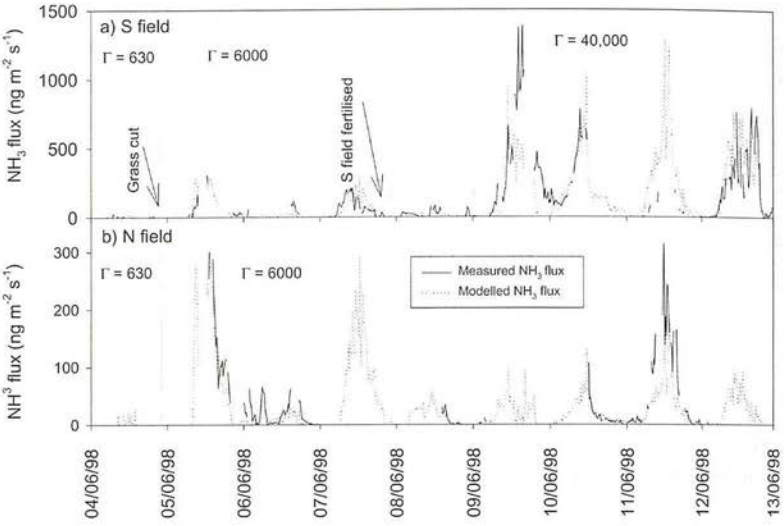

Figure 5. Measured and predicted flux using the canopy compensation point model, shown separately for (a) S field and (b) the N field.

taking account of atmospheric deposition (2.3 kg N ha^{-1} yr^{-1}) the net emission flux corresponds to 0.7% of the N applied. Although this is a small net emission flux it is significant due to the large area of the U.K. covered by grasslands (currently 65 574 km^2, Fuller *et al.*, 1994).

3.3. Parameterisation of NH_3 exchange

It is necessary to parameterise NH_3 exchange in order to interpret the measurements and investigate the mechanisms for exchange, as well as to develop parameterisations for modelling NH_3 exchange on a U.K. or European scale. An initial parameterisation of the NH_3 exchange using a 'canopy compensation point' model (Section 2.1) is shown in Figure 5. The modelled flux is shown against measured flux for the two fields separately; it is necessary to do this because of the different timing of management activities on the two fields.

R_a and R_b were derived from micrometeorological measurements (Sutton *et al.* (1993), whilst R_s and R_w were parameterised as follows:

$$R_w = R_{w,\min} \exp\left((100 - h)/a\right) \tag{4}$$

$$R_s = R_{s,\min}\left(1 + \frac{\beta_s}{S_t}\right), \tag{5}$$

where $R_{w,\min}$ is the minimum cuticular resistance, h is relative humidity (%), a is a constant controlling the increase of R_w with decreasing relative humidity, $R_{s,\min}$ is the minimal stomatal resistance, S_t is solar radiation and β_s is a constant controlling

he decrease of R_s with S_t. The values used in the prediction presented here were: $R_{s,\min} = 30$ s m^{-1}, $a = 7$, $R_{s,\min} = 100$ s m^{-1} and $\beta_s = 60$ W m^{-2}. Lastly, a arameterisation for χ_s was required. χ_s is a strong function of temperature and s also a function of the ratio $\Gamma = [NH_4^+]/[H^+]$ in the apoplast (intercellular fluids):

$$\chi_s = \frac{161500}{(T_s + 273.15)} \exp\left(-\frac{10,378}{T_s + 273.15}\right) \frac{NH_4^+}{H^+}, \quad (6)$$

here T_s is the temperature of the canopy in °C (Nemitz *et al.*, 2000). The apolastic ratio is independent of temperature and so is a useful indicator of the emission potential of an ecosystem.

The dynamics of the fluxes before and after the cutting and fertilising are well eproduced by accounting for three different values of the apoplastic ratio, (precut: = 630, postcut: $\Gamma = 6000$, post fertilising: $\Gamma = 40\,000$). This good agreement s partly a consequence of the strong dependence of NH_3 exchange on turbulence, emperature and light intensity which are well described in the model. However, hese results do show Γ varies in response to seasonal changes and management ctivities and that relatively approximate values of Γcan allow a good simulation f the NH_3 bi-directional flux. Current national deposition models for NH_3 assume constant Γ (= 3800) for the whole year (Smith *et al.*, 2000); future work will nvestigate the sensitivity of such models to seasonal variation of Γ.

4. Conclusions

ong-term measurements of NH_3 exchange have been successfully conducted over n intensively managed grassland for 19 months using the aerodynamic gradient ethod. Enhanced emissions were observed following grass cutting (up to 300 ng $^{-2}$ s^{-1}) and fertilising (up to 1400 ng m^{-2} s^{-1}) lasting for up to three weeks fter the cut. Emissions over the grassland prior to cutting were of an order of agnitude less than the cutting emissions. The intensive grassland acted as a net ource of ammonia (1.8 kg N ha^{-1} yr^{-1}) equating to 0.7% of the fertiliser N pplied. The dynamics of NH_3 exchange can be well reproduced by introducing seasonally varying apoplastic ratio of $[NH_4^+]/[H^+]$ into the canopy compensation oint resistance model. These results demonstrate the strength of long-term, high emporal resolution measurements, which are an important tool for improving our nderstanding of diurnal, seasonal and annual patterns of NH_3 exchange.

Acknowledgements

his work was supported by the U.K. Department of the Environment, Transport nd the Regions (EPG 1/3/94) and by the EU under the GRAMINAE project

(ENV4-CT98-0722). We are grateful to the University of Edinburgh for access to the field site.

References

Bobbink, R.: 1998, 'Impacts of trosospheric ozone and airborne nitrogenous pollutants on natural and semi-natural ecosystems: A commentary', *New Phytol.* **139**, 161–168.

Bull, K. R. and M. A. Sutton.: 1998, 'Critical loads and the relevance of ammonia to an effects based nitrogen protocol', *Atmos. Environ.* (Ammonia Special Issue), **32**, 565–572.

CLAG (Critical Loads Advisory Group): 1997, 'Deposition fluxes of acidifying compounds in the United Kingdom', Sub-group report on Deposition Fluxes. Department of Environment, Transport and Regions, London, U.K.

Fangmeier, A., Hadwiger-Fangmeier, A., Van der Eerden, L. and Jäger, H. J.: 1994, 'Effects of atmospheric ammonia on vegetation- a review', *Environ. Pollut.* **86**, 43–82.

Farquhar, G. D., Firth, P. M., Wetselaar, R. and Wier, B.: 1980, 'On the gaseous exchange of ammonia between leaves and the environment: determination of the ammonia compensation point', *Plant Physiol.* **66**, 710–714.

Fowler, D., and Unsworth M. H.: 1979, 'Turbulent transfer of sulphur dioxide to a wheat crop', *Q. J. R. Meteorol. Soc.* **105**, 767–783.

Fuller, R. M., Groom, G. B. and Jones, A. R.: 1994, 'The land cover map of Great Britain: An automated classification of landsat thematic mapper data', *Photogrammetric Engineering and Remote Sensing* **60**, 553–562.

Gouw, J. A., Carleton, J. H., Custer, T. G. and Fall, R.: 1999, 'Emissions of volatile organic compounds from cut grass and clover are enhanced by the drying process', *Geophys. Res. Lett.* **26**, 811–814.

Mannheim, T., Braschkat, J. and Marschner, H.: 1997, 'Ammonia emissions from senescing plants and during decompostion of crop residues', *Z. Pflanzenernähr. Bodenk.* **160**, 125–132. (in German).

Nemitz, E., Sutton, M. A., Fowler, D., Schjørring, J. K., Husted, S. and Wyers, G. P.: 2000, 'Resistance modelling of ammonia exchange above oilseed rape', *Agric. Forest Meteorol.* **105**, 405–425.

Schjoerring, J. K., Husted, S. and Mattsson, M.: 1998, 'Physiological parameters controlling plant-atmosphere exchange', *Atmos. Environ.* **32**, 491–498.

Scheupp, P. H., Leclerc, M. Y., MacPherson, J. I. and Desjardins, R. L.: 1990, 'Footprint prediction of scalar fluxes from analytical solutions of the diffusion equation', *Bound.-Layer Met.* **50**, 355–373.

Sutton, M. A., Fowler, D. and Moncrieff, J. B.: 1993, 'The exchange of atmospheric ammonia with vegetated surfaces I: Unfertilized vegetation', *Q. J. R. Meteorol. Soc.* **119**, 1023–1045.

Sutton, M. A., Schjoerring, J. K. and Wyers, G. P.: 1995, 'Plant – atmosphere exchange of ammonia', *Phil. Trans. R. Soc. Lond., A* **351**, 261–278.

Sutton, M. A., Milford, C., Dragosits, U., Singles, R., Fowler, D., Ross, C., Hill, R., Jarvis, S. C., Pain, B. P., Harrison, R., Moss, D., Webb, J., Espenhahn, S. E., Halliwell, C., Lee, D. S., Wyers, G. P., Hill, J. and ApSimon, H. M.: 1997, 'Gradients of Atmospheric Ammonia Concentrations and Deposition Downwind of Ammonia Emissions: First Results of the ADEPT Burrington Moor Experiment', in B. P. Pain and S. C. Jarvis (eds), *Gaseous Exchange with Grassland Systems*, CAB International, Wallingford, U.K., pp. 131–139.

van Breemen, N. and van Dijk, H. F. G.: 1988, 'Ecosystem effects of atmospheric deposition of nitrogen in The Netherlands', *Env. Pollut.* **54**, 249–274.

Whitehead, D. C. and Lockyer, D. R.: 1989, 'Decomposing grass herbage as a source of ammonia in the atmosphere', *Atmos. Environ.* **23**, 1867–1869.

Wyers, G. P., Otjes, R. P. and Slanina, J.: 1993, 'A continuous flow denuder for the measurement of ambient concentrations and surface fluxes of ammonia', *Atmos. Environ.* **27A**, 2085–2090.

Plant and Soil **238:** 97–110, 2002.

Seasonal variability of apoplastic NH_4^+ and pH in an intensively managed grassland

Benjamin Loubet[1,3], Celia Milford[2], Paul W. Hill[2], Y. Sim Tang[2], Pierre Cellier[1] & Mark A. Sutton[2]

[1]*Institut National de la Recherche Agronomique (INRA), 78850 Thiverval-Grignon, France.*
[2]*Centre for Ecology and Hydrology (CEH), Bush Estate, Penicuik, EH26 0QB, Scotland.*
[3]*Corresponding author*

Received 22 March 2001. Accepted in revised form 27 September 2001

Key words: ammonia, apoplast, compensation point, *Lolium perenne* L., pH

Abstract

The stomatal compensation point of ammonia (χ_s) is a major factor controlling the exchange of atmospheric ammonia (NH_3) with vegetation. It is known to depend on the supply of nitrogen and to vary among plant species, but its seasonal variation has not yet been reported for grassland. In this study, we present the temporal variation of apoplastic NH_4^+ concentration ($[NH_4^+]_{apo}$) and pH (pH_{apo}) measured in leaves of *Lolium perenne* L. in a grassland, through two periods of cutting / fertilisation, followed by a livestock grazing period. The total free NH_4^+ concentration measured in foliage ($[NH_4^+]_{fol}$), and soil mineral NH_4^+ and NO_3^- concentration are also presented. The value of $[NH_4^+]_{apo}$ varied from less than 0.01 mM to a maximum of 0.5 mM occurring just after fertilisation, whereas the apoplastic pH ranged from pH 6 to 6.5 for most of the time and increased up to pH 7.8, 9 days after the second fertilisation, when grazing started. $[NH_4^+]_{fol}$ varied between 20 and 50 μg N-NH_4^+ g^{-1} f.w. The compensation point at 20°C, ranged from 0.02 μg NH_3 m^{-3} between the fertilisations to 10 μg NH_3 m^{-3} just after the second fertilisation. The reasons for these seasonal changes are discussed, with respect to plant metabolism and the concentration of ammonium and nitrate in the soil.

Introduction

The stomatal compensation point for ammonia (χ_s) is the NH_3 concentration in the sub-stomatal cavity of a plant at equilibrium with ammonium in the apoplast. It is a major parameter controlling the strength and the direction of NH_3 exchange between vegetation and the atmosphere (Sutton et al., 1995). It has been shown that, due to differences in χ_s, fertilised crops can volatilise ammonia (Francis et al., 1997; Schjørring et al., 1993a), whereas deposition is more likely for semi-natural ecosystems (Fléchard and Fowler, 1998; Sutton et al., 1994). Therefore, a better characterisation of χ_s in relation to nitrogen supply, management practices, and plant species, is crucial to understand NH_3 exchange with vegetation.

The stomatal compensation point is often assessed from simultaneous measurement of fluxes and concentration either by micrometeorological techniques (Fléchard and Fowler, 1998) or by chamber measurements (Hill, 1999; Mattsson and Schjørring, 1996). Another technique, is based on the determination of the leaf apoplastic NH_4^+ concentration ($[NH_4^+]_{apo}$) and pH (pH_{apo}) by means of apoplastic extraction (Husted and Schjørring, 1995). The two techniques are complementary. The apoplast extraction technique can give a measure of the local variability of χ_s, and is independent of any cuticular interactions, which may affect the micrometeorological and chamber estimates (Fléchard et al., 1999; Sutton et al., 1995).

When combined with measurement of plant N content, free NH_4^+ in leaf foliage ($[NH_4^+]_{fol}$) and soil chemistry, the extraction technique provides a basis to analyse the interactions involved in the variation of χ_s with time. The assimilation of NH_x in the leaves, and therefore $[NH_4^+]_{apo}$, are related to the metabolic

activity (Yin et al., 1996), most probably through the activity of the glutamine synthetase enzyme (GS), as shown by several laboratory experiments (Mattsson and Schjørring, 1996; Olsen et al., 1995; Pearson et al., 1998). The decrease of GS activity is also thought to be responsible for NH_3 emissions from senescing leaves (Farquhar et al., 1979; Pearson et al., 1998 Schjørring et al. 1993b; Woodall et al., 1996).

It has been shown for several species that χ_s increased with increasing nitrogen supply to the roots (Hill, 1999; Mattsson and Schjørring, 1996, 1999). However, the quantitative relationship between the amount of N supplied to the plant and χ_s is still not clear, because both $[NH_4^+]_{apo}$ and pH_{apo}, which determine χ_s, are affected by root uptake of nitrogen. Indeed, Olsen et al. (1995) found a systematic increase of $[NH_4^+]_{fol}$ in leaves of oilseed rape with increasing N supply (either as NO_3^- or NH_4^+), but this increase was not correlated with NH_3 emissions, which suggests that χ_s did not increase. This may be due to the change of pH_{apo}, which seems to increase with NO_3^- supply, and may decrease with NH_4^+ supply (Hoffmann et al., 1992; Sutton et al., 1995; Yin and Raven, 1997).

In this paper, we report the results of a 5-month experiment, in intensively managed grassland in southern Scotland. The apoplastic extraction approach was applied to assess the effects of cutting, fertilising and grazing on $[NH_4^+]_{apo}$, pH_{apo}, and χ_s. In parallel, soil ammonium and nitrate concentration were measured to provide a basis for analysing the processes involved in controlling χ_s.

Material and methods

The experimental field and sampling

The measurements reported here were made as part of an integrated experiment under the EU GRAMINAE (GRassland AMmonia INteractions Across Europe) project (Sutton et al., 2001). Experimentation took place in two intensively managed grassland fields at Bush Estate (near Edinburgh, Scotland) (Milford et al., 1999). Both fields received 270 kg N ha^{-1} yr^{-1} (27 g N m^{-2} yr^{-1}) as compound fertiliser in pellet form (Kemira N-P-K (26%, 5%, 10%)) with the N as ammonium nitrate. Species composition was dominated by *L. perenne* (>90%). The two fields are referred hereafter as north and south fields, according to their relative position. They were cut and fertilised three times during the year at different times, and then grazed from late summer onwards by cattle and sheep (Table 1). We present measurements of $[NH_4^+]_{apo}$ and pH_{apo} in leaves of *L. perenne*, from May 1998 to October 1998, which covers the last two cutting/fertilisation events, and the grazing period. The grazing was variable, with an average stocking density of approximately 1 livestock unit per hectare, and in maximum periods up to 11 livestock units ha^{-1} (Table 1). There is a period, after the first cut, from the 15 June–10 July, when the data were discarded, due to problems in the extraction technique.

Samples of *L. perenne* were taken from four random locations in the field. Leaves were cut higher than 3 cm above the ground. All leaves sampled were still attached to the plant, and no litter leaves were taken. In the laboratory, located 500 m from the field, the four samples were homogenized, and green leaves only were cut into segments of 3–5 cm for apoplastic extraction. A segment of 0.5 cm was cut from each leaf for determination of $[NH_4^+]_{fol}$. After the field was cut, the grass left was very short (~5 cm), and in order to obtain sufficient plant material, leaves had to be sampled from more than four locations. After the cuts, mainly stubble was left, and the proportion of senescing leaves increased. In order to minimise the sampling bias, only green leaves, above the stubble, were sampled following the cut. After a few days, fresh re-growing leaves were also sampled.

Additional measurements of $[NH_4^+]_{fol}$ were made in order to assess the detailed time evolution of $[NH_4^+]_{fol}$. The grass sampled for this purpose included older leaves that were avoided for apoplastic extraction (due to contamination problems). This lead to two sets of data for $[NH_4^+]_{fol}$ after cutting, one for green leaves, which corresponds to the same samples as for $[NH_4^+]_{apo}$ and pH_{apo}, and one for 'yellow-green' leaves, corresponding to live older leaves, but not detached (no dead litter was sampled).

Determination of the leaf tissue NH_4^+ concentration ($[NH_4^+]_{fol}$)

The leaf segments were cut into smaller pieces, frozen in a ceramic mortar with liquid nitrogen (−210 °C), and quickly ground into a powder with a ceramic pestle. Two samples of approximately 0.1 g of this powder were taken, weighed, and put into a 1.5 ml Eppendorf tube with 1 ml of de-ionised water. The samples were shaken a few seconds by hand, left between 2 and 5 minutes to equilibrate. The samples were then centrifuged for 10 minutes, at 2000 g, and

Table 1. Dates of cutting, lifting, fertilising and grazing in the north and south fields during 1998, together with the amount of nitrogen supplied as compound (N-P-K) fertiliser, and estimated livestock units during the grazing period

Event	North field		South field	
	Date	N supply[a] kg N ha^{-1}	Date	N supply[a] kg N ha^{-1}
Fertilising	28-03-1998	104	28-03-1998	104
Cutting	05-06-1998		05-06-1998	
Lifting	13-06-1998		08-06-1998	
Fertilising	13-06-1998	104	09-06-1998	104
Cutting	31-07-1998		28-07-1998	
Lifting	02-08-1998		02-08-1998	
Fertilising	05-08-1998	65	05-08-1998	65
		livestock[a] units ha^{-1}		**livestock[a] units ha^{-1}**
Grazing	10-08-1998 onwards	Mean: 1.1 Max: 11.2	10-08-1998 onwards	Mean: 0.7 Max: 10.2

[a] 1 ha = 10^4 m^2.

4 °C, to separate the plant material from the solution. The supernatant was then decanted and filtered with cotton wool plugs as syringe-tip filters to remove large particles (note that it is not necessary to perform micro filtration since the AMFIA system involves diffusion of NH_3 across a membrane into a counter flow of deionised water), and remaining plant tissues. The filtered solution was then frozen in liquid nitrogen, and stored in a freezer at −18 °C, prior to analysis for NH_4^+, with an AMmonium Flow Injection Analyser (AMFIA, ECN, Netherlands). $[NH_4^+]_{fol}$ was then calculated as:

$$[NH_4^+]_{fol} = [NH_4^+]_{sol} \times \frac{1 + m_{fw}}{m_{fw}} \times \frac{M_N}{M_{NH4}}, \quad (1)$$

where $[NH_4^+]_{sol}$ is the NH_4^+ concentration of the filtered solution (μg NH_4^+–N g^{-1}), $[NH_4^+]_{fol}$ is in units of μmol NH_4^+ g^{-1} f.w., M_N and M_{NH4} are the molecular mass of nitrogen and ammonium respectively (g mol^{-1}), and m_{fw} is the mass of fresh leaves (g).

The extraction technique does not guarantee that all NH_4^+ is extracted from tissues. However, the grinding and freeze–thaw processing ought to be enough to disrupt the cells, and the large volume of water relative to the plant tissue should ensure that almost all free NH_4^+ was extracted. Furthermore, assuming that the degree of extraction is constant between extracts, this method gives an indication of tissue NH_4^+ concentration that can be used to analyse its variation with time.

Apoplastic extractions

Extraction technique

The vacuum infiltration technique, slightly modified from the method of Husted and Schjørring (1995), was used to determine $[NH_4^+]_{apo}$ and pH_{apo}. Leaf segments were cut, successively washed with tap water and de-ionised water, in order to avoid any contamination from fertiliser or animal excrements. The cleaning was found to be essential, especially during the grazing period, when leaf surfaces could be heavily contaminated with NH_4^+. Tests proved that this cleaning was sufficient to avoid any noticeable contamination. The clean leaf segments were separated into four replicates, infiltrated with an indigo carmine solution (50 μmol l^{-1}), using a 60 mL syringe by successively creating vacuum and pressure by hand. The infiltrated leaves were dried with clean laboratory tissues, and the apoplastic solution was then extracted by centrifugation at 500 *g* for 10 min at 4 °C. The time lapse between infiltration and extraction of the leaves was about 5 min. The extracted solution was then

frozen in liquid nitrogen and stored at −18 °C prior to analysis. The whole treatment took about 20 min from the cutting of the leaves until the end of the extraction. The infiltration was made at room temperature (15–20 °C), and the extracted volume varied between 80 and 200 μl.

Analysis of pH and NH_4^+ concentration in the apoplast (pH_{apo} and $[NH_4^+]_{apo}$)

The pH of the extracted solution was measured using a semi-micro pH electrode (Mettler Toledo, Inlab 423, Electroly, 9811). $[NH_4^+]$ of the extracted solution was determined with AMFIA, using calibration solutions (NH_4Cl in de-ionised water) of 0.1 and 1.0 μg NH_4^+ kg^{-1} or 1.0 and 10 μg NH_4^+ kg^{-1} depending on the concentration of the samples. De-ionised water was used for the zero standard. Within the range of dilutions of the extracts, Nielsen and Schjørring (1998) and Hill et al. (2001) have shown that the apoplastic pH is buffered, and therefore, in contrast to Husted and Schjørring (1995), no dilution correction for $[H^+]_{apo}$ dilution was applied. Nielsen and Schjørring (1998) have also shown, for *Brassica napus* L., that $[NH_4^+]_{apo}$ tended to be regulated during infiltration, by rapid exchange of NH_4^+ and H^+ through the cell walls. However, Hill et al. (2001), did not find such a homeostasis for $[NH_4^+]_{apo}$ in *Luzula sylvatica* (Huds.) Gaud. In the absence of further information regarding infiltration of *L. perenne*, no correction was applied for dilution effects on $[NH_4^+]_{apo}$.

Test for cytoplasmic contamination

Cytoplasmic contamination of the apoplast during the extraction procedure was tested by performing the extraction using a buffered solution (0.1 M N-tris[hydroxymethyl]methyl-2-aminoethanesulphonic acid, 2 mM dithiothreitol and 0.2 mM EDTA), and comparing the activity of the enzyme Malate Dehydrogenase (MDH) (EC 1.1.1.37) in the apoplastic extracts to its activity in the leaf homogenates, as described in Husted and Schjørring (1995). Based on four replicates, the MDH activity in the apoplastic extracts was less than 0.3% of that in the bulk extracts. Although this ratio is very low, since $[NH_4^+]_{fol}$ is much larger than $[NH_4^+]_{apo}$, calculation shows that the contamination of the apoplastic extract with cytoplasmic ammonium may lead to an overestimate in $[NH_4^+]_{apo}$ of up to 8%.

Calculation of the ammonia stomatal compensation point (χ_s) and uncertainty

The stomatal compensation point concentration (χ_s) was calculated from $[NH_4^+]_{apo}$ and pH_{apo} using the following equation, which expresses the NH_x equilibrium at the apoplast-atmosphere interface:

$$\chi_{s(20)} = M_{NH3} \times K_{H_{20}} \times K_{D_{20}} \times \frac{[NH_4^+]_{apo}}{[H^+]_{apo}} \times 10^9 \quad (2)$$

where $\chi_{s(20)}$ is the stomatal compensation point at 20 °C (in μg NH_3 m^{-3}) M_{NH_3} is the molecular mass of NH_3 (in g mol^{-1}), $K_{H_{20}}$ is the dimensionless Henry dissociation constant at 20 °C, $K_{D_{20}}$ is the acidity dissociation constant of the acid-base couple NH_3/NH_4^+ at 20 °C (in mol l^{-1}), and $[H^+]_{apo}$ and $[NH_4^+]_{apo}$ are in mol l^{-1}. The product $K_{H_{20}} \times K_{D_{20}}$ was 2.25×10^{-13} mol l^{-1}. The ratio of $[NH_4^+]_{apo}$ to $[H^+]_{apo}$, called Γ, is temperature independent and is therefore often used as a non-dimensional variable instead of $\chi_{s(20)}$ (Sutton et al., 1995, 2001). The relationship between the two variables is: $\Gamma = 262\ \chi_{s(20)}$, with the units given above.

Based on the ratio of the standard deviation to the mean for the 4 replicate measurements of $[NH_4^+]_{apo}$ at each time-point, an average standard deviation of 58% for $[NH_4^+]_{apo}$ was estimated for the whole period. Using the same approach, an average standard deviation of 0.3 pH units was found for pH_{apo}. These estimates represent the average scatter of the data at each time point, which is a more robust estimate of the uncertainty of the method than standard deviation at each time point. However, the error varied with time: it was larger after cutting and fertilisation. The combination of these averaged standard deviation with Eq. (2), allowed assessment of the uncertainty in $\chi_{s(20)}$, which can be expressed in terms of a relative range of variation [20%; 240%]. The non-symmetry of the uncertainty is due to the logarithmic relationship between $[H^+]_{apo}$ and pH_{apo}.

Measurements of soil $[NH_4^+]$ and $[NO_3^-]$

Soil measurements were determined for the South and the North field separately due to different timing of management activities. Five soil cores (separated into two layers: 0–0.15 m and 0.15–0.30 m) were taken in each field along a horizontal transect from the measurement equipment. The samples were bulked and a sub-sample (approximately 100g) was analysed for moisture content (% weight loss on drying for 24 h

at 105 °C). Another sub-sample was frozen at −18°C, and extracted at a later date (15 g soil extracted with 50 mL 1M KCL), and then analysed for soil available NH_4^+ and NO_3^- by colorimetry (Henriksen and Selmer-Olsen, 1970). Soil measurements were made fortnightly throughout the year and at greater frequency before and after management activities (e.g. cutting, fertilising).

Results

Leaf apoplastic ammonium ($[NH_4^+]_{apo}$)

Figure 1 shows $[NH_4^+]_{apo}$ in leaves of *L. perenne*, measured from the 29 May to the 2 October. There was a large temporal variability during the period. Two weeks after the first fertilization, $[NH_4^+]_{apo}$ was between 0.006 ± 0.001 mM and 0.03 ± 0.009 mM, for both fields (average ± standard deviation over the four replicates). By contrast, 8–10 days following the second fertilisation, there was a substantial increase of $[NH_4^+]_{apo}$, up to 0.6 ± 0.4 mM in both fields. Such an increase was also observed after the first fertilisation, although only one measurement is available. Figure 1 shows no significant increase of $[NH_4^+]_{apo}$ in the periods after cutting but before fertilisation. Following the second fertilisation, during the grazing period, $[NH_4^+]_{apo}$ was as small as between the two fertilisation events.

Leaf apoplastic pH (pH_{apo})

Figure 2 shows pH_{apo} in leaves of *L. perenne*. On average, pH_{apo} increased over the period, and ranged from below pH 5.7 to above pH 7.8. The pattern is very different from that of $[NH_4^+]_{apo}$ during the same period (Figure 1). Indeed, before the 13/08, pH_{apo} varied within the range pH 5.6–pH 6.9, but then increased sharply on the 14/08 (9 days after fertilisation, and also 4 days after grazing has started) and then decreased slowly to a value between pH 6 and pH 6.8 (more than 30 days later). Figure 2 shows that neither cuts nor fertilization had an immediate effect on pH_{apo}.

Compensation point ($\chi_{s(20)}$) and Γ

Measured $[NH_4^+]_{apo}$ and pH_{apo} were used to assess Γ, the ratio of $[NH_4^+]_{apo}$ to $[H^+]_{apo}$ (Figure 3). Values of $\chi_{s(20)}$ are given in a separate axis. Before 05/08, Γ ranged roughly between 6 and 70, which corresponds to $\chi_{s(20)}$ ranging from 0.04 and 0.5 μg NH_3 m^{-3}. Then, as with $[NH_4^+]_{apo}$, Γ increased sharply the day after the second fertilisation, to reach values larger than 2000, which corresponds to $\chi_{s(20)}$ = 14 μg NH_3 m^{-3}. Γ then decreased slowly, to reach its previous level 20 days later. The evolution of Γ after fertilisation varied more in the northern field, but the trend is similar in both fields.

It is striking to note that Γ, and therefore $\chi_{s(20)}$, did not increase in both fields after the first cut/fertilisation event, even though more nitrogen was supplied than in the second fertilisation. Although there is only one data point available immediately after the first fertilisation, which prevents definitive conclusions, the small Γ after the first fertilisation is attributed to a small pH_{apo} (Figure 2), while $[NH_4^+]_{apo}$ increased (Figure 1).

Total free ammonium in leaves ($[NH_4^+]_{fol}$)

Figures 4a and 4b show the total free ammonium concentration in green healthy leaves, and live yellow-green leaves of *L. perenne* respectively. Figure 4a shows that before the second fertilisation, $[NH_4^+]_{fol}$ in green leaves was stable at around 20 μg NH_4^+-N g^{-1} f.w., and even lower before the first fertilisation. Two days after the first fertilisation, $[NH_4^+]_{fol}$ in green leaves increased up to 80 μg N-NH_4^+ g^{-1} f.w. in the south field, but did not increase in the north field (only one measurement 6 days after fertilisation). After the second fertilisation, $[NH_4^+]_{fol}$ in green leaves increased again to almost 80 μg NH_4^+-N g^{-1} f.w. in the north field but not in the south field. However, in both fields, $[NH_4^+]_{fol}$ in green leaves increased later, to reach a peak 8–9 days after the second fertilisation, at the same time as pH_{apo} reached a maximum (Figure 2), and $[NH_4^+]_{apo}$ started to decrease down to its original level (Figure 1). From the 26 August onwards, $[NH_4^+]_{fol}$ in green leaves stabilised at 30 μg NH_4^+-N g^{-1} f.w., a level slightly higher than prior to the second fertilisation.

Figure 4b shows that the 'yellow-green' leaves, i.e. older leaves, have similar $[NH_4^+]_{fol}$ as green leaves in between fertilisation events, but represent a very different pattern after cutting and fertilisation. A few days after the first fertilisation, $[NH_4^+]_{fol}$ of yellow–green leaves increased to 80 μg NH_4^+-N g^{-1} f.w. in the south field and 180 μg NH_4^+-N g^{-1} f.w. in the north field. $[NH_4^+]_{fol}$ of yellow–green leaves then decreased slowly to its original level in about three weeks. After the second cut, $[NH_4^+]_{fol}$ of yellow-green leaves increased up to 220 μg NH_4^+–N g^{-1} f.w.

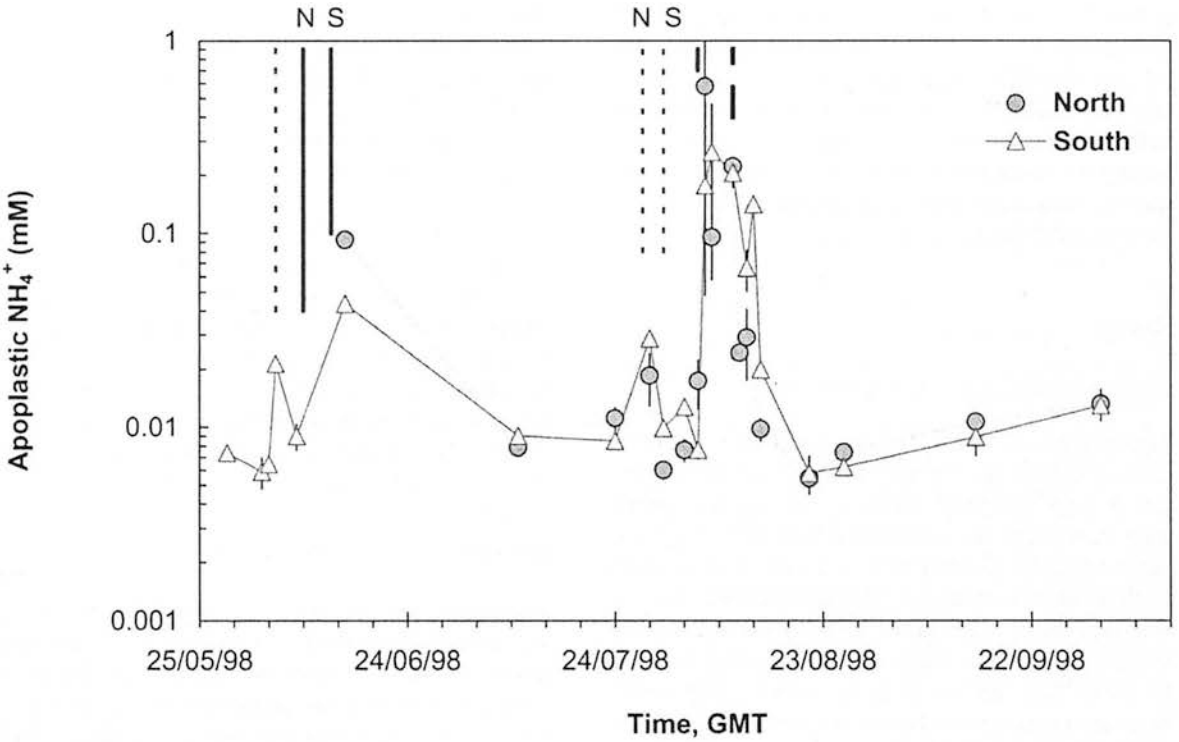

Figure 1. Apoplastic NH_4^+ concentration in leaves of *Lolium perenne* L. ($[NH_4^+]_{apo}$), measured in two fields of intensively managed grassland, at Bush Estate (Scotland). Vertical lines show management events (see Table 1): *dotted lines = cut*, *bold line = fertilisation*, and *bold dashed lines = grazing*. Here, N and S stand for north and south fields, respectively. Fertilisation consisted of 104 kg N ha^{-1} (10.4 g m^{-2}) and 65 kg N ha^{-1} (6.5 g m^{-2}) for the first and the second fertilisation, respectively. Error-bars indicate the standard deviation over 4 replicates.

in the south field and 180 μg NH_4^+–N g^{-1} f.w. in the north field, and then decreased in both fields to reach its original level just after fertilisation. Since in both fields, $[NH_4^+]_{fol}$ of yellow–green leaves behave similarly, this gives confidence that the pattern is not only scatter, but also reveals a different behaviour between $[NH_4^+]_{fol}$ in green and yellow–green leaves.

Soil NO_3^- and NH_4^+ concentration

Figure 5 shows the $[NH_4^+]_{soil}$ and $[NO_3^-]_{soil}$ of two soil layers (0–0.15 m and 0.15–0.3 m). Both $[NH_4^+]_{soil}$ and $[NO_3^-]_{soil}$ are quite variable throughout the period. Some general features can be observed: after the first cut/fertilisation, NH_4^+ concentration is rather large, and NO_3^- concentration is rather low, while it is the opposite after the second fertilisation. Whereas after the first cut/fertilisation, $[NH_4^+]_{soil}$ stays high and $[NO_3^-]_{soil}$ decreases, both $[NH_4^+]_{soil}$ and $[NO_3^-]_{soil}$ increase immediately after the second cut, before fertilisation.

Discussion

Seasonal variation of apoplastic pH

The apoplastic pH (Figure 2) ranged from pH 5.3 to pH 7.8. The maximum is slightly higher than reported measurements using a range of techniques (Hanstein et al., 1999; Hoffmann et al., 1992; Husted and Schjørring, 1995; Husted et al., 2000; Pearson et al., 1998). The most striking feature in Figure 2 is the sharp increase of pH_{apo}, 9 days after the second fertilisation, and 4 days after the start of grazing. It is very unlikely that this peak was due to contamination during extraction because: (i) both fields show the same pattern, (ii) the peak appears lately, while contamination would have occurred just after fertilisation or start of grazing, and (iii) the smooth decrease after the peak could not be explained by a contamination effect. In addition, the extraction protocol was specifically designed to avoid contamination through the leaf washing procedure.

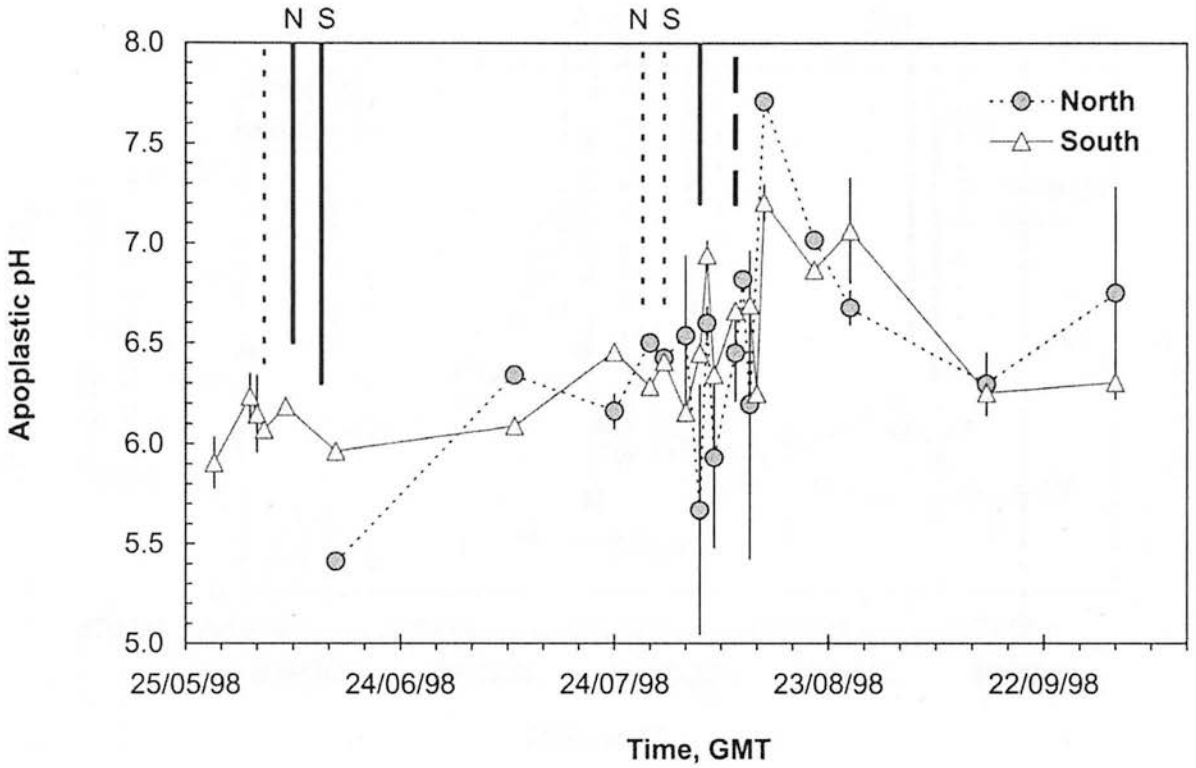

Figure 2. Apoplastic pH in leaves of *Lolium perenne* L. (pH_{apo}), measured in two fields of intensively managed grassland, at Bush estate (Scotland) during a cutting-fertilising event. Vertical lines show management events (see Table 1): *dotted lines = cut, bold line = fertilisation,* and *bold dashed lines = grazing*. Here, N and S stand for north and south fields, respectively. Fertilisation consisted of 104 kg N ha^{-1} (10.4 g m^{-2}) and 65 kg N ha^{-1} (6.5 g m^{-2}) for the first and the second fertilisation, respectively. Error-bars indicate the standard deviation over 4 replicates.

Once the assumption of contamination has been dismissed, other factors can be evaluated. It has previously been shown, both with theoretical arguments and laboratory experiments, that absorption of NH_4^+ by the roots may lead to acidification of the apoplast (Hoffmann et al., 1992; Raven, 1985), whereas NO_3^- uptake gives rise to alcalinisation of the apoplast (Farquhar et al., 1983; Hoffmann et al., 1992). The patterns of $[NH_4^+]_{soil}$ and $[NO_3^-]_{soil}$ (Figure 5) support the hypothesis that pH_{apo} is linked to the ratio of $[NO_3^-]_{soil}$ to $[NH_4^+]_{soil}$; a plot of pH_{apo} against the ratio $[NH_4^+]_{soil}/[NO_3^-]_{soil}$ for the whole period, showed a lightly negative, though very scattered correlation ($R^2 = 0.14$, slope = −0.04, data not shown). Moreover, as suggested by the recent findings of Louahlia et al. (2000) on *L. perrenne*, the potential NH_4^+ uptake rate decreases to reach a minimum about 10 days after defoliation and fertilisation, whereas the potential NO_3^- uptake rate shows a maximum around 10–15 days following defoliation and fertilisation. This suggests that, the peak of pH_{apo} is most likely due to a larger ratio of NO_3^- to NH_4^+ uptake, resulting from the larger $[NO_3^-]_{soil}$ to $[NH_4^+]_{soil}$ ratio and the larger root uptake ratio. As another element to confirm this hypothesis, Louahlia et al. (2000) have shown, in field conditions, that the part of N allocated to regrowing leaves, coming from current root uptake increases from 30% to 70% between 10 and 15 days following defoliation.

Change of apoplastic NH_4^+ in relation to management events

The apoplastic NH_4^+ concentration, measured in healthy green leaves between fertilisations, is comparable to that reported by other authors for *L. perenne* (Herrmann et al., 1999; Mattsson and Schjørring, 1999). After fertilisation, $[NH_4^+]_{apo}$ is comparable to reported measurements on plants receiving large amounts of nitrogen (Husted and Schjørring, 1995;

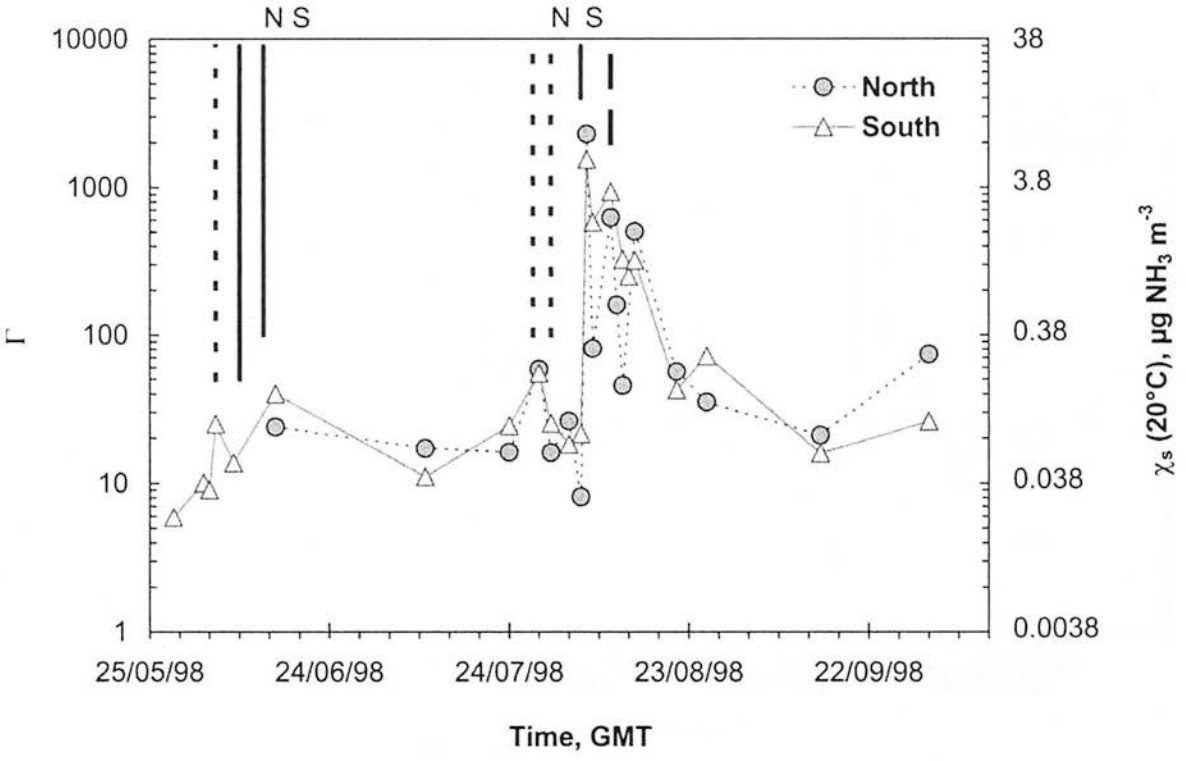

Figure 3. Evolution of the ratio of $[NH_4^+]_{apo}$ to $[H^+]_{apo}$ (Γ) in leaves of *Lolium perenne* L., measured in two fields of intensively managed grassland, at Bush estate (Scotland) during a cutting-fertilising event. Also given is the compensation point concentration at 20 °C ($\chi_{s\,20}$). Vertical lines show management events (see Table 1): *dotted lines = cut, bold line = fertilisation*, and *bold dashed lines = grazing*. Here, N and S stand for north and south fields, respectively. Fertilisation consisted of 104 kg N ha^{-1} (10.4 g m^{-2}) and 65 kg N ha^{-1} (6.5 g m^{-2}) for the first and the second fertilisation, respectively.

Hanstein et al., 1999; Husted et al., 2000; Mattsson and Schjørring, 1996).

In both fields, $[NH_4^+]_{apo}$ did not increase after cutting, but increased roughly 10 days later, just after fertilisation (Figure 1). This pattern of $[NH_4^+]_{apo}$ might be linked to the cutting as well as the fertilisation. Indeed, previous studies on the dynamics of grass regrowth (Jarvis and Macduff, 1989; Mattsson and Schjørring, 1999; Ourry et al., 1990; Sutton et al., 2001) suggests that in *L. perenne*, for a period of 7–15 days following defoliation, the proportion of N coming from root uptake of NH_4^+ or NO_3^- can be reduced, compared to N remobilised from reserves in the remaining plant (Louahlia et al., 2000; Ourry et al., 1988, 1994). This nitrogen transfer to growing leaves mainly originates from roots and stubble and possibly remaining older leaves, and could lead to a large NH_4^+ production in the senescing tissues (Pearson et al., 1998; Schjørring, 1991). Indeed, Ourry et al. (1989) report that the content of soluble proteins decreases by 30–40% in older tissues during the week after cutting, and Louahlia et al. (2000) report, during the same period, a 47 and 43% decrease in N-content of the roots and stubble, respectively. However, if as reported by Tourraine et al. (1988), nitrogen is transported as organic acids or amines, which are directly assimilated in the developing leaves, $[NH_4^+]_{apo}$ might remain low in the growing tissues during the first week following cutting. This may explain why $[NH_4^+]_{apo}$ of green leaves did not noticeably increase in the week following cutting (Figure 1). More work is needed to understand how nitrogen is transported from roots and stubble to younger leaves following defoliation in *L. perenne*.

The sudden increase of $[NH_4^+]_{apo}$ observed following both fertilisation events (Figure 1), can be explained by three hypotheses:

(H1) During a few days following cutting, the proportion of N coming from root uptake used in regrowing tissue, is very small (Louahlia et

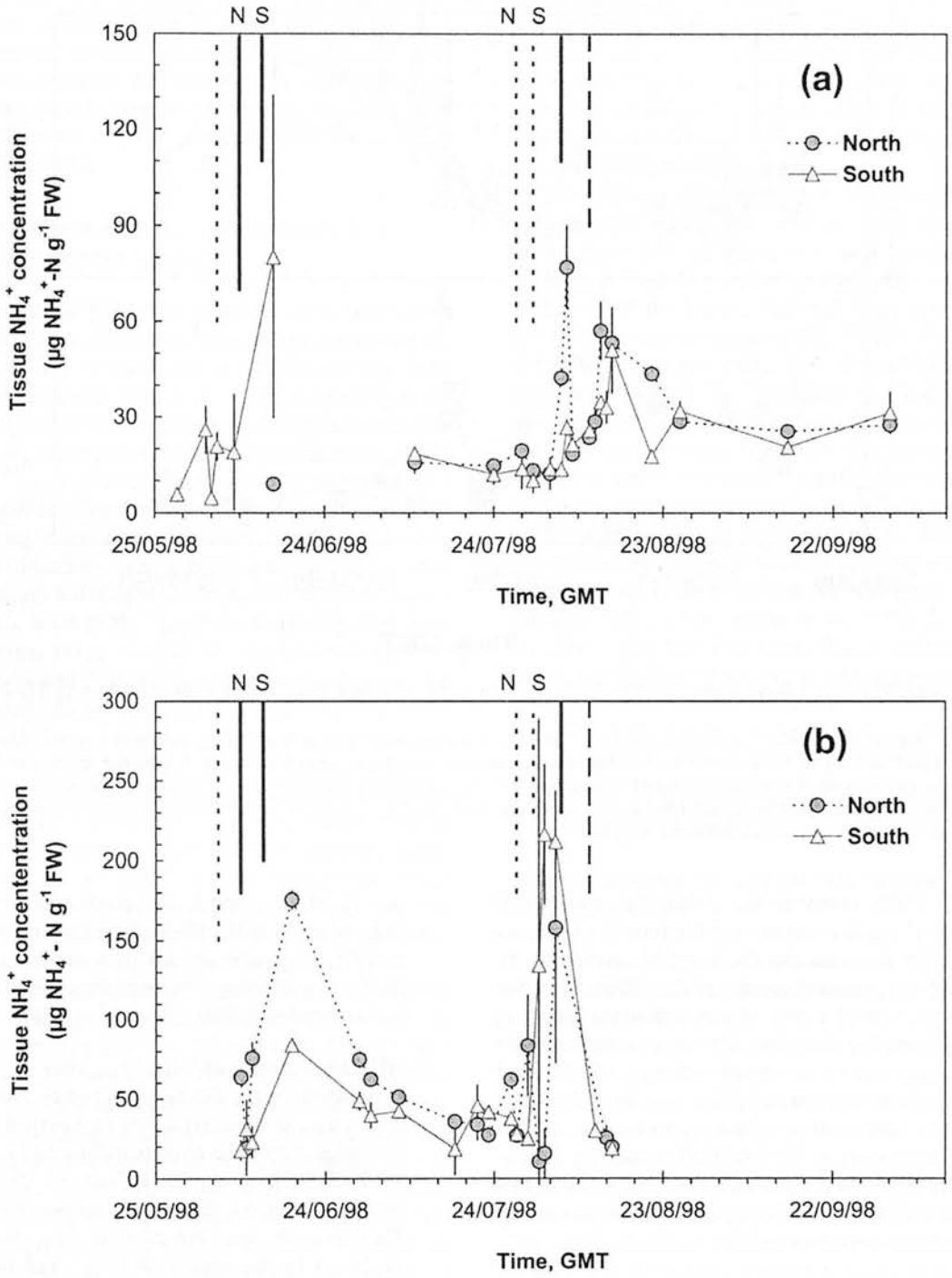

Figure 4. Tissue NH_4^+ concentration in leaves of *Lolium perenne* L. ($[NH_4^+]_{fol}$), measured in two fields of intensively managed grassland, during a cutting–fertilisation–grazing period. **(a)** $[NH_4^+]_{fol}$ for green leaves (same samples as $[NH_4^+]_{apo}$ and pH_{apo}), and **(b)** $[NH_4^+]_{fol}$ for 'yellow–green' leaves (older leaves). Vertical lines show management events (see Table 1): *dotted lines = cut*, *bold line = fertilisation*, and *bold dashed lines = grazing*. Here, N and S stand for north and south fields, respectively. Fertilisation consisted of 104 kg N ha^{-1} (10.4 g m^{-2}) and 65 kg N ha^{-1} (6.5 g m^{-2}) for the first and the second fertilisation, respectively. Error-bars indicate the standard deviation over 4 replicates.

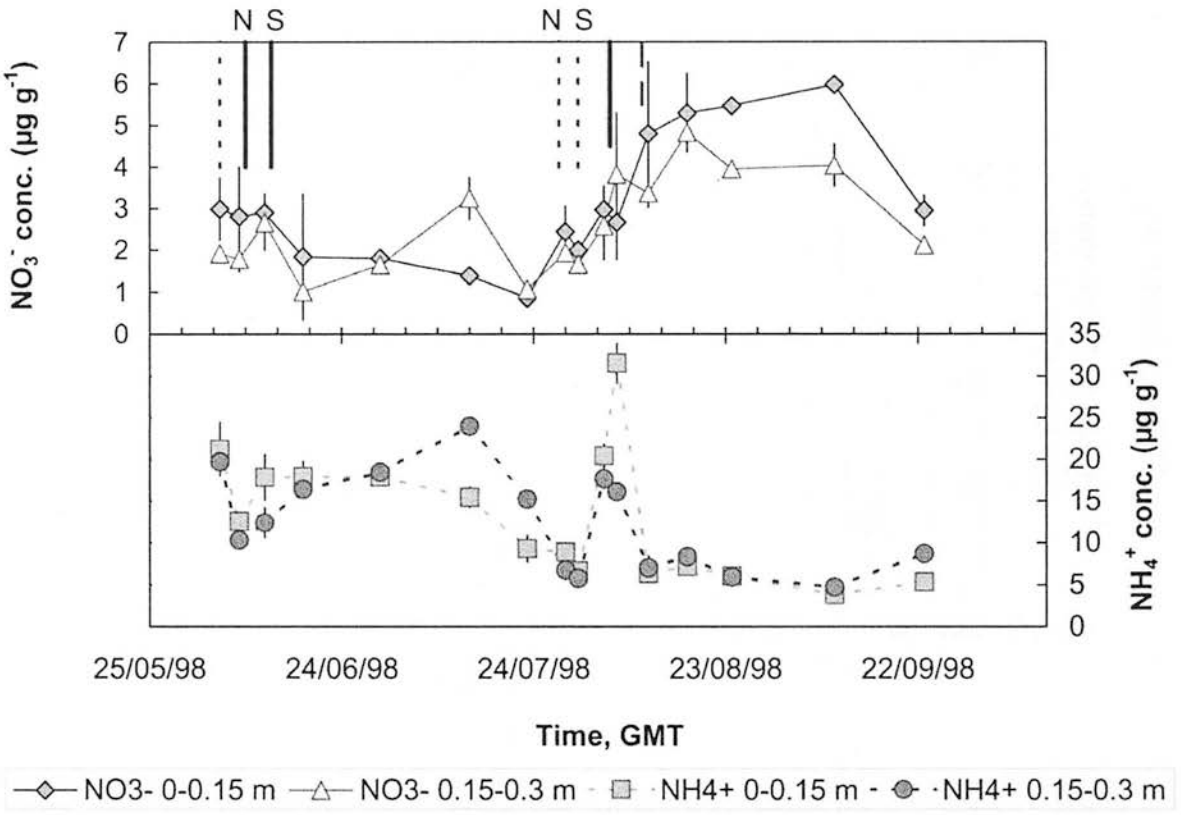

Figure 5. Soil NH_4^+ and NO_3^- concentration, in $\mu g\ g^{-1}$ of dry soil, (named $[NH_4^+]_{soil}$ and $[NO_3^-]_{soil}$, respectively), in two layers of soil: 0–0.15 m and 0.15–0.3 m. No distinction is made between the south and north field. Vertical lines show management events (see Table 1): *dotted lines = cut, bold line = fertilisation,* and *bold dashed lines = grazing*. Here, N and S stand for north and south fields, respectively. Fertilisation consisted of 104 kg N ha^{-1} (10.4 g m^{-2}) and 65 kg N ha^{-1} (6.5 g m^{-2}) for the first and the second fertilisation respectively. Error-bars indicate the standard deviation over 4 replicates.

al., 2000; Ourry et al., 1990). The increase of $[NH_4^+]_{apo}$ is coherent with the time at which root uptake becomes the dominant N source for regrowing tissues (Louahlia et al., 2000). Since the proportion of active photosynthesising leaves is still small at that time, the nitrogen that is taken up may not be completely utilised, which might explain the increase of $[NH_4^+]_{apo}$ until the metabolic activity of the plant comes back to normal (Ourry et al., 1988, 1994). Mattsson and Schjørring (1999) have indeed shown, for *L. perenne*, that the $[NH_4^+]_{apo}$ reaches a peak 6 days after cutting, and then decreases again.

(H2) The $[NH_4^+]_{apo}$ increase immediately after fertilisation may be due to the increase of $[NH_4^+]_{soil}$, coupled with an active uptake of NH_4^+ by the regrowing plant (as shown by Louahlia et al., 2000), and by the subsequent transport of NH_4^+ to the foliar apoplast in the xylem (e.g., Mattson et al., 1998). Note that the increase of $[NH_4^+]_{apo}$ corresponds to a narrow peak in $[NH_4^+]_{soil}$. Moreover, the logarithm of $[NH_4^+]_{apo}$ is correlated with $[NH_4^+]_{soil}$ ($R^2 = 0.29$).

(H3) The increase of $[NH_4^+]_{apo}$ after the second fertilisation might also be explained by NO_3^- uptake from soil since, (i) during regrowth, nitrate is also taken up by the roots (Chaillou and Lamaze, 1997; Saravitz et al., 1994), and (ii) $[NO_3^-]_{soil}$ increased after the second fertilisation (Figure 5). Therefore, the increase of $[NH_4^+]_{apo}$ could be explained by the uptake of NO_3^- and the subsequent reduction to NH_4^+ either in the roots or in the leaves. However, this process alone can not explain the observed pattern of $[NH_4^+]_{apo}$, since $[NH_4^+]_{apo}$ and $[NO_3^-]_{soil}$ are not correlated ($R^2 = 0.05$).

The observed increase of $[NH_4^+]_{apo}$ following fertilisation events (Figure 1), may well be due to a combination of all of the processes given in the three hypotheses above: the restart of the nitrogen uptake by roots; photosynthesis still not fully efficient; large concentrations of NH_4^+ and NO_3^- in the soil at that time (Figure 5).

Change of total free NH_4^+ content in leaves, in relation to management events

The measured $[NH_4^+]_{fol}$ in green and yellow–green leaves (Figure 4a, b) is in the range previously reported in the literature for several intensively managed species (Pearson et al., 1998; Schjørring et al., 1993b), although it is higher than reported measurements on *L. perenne* (Mattsson and Schjørring, 1999). $[NH_4^+]_{fol}$ of green leaves (Figure 4a) increased for a short period after both fertilisation events, but there was a more continuous increase after the second cutting/fertilisation event to reach a maximum just after grazing started (Figure 3). Note that this peak corresponds to when $[NH_4^+]_{apo}$ starts decreasing (Figure 1), and when pH_{apo} reaches its maximum (Figure 2). Mattsson and Schjørring (1999) have observed the same correlations between $[NH_4^+]_{fol}$ of healthy leaves and $[NH_4^+]_{apo}$, following cutting of *L. perenne*. The large $[NH_4^+]_{apo}$ observed after fertilisation indicates an accumulation of NH_4^+ in the leaves, which induces an increase of $[NH_4^+]_{fol}$, since the metabolism is not still efficient. Then, as photosynthetic activity increases, the NH_4^+ is taken up by roots, which might explain the quick drop of $[NH_4^+]_{apo}$, and why $[NH_4^+]_{fol}$ decreases more slowly, following the metabolic activity coming back to its optimum level.

The measured $[NH_4^+]_{fol}$ in live yellow–green leaves (Figure 4b) gives additional information on the pattern of $[NH_4^+]_{fol}$ following the first fertilisation, and the second cut. After the first fertilisation, $[NH_4^+]_{fol}$ in yellow–green leaves increased to a peak value and then started decreasing to eventually reach the original level three weeks later. After the second cut, $[NH_4^+]_{fol}$ in yellow–green leaves increased before fertilisation (Figure 4b), but no increase was observed either in $[NH_4^+]_{fol}$ or in $[NH_4^+]_{apo}$ of green leaves. This may be explained by the breakdown of the proteins in older leaves (Ourry et al., 1989; Schjørring, 1991; Pearson et al., 1998), which is promoted following cutting (Louahlia et al., 2000).

In the range 0–60 μg $N\text{–}NH_4^+$ g^{-1} FW for green leaves, pH_{apo} is positively correlated with $[NH_4^+]_{fol}$ ($R^2 = 0.56$, slope = 0.03, data not shown). If this relationship were to be verified for other species, two important results would be drawn: (i) plants with larger $[NH_4^+]_{fol}$ have larger χ_s although $[NH_4^+]_{apo}$ might not be larger; (ii) measurement of $[NH_4^+]_{fol}$ could be used as a useful indicator of the pH_{apo} which is more complicated to measure.

The different patterns of $[NH_4^+]_{fol}$ in green and yellow–green leaves give rise to many questions, but suggests that: (i) There is a large variability of $[NH_4^+]_{fol}$ within the canopy, which may be linked to the age of the leaves. This has been already observed for *Luzula sylvatica* (Hill, 1999). (ii) If such variability exists for $[NH_4^+]_{fol}$, similar differences may also exist for $[NH_4^+]_{apo}$ and pH_{apo}. Indeed, Hill (1999) reports a large variability of pH_{apo} with leaf age in *Luzula sylvatica*. This shows that the extraction technique, which is limited to healthy leaves to avoid apoplastic contamination during centrifugation, may not be representative of the whole canopy. Moreover, (iii) micrometeorological measurements have demonstrated that ammonia is emitted after grassland cutting (Milford et al., 1999; Sutton et al., 1998; Sutton et al., 2001). The fact that $[NH_4^+]_{fol}$ in yellow-green leaves increased after cutting is an encouraging result suggesting that NH_3 emissions may result from the effect of the cut increasing $[NH_4^+]_{apo}$ in yellow–green leaves, as well as from the better exposure of these leaves (that were deep within the canopy before cutting) to the free atmosphere following cutting.

Seasonal variation of Γ and the NH_3 stomatal compensation point

Before the second fertilisation, measured Γ (Figure 3) was among the smallest reported values ($\Gamma = 20$) (Hanstein et al., 1999; Sutton et al., 1992), whereas, it increased to roughly $\Gamma = 2000$ just after fertilisation, and stayed higher than 100 for more than 10 days afterwards, which is in the range of many reported values for well fertilised vegetation (Husted and Schjørring, 1995; Schjørring, 1997). The corresponding $\chi_{s(20)}$ cover the range of semi-natural to slightly fertilised vegetation as reported by previous work: 0.02–10 μg NH_3 m^{-3}. It should be noted that there is currently some uncertainty as to whether the present bioassay approach leads to underestimation of the value of Γ and χ_s (Hill et al., 2001). A possible reason for this would be spatial heterogeneity of $[NH_4^+]$ and $[H^+]$ in the apoplast, which is averaged in the extractions. However, Hill et al. (2001) agree that despite this un-

certainty, there is no evidence to doubt the relative differences in relation to treatments or management events, such as are reported here.

The pattern of observed Γ values results from a combination in the changes of $[NH_4^+]_{apo}$ and pH_{apo} over time. The changes in pH_{apo} have a large influence, and this is shown by the increase of $[NH_4^+]_{apo}$ after the first fertilisation, which is not reproduced in Γ, due to a low pH_{apo}. Also, no increase of Γ is observed after both of the cutting events, which is contradictory to ammonia fluxes observed above the grassland, after both cuts (Milford et al., 1999; Sutton et al., 2001). The difference between the dynamics of measured Γ, for green leaves, and the ammonia fluxes after cutting, raises the question of an extra source within the canopy. A likely hypothesis is that either the litter leaves (Nemitz et al., 2000), or the older yellow-green leaves contribute to this extra source, during the remobilization of nitrogen following cutting (Schjørring et al., 1993b; Mattsson and Schjørring, 1996). Although $[NH_4^+]_{apo}$ was not determined for older yellowing leaves, $[NH_4^+]_{fol}$ in this fraction of leaves increased substantially following cutting (Figure 4b), which supports this hypothesis. Further comparison of the micrometeorological fluxes with the apoplastic measurements presented in this study will push forward our understanding of the exchange of NH_3 between grassland and the atmosphere. However, such a comparison is beyond the scope of this paper, since it requires a detailed description of the micrometeorological measurements as well as surface exchange models.

Conclusions

Measurements have shown a large seasonal variability of $[NH_4^+]_{apo}$ and pH_{apo}, and also of $[NH_4^+]_{fol}$ in leaves of *L. perenne*. The $[NH_4^+]_{apo}$ of green leaves varied from roughly 0.01 mM in between fertilisation events, to more than 0.4 mM following fertilisation. It is suggested that the change in $[NH_4^+]_{apo}$ was a consequence of the combination of the regrowth process following cutting, and fertilisation.

The pH_{apo}, which was below pH 6.5 during the first part of the season increased up to pH 7.8, 9 days after fertilisation and 4 days after the grazing started. This increase is correlated with an increase in $[NH_4^+]_{fol}$ of green leaves ($R^2 = 0.56$), and slightly correlated with an increase of the ratio of mineral nitrate to mineral ammonium content in the soil ($R^2 = 0.14$). The peak in pH_{apo} also corresponds to a sudden decrease in $[NH_4^+]_{apo}$. The seasonal variability of pH_{apo} and $[NH_4^+]_{apo}$, resulted in a change in $\chi_{s(20)}$, from very low $\chi_{s(20)}$ characterising semi-natural ecosystems (0.02 μg NH_3 m^{-3}), to large $\chi_{s(20)}$, encountered in well-fertilised vegetation (10 μg NH_3 m^{-3}), although it is recognized that the bioassay results may be underestimates.

More research is needed to understand the processes leading to the seasonal change of the compensation point, which this study has shown to be large. The coupling of models describing the transfer of nitrogen in the plant, with soil and apoplastic measurements, would be a way forward to explore the mechanisms involved in the temporal variability of χ_s. The exploration of the spatial variability of $\chi_{s(20)}$ within a plant, as may be induced by leaf age, would also help to interpret the differences observed between apoplastic measurements and ammonia fluxes above the canopy following cutting.

Acknowledgements

This study has been partly funded by the French Ministries of Agriculture and Research Technologies and Education, the European project GRAMINAE (ENV 4V – CT98 0722), the UK Department of Environment, Transport and the Regions (DETR) and the Natural Environment Research Council (NERC). We thank Mr Lawrence Hodgson-Jones of the University of Edinburgh for access to the experimental field site.

References

Chaillou S and Lamaze T 1997 Nutrition ammoniacale des plantes. *In* Assimilation De L'azote Chez Les Plantes, Aspects Physiologique, Biochimique et Moléculaire. Ed. J F Morot-Gaudry. pp 422. INRA editions, Paris.

Farquhar G D, Wetselaar R and Weir B 1983 Gaseous nitrogen loss from plants. *In* Loss of Gaseous nitrogen from Plant–Soil Systems. Eds. J R Freney, J R Simpson. pp 159–180. Nijhoff/ Dr. W. Junk publishers, The Hague.

Farquhar G D, Wetsselaar R and Firth P M 1979 Ammonia volatilization from senescing leaves of maize. Science (Wash. D.C.) 203, 1257–1258.

Fléchard C R and Fowler D 1998 Atmospheric ammonia at a moorland site. II: Long-term surface-atmosphere micrometeorological flux measurements. Quart. J. R. Met. Soc. 124, 759–791.

Fléchard C R, Fowler D, Sutton M A and Cape J N 1999 A dynamic chemical model of bi-directional ammonia exchange between semi-natural vegetation and the atmosphere. Quart. J. R. Met. Soc. 125, 2611–2641.

Francis D D, Schepers S J and Sims A L 1997 Ammonia exchange from corn foliage during reproductive growth. Agroclimatology J. 89, 941–946.

Hanstein S, Mattsson M, Jaeger H J and Schjørring J K 1999 Uptake and utilization of atmospheric ammonia in three native Poaceae species: leaf conductance, composition of apoplastic solution and interactions with root nitrogen supply. New. Phytol. 141, 71–83.

Henriksen A and Selmer-Olsen A R 1970 Automatic methods for determining nitrate and nitrite in water and soil extracts. Analyst 95, 514–518.

Herrmann B, Blatter A, Jones S, Hinderling-Schwob J, Fuhrer J and Neftel A 1999 Influence of symbiotic nitrogen fixation on NH_3 exchange between grass clover crop and the atmosphere at two levels of N application: an experimental approach. *In* Proc. 10th Nitrogen Workshop, Copenhagen, August 1999. II.42. RVAU, Copenhagen.

Hill P W 1999 Physiological aspects of the exchange of gaseous ammonia between *Luzula sylvatica* Huds. (Gaud.) and the atmosphere. Ph.D. Thesis, University of Dundee, UK. 216 pp.

Hill P W, Raven J A, Loubet B, Fowler D and Sutton M A 2001 Comparison of gas exchange and bioassay determinations of the ammonia compensation point in *Luzula sylvatica* (Huds.) Gaud. Plant Physiol. 125, 476–487.

Hoffmann B, Plaenker R and Mengel K 1992 Measurements of pH in the apoplast of sunflower leaves by means of fluorescence. Physiol. Plant. 84, 146–153.

Husted S and Schjørring J K 1995 Apoplastic pH and ammonium concentration in leaves of *Brassica napus* L. Plant Physiol. 109, 1453–1460.

Husted S, Schjørring J K, Nielsen K H, Nemitz E and Sutton M A 2000 Stomatal compensation points for ammonia in oilseed rape plants under field conditions. Agric. Forest Meteorol. 105, 371–383.

Jarvis S C and Macduff J H 1989 Nitrate nutrition of grasses from steady state supplies in flowing solution culture following nitrate deprivation and or defoliation. J. Exp Bot. 218, 965–975.

Louahlia S, Lainé P, Thornon B, Ourry A and Boucaud J 2000 The role of N-remobilisation and the uptake of NH_4^+ and NO_3^- by *Lolium perenne* L. in laminae growth following defoliation under field conditions. Plant Soil 220, 175–187.

Mattsson M and Schjørring J K 1996 Ammonia emission from young barley plants: influence of N source, light/dark cycles and inhibition of glutamine synthetase. J. Exp. Bot. 47, 477–484.

Mattsson M E and Schjørring J K 1999 Controlled environment chamber measurements of ammonia exchange in two grass species. *In* Proc. 10^{th} nitrogen Workshop, Copenhagen, August 1999. II.46. RVAU, Copenhagen.

Mattsson M, Husted S, Schjørring J K 1998 Influence of nitrogen nutrition and metabolism on ammonia volatilisation in plants. Nutrient Cycling in Agroecosystems 32, 491–498.

Milford C, Sutton M A, Theobald M and Nemitz E 1999 Fluxes of ammonia with an intensively managed cut grassland in southern Scotland. *In* Proc. 10^{th} nitrogen Workshop, Copenhagen, August 1999. II.47. RVAU, Copenhagen.

Nemitz E, Sutton M A, Schjørring J K, Husted S and Wyers G P 2000 Resistance modelling of ammonia exchange over oilseed rape. Agric. Forest Meteorol. 105, 405–425.

Nielsen K H and Schjørring J K 1998 Regulation of apoplastic NH_4^+ concentration in leaves of oilseed rape. Plant Physiol. 118, 1361–1368.

Olsen C, Mattsson M and Schjørring J K 1995 Ammonia volatilization in relation to nitrogen nutrition of young *Brassica napus* plants growing with controlled nitrogen supply. J. Plant Physiol. 147, 306–312.

Ourry A, Bigot J and Boucaud J 1989 Protein mobilization from stubble and roots and proteoytic activities during post-clipping re-growth of perennial ryegrass. J. Plant Physiol. 134, 298–303.

Ourry A, Boucaud J and Duyme M 1990 Sink control of nitrogen assimilation during re-growth of ryegrass. Plant Cell Environ. 13, 185–189.

Ourry A, Boucaud J and Salette J 1988 Nitrogen mobilization from stubble and roots during re-growth of ryegrass. J. Exp. Bot. 39, 803–809.

Ourry A, Kim T H and Boucaud J 1994 Nitrogen reserve mobilization during regrowth of *Medicago sativa* L.: relationship between their availability and regrowth yield. Plant Physiol. 105, 831–837.

Pearson J, Clough E C M, Woodall J, Havill D C and Zhang X H 1998 Ammonia emissions to the atmosphere from leaves of wild plants and Hordeum vulgare treated with methionine sulphomine. New Phytol. 138, 37–48.

Raven J A 1985 pH regulation in plants. Sci. Prog. Oxford 69, 495–509.

Saravitz C H, Chaillou S, Musset J, Raper C D and Morot-Gaudy J F 1994 Influence of nitrate on uptake of ammonium by nitrogen-depleted soybean: is the effect located in roots or shoot? J. Exp. Bot. 45, 1575–1584.

Schjørring J K, 1991 Ammonia emission from foliage of growing plants. *In* Trace Gas Emissions by Plants. Eds. T D Sharkey, H A Mooney and E A Holland). pp 269–292. Academic Press inc., New York.

Schjørring J K , Kyllingsbaek A, Mortensen J V and Byskov-Nielsen S 1993a Field investigation of ammonia exchange between barley plants and the atmosphere. I. Concentration profiles and flux densities of ammonia. Plant Cell Environ. 16, 161–168.

Schjørring J K, Kyllingsbaek A, Mortensen J V and Byskov-Nielsen S 1993b Field investigation of ammonia exchange between barley plants and the atmosphere. II. nitrogen reallocation, free ammonium content and activities of ammonium-assimilating enzymes in different leaves. Plant Cell Environ. 16, 169–178.

Schjørring J K 1997 Plant-Atmosphere Ammonia Exchange. Quantification, physiology regulation and interaction with environmental factors. D.Sc. Degree. 55 pp. Royal Veterinary and Agricultural University, Copenhague, Danmark.

Sutton M A, Moncrieff J B and Fowler D 1992 Deposition of atmospheric ammonia to moorlands. Environ. Pollut. 75, 15–24.

Sutton M A, Milford C, Nemitz E, Theobald M R, Hill P W, Fowler D, Schjørring J K, Mattsson M E, Nielsen K H, Husted S, Erisman JW, Otjes R Hensen A, Mosquera J, Cellier P, Loubet B, David M, Génermont S, Neftel A, Blatter A, Herrmann B, Jones SK, Horvath L, Führer E, Mantzanas K, Koukoura Z, Gallagher M, Williams P, Flynn M and Riedo M 2001 Biosphere-atmosphere interactions of ammonia with grasslands: experimental strategy and results from a new European initiative. Plant Soil 228, 131–145.

Sutton M A, Milford C, Dragosits U, Place C J, Singles R J, Smith R I, Pitcairn C E R, Fowler D, Hill J, ApSimon H M Ross C, Hill R, Jarvis S C, Pain B F, Phillips V C, Harrison R, Moss D, Webb J, Espenhahn S E, Lee D S, Hornung M, Ullyett J, Bull K R, Emmett B A, Lowe J and Wyers G P 1998 Dispersion, deposition and impacts of atmospheric ammonia: quantifying local budgets and spatial variability. Environ. Pollut. (Nitrogen Special Issue) 102, S1, 349–361.

Sutton M A, Schjørring J K and Wyers G P 1995 Plant-atmosphere exchange of ammonia. Phil. Trans. Roy. Soc. Lond. A 351, 261–278.

Sutton M A, Asman W A H and Schjørring J K 1994 Dry deposition of reduced nitrogen. Tellus 46, 255–273.

Tourraine B, Grignon N and Grignon C 1988 Charge balance in NO_3^- fed soybean. Estimation of K^+ and carboxylate recirculation. Plant Physiol. 88, 605–612.

Woodall J, Boxall J G, Forde B G and Pearson J 1996 Changing perspective in plant nitrogen metabolism: the central role of glutamine synthetase. Science 79, 1–26.

Yin Z -H, Kaiser W M, Heber U and Raven J A 1996 Acquisition and assimilation of gaseous ammonia as revealed by intecellular pH changes in leaves of higher plants. Planta 200, 380–387.

Yin Z-H and Raven J A 1997 A comparison of the impacts of various nitrogen sources on acid-base balance in C_3 *Triticum aestivum* L. And C_4 *Zea mays* L. Plants. J. Exp. Bot. 48, 315–324.

Section editor: H. Lambers

ELSEVIER

Ecological Modelling 158 (2002) 83–110

ECOLOGICAL MODELLING

www.elsevier.com/locate/ecolmodel

Coupling soil–plant–atmosphere exchange of ammonia with ecosystem functioning in grasslands

Marcel Riedo [a], Celia Milford [a], Martin Schmid [b,1], Mark A. Sutton [a,*]

[a] *Centre for Ecology and Hydrology (CEH) Edinburgh, Bush Estate, Penicuik, Midlothian EH26 0QB, UK*
[b] *Federal Research Station for Agroecology and Agriculture (FAL), Zurich-Reckenholz, Switzerland*

Received 9 May 2001; received in revised form 3 May 2002; accepted 28 May 2002

Abstract

The exchange of ammonia (NH_3) between the atmosphere and the land surface is controlled by both atmospheric and land surface processes and can thus be bi-directional. Whether emission or deposition occurs depends on the nitrogen (N) status of the ecosystem. Resistance models have been developed to represent this bi-directional pattern of NH_3 exchange. Major pathways include exchange with leaf cuticles, plant tissues (via stomata) and with the soil surface. However, the parameters that quantify the emission potential of the foliage and ground surface, the NH_3 stomatal compensation point, χ_s, and the soil surface NH_3 concentration, χ_{soil}, respectively, are entirely empirical in these models and do not consider the influence of the plant and soil N status. On the other side, grassland ecosystem models simulate the ecosystem N dynamics, but until now NH_3 biosphere–atmosphere exchange was only treated in a very simple manner. A two-layer resistance model for NH_3 exchange has thus been combined with the grassland ecosystem model PaSim in order to link NH_3 exchange with the ecosystem N dynamics. For this purpose, the plant substrate N pool in previous versions of PaSim has been divided between apoplastic and symplastic compartments, and the apoplastic substrate N pool has been linked to the stomatal NH_3 exchange. In addition, soil ammoniacal N (NH_x) has been partitioned between the soil surface and several soil layers, and the soil surface NH_3 exchange has been linked to the soil surface ammonium (NH_4^+). The new combined model has been parameterised and applied to an intensively managed grassland site in Southern Scotland. The comparison with micrometeorological measurements of NH_3 fluxes has shown that the model can qualitatively reproduce the effects of cutting and fertilisation on the net NH_3 exchange above the canopy. In particular, the model reproduces the expected strong coupling of the NH_3 exchange with the dynamics of the apoplastic substrate N pool. However, peak NH_3 emissions are underestimated, and it is postulated that this could be related to the representation of leaf litter emissions from the soil surface in the model, and to the simulated soil NH_x dynamics. Nevertheless, this new version of PaSim is a valuable tool for investigating the influence of different management scenarios or of climate change on NH_3 exchange.

Keywords: Ammonia fluxes; Grassland; Resistance model; Ecosystem model; Compensation point

* Corresponding author. Tel.: +44-131-445-4343; fax: +44-131-445-3943
E-mail address: ms@ceh.ac.uk (M.A. Sutton).
[1] Present address: EAWAG, Limnological Research Centre, 6047 Kastanienbaum, Switzerland.

0304-3800/02/$ - see front matter
PII: S0304-3800(02)00169-2

1. Introduction

NH_3 deposition is of concern since it contributes to eutrophication and acidification of semi-natural ecosystems (Fangmeier et al., 1994; Bull and Sutton, 1998; Aneja et al., 2001; Erisman, 2001). In contrast to many other pollutant gases, which are consistently deposited, the exchange of NH_3 between the atmosphere and the land surface is controlled by both atmospheric and land surface processes and can be bi-directional. Whether emission or deposition occurs depends on the nitrogen (N) status of the ecosystem. For intensively managed agricultural ecosystems, the N balance is mainly driven by agricultural fertilisation (Schjoerring, 1991; Sutton et al., 1993a, 2001; Harper et al., 1996), but on unfertilised semi-natural and natural ecosystems, deposition of atmospheric NH_3 is usual (Sutton et al., 1993b; Duyzer, 1994; Wyers and Erisman, 1998), and with other forms of fixed nitrogen (e.g. wet deposition of NH_4^+ and NO_3^-, dry deposition of HNO_3 and NO_2) can influence biodiversity. There are important feedback effects of ecosystems on the atmosphere: intense long-term N inputs may lead to changes in the ecosystem functioning, related to increased N status of the vegetation and litter, that decrease net N input to the ecosystem (Sutton et al., 1995a). In addition, intensively managed agricultural systems have a large potential for NH_3 emission, and thus influence the atmospheric N balance.

Resistance models have been developed to represent this bi-directional pattern of NH_3 biosphere–atmosphere exchange (Sutton and Fowler, 1993; Sutton et al., 1995b; Flechard et al., 1999; Nemitz et al., 2001). Major pathways include exchange with leaf cuticles, plant tissues (via stomata) and with litter or the soil surface. For the cuticular exchange pathway, both instantaneous resistance models (Sutton et al., 1995b; Nemitz et al., 2001) and dynamic models (Sutton et al., 1998a; Flechard et al., 1999) have been developed. The emission potential of the internal leaf tissues and ground surface are given by the NH_3 gas concentrations at equilibrium with the NH_4^+ concentration in the apoplastic water film, χ_s ($\mu g\ NH_3\ m^{-3}$), referred to as the 'stomatal compensation point', and the soil surface concentration, χ_{soil} ($\mu g\ NH_3\ m^{-3}$), respectively. Values of χ_s are calculated through a thermodynamic temperature function of apoplastic NH_4^+ and H^+ concentration (Sutton et al., 1998a; Nemitz et al., 2001). While there are sound experimental grounds to parameterise the temperature function, the apoplastic NH_4^+ is entirely empirical in these models. They thus do not consider the dynamic dependency of the apoplastic NH_4^+ concentration on factors such as management, supply of N to the roots, plant N level and development stage (Sutton et al., 1993b; Whitehead, 1995; Schjoerring et al., 1998). A similar limitation applies to χ_{soil} (Nemitz et al., 2001): the soil surface NH_4^+ concentration is given empirically, and not related to the soil N dynamics. There is consequently a need to link the recent developments in modelling bi-directional NH_3 exchange with modelling of ecosystem functioning.

Process based ecosystem models cover the dynamics of carbon (C), N, water and energy fluxes of the ecosystem in relation to management practice, and local climate and soil conditions (e.g. Chen et al., 1996; Foy et al., 1999; Parton et al., 1998; Li et al., 1992; Shiyomi et al., 2000; Thornley and Verberne, 1989; Thornley, 1998; Riedo et al., 1998). Most attention in such models with regard to N fluxes with the atmosphere has been given to the estimation of N_2O emissions (e.g. Frolking et al., 1998). However, other important parts of the N exchange between atmosphere and ecosystem were until now treated in a very simple manner, if at all. In particular, modelling the exchange of NH_3 is an area that has received little attention within process-based ecosystem models. NH_3 exchange was so far not represented as a bi-directional flux, but instead the amount of NH_3 deposition was given as a driving variable for model simulations (Riedo et al., 1998; Thornley, 1998), and soil NH_3 emission did not depend on factors such as wind speed and soil pH (Thornley, 1998). In the CENTURY model, N losses through volatilisation are assumed to be proportional to gross N-mineralisation (Parton et al., 1987). In the DNDC model (Li et al., 1992) ammonia volatilisation from the soil is calculated as a function of the ammonia concentration in the soil liquid phase,

but there is no consideration of bi-directional fluxes.

The objective of this study was to improve the representation of ammonia fluxes between the atmosphere and ecosystem in an ecosystem model, and to allow the consideration of the interactions between N exchange and ecosystem functioning. To do this, a resistance model for gaseous NH_3 exchange (Sutton et al., 1995b; Nemitz et al., 2001) was coupled with the dynamic grassland ecosystem model PaSim. PaSim simulates above- and below-ground dry matter production of cut, fertilised or grazed grassland ecosystems relative to fluxes of C, N, water, and energy (Riedo et al., 1998). In earlier work it was mainly used to investigate the sensitivity of productivity and C sequestration in intensively managed grassland ecosystems to elevated atmospheric CO_2 and climate change (Riedo et al., 1999, 2000, 2001). To our knowledge the present work is the first attempt to couple NH_3 exchange using a bi-directional resistance model with a dynamic model of grassland ecosystem functioning. This approach is obviously a major advance compared with the existing bi-directional NH_3 exchange models, which do not consider the dynamics of ecosystem functioning (e.g. Sutton et al., 1995b; Flechard et al., 1999; Nemitz et al., 2001) as it enables the interactions with grassland management and environmental change to be addressed. Equally, it is a significant advance compared with the existing dynamic ecosystem models (e.g. Thornley, 1998; Riedo et al., 1998; Frolking et al., 1998), in that it provides a mechanistic treatment of bi-directional NH_3 exchange coupled to both soil and plant processes. While the work reported here has been applied in a grassland model, it should be noted that the principles of bi-directional ammonia exchange applied here are equally applicable to other systems, such as forest and arable crops.

In previous versions of PaSim, plant N was divided between substrate and structural N. Such a division is also made by the Hurley Pasture Model (Thornley, 1998), but not by other grassland models. This had the advantage for modelling NH_3 exchange that substrate N is expected to be more closely coupled to apoplastic NH_4^+ than total plant N. In an initial analysis, the temporal changes in substrate N were also found to relate at least qualitatively to field measurements of apoplastic NH_4^+ and NH_3 fluxes (Sutton et al., 2001). For this study, a new PaSim version was developed, in which substrate N is partitioned explicitly into apoplastic and symplastic fractions, and it has been hypothesised that the value of χ_s used in the resistance models is linked to the apoplastic substrate N. In order to simulate the source–sink strength of the soil surface, the single layer approach for soil ammoniacal N in previous PaSim versions (Riedo et al., 1998) has been expanded in order to deal with NH_4^+ concentrations in different soil layers and the soil surface. This is crucial to modelling NH_3 release from the soil surface, as has been demonstrated for volatilisation of liquid manure by Genermont et al. (1998).

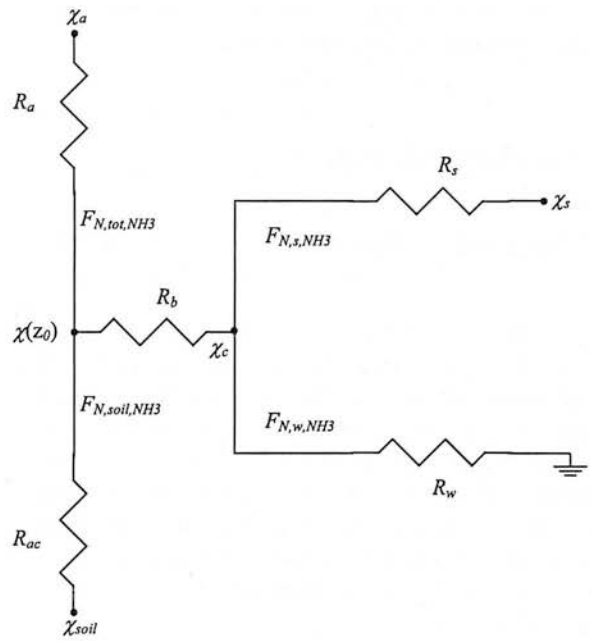

Fig. 1. Two-layer resistance model (Nemitz et al., 2001) used to describe NH_3 exchange in the grassland ecosystem model PaSim. The net canopy NH_3 exchange, F_{N,tot,NH_3}, is determined by NH_3 transfer through the stomata, F_{N,s,NH_3}, deposition to leaf cuticles, F_{N,w,NH_3}, and exchange with the soil surface, $F_{N,soil,NH_3}$. The resistances controlling the fluxes are the leaf stomata resistance R_s, the cuticular resistance R_w, the aerodynamic resistance R_a, the leaf boundary resistance R_b, and the in-canopy aerodynamic resistance R_{ac}.

The present paper reports the development of the coupled NH_3 exchange-grassland ecosystem model. The model is parameterised using a range of literature information and by reference to micrometeorological flux measurements carried out in 1998 applying the aerodynamic gradient method at an intensively managed grassland field site in Southern Scotland (Sutton et al., 2001; Milford et al., 2001). The model is then assessed in relation to flux measurements for 1999 at the same field site. A sensitivity analysis is also presented for the new model parameters determining NH_3 exchange.

With such a combined model the effects of e.g. fertilisation, plant decomposition, and leaf N on the NH_3 exchange can directly be simulated. In view of the constraints on field measurements both in the number of sites, and in the duration of measurements, such a combined grassland ecosystem model is thus a valuable tool to investigate the influence of different management scenarios or of climate change on NH_3 exchange.

2. Material and methods

2.1. Model description

2.1.1. Model overview

PaSim is a dynamic grassland ecosystem model. It simulates above- and below-ground dry matter production of cut, fertilised or grazed grassland ecosystems relative to fluxes of C, N, water, and energy. This paper describes and uses the new version 3.5 of PaSim. Descriptions of previous PaSim versions can be found elsewhere (Riedo et al., 1998, 1999, 2000; Schmid et al., 2000a,b; Schmid, 2001).

The main changes in this new PaSim version are the incorporation of a NH_3 exchange resistance model, the partitioning of plant substrate N into apoplastic and symplastic substrate N, and the partitioning of soil NH_x and NO_3^- among a soil surface layer (only for NH_x) and several soil layers. Other minor changes are described in the Appendix A.

2.1.2. NH_3 exchange

For a NH_3 resistance model to be included into PaSim the resistance model had to fulfil two criteria: it had to represent all the different sources and sinks relevant for a grassland ecosystem, and it had to fit into the frame of PaSim, i.e. its level of detail should be in accordance with the level of detail of PaSim. It was considered that models describing the temporal dynamics of cuticle adsorption–desorption (Sutton et al., 1998a; Flechard et al., 1999) were over-complex for the present purpose, especially since they require time steps down to a few seconds (in contrast to a PaSim time step of about half an hour). The 'canopy compensation point' approach developed by Sutton and Fowler (1993) was therefore applied, whereby bi-directional stomatal fluxes are offset against deposition to leaf cuticles, with the latter constrained by a cuticular resistance (R_w). Nemitz et al. (2001) have recently modified this from a one-layer to a two-layer approach, which is thus able to deal with litter/soil emissions. Although a more detailed three-layer model was also available (Nemitz et al., 2000), the two-layer resistance model (2LRM) was found to be the optimum compromise between simplicity and accuracy (Nemitz et al., 2001), and it has a level of detail that is comparable to the various components of PaSim.

The 2LRM is fully described by Nemitz et al. (2001). Here, only a short overview is given, and some differences in the implementation are mentioned. The resistance scheme for the 2LRM is shown in Fig. 1. The model includes bi-directional foliar stomatal exchange, F_{N,s,NH_3} (kg N m^{-2} per day), deposition to leaf cuticles, F_{N,w,NH_3} (kg N m^{-2} per day), and NH_3 exchange with a ground layer, $F_{N,soil,NH_3}$ (kg N m^{-2} per day), with ground emissions originating from fertiliser evaporation, soil, and decomposing plant parts. The emission potential of the foliage and ground surface are given by the NH_3 stomatal compensation point, χ_s, and the soil surface NH_3 concentration, χ_{soil}, respectively. From these concentrations together with transfer resistances of the different exchange pathways, and with the NH_3 concentration at a reference height above the canopy, χ_a (μg NH_3 m^{-3}), the net canopy NH_3 exchange flux,

F_{N,tot,NH_3} (kg N m^{-2} per day), can be determined. However, as mentioned above, the determination of the NH_4^+ concentration of the apoplast and the soil surface, from which χ_s and χ_{soil} are derived, are completely empirical in the 2LRM. Through the coupling of the 2LRM with PaSim as described here, χ_s and χ_{soil} can be related to the N dynamics of the plants and the soil surface, respectively.

In the 2LRM, it is not considered what happens with the NH_3 deposited to leaf cuticles. However, a grassland ecosystem model like PaSim has a much longer time scale than a 2LRM, and the dynamics of this NH_3 pool has thus to be taken into account. In the new version of PaSim, NH_3 dry deposited on the leaf cuticle is washed to the soil surface pool through precipitation (Sutton et al., 1993b).

In previous versions of PaSim, transfer resistances of the different exchange pathways were already represented in order to calculate evapotranspiration (except for the cuticular resistance, R_w) (Riedo et al., 1998). These resistances are now also used to calculate NH_3 biosphere–atmosphere exchange. A sensitivity analysis showed that the differences in the representations of these resistances in PaSim and in the 2LRM (Nemitz et al., 2001) could be ignored. In calculating the stomatal resistance for NH_3, the theoretical difference in diffusivity between NH_3 value and H_2O value has been applied according to the ratio of their molecular diffusivities (0.92). However, some laboratory studies have suggested that NH_3 may in practice have a much smaller stomata resistance than H_2O (Husted, 1997; Schjoerring et al., 1998). It is possible that this effect is due to interaction with the leaf cuticle resistance (Wyers and Erisman, 1998; Sutton et al., 2001), but this interaction has not been included in the present version of the model. The cuticular resistance R_w (s m^{-1}) is given by:

$$R_w = R_{w,min} \exp^{(100-RH)/b_{cuticles}} \quad (1)$$

where the values for the parameters $R_{w,min}$ and $b_{cuticles}$ were chosen according to Milford et al. (2001), Sutton et al. (2001), and RH is relative humidity as %.

2.1.3. Apoplastic and symplastic substrate N pools

The NH_3 stomatal compensation point, χ_s (Fig. 1), is given by:

$$\chi = \frac{K_{a,NH_4^+,T}}{K_{h,NH_3,T}} \frac{[NH_4^+]_{apo}}{10^{-pH_{apo}}} 1.70 \times 10^{10}$$

$$= \frac{K_{a,NH_4^+,T}}{K_{h,NH_3,T}} \Gamma \times 1.70 \times 10^{10} \quad (2)$$

where $K_{a,NH_4^+,T}$ (M) and $K_{h,NH_3,T}$ (dimensionless) are the dissociation constant and the Henry equilibrium constant, respectively, which both depend on leaf temperature T_l (Sutton et al., 1994), pH_{apo} is the apoplastic pH, and Γ_s is the NH_4^+ to H^+ concentration ratio in the apoplast. The factor 1.70×10^{10} converts between the units of $[NH_4^+]_{apo}$ and χ_s. The apoplastic NH_4^+ concentration $[NH_4^+]_{apo}$ is closely coupled to the plant N dynamics. It reflects the balance between reactions that produce ammonia in plant tissues (nitrate reduction, photorespiration, phenylpropanoid pathway, degradation of transport amides and proteolysis) and the reactions (associated with GS–GOGAT, ADH–GDH, carbamoyl phosphate synthetase) that assimilate it (Husted, 1997). In previous versions of PaSim, total plant N was divided between structural N, $W_{N,struct}$ (kg N m^{-2}), and plant substrate N, $W_{N,sub}$ (kg N m^{-2}), i.e. the freely available plant N, which can be used for e.g. growth of structural plant material, or protein synthesis. However, preliminary examinations revealed (data not shown) that neither the total plant N concentration per unit mass of total plant dry matter, N_{tot} (kg N kg^{-1} DM), nor the substrate N concentration per structural plant dry matter, N_{sub} (kg N kg^{-1} structural DM), show the detailed temporal behaviour of $[NH_4^+]_{apo}$ observed in measurements. The plant substrate N pool has thus been divided in PaSim into apoplastic substrate N, $W_{N,apo}$ (kg N m^{-2}), and substrate N in cell internal pools, combined into the symplastic substrate N, $W_{N,sym}$ (kg N m^{-2}) (Fig. 2), and it is assumed that $[NH_4^+]_{apo}$ is closely coupled to the apoplastic substrate N pool (see Eq. (9) below).

The separation of the apoplast from the symplast in PaSim, and the assumed close coupling of

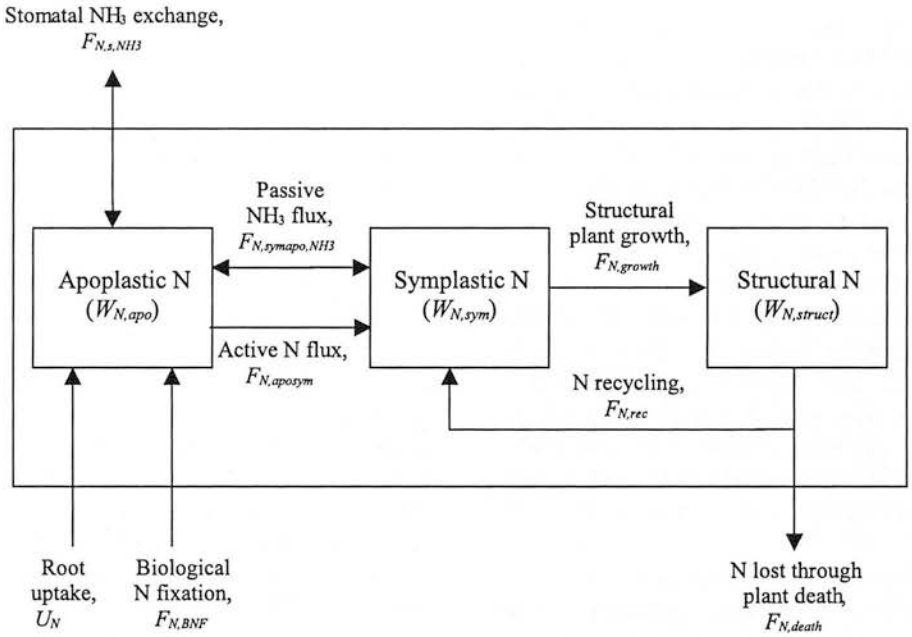

Fig. 2. Plant N in PaSim is divided among structural N $W_{N,struct}$, apoplastic substrate N $W_{N,apo}$, and symplastic substrate N $W_{N,sym}$. All input/output fluxes of the N pools are shown except for the losses from grazing and cutting. The governing equations for $W_{N,apo}$ and $W_{N,sym}$ are given in Eqs. (3) and (4), for $W_{N,struct}$ see (Riedo et al., 1998).

the stomatal compensation point to the apoplastic substrate N, is based on observations of the xylem transport of NH_x and the biochemical pathways involving NH_x that result in several aqueous NH_x pools in cell compartments (Husted, 1997). NH_4^+ is taken up by the roots, and after the translocation from roots to shoots in the xylem, it is moved from the stem sap to the leaf apoplast and absorbed into the leaf cells (Finnemann and Schjoerring, 1999). This NH_4^+ pathway and the observation that there is a close connection between the leaf apoplast and the xylem compartment (Mattsson et al., 1998), have been represented in PaSim through the following equations for the dynamics of plant apoplastic and symplastic substrate N:

$$\frac{dW_{N,apo}}{dt} = U_N + F_{N,BNF} + F_{N,symapo,NH_3} - F_{N,s,NH_3} - \frac{W_{N,apo}}{W_{N,sub}} F_{N,grazing,sub} - F_{N,aposym} \quad (3)$$

$$\frac{dW_{N,sym}}{dt} = F_{N,rec} + F_{N,aposym} - F_{N,growth} - \frac{W_{N,sym}}{W_{N,sub}} F_{N,grazing,sub} - F_{N,symapo,NH_3} \quad (4)$$

These two pools represent not only N substrate in the leaves, but the total plant N substrate. N is taken up by the roots (U_N (kg N m^{-2} per day) in (Eq. (3)), and transported in various compounds through the xylem to the plant apoplastic substrate N pool $W_{N,apo}$. The flux U_N and the two pools $W_{N,apo}$ and $W_{N,sym}$ not only include NH_x, but also other N compounds, including NO_3^-. However, the model described here does not distinguish between effects of root NO_3^- uptake as compared with root NH_4^+ uptake. From $W_{N,apo}$ NH_4^+ is moved through an active process across the plasmalemma ($F_{N,aposym}$ (kg N m^{-2} per day) in Eq. (3)) to the symplastic substrate N pool $W_{N,sym}$. An active NH_4^+ transport system from the apoplast into the leaf cells has been suggested because the leaf apoplast has much lower NH_4^+ concentra-

tions than the leaf tissue (Finnemann and Schjoerring, 1999). The rate of the active NH_4^+ flux across the plasmalemma, $F_{N,aposym}$, depends on apoplastic NH_4^+ concentration and temperature (Nielsen and Schjoerring, 1998), and is thus calculated as:

$$F_{N,aposym} = k_{aposym,T} N_{apo} W_{sh} \quad (5)$$

where the rate parameter $k_{aposym,T}$ depends on leaf temperature T_l, N_{apo} is the apoplastic substrate N concentration per structural plant dry matter, (kg N kg^{-1} structural DM), and W_{sh} is the shoot structural dry matter (kg DM m^{-2}). For $k_{aposym,T}$ the same temperature response has been assumed as for other plant processes (Riedo et al., 2000).

In addition to the active NH_4^+ flux from the apoplast to the symplast, the two substrate N pools are also connected through passive NH_3 diffusion across the plasmalemma, $F_{N,symapo,NH_3}$ (kg N m^{-2} per day) Eqs. (3) and (4)). A steep NH_3 gradient between the neutral pH conditions in the cytoplasm and more acidic conditions in the apoplast favours NH_3 diffusion through the plasmalemma from the symplast to the apoplast (Husted, 1997; Lee and Ayling, 1993). Because NH_3 has high membrane permeability, this diffusion flux can be important, as can be seen e.g. through the observation that inhibition of glutamine synthetase (GS) causes a rapid increase in NH_3 emission (Sutton et al., 1995b; Mattsson et al., 1998). Fick's law can be applied to calculate NH_3 diffusion through the plasmalemma:

$$F_{N,symapo,cell,NH_3} = ([NH_3]_{sym} - [NH_3]_{apo}) P_{NH_3,T} \times 1.21 \quad (6)$$

Here, $F_{N,symapo,cell,NH_3}$ (kg N m^{-2} cell surface per day) is the NH_3 diffusion on a per cell surface basis, $P_{NH_3,T}$ (m s^{-1}) is NH_3 permeability of the plasmalemma (depending on leaf temperature), $[NH_3]_{sym}$ and $[NH_3]_{apo}$ (M) are the concentrations of symplastic and apoplastic NH_3, and 1.21 is a unit conversion factor. As for $k_{aposym,T}$, the temperature response of $P_{NH_3,T}$ has been assumed to be the same as for other plant processes (Riedo et al., 2000). The NH_3 diffusion on a cell area basis is converted to a diffusion on a ground area basis, $F_{N,symapo,NH_3}$ (kg N m^{-2} per day), through the equation

$$F_{N,symapo,NH_3} = F_{N,symapo,cell,NH_3} CAI \times LAI \quad (7)$$

where CAI is the cell area index (m^2 cell surface per m^2 leaf surface), and LAI is the leaf area index. The symplastic and apoplastic NH_3 concentrations in Eq. (6) are related to the symplastic and apoplastic NH_4^+ concentrations through the dissociation equilibria:

$$[NH_3]_{sym} = K_{a,NH_4^+,T} 10^{pH_{sym}} [NH_4^+]_{sym}$$

$$[NH_3]_{apo} = K_{a,NH_4^+,T} 10^{pH_{apo}} [NH_4^+]_{apo} \quad (8)$$

Symplastic and apoplastic NH_4^+ concentrations are calculated from molar symplastic and apoplastic substrate N concentrations, $[N]_{sym}$ and $[N]_{apo}$ (M), respectively:

$$[NH_4^+]_{sym} = f_{NH_4^+,N_{sym}} [N]_{sym}$$

$$[NH_4^+]_{apo} = f_{NH_4^+,N_{apo}} [N]_{apo} \quad (9)$$

The molar concentrations $[N]_{sym}$ and $[N]_{apo}$ are calculated according to the Appendix A, and the dimensionless fraction $f_{NH_4^+,Nsym}$ is assumed to be constant. The fraction of NH_4^+ in N_{apo}, $f_{NH_4^+,Napo}$, is assumed to have a constant value of $f_{NH_4^+,Napo,min}$ for periods of background levels of N_{apo} (N_{apo} below N_{apo1}), but to increase linearly up to a maximum of $f_{NH_4^+,N_{apo,max}}$ for values of N_{apo} between N_{apo1} and N_{apo2}. This dependency of $f_{NH_4^+,N_{apo}}$ on N_{apo} was chosen because it has been shown for the xylem (which is closely linked to the apoplast), that the NH_4^+ fraction of the total amount of inorganic and organic N translocated in the xylem sap strongly depends on the amount of N supply (Finnemann and Schjoerring, 1999).

The remaining N fluxes in Eqs. (3) and (4) are biological N fixation, $F_{N,BNF}$ (kg N m^{-2} per day), bi-directional NH_3 stomatal exchange, F_{N,s,NH_3} (kg N m^{-2} per day) (Fig. 1), substrate N loss from both apoplast and symplast through grazing, $F_{N,grazing,sub}$ (kg N m^{-2} per day), N recycling from dead plant material, $F_{N,rec}$ (kg N m^{-2} per day), and N used for growth of structural plant material $F_{N,growth}$ (kg N m^{-2} per day).

2.1.4. Soil mineral N and soil NH_3 emission

NH_3 emission from the soil surface layer, $F_{N,soil,NH_3}$ (kg N m^{-2} per day), originating from

fertiliser evaporation, soil, and decomposing plant parts, depends on the soil surface NH_3 concentration, χ_{soil} (Fig. 1), at equilibrium with the NH_4^+ concentration in the soil surface solution, $[NH_4^+]_{aq,surface}$ (μg N m^{-3}) (see Eq. (11) below). The value of $[NH_4^+]_{aq,surface}$ is a fraction of the total ammoniacal N of the soil surface, $N_{amm,surface}$ (kg N m^{-2}). This ammoniacal N of the soil surface is a new pool in PaSim (Fig. 3), and several assumptions have been made concerning this pool: (1) $N_{amm,surface}$ is partitioned among gaseous and aqueous NH_3 and aqueous NH_4^+ according to the Henry and dissociation equilibria (Sutton et al., 1994), (2) $N_{amm,surface}$ is uniformly distributed in a layer on the soil surface with a constant thickness of $d_{surface}$, (3) the actual and saturated volumetric water content of this layer are assumed to be the same as for the soil layer 1 ($\theta_s(1)$ and $\theta_{s,sat}(1)$), and (4) its temperature is given by the soil surface temperature, T_{ss}. With these assumptions the following equation can be derived for $[NH_4^+]_{aq,surface}$:

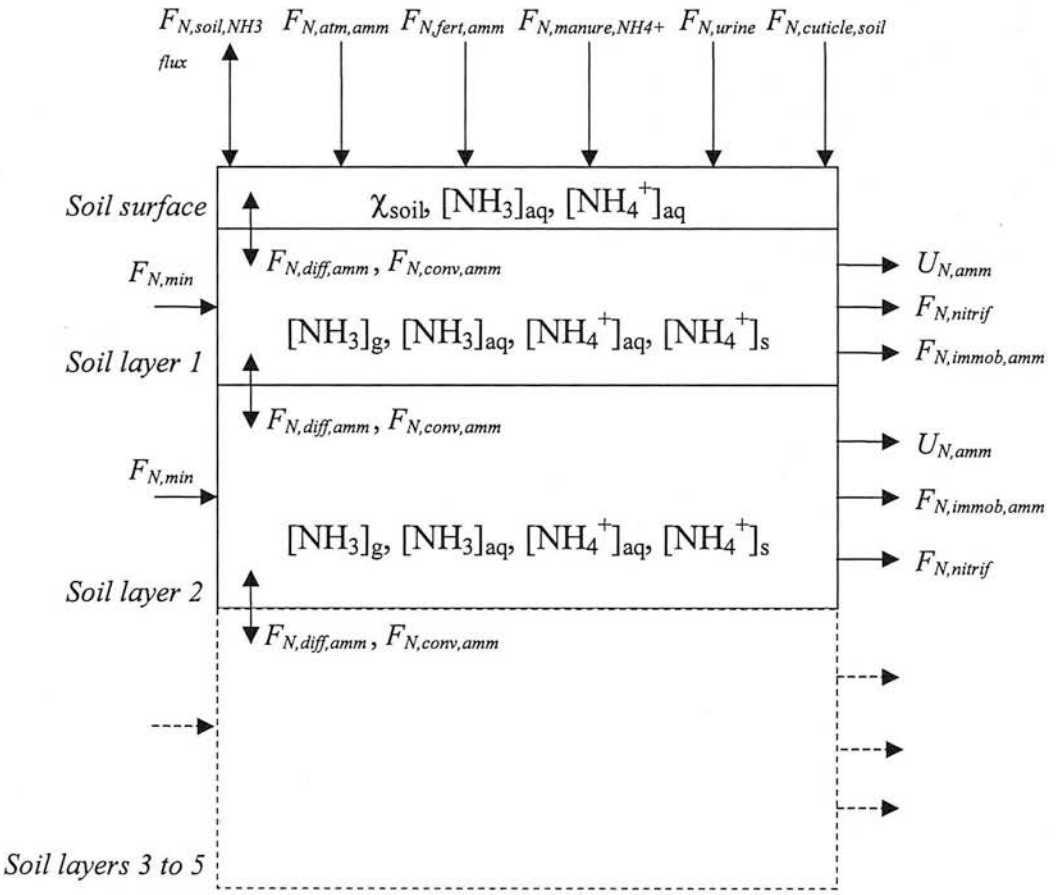

Fig. 3. Soil ammoniacal N in PaSim is divided among soil surface NH_x, and NH_x in the different soil layers. Soil surface NH_x is partitioned between aqueous NH_4^+, and gaseous and aqueous NH_3. Soil ammoniacal N is partitioned between aqueous and exchangeable solid NH_4^+, and gaseous and aqueous NH_3. All input/output fluxes of the soil N pools are shown. The governing equations for the soil NH_x pools are given in Eqs. (12) and (13). For meaning of symbols see text and Nomenclature.

$$[NH_4^+]_{aq,surface} = \frac{N_{amm,surface}10^9/d_{surface}}{((\theta_{s,sat}(1) - \theta_s(1))K_{a,NH_4^+,T}/K_{h,NH_3,T} + \theta_s(1)K_{a,NH_4^+,T}(1))10^{pH_{soil}} + \theta_s(1)} \quad (10)$$

where pH_{soil} is the soil pH, and 10^9 converts between μg and kg. The NH_3 soil surface concentration can then be calculated from:

$$\chi_{soil} = \frac{K_{a,NH_4^+,T}}{K_{h,NH_3,T}} \frac{[NH_4^+]_{aq,surface}}{10^{-pH_{soil}}} \frac{17}{14} \quad (11)$$

The dynamics of the ammoniacal N of the soil surface is given by:

$$\begin{aligned}\frac{dN_{amm,surface}}{dt} &= F_{N,atm,amm} + F_{N,fert,amm} + F_{N,manure,NH_4^+} + F_{N,urine} \\ &+ F_{N,cuticle,soil} - F_{N,conv,amm}(0) - F_{N,diff,amm}(0) \\ &- F_{N,soil,NH_3} \end{aligned} \quad (12)$$

where $F_{N,atm,amm}$ (kg N m^{-2} per day) is atmospheric NH_x–N deposition other than gaseous NH_3, $F_{N,fert,amm}$ (kg N m^{-2} per day) is NH_4^+ from mineral fertilisation, $F_{N,manure,NH_4^+}$ (kg N m^{-2} per day) is NH_x–N from manure application, $F_{N,urine}$ (kg N m^{-2} per day) is NH_x–N from hydrolysis of urine excreted by grazing animals, $F_{N,cuticle,soil}$ (kg N m^{-2} per day) is NH_x–N from the leaf cuticle washed to the soil surface through precipitation, and $F_{N,soil,NH_3}$ (kg N m^{-2} per day) is soil surface exchange of gaseous NH_3. The ammoniacal N of the soil surface is coupled with the ammoniacal N in soil layer 1 through convection, $F_{N,conv,amm}(0)$ (kg N m^{-2} per day), and diffusion, $F_{N,diff,amm}(0)$ (kg N m^{-2} per day) (see Appendix A).

In contrast to previous versions of PaSim, soil ammoniacal N is now divided among different soil layers (Fig. 3), and for each layer the dynamics is given by:

$$\begin{aligned}\frac{dN_{amm}(h)}{dt} &= F_{N,min}(h) + F_{N,conv,amm}(h-1) \\ &+ F_{N,diff,amm}(h-1) - U_{N,amm}(h) \\ &- F_{N,nitrif}(h) - F_{N,immob,amm}(h) \\ &- F_{N,conv,amm}(h) - F_{N,diff,amm}(h) \end{aligned} \quad (13)$$

The vertical NH_x convection and diffusion fluxes in Eq. (13), $F_{N,conv,amm}(h)$ and $F_{N,diff,amm}(h)$, depend on the partitioning of $N_{amm}(h)$ among the different phases in the soil (see Appendix A). The remaining fluxes are N mineralisation, $F_{N,min}(h)$ (kg N m^{-2} per day), root NH_4^+ uptake, $U_{N,amm}(h)$ (kg N m^{-2} per day), nitrification, $F_{N,nitrif}(h)$ (kg N m^{-2} per day), and NH_4^+ immobilisation, $F_{N,immob,amm}(h)$ (kg N m^{-2} per day). Because of the close coupling between soil ammoniacal N and soil nitrate (NO_3^-) through nitrification, different soil layer pools have also been introduced for NO_3^- (see Appendix A). In contrast to the ammoniacal N pool of the soil surface, in the soil layers the exchangeable soil solid phase is also represented in addition to the gaseous and aqueous phases (see Appendix A).

In the 2LRM for NH_3 exchange included into PaSim, soil NH_3 emission from the soil surface depends on χ_{soil}, which is in equilibria with soil surface NH_4^+, and thus also closely coupled to soil NH_4^+. The different sources of NH_3 emission from the soil surface, i.e. fertiliser evaporation, soil NH_4^+, decomposing plant parts, and animal excreta, contribute to soil NH_3 emission indirectly through their influence on soil and soil surface NH_4^+ (Eqs. (12) and (13)). This representation of soil NH_3 emission in the new PaSim version described here replaces the previous empirical relationships in previous PaSim versions for NH_3 loss from different sources (volatilisation from mineral N fertilisation, animal excreta, and soil NH_4^+).

2.1.5. Numerical techniques

Owing to the changes in this new PaSim version, including vertical soil NH_x convection and diffusion fluxes, the model now includes processes which differ in their time constants by orders of magnitude. This problem has been solved by dividing the model into different parts, which run each with an appropriate integration time step. Tests have been carried out to optimise these time steps for accuracy and efficiency.

2.2. Model parameterisation

Where possible, the values for the new model parameters in PaSim (plant and soil parameters in Table 1) were directly or indirectly derived from the literature. However, this was not always possible, and in these cases best estimates were used, or the parameter values were chosen in order to fit model simulations to measurements in 1998 at a grassland field site in Southern Scotland (see Section 2.3 for the site description).

The maximal fraction of NH_4^+ in N_{apo}, $f_{NH_4^+,Napo,max}$, was estimated to be 10%, because measurements for the xylem, which is strongly coupled to the apoplast, have shown that NH_4^+ constituted up to 11% of the total amount of inorganic and organic N translocated in the xylem sap (Finnemann and Schjoerring, 1999). In contrast, $f_{NH_4^+,Napo,min}$ was set in such a way that the simulated ground level NH_3 biosphere–atmosphere exchange (i.e. the exchange in absence of management influences) was close to the exchange measured in 1998 at the Southern Scotland field site (Milford et al., 2001). Due to lack of data, the constant fraction of NH_4^+ in N_{sym}, $f_{NH_4^+,Nsym}$, was set to the maximal value of NH_4^+ in N_{apo}.

The fraction of NH_4^+ in N_{apo}, $f_{NH_4^+,Napo}$, increases for values of N_{apo} between N_{apo1} and N_{apo2}. N_{apo1} was chosen in such a way that for

Table 1
New plant, soil and input parameters in PaSim

Plant parameters			
$b_{cuticles}$	Parameter for R_w	7	Sutton et al., 2001
$f_{NH_4^+,N_{apo,max}}$	Maximal fraction of NH_4^+ in N_{apo}	0.1 mol mol^{-1}	Finnemann and Schjoerring, 1999
$f_{NH_4^+,N_{apo,min}}$	Minimal fraction of NH_4^+ in N_{apo}	0.05 mol mol^{-1}	Calibration for Southern Scotland
$f_{NH_4^+,Nsym}$	Fraction of NH_4^+ in N_{sym}	0.1 mol mol^{-1}	Estimation
f_{H_2Oapo}	Fraction of leaf water in apoplast	0.15	Husted and Schjoerring, 1995; Nielsen and Schjoerring, 1998
$k_{aposym,20}$	Rate parameter at 20 °C for $F_{n,aposym}$	10 per day	Schjoerring et al., 1998
N_{apo1}	Parameter for $f_{NH_4^+,N_{apo}}$	0.0002 kg N (kg DM)$^{-1}$	Calibration for Southern Scotland
N_{apo2}	Parameter for $f_{NH4+,N_{apo}}$	0.0005 kg N (kg DM)$^{-1}$	Calibration for Southern Scotland
$P_{NH_3,20}$	NH_3 permeability of the plasmalemma at 20 °C	4.0×10^{-9} m s^{-1}	Calibration for Southern Scotland
$R_{w,min}$	Parameter for R_w	30 s m^{-1}	Sutton et al., 2001
CAI	Cell area index	50 m^2 cell surface (m^2 leaf surface)$^{-1}$	Estimation based on leaf thickness of 8 cells
$W_{plantfresh2dry}$	Shoot dry to fresh weight ratio	0.3 kg DM (kg FM)$^{-1}$	Finnemann and Schjoerring, 1998
Soil parameters			
$d_{surface}$	Thickness of soil surface ammoniacal N layer	1 mm	Estimation
Input parameters			
$a_{NH_4^+ads}(h)$	Parameter for Freundlich equation for NH_4^+ partitioning in soil layer h	1.076	Singh and Nye, 1984
$b_{NH_4^+ads}(h)$	Parameter for Freundlich equation for NH_4^+ partitioning in soil layer h	0.66	Singh and Nye, 1984
PH_{apo}	Apoplastic pH	6.2	Loubet et al., 2002
PH_{sym}	Symplastic pH	7.0	Husted, 1997
pH_{soil}	Soil pH	5.6	Milford et al., 2001

Parameter values used for simulations for Southern Scotland field site in 1998 and 1999.

background conditions, i.e. periods without management interventions, the simulated values of N_{apo} for the Southern Scotland field site in 1998 were below N_{apo1}. The parameter N_{apo2} was set to a value that the simulated values of N_{apo} for the Southern Scotland field site in 1998 reached within one or two days after a fertilisation event.

Once the parameters for the calculation of $[NH_4^+]_{apo}$ and $[NH_4^+]_{sym}$ from Eq. (9) were set, $k_{aposym,20}$ (see Eq. (5)) was determined in such a way that the ratio between the apoplastic and symplastic NH_4^+ concentrations, $[NH_4^+]_{apo}$ and $[NH_4^+]_{sym}$, was around 1/10 for background conditions, i.e. periods without management influences. This ratio 1/10 reflects measured ratios between apoplastic and bulk leaf NH_4^+ concentrations (Schjoerring et al., 1998). The assumption made here is that the symplastic NH_4^+ concentration has approximately the same value as the measured leaf bulk NH_4^+ concentration. It should be noted that in the model the vacuole is implicitly included into the symplast N pool.

The above mentioned parameterisation of $k_{aposym,20}$ *was only possible with the arbitrary assumption that the passive* NH_3 *diffusion through the plasmalemma,* $F_{N,symapo,NH_3}$, is an order of magnitude smaller than the active N transport through the plasmalemma, $F_{N,aposym}$. The same assumption was used to determine a value for the NH_3 permeability of the plasmalemma, $P_{NH_3,T}$ (see Eq. (6)). The value for CAI (see Eq. (7)) was estimated from an average number of cells per leaf area, and from an average cell surface area.

The value for the fraction of leaf water that is in the apoplast, f_{H_2Oapo}, was estimated from data reported by Husted and Schjoerring (1995), Nielsen and Schjoerring (1998). The shoot dry to fresh weight ratio, $W_{plantfresh2dry}$ (kg DM kg^{-1} FM), was estimated from data given by Finnemann and Schjoerring (1998).

The thickness of the soil surface NH_4^+ layer, $d_{surface}$, was determined from a set of simulations with different values of $d_{surface}$ at the Southern Scotland field site for 1998 as the best compromise between accuracy and requirements to the model time step associated with the soil surface NH_4^+ pool.

2.3. Model application for a grassland site in Southern Scotland

The new PaSim version described here is applied to an intensive grassland field site in Southern Scotland (Long 3°2′ W, Lat 55° 52′ N, elevation 190 m a.s.l.). The field site was composed of at least 90% *Lolium perenne*, received about 270 kg $NH_4^+NO_3^-$–N ha^{-1} per year, was cut twice a year for silage, and was used for cattle and sheep grazing from August onwards (see Figs. 7 and 9 for details). The model performance could be compared with micrometeorological measurements of NH_3 fluxes and other ecosystem variables that were carried out during the growing seasons of 1998 and 1999. Detailed descriptions of the site and the field measurements are given by Milford et al. (2001).

The model input parameters, including hourly weather data for the two years, were available or could be derived from the field measurements. For the model input parameters that are new to the PaSim version described here, the values are given in Table 1. Atmospheric NH_x deposition other than gaseous NH_3 was assumed to be 5.3 kg N ha^{-1} per year, and atmospheric NO_3^- deposition was set to 5.5 kg N ha^{-1} per year (Sutton et al., 1993b). As in PaSim only grazing by lactating cows, but not by sheep is represented, the sheep stocking density was converted into a cattle stocking density using a livestock unit of 0.08 for sheep. In order to receive representative initial conditions of the model state variables for this site, a steady state simulation had to be carried out. This steady state simulation required weather data over sufficient years that represent the climate at this site. However, only daily long-term meteorological data were available (Land Surface Observation Stations Data for the Bush House station from the UK MetOffice), and PaSim, which required hourly weather data in previous versions, had thus to be expanded to cope with daily weather input data. This was done according to Thornley (1998). A sensitivity analysis that was done for a Swiss site, for which both hourly and daily long term weather data were available, showed that the results of a steady state simulation are not sensitive to the use of daily or hourly weather input data.

2.4. Sensitivity analysis

A sensitivity analysis was carried out for the Southern Scotland site to investigate the sensitivity of the NH_3 fluxes cumulated over the vegetation period of 1998 to the new model and input parameters of PaSim (parameters in Table 1). For each of these parameters, two model simulations were carried out, one with a 25% decrease, and one with a 25% increase in the parameter value.

3. Results

3.1. Model application for grassland site in Southern Scotland

3.1.1. Seasonal dynamics of plant N compartments and fluxes

The comparison of the simulated time courses of plant N variables over the vegetation period of 1998 shows that the relative temporal variability is greater for N_{apo} than for N_{sub}, and greater for N_{sub} than for N_{tot} (Fig. 4a and b). N_{sub} and N_{apo} show fast responses to fertilisation and, to a lesser amount, to cutting. In contrast, the response of N_{tot} is slower and smaller for both fertilisation and cutting events. While N_{tot} and N_{sub} peak at about the same values after both cutting/fertilisation events, N_{apo} shows a larger peak in June than in August. As is expected from Eq. (9), Γ_s follows the time course of N_{apo}, but shows a larger increase due to the increased fraction of NH_4^+ in N_{apo} during periods of increased substrate N levels (Fig. 4b). Similar model results have been obtained for the vegetation period of 1999 (data not shown).

In the absence of biological N fixation and without grazing, the dynamics of apoplastic substrate N are determined by the fluxes U_N, $F_{N,symapo,NH_3}$, $F_{N,aposym}$ and F_{N,s,NH_3} (Eq. (3)). However, both $F_{N,symapo,NH_3}$ and F_{N,s,NH_3} are very small compared with U_N and $F_{N,aposym}$, as Fig. 5 shows for the cutting/fertilisation events of both June and August 1998. During some days after cutting, the balance between U_N and $F_{N,aposym}$ *shifted towards* U_N, leading to a small increase in N_{apo} both in June and August (Figs. 4 and 5). This shift was much more pronounced during some days after fertilisation, and more so for the June than for the August fertilisation, leading to large increases in N_{apo}.

3.1.2. Component fluxes of NH_3 exchange in 1998

Cutting in June 1998 led to a small increase in simulated F_{N,s,NH_3} (Fig. 6a) and the simulated net NH_3 exchange above the canopy, F_{N,tot,NH_3} (Fig. 6b). However, the simulated increase in F_{N,tot,NH_3} was much smaller than the increase in F_{N,tot,NH_3} after cutting recorded in the micrometeorological measurements (Milford et al., 2001) (Fig. 6b). After the fertilisation in June 1998, a much larger increase in the simulated net canopy NH_3 exchange occurred than after cutting, which is consistent with the measured values (Fig. 6b). By contrast, the peak NH_3 emissions were larger in the measurements than in the simulations. During the first two days after fertilisation, this increase was mainly caused by an increase in simulated soil NH_3 emission, but after the third day the stomata flux was the only component contributing to the simulated canopy NH_3 emission (Fig. 6a). During this period, only a small part of the simulated NH_3 emission from stomata was deposited on the leaf cuticle and the soil surface, while the main part was emitted to the air above the canopy (Fig. 6a). The same qualitative simulation results were found for the second cutting and fertilisation events in 1998 (data not shown).

3.1.3. Seasonal net NH_3 exchange above canopy in 1998

The daily averaged values of the simulated and measured net canopy NH_3 exchange are shown for the vegetation period 1998 in Fig. 7. Although only a restricted amount of measured data is available for the period after the second cut/fertilisation event in 1998, the measured emissions nevertheless seem to be much smaller than after the June cutting/fertilisation. In contrast, a smaller difference between the first and second period was obtained in the simulations. The cumulative simulated NH_3 emission related to fertilisation was 0.97 kg N ha^{-1} in June, and 0.74 kg N ha^{-1} in August 1998. From the simulated seasonal dynamics of Γ_s (Fig. 4b), and the larger N fertilisation amount in

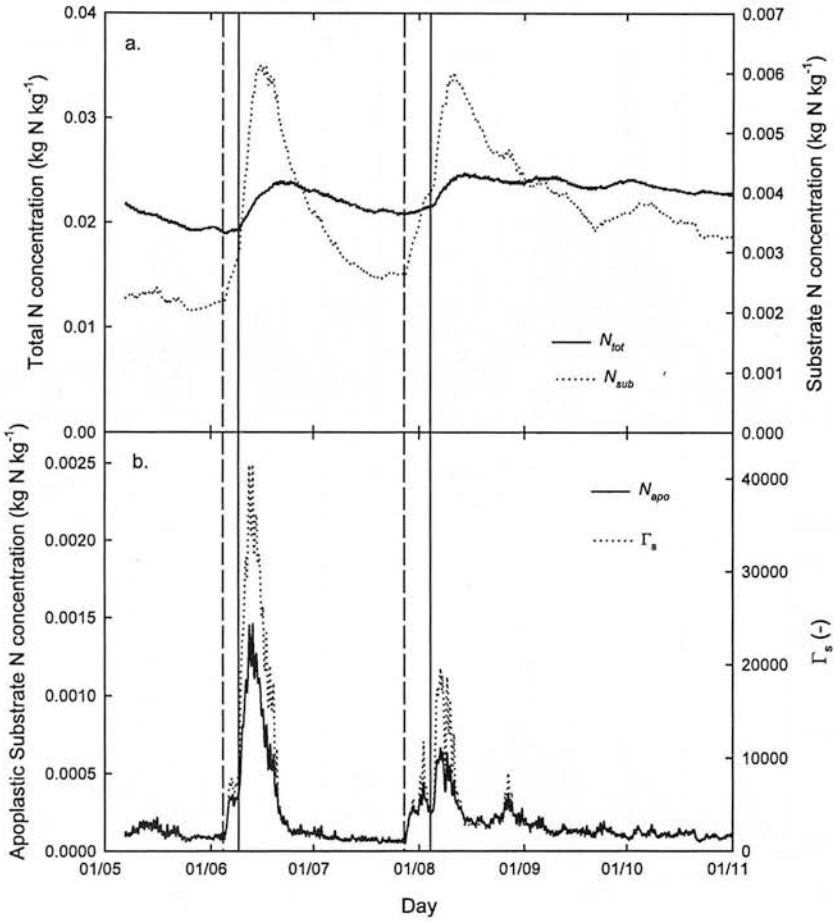

Fig. 4. Simulated seasonal dynamics of plant N variables and Γ_s for the growing season of 1998 at the Southern Scotland field site. (a) Plant total N concentration N_{tot}, plant substrate N concentration N_{sub}. (b) Apoplastic substrate N concentration N_{apo}, apoplastic NH_4^+ to H^+ concentration ratio Γ_s. The N concentrations are given as dry weight. Vertical lines indicate cutting (dashed lines) and $NH_4^+NO_3^-$ fertilisation (solid lines). For fertiliser amounts see Fig. 7.

June than in August, it would have been expected that the difference in the simulated net canopy NH_3 exchange between June and August would have been in better agreement with the measurements. However, the reason why this is not the case is that the leaf temperature was significantly lower during the days after the June fertilisation than after the August fertilisation (Fig. 8). As the stomatal compensation point χ_s depends on both Γ_s and leaf temperature (Eq. (2)), the difference between June and August was smaller for χ_s than for Γ_s (Fig. 8). Although grazing started in August 1998, only small NH_3 emissions were visible in the simulations (Fig. 7). In contrast, the measurements showed some emission peaks, which could be related to grazing.

3.1.4. Seasonal net NH_3 exchange above canopy in 1999

As an independent test, the model was compared with fluxes measured during 1999 (Fig. 9). For the first cut/fertilisation event, the simulations show a close agreement with the measurements concerning the temporal variability (the measured and modelled peak NH_3 emissions last until the 18–19 June), but as in 1998 not concerning the magnitude of the emission peaks. The simulated cumulative net canopy NH_3 emission was much

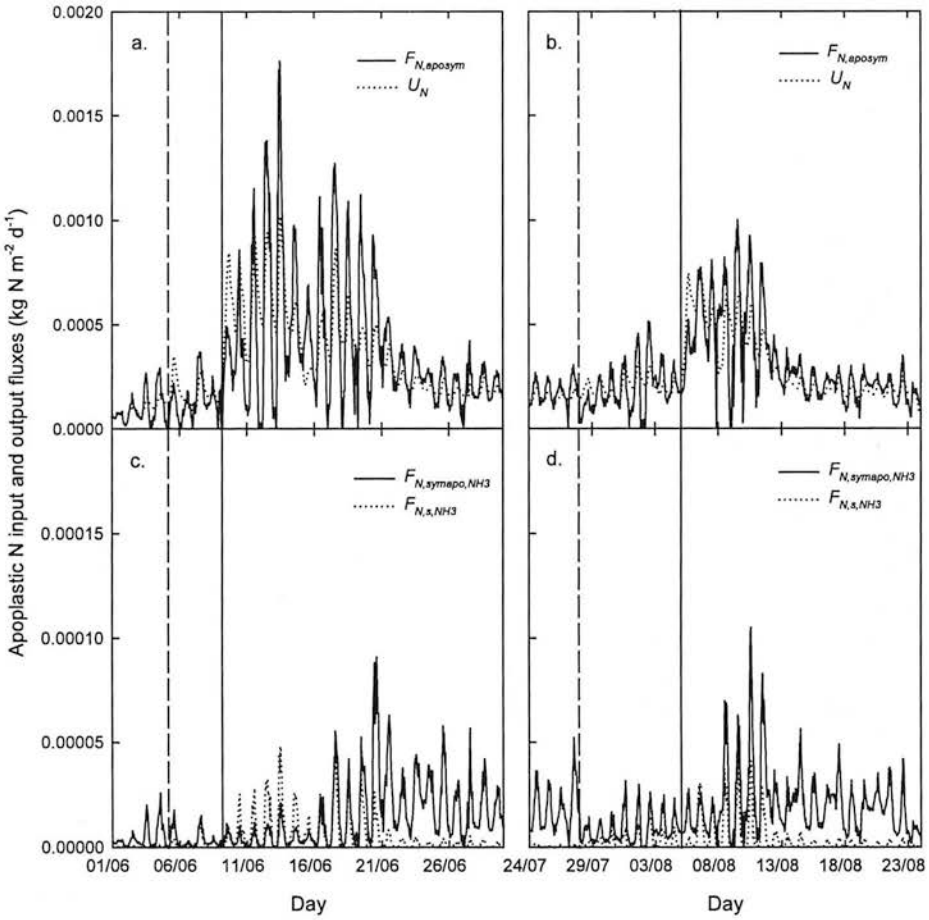

Fig. 5. N fluxes influencing apoplastic substrate N (see Eq. (3)) as simulated for the first (a and c) and second (b and d) cutting/fertilisation events in 1998 at the Southern Scotland field site. (a and b) Active substrate N flux from apoplast to symplast $F_{N,aposym}$, total root NH_4^+ uptake $U_{N,amm}$. (c and d) NH_3 diffusion between apoplast and symplast $F_{N,symapo,NH_3}$, NH_3 flux through stomata F_{N,s,NH_3}. Vertical lines indicate cutting (dashed lines) and $NH_4^+NO_3^-$ fertilisation (solid lines). For fertiliser amounts see Fig. 7.

higher in June (0.89 kg N ha^{-1}) than in August (0.24 kg N ha^{-1}). For the second cutting/fertilisation event, no comparison between simulations and measurements is possible for the August period due to lack of measurements. As in 1998, grazing took place after the second cut in 1999. While again only a small effect on NH_3 exchange was visible in the simulations, much larger emissions were measured in 1999 than in 1998.

3.1.5. Soil NH_x and NO_3^- concentrations

Several discrepancies occurred between simulated and measured values of soil NH_x and NO_3^- (data not shown). The measured soil NH_x concentrations showed large increases immediately after both cutting events of 1998 (Milford et al., 2001), but the simulated concentrations increased only after fertilisation (data not shown). Later on, the high levels of soil NH_x after fertilisation decreased much slower in the measurements than in the simulations after the June fertilisation, but at a comparable rate after the August fertilisation. Concerning NO_3^-, significant increases in concentrations after the $NH_4^+NO_3^-$ fertilisation events in 1998 only occurred in the simulations, but not in the measurements.

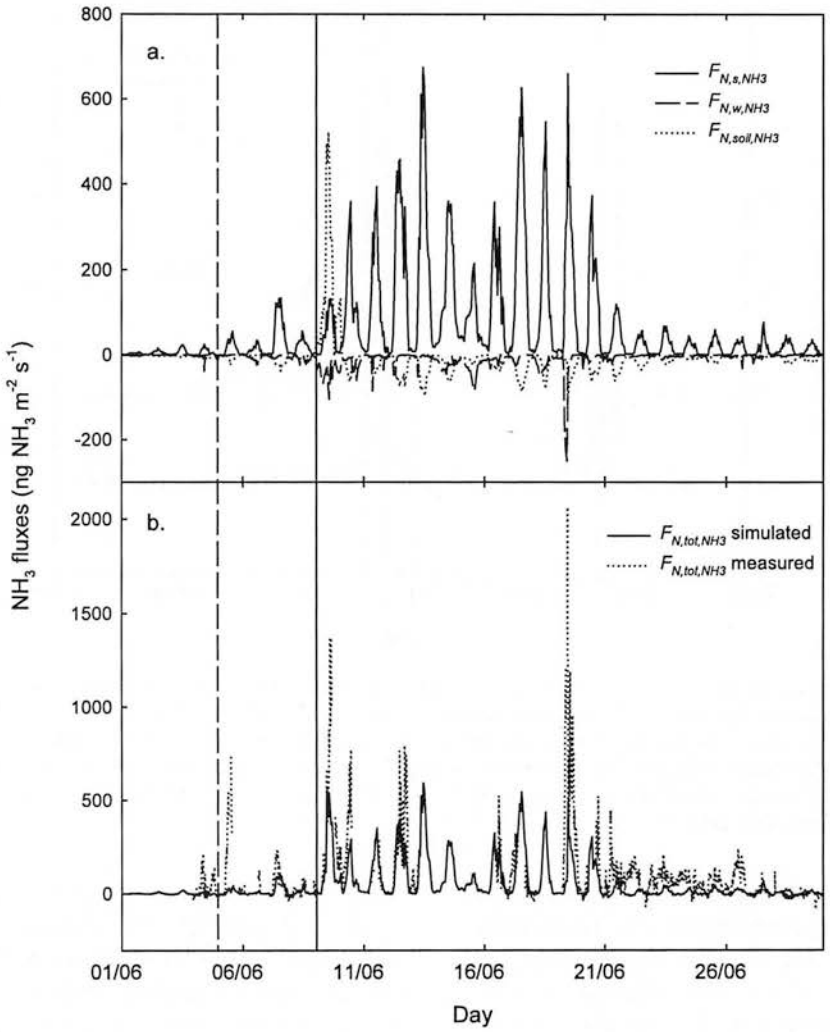

Fig. 6. Simulated and measured NH_3 fluxes in June 1998 at the Southern Scotland field site. (a) Simulated NH_3 component fluxes: NH_3 flux through stomata F_{N,s,NH_3}, cuticular NH_3 uptake F_{N,w,NH_3}, and soil surface NH_3 exchange $F_{N,soil,NH_3}$. (b) Comparison of simulated and measured (Milford et al., 2001) net canopy NH_3 exchange F_{N,tot,NH_3}. The measurements shown are averages over 15 min periods. Vertical lines indicate cutting (dashed lines) and $NH_4^+NO_3^-$ fertilisation (solid lines). For fertiliser amount see Fig. 7.

3.2. Sensitivity analysis

The results of the sensitivity analysis are shown in Table 2. The parameters are listed according to the sensitivity of the simulated net canopy NH_3 exchange cumulated over the vegetation period of 1998 to parameter changes of $\pm 25\%$. In general, the net canopy NH_3 exchange is more sensitive to the parameters that have an important direct influence on N_{apo}, than on parameters that influence the soil surface NH_3 exchange or the cuticular NH_3 uptake.

4. Discussion

In current resistance models (Sutton et al., 1995b; Nemitz et al., 2001) the influence of factors such as management, supply of N to the roots and plant N level on NH_3 exchange is not represented,

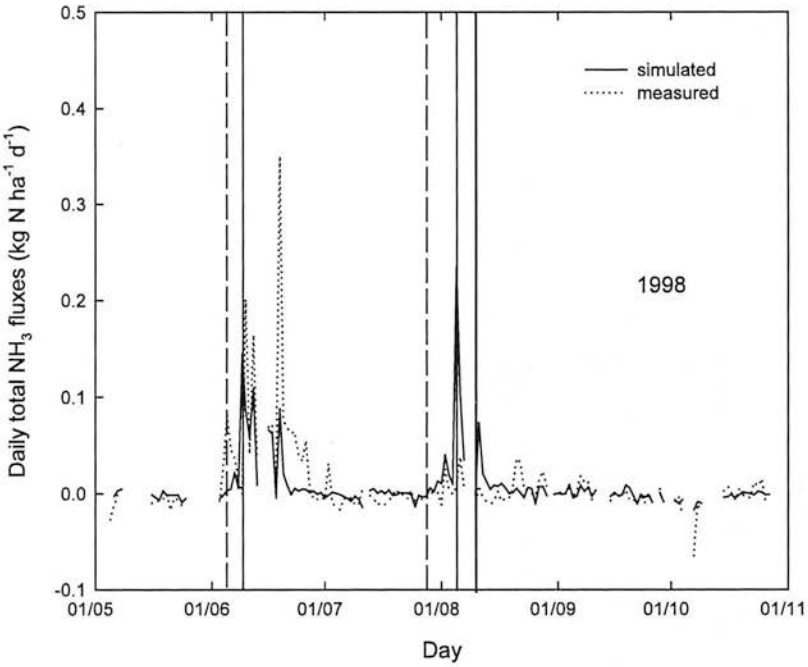

Fig. 7. Simulated and measured (Milford et al., 2001) seasonal dynamics of net canopy NH_3 exchange F_{N,tot,NH_3} for the growing season of 1998 at the Southern Scotland field site. The measured values shown are daily averages of the available 15-min average values. The simulated values shown are the daily averages for the same 15-min periods for which measurements were available. Vertical lines indicate cutting (dashed lines), $NH_4^+NO_3^-$ fertilisation (solid lines), and start of grazing (bold solid lines). Amounts and dates of fertilisation: 104 kg N ha^{-1} on the 28th of March, 104 kg N ha^{-1} on the 9th of June, and 65 kg N ha^{-1} on the 5th of August. Grazing continued until after 1 November 1998.

instead apoplastic and soil surface NH_4^+ concentrations have to be chosen empirically. In contrast, PaSim delivers a frame in which these factors can be modelled, and allows investigation of their influence on NH_3 exchange through the coupling of apoplastic and soil surface NH_4^+ with the plant and soil N dynamics.

4.1. Influence of cut on NH_3 exchange

Where measurements were available for the periods between cutting and fertilisation, these showed for both 1998 and 1999 significant NH_3 emissions (Figs. 7 and 9). The model can reproduce these NH_3 emissions after cutting, although they were generally lower than in the measurements (Figs. 7 and 9). In the simulations, these increases were caused by an increase in the stomata emissions (Fig. 6a), due to increased values of N_{apo} and thus $[NH_4^+]_{apo}$. This simulated contribution of increases in stomatal NH_3 emissions to net canopy NH_3 emissions after cutting is confirmed by measurements of $[NH_4^+]_{apo}$ after cutting under controlled conditions for *L. perenne* and *B. erectus* (Mattsson and Schjoerring, 1999; Sutton et al., 2001). These show an increase in apoplastic NH_4^+ concentrations after cutting. However, this increase did not occur until 5 days after cutting, while the measurements for the Southern Scotland site showed an immediate increase of net canopy NH_3 exchange on the day of cutting for June 1998 (Fig. 6b). It could thus be that the underestimation of the emission peaks after cutting in the simulations is not caused by an underestimation of stomata NH_3 emission, but because other significant sources of NH_3 emission after cutting are underestimated or not represented at all in the model, including (i) NH_3 leaking from remaining shoot material damaged through cutting; (ii) direct emission from leaf litter on the soil

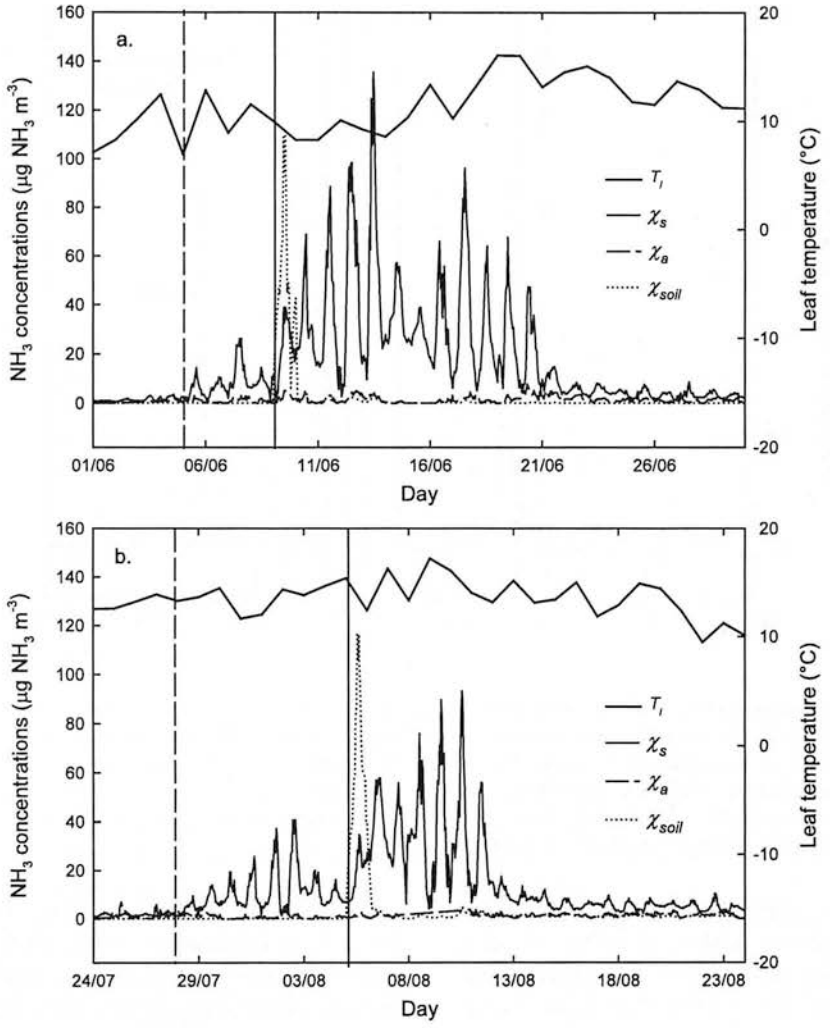

Fig. 8. NH_3 concentrations and leaf temperature for the first (a) and second (b) cutting/fertilisation events in 1998 at the Southern Scotland field site. Shown are the simulated stomatal NH_3 compensation point χ_s, the measured NH_3 concentration at 2 m above the soil surface χ_a (a model input parameter used for the simulations), the simulated soil surface NH_3 concentration χ_{soil}, and the simulated leaf temperature T_l. The temperature values shown are daily values. Vertical lines indicate cutting (dashed lines) and $NH_4^+NO_3^-$ fertilisation (solid lines). For fertiliser amounts see Fig. 7.

surface (Whitehead and Lockyer, 1989); (iii) NH_3 emission from yellow leaves at the bottom of the canopy still attached to the stem (Loubet et al., 2002); (iv) increased soil NH_4^+ concentrations after cutting. The sources (ii) and (iii) seem not to be related to cutting, but it could be that during periods of high plant shoot matter, the emissions from soil surface leaf litter or yellow leaves at the bottom of the canopy are reabsorbed through the stomata and cuticles, and only after a cut could NH_3 from these sources escape to the atmosphere. Although plant decomposition (including leaf litter) is modelled in PaSim, this is done as part of the soil biology submodel, and NH_4^+ released through decomposition is a substrate for several competing processes (e.g. nitrification, immobilisation, adsorption). In contrast, NH_x released from leaf litter decomposition on the soil surface could more easily be emitted as NH_3. Evidence for NH_3 emission from yellow leaves comes from

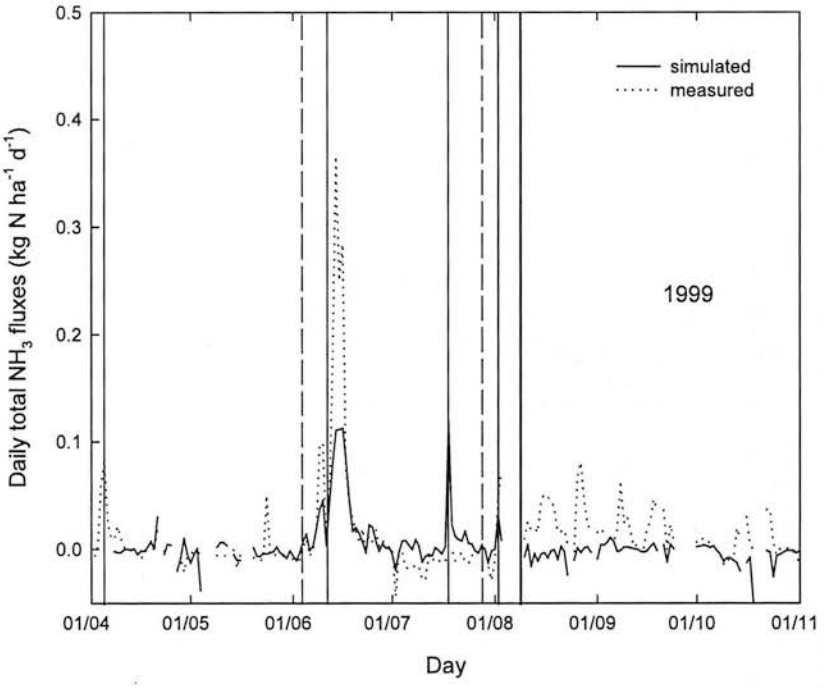

Fig. 9. Simulated and measured (Milford et al., 2001) seasonal dynamics of net canopy NH_3 exchange F_{N,tot,NH_3} for the growing season of 1999 at the Southern Scotland field site. The measured values shown are daily averages of the available 15-min average values. The simulated values shown are the daily averages for the same 15-min periods for which measurements were available. Vertical lines indicate cutting (dashed lines), $NH_4^+NO_3^-$ fertilisation (solid lines), and start of grazing (bold solid lines). Amounts and dates of fertilisation: 117 kg N ha^{-1} on the 4th of April, 91 kg N ha^{-1} on the 11th of June, 39 kg N ha^{-1} on the 18th of July, and 39 kg N ha^{-1} on the 2nd of August. Grazing continued until after 1 November 1998.

measurements that show higher $[NH_4^+]_{apo}$ for yellow than for green leaves (Loubet et al., 2002). Several studies have shown a large decrease of root NH_4^+ uptake after cutting (e.g. Louahlia et al., 2000), and this could lead to a significant increase in soil NH_4^+ concentrations after cutting. While PaSim does reproduce this root behaviour, it probably underestimates it significantly. A strong hint for this is that for the Southern Scotland site only the measurements showed a significant increase in soil NH_x after cutting (Milford et al., 2001), but not the simulations (data not shown).

4.1.1. Influence of fertilisation on NH_3 exchange

Fertilization led instantly to large simulated canopy NH_3 emissions within the same day for all fertilisation events in both 1998 and 1999 (Figs. 7 and 9). These emission periods lasted for between 3 and 12 day after cut/fertilisation events, and for both years they were shorter after the second cut/fertilisation event than after the first. For 1998, this period of increased emission was longer in the measurements than in the simulations in June, but shorter in August. A good agreement was visible for June 1999, while for August 1999, it is not clear how long the influence of fertilisation on the emissions lasted, because this effect was overlapped by emissions from another source, probably grazing. Although some discrepancies occurred between simulations and measurements concerning the length of the period after fertilisation with increased NH_3 emission, this comparison nevertheless indicates that N_{apo} is an appropriate plant N compartment to be linked to χ_s, in contrast to N_{sub} or N_{tot}. This is further confirmed by the fact that the model parameter by which the length of the simulated NH_3 emission period after fertilisation is mainly determined, $k_{aposym,20}$ (Eq. (5)), has been derived from literature data and not

Table 2
Sensitivity analysis for new parameters in PaSim

	F_{N,tot,NH_3}		F_{N,s,NH_3}		F_{N,w,NH_3}		$F_{N,soil,NH_3}$	
	−25%	+25%	−25%	+25%	−25%	+25%	−25%	+25%
$W_{plantfresh2dry}$	−50.7	65.1	−39.0	50.0	−15.9	20.4	−31.8	40.6
$k_{aposym,20}$	63.9	−36.4	48.6	−27.8	18.2	−10.7	40.0	−22.9
$[H^+]_{apo}$	51.8	−30.8	39.8	−23.7	16.4	−9.8	32.5	−19.3
F_{H_2Oapo}	48.9	−29.6	37.6	−22.8	15.6	−9.4	30.7	−18.6
$F_{NH_4^+,N_{apo,max}}$	−19.7	19.4	−15.3	15.0	−6.2	6.2	−13.0	12.8
$F_{NH_4^+,N_{apo},min}$	−17.8	17.8	−13.6	13.5	−5.6	5.6	−10.5	10.4
$B_{cuticles}$	9.1	−9.4	−1.3	1.3	−30.8	31.6	5.9	−6.0
N_{apo2}	6.5	−5.1	4.9	−3.9	1.5	−1.5	4.3	−3.4
$b_{NH_4^+ads}(h)$	7.7	−3.4	−2.3	−1.1	1.9	−1.2	−43.7	6.7
$R_{w,min}$	−6.6	4.4	0.9	−0.7	22.2	−14.9	−4.2	2.8
$[H^+]_{soil}$	4.3	−6.4	−1.9	−0.9	0.7	−1.8	−27.4	20.1
N_{apo1}	3.7	−2.9	2.8	−2.2	1.1	−0.8	2.4	−1.9
$[H^+]_{sym}$	3.5	−2.1	2.7	−1.6	1.0	−0.6	2.2	−1.3
$F_{NH_4^+,Nsym}$	−2.6	2.5	−1.9	1.9	−0.7	0.7	−1.6	1.6
$P_{NH_3,20}$	−2.4	2.4	−1.8	1.8	−0.7	0.6	−1.5	1.5
CAI	−2.4	2.4	−1.8	1.8	−0.7	0.6	−1.5	1.5
$a_{NH_4^+ads}(h)$	−1.1	−2.1	−1.4	−1.3	−0.5	−0.8	−3.9	0.9
$D_{surface}$	0.4	−0.3	0.0	0.0	0.1	−0.1	−1.4	1.3

The model sensitivity to parameter changes of ±25% was determined for simulated NH_3 fluxes (see Fig. 1) integrated over the growing season of 1998 at the Southern Scotland field site. The parameters are listed in decreasing order of the average of the modulus values of the relative changes in F_{N,tot,NH_3}.

from a fit to the measurements (see Section 2.2). However, the above mentioned postulated connection between the time scales of the measured net canopy NH_3 emission and of N_{apo} is based on the assumption that except for the two first days after fertilisation, the stomata are the main source of the net canopy NH_3 emission, as has been simulated (Fig. 6a; data only shown for June 1998). The importance of the stomata as a source for NH_3 emission after fertilisation has indeed been reported for intensively managed fertilised grassland (Harper et al., 1996; Sutton et al., 1998b).

In contrast to the satisfactory qualitative agreement between simulations and measurements concerning the length of the periods with increased NH_3 emission after fertilisation, the large measured peak emissions in June of 1998 and 1999 could not be quantitatively reproduced with the model (Figs. 7 and 9) (while some parameter values were chosen in order to fit model simulations to measurements in 1998, this fit did not include the peak NH_3 emissions). Similarly, the simulated proportions of the amount of fertilised $NH_4^+NO_3^-$–N lost through canopy NH_3 emission were at the lower end of the values reported elsewhere. While the simulated proportions were in the range of 0.5–1.1%, van der Weerden and Jarvis (1997) estimated a value of 1.6% for grassland in the UK, and according to Whitehead (1995), they are typically between 1 and 3% for temperate grassland areas. The reason for this underestimation of the net canopy NH_3 emission peaks after fertilisation in the simulations is probably not caused by an underestimation in the stomatal NH_3 emission, because the simulated values for the stomatal compensation point (Fig. 8a) are above the range of values obtained in measurements (Schjoerring et al., 1998). For the same reason, too small a value for apoplastic pH, a highly uncertain parameter, is probably also not the reason why the simulated NH_3 emissions are too small. But it could be that PaSim still underestimates the soil NH_3 emissions after fertilisation, although the incorporation of a soil surface NH_x layer and the layering of soil NH_x brought a

significant improvement over previous PaSim versions with only a single soil NH_x layer (data not shown). Reasons could be that the immediate incorporation of fertilised N into the soil surface solution in PaSim is not an adequate description of the processes influencing the fertiliser granules, or that the used value for soil pH is too small. For the same reason as mentioned above for NH_3 emission from leaf litter, the model could underestimate the NH_3 emission from granules because it exposes the fertilised NH_4^+ to different processes competing for this substrate. Due to the uncertainty in the measurement of soil pH, and the large model sensitivity to this parameter (Table 2), it is easily possible that it is the cause for an underestimation of soil NH_3 emission in the simulations. The fraction of NH_3 emission loss from fertilisers containing NH_4^+ does indeed show a large dependency on the soil pH (Whitehead, 1995).

4.1.2. Influence of grazing on NH_3 exchange

Only very small effects of grazing on NH_3 exchange were visible in the simulations for both 1998 and 1999. However, as the cumulative simulated amount of animal excreta N was 41 kg N ha^{-1} in 1998, and 46 kg N ha^{-1} in 1999, and with the assumption that about 5% is emitted as NH_3 (Menzi et al., 1997), a NH_3 emission from grazing of about 2 kg N ha^{-1} would have been expected. In addition, significant NH_3 emissions during grazing were visible in the measurements for 1999. The reasons responsible for the underestimation of soil surface NH_3 emissions after fertilisation are probably also partly responsible for the underestimation of NH_3 emissions related to grazing. It has been postulated that urine is partially retained by leaves and dead leaf litter of grasslands, and that there is thus an increase in the amount of NH_3 emission, because the litter on the soil surface provides a surface for urease activity, reduces contact between the urine and the soil, and has little cation exchange capacity (Whitehead, 1995).

4.1.3. Influence of plant development stage on NH_3 exchange

For cereals, bimodal patterns of NH_3 emissions related to development stage have been observed, and may be related to the gradual appearance of senescing leaves and anthesis-induced depression in N uptake capacity and transport (Schjoerring et al., 1998; Mattsson et al., 1993). However, it could be that these factors are less important for intensively managed grasslands, because, due to cutting, these are mainly in the vegetative development stage during the growing season, and because in contrast to cereals, the dominating grassland species undergo a constant turnover of leaves, with new leaves constantly growing and senescing during the whole season. Consequently, these factors were not represented in PaSim.

4.1.4. Uncertainties in the modelling of net canopy NH_3 exchange with PaSim

Uncertainties in the modelling of net canopy NH_3 exchange are related to the way the relevant processes are represented in PaSim, to model parameters, and to the input parameters. Several uncertainties concerning the representation of processes in PaSim have been mentioned above. A further uncertainty arises because PaSim does not consider the form of N taken up by the roots. However, it has been shown that plants absorbing NH_4^+ have higher NH_3 emissions compared with plants absorbing NO_3^- (Mattsson and Schjoerring, 1996; Schjoerring et al., 1998). This could explain the lack of late summer emissions, and indicates the importance of further work to quantify the controls on apoplastic NH_4^+.

Concerning the model parameters and the input parameters, the largest uncertainty is associated to the parameters that directly influence apoplastic NH_x, because small changes in these parameters lead to large changes in the NH_3 exchange (Table 2). Significant improvements in the modelling of NH_3 exchange could thus be achieved by considering factors that can influence these parameters. Concerning the parameter $W_{\text{plantfresh2dry}}$, the shoot dry to fresh weight ratio (see Table 1 and Eq. (A1)), this could only be achieved by introducing a new plant water content pool into the PaSim model. However, this is beyond the scope of the current PaSim version. It would probably be more promising to incorporate further experimental evidence about the factors controlling the active NH_4^+ transport system across the plasmalemma,

and about apoplastic pH. For example, it has been shown that apoplastic pH is higher for NO_3^- than for NH_4^+ nutrition, and that it seems to increase with increasing soil NO_3^- concentrations in the root medium (Schjoerring et al., 1998). The value of NH_3 permeability of the plasmalemma, $P_{NH_3,T}$, is also uncertain and was fitted here with the arbitrary assumption that the passive NH_3 diffusion through the plasmalemma, which is determined by $P_{NH_3,T}$, is an order of magnitude smaller than the active N transport through the plasmalemma (see Section 2.2). Subsequent literature search revealed some data on NH_3 plasmalemma permeability for various organisms, with values being in the range of 5.7×10^{-6}–7.8×10^{-4} m s^{-1} (Kleiner, 1985; Ritchie, 1987; Raven et al., 1992; Priver et al., 1993; Lande et al., 1995). Incorporation of a value in this range in the model led to a poorer agreement with measurements, and N_{apo} tracking N_{sym} directly. The original, much lower value in the model of $P_{NH_3,20}$ (Table 1) has therefore been retained. It is possible that there is an additional resistance in the cell between the plasmalemma and the substomatal cavities, and thus could account for the need to apply a lower effective value of $P_{NH_3,20}$.

5. Conclusions

A two-layer resistance model for soil–plant–atmosphere exchange of gaseous NH_3 has been coupled with the grassland ecosystem model PaSim, in order to link NH_3 exchange with the plant and soil N status. This is a significant improvement over the empirical treatment in a 2LRM of the stomatal compensation point χ_s and the soil surface NH_3 concentration, and over the empirical calculation of NH_3 emissions in previous grassland models. It has been shown that through the introduction of an apoplastic substrate N pool in PaSim it is now possible to relate χ_s in a satisfactory way to the plant internal N dynamics. Similarly, the introduction of a NH_x pool of the soil surface and the partitioning of soil NH_x among different soil layers is an improvement over previous PaSim versions in relation to biosphere–atmosphere gas exchange (see also Schmid, 2001 for gaseous emissions related to denitrification).

However, it has to be mentioned that concerning NH_3 exchange there are still some uncertainties remaining. It is not clear at the moment whether the underestimation of NH_3 emission peaks after cutting and fertilisation in the simulations is related to the way the NH_3 sources that are considered in this version of PaSim are represented and parameterised, or whether this discrepancy occurs because other important NH_3 sources are not yet incorporated in PaSim. The work reported here represents the first time that the ecosystem dynamics of the NH_3 compensation point have been modelled, and it is hoped that this will stimulate further experimental research allowing improved parameterisation to be developed.

Although improvements are still necessary in PaSim concerning the simulation of NH_3 exchange, a very useful tool is now available that can be used to investigate short and long term interactions between NH_3 exchange and the ecosystem N status under various scenarios of different management scenarios or climate change.

6. Nomenclature (see also Table 1 for PaSim parameters)

$D_{aqueous}(h)$	aqueous diffusion coefficient of soil layer h (m^2 s^{-1})
$D_{gaseous}(h)$	gaseous diffusion coefficient of soil layer h (m^2 s^{-1})
$F_{H_2O,CapRise}(h)$	capillary rise from soil layer $h+1$ to h (m per day)
$F_{H_2O,Drainage}(h)$	drainage from soil layer h to $h+1$ (m per day)
$F_{H_2O,Infiltration}(h)$	soil water infiltration (m per day)
$f_{immprevamm}$	parameter for immobilisation partitioning
$F_{N,aposym}$	active substrate N flux from apoplast to symplast (kg N m^{-2} per day)
$F_{N,atm,amm}$	atm. NH_x–N deposition other than gaseous NH_3 (kg N m^{-2} per day)

$F_{N,atm,nit}$ atm. NO_3^- deposition (kg N m^{-2} per day)

$F_{N,BNF}$ biological N fixation (kg N m^{-2} per day)

$F_{N,conv,amm}(h)$ convective NHx transport from soil layer h to $h+1$ (kg N m^{-2} per day)

$F_{N,cuticle,soil}$ N flux from cuticle to soil surface (kg N m^{-2} per day)

$F_{N,death}$ N lost through plant death (kg N m^{-2} per day)

$F_{N,diff,aq,NH_3}(h)$ Aqueous NH_3 diffusion from soil layer h to $h+1$ (kg N m^{-2} per day)

$F_{N,diff,aq,NH_4^+}(h)$ aqueous NH_4^+ diffusion from soil layer h to $h+1$ (kg N m^{-2} per day)

$F_{N,diff,g,NH_3}(h)$ gaseous NH_3 diffusion from soil layer h to $h+1$ (kg N m^{-2} per day)

$F_{N,diff,amm}(h)$ NH_x diffusion from soil layer h to $h+1$ (kg N m^{-2} per day)

$F_{N,fert,amm}$ NH_4^+ input from mineral fertilisation (kg N m^{-2} per day)

$F_{N,fert,nit}$ NO_3^- input from mineral fertilisation (kg N m^{-2} per day)

$F_{N,grazing,sub}$ substrate N loss through grazing (kg N m^{-2} per day)

$F_{N,growth}$ N used for growth of structural plant material (kg N m^{-2} per day)

$F_{N,immob}$ total soil N immobilisation (kg N m^{-2} per day)

$F_{N,immob,amm}(h)$ NH_4^+ immobilisation in soil layer h (kg N m^{-2} per day)

$F_{N,immob,nit}(h)$ NO_3^- immobilisation in soil layer h (kg N m^{-2} per day)

$F_{N,leach,nit}(h)$ NO_3^- leaching from soil layer h to $h+1$ (kg N m^{-2} per day)

$F_{N,manure,NH_4^+}$ NH_4^+ input from manure application (kg N m^{-2} per day)

$F_{N,min}(h)$ N mineralization in soil layer h (kg N m^{-2} per day)

$F_{N,nitdenitrif}(h)$ NO_3^- used in denitrification (kg N m^{-2} per day)

$F_{N,nitrif}(h)$ nitrification in soil layer h (kg N m^{-2} per day)

$F_{N,rec}$ N recycling from dead plant material (kg N m^{-2} per day)

$F_{N,s,NH3}$ NH_3 flux through stomata (kg N m^{-2} per day)

$F_{N,soil,NH3}$ soil surface NH_3 exchange (kg N m^{-2} per day)

$F_{N,symapo,NH3}$ NH_3 diffusion between apoplast and symplast (kg N m^{-2} per day)

$F_{N,symapo,cell,NH3}$ passive NH_3 diffusion flux per cell surface area (kg N m^{-2} cell surface per day)

$F_{N,tot,NH3}$ net canopy NH_3 exchange (kg N m^{-2} per day)

$F_{N,urine}$ NH_x–N from urine excreted by grazing animals (kg N m^{-2} per day)

$F_{N,w,NH3}$ cuticular NH_3 uptake (kg N m^{-2} per day)

$f_{NH4+,N_{apo}}$ molar fraction of NH_4^+ in N_{apo} (mol mol^{-1})

$f_{N2Onitrif}(h)$ fraction of nitrified NH_4^+–N converted to N_2O

$f_{root}(h)$ fraction of roots in soil layer h

$k_{aposym,T}$ rate parameter (per day)

$K_{a,NH4+,T}$ dissociation constant of NH_4^+ (M)

$K_{h,NH3,T}$ henry equilibrium constant of NH_3

LAI leaf area index (m^2 leaf surface m^{-2})

N_{apo} apoplastic substrate N concentration (kg N kg^{-1} structural DM)

$[N]_{apo}$ molar apoplastic substrate N concentration (M)

$N_{amm}(h)$ ammoniacal N in soil layer h (kg N m^{-2})

$N_{amm,surface}$ ammoniacal N of soil surface (kg N m^{-2})

$N_{nit}(h)$ NO_3^-–N in soil layer h (kg N m^{-2})

N_{sub} plant substrate N concentration (kg N kg^{-1} structural DM)

N_{sym} symplastic substrate N concentration (kg N kg^{-1} structural DM)

$[N]_{sym}$	molar symplastic substrate N concentration (M)
N_{tot}	plant total N concentration (kg N kg^{-1} DM)
$[NH_3]_{apo}$	molar concentration of apoplastic NH_3 (M)
$[NH_3]_{sym}$	molar concentration of symplastic NH_3 (M)
$[NH_3]_{aq,surface}$	NH_3–N in aqueous phase of soil surface (μg N m^{-3})
$[NH_3]_{aq}(h)$	NH_3–N in soil aqueous phase of soil layer h (μg N m^{-3})
$[NH_3]_{g,surface}$	NH_3–N in gaseous phase of soil surface (μg N m^{-3})
$[NH_3]_g(h)$	NH_3–N in soil gaseous phase of soil layer h (μg N m^{-3})
$[NH_4^+]_{apo}$	molar concentration of apoplastic NH_4^+ (M)
$[NH_4^+]_{sym}$	molar concentration of symplastic NH_4^+ (M)
$[NH_4^+]_{aq,surface}$	NH_4^+–N in aqueous phase of soil surface (μg N m^{-3})
$[NH_4^+]_{aq}(h)$	NH_4^+–N in soil aqueous phase of soil layer h (μg N m^{-3})
$[NH_4^+]_s(h)$	NH_4^+–N in soil solid phase of soil layer h (μg N kg^{-1} dry soil)
$P_{NH_3,T}$	NH_3 permeability of the plasmalemma (m s^{-1})
R_a	aerodynamic resistance (s m^{-1})
R_{ac}	in-canopy aerodynamic resistance (s m^{-1})
R_b	leaf boundary resistance (s m^{-1})
RH	relative humidity (%)
R_s	leaf stomata resistance (s m^{-1})
R_w	cuticular resistance (s m^{-1})
T_l	leaf temperature (K)
T_{ss}	soil surface temperature (K)
$U_{N,amm}$	total root NH_4^+ uptake (kg N m^{-2} per day)
$U_{N,amm}(h)$	root NH_4^+ uptake from soil layer h (kg N m^{-2} per day)
$U_{N,nit}(h)$	root nitrate uptake from soil layer h (kg N m^{-2} per day)
$W_{N,apo}$	Substrate N in apoplast (kg N m^{-2})
$W_{N,struct}$	plant structural N (kg N m^{-2})
$W_{N,sym}$	Substrate N in symplast (kg N m^{-2})
$W_{N,sub}$	total plant substrate N (kg N m^{-2})
W_{sh}	plant structural shoot dry matter (kg structural DM m^{-2})
W_{shtot}	total plant shoot dry matter (kg DM m^{-2})
$z_s(h)$	depth of soil layer h (m)
χ_a	NH_3 concentration at 2m above soil surface (μg NH_3 m^{-3})
χ_c	NH_3 concentration at leaf surface (μg NH_3 m^{-3})
χ_s	stomatal NH_3 compensation point (μg NH_3 m^{-3})
χ_{soil}	soil surface NH_3 concentration (μg NH_3 m^{-3})
$\chi(z_0)$	NH_3 concentration at in-canopy exchange layer (μg NH_3 m^{-3})
Δt	model time step (day)
Γ_s	apoplastic NH_4^+ to H^+ concentration ratio
$\theta_s(h)$	volumetric water content in soil layer h (m^3 m^{-3})
$\theta_{s,sat}(h)$	volumetric water content at saturation in soil layer h (m^3 m^{-3})
$\rho_b(h)$	bulk density in soil layer h (kg dry soil m^{-3})

Acknowledgements

This work was supported by the Swiss National Science Foundation through a TMR fellowship, and it contributed to the EU project 'GRAMINAE' (CT98-0722). MAS is grateful for support from the UK Department for Environment, Food and Rural Affairs (contract EPG 1/3/94).

Appendix A

Molar apoplastic and symplastic substrate N concentrations

The molar symplastic and apoplastic NH_4^+ concentrations used in Eq. (9), $[N]_{sym}$ and $[N]_{apo}$ (M), are calculated from the symplastic and apoplastic substrate N concentrations per struc-

tural dry matter, N_{sym} and N_{apo} (kg N (kg structural DM)$^{-1}$), as:

$$[N]_{sym} = \frac{N_{sym}(W_{sh}/W_{shtot})(W_{plantfresh2dry}/1 - W_{plantfresh2dry})}{(1 - f_{H_2Oapo})/0.014}$$

$$[N]_{apo} = \frac{N_{apo}(W_{sh}/W_{shtot})(W_{plantfresh2dry}/1 - W_{plantfresh2dry})}{f_{H_2Oapo}/0.014} \quad (A1)$$

where W_{sh} is the shoot structural dry matter (kg structural DM m^{-2}), and W_{shtot} is the total shoot dry matter (kg DM m^{-2}). The two new model parameters f_{H_2Oapo} and $W_{plantfresh2dry}$ (kg DM kg^{-1} FM) represent the fraction of leaf water that is in the apoplast, and the shoot dry to fresh weight ratio, respectively. The constant 0.014 is a unit conversion factor.

Soil ammoniacal species

In each soil layer, the soil ammoniacal N is divided among gaseous and aqueous NH_3, and aqueous and exchangeable soil solid NH_4^+. Total ammoniacal N in soil layer h, $N_{amm}(h)$ (kg N m^{-2}), is then given by:

$$\frac{N_{amm}(h)}{(z_s(h) - z_s(h-1))10^{-6}} = (\theta_{s,sat}(h) - \theta_s(h))[NH_3]_g(h) + \theta_s(h)[NH_3]_{aq}(h) + \theta_s(h)[NH_4^+]_{aq}(h) + \rho_b(h)10^3[NH_4^+]_s(h) \quad (A2)$$

where $[NH_3]_g(h)$ (μg N m^{-3}) is NH_3 in the soil gaseous phase of soil layer h, $[NH_3]_{aq}(h)$ (μg N m^{-3}) is NH_3 in the soil aqueous phase of soil layer h, $[NH_4^+]_{aq}(h)$ (μg N m^{-3}) is NH_4^+ in the soil aqueous phase of soil layer h, and $[NH_4^+]_s(h)$ (μg N kg^{-1} dry soil) is NH_4^+ in the exchangeable soil solid phase of soil layer h. Furthermore, for each soil layer h, $z_s(h)$ (m) is the depth of the soil layer, $\theta_s(h)$ and $\theta_{s,sat}(h)$) (m^3 m^{-3}) are the actual and saturated volumetric soil water content, and $\rho_b(h)$ (kg dry soil m^{-3}) is the bulk density. The equilibrium describing the partitioning of NH_4^+ among the aqueous and the exchangeable solid phase is given by a Freundlich equation with the parameters $a_{NH_4^+ ads}(h)$ and $b_{NH_4^+ ads}(h)$ (Singh and Nye, 1984):

$$[NH_4^+]_s(h) = a_{NH_4^+ ads}(h)[NH_4^+]_{aq}(h)^{b_{NH_4^+ ads}(h)} \quad (A3)$$

An implicit assumption behind the partitioning of ammoniacal N for each soil layer is that the equilibrium between the different NH_x species is 'instantaneous' compared with the speed of vertical exchanges. Combining Eq. (A2) with the Henry and dissociation equilibria and Eq. (A3) yields an equation for $[NH_4^+]_{aq}(h)$ for each soil layer h:

$$\frac{N_{amm}(h)}{(z_s(h) - z_s(h-1))10^{-6}} = (\theta_{s,sat}(h) - \theta_s(h))\frac{K_{a,NH_4^+,T}(h)}{K_{h,NH_3,T}(h)10^{-pH_{soil}}}[NH_4^+]_{aq} \times (h) + \theta_s(h)K_{aNH_4^+}(h)10^{pH_{soil}}[NH_4^+]_{aq}(h) + \theta_s(h)[NH_4^+]_{aq}(h) + \rho_b(h)10^3 a_{NH_4^+ ads}(h) \times [NH_4^+]_{aq}(h)^{b_{NH_4^+ ads}(h)} \quad (A4)$$

A root finding method which combines Newton–Raphson and bisection is used to obtain $[NH_4^+]_{aq}(h)$ from Eq. (A4) for each soil layer h.

Vertical soil NH_x fluxes

Vertical NH_x exchange between the soil surface layer and the soil layer 1 (Eq. (12)), and between adjacent soil layers (Eq. (13)) is assumed to occur through convective transport in the aqueous phase, and through diffusion in both the gaseous and aqueous phase (van der Molen et al., 1990). The convective NH_x flux from the soil surface to soil layer 1, $F_{N,conv,amm}(0)$, is given by:

$$F_{N,conv,amm}(0) = ([NH_4^+]_{aq,surface} + [NH_3]_{aq,surface})F_{H_2O,Infiltration}10^{-9} \quad (A5)$$

where $F_{H_2O,Infiltration}$ (m per day) is soil water infiltration (Riedo et al., 2000), and $[NH_3]_{aq,surface}$ (μg N m^{-3}) is the soil surface NH_3 concentration. The convective NH_x flux between soil layers h and

$h+1$ is given by:

$$F_{\mathrm{N,conv,amm}}(h) = ([\mathrm{NH_4^+}]_{\mathrm{aq}}(h) + [\mathrm{NH_3}]_{\mathrm{aq}}(h))F_{\mathrm{H_2O,Drainage}}(h)10^{-9} - ([\mathrm{NH_4^+}]_{\mathrm{aq}}(h+1) + [\mathrm{NH_3}]_{\mathrm{aq}} \times (h+1))F_{\mathrm{H_2O,CapRise}}(h)10^{-9} \quad \text{(A6)}$$

where $F_{\mathrm{H_2O,Drainage}}(h)$ (m per day) is soil water drainage, $F_{\mathrm{H_2O,CapRise}}(h)$ (m per day) is soil water capillary rise (Riedo et al., 2000), and 10^{-9} converts between μg and kg. The diffusive NH_x fluxes $F_{\mathrm{N,diff,amm}}(h)$ in Eqs. (12) and (13) are the sum of gaseous NH_3 diffusion, $F_{\mathrm{N,diff,g,NH_3}}(h)$ (kg N m^{-2} per day), aqueous NH_3 diffusion, $F_{\mathrm{N,diff,g,NH_3}}(h)$ (kg N m^{-2} per day), and aqueous NH_4^+ diffusion, $F_{\mathrm{N,diff,aq,NH_4^+}}(h)$ (kg N m^{-2} per day), which are calculated as:

$$F_{\mathrm{N,diff,g,NH_3}}(h) = D_{\mathrm{gaseous}}(h,\ h+1) \times \frac{([\mathrm{NH_3}]_{\mathrm{g}}(h) - [\mathrm{NH_3}]_{\mathrm{g}}(h+1))}{(z_{\mathrm{s}}(h+1) - z_{\mathrm{s}}(h-1))/2}\ 10^{-9} \times 86400 \quad \text{(A7)}$$

$$F_{\mathrm{N,diff,aq,NH_3}}(h) = D_{\mathrm{aqueous}}(h,\ h+1) \times \frac{([\mathrm{NH_3}]_{\mathrm{aq}}(h) - [\mathrm{NH_3}]_{\mathrm{aq}}(h+1))}{(z_{\mathrm{s}}(h+1) - z_{\mathrm{s}}(h-1))/2}\ 10^{-9} \times 86400 \quad \text{(A8)}$$

$$F_{\mathrm{N,\ diff,\ aq,\ NH_4^+}}(h) = D_{\mathrm{aqueous}}(h,\ h+1) \times \frac{([NH_4^+]_{\mathrm{aq}}(h) - [NH_4^+]_{\mathrm{aq}}(h+1))}{(z_{\mathrm{s}}(h+1) - z_{\mathrm{s}}(h-1))/2}\ 10^{-9} \times 86400 \quad \text{(A9)}$$

where $D_{\mathrm{aqueous}}(h,h+1)$ is the weighted mean for soil layers h and $h+1$ of $D_{\mathrm{aqueous}}(h)$ (m s^{-1}), the aqueous diffusion coefficient, and $D_{\mathrm{gaseous}}(h,h+1)$ is the weighted mean for h and $h+1$ of $D_{\mathrm{gaseous}}(h)$ (m s^{-1}), the gaseous diffusion coefficient. The factors 10^{-9} and 86400 convert units. The aqueous and gaseous diffusion coefficients are calculated according to van der Molen et al. (1990). For the diffusion between the soil surface and soil layer 1, the diffusion coefficients of soil layer 1 are used, $[\mathrm{NH_3}]_{\mathrm{g}}(0)$ is equal to $[\mathrm{NH_3}]_{\mathrm{g,surface}}$, $[\mathrm{NH_3}]_{\mathrm{aq}}(0)$ is equal to $[\mathrm{NH_3}]_{\mathrm{aq,surface}}$, $[\mathrm{NH_4^+}]_{\mathrm{aq}}(0)$ is equal to $[\mathrm{NH_4^+}]_{\mathrm{aq,surface}}$, and $z_{\mathrm{s}}(-1)$ and $z_{\mathrm{s}}(0)$ are zero. $[\mathrm{NH_3}]_{\mathrm{g,surface}}$, $[\mathrm{NH_3}]_{\mathrm{aq,surface}}$, and $[\mathrm{NH_4^+}]_{\mathrm{aq,surface}}$ are given by Eq. (10) and the Henry and dissociation equilibria (Sutton et al., 1994).

Partitioning of NO_3^- among different soil layers

Similar to soil ammoniacal N, NO_3^- has also been divided among the different soil layers. For soil layer 1, the NO_3^- dynamics is given by:

$$\frac{\mathrm{d}N_{\mathrm{nit}}(1)}{\mathrm{d}t} = F_{\mathrm{N,atm,nit}} + F_{\mathrm{N,fert,nit}} + (1 - f_{\mathrm{N_2Onitrif}}(1))F_{\mathrm{N,\ nitrif}}(1) + F_{\mathrm{N,nitdenitrif}}(1) - U_{\mathrm{N,nit}}(1) - F_{\mathrm{N,immob,nit}}(1) - F_{\mathrm{N,leach,nit}}(1) \quad \text{(A10)}$$

and for the remaining layers by:

$$\frac{\mathrm{d}N_{\mathrm{nit}}(h)}{\mathrm{d}t} = (1 - f_{\mathrm{N_2Onitrif}}(h))F_{\mathrm{N,nitrif}}(h) + F_{\mathrm{N,nitdenitrif}}(h) + F_{\mathrm{N,leach,nit}}(h-1) - U_{\mathrm{N,nit}}(h) - F_{\mathrm{N,immob,nit}}(h) - F_{\mathrm{N,leach,nit}}(h) \quad \text{(A11)}$$

where $F_{\mathrm{N,atm,nit}}$ is atm. NO_3^- deposition, $F_{\mathrm{N,fert,nit}}$ NO_3^- is input from mineral fertilisation, $F_{\mathrm{N,nitrif}}(h)$ is nitrification, $F_{\mathrm{N,nitdenitrif}}(h)$ is NO_3^- used in denitrification, $U_{\mathrm{N,nit}}(h)$ is root nitrate uptake, $F_{\mathrm{N,immob,nit}}(h)$ is NO_3^- immobilisation, and $F_{\mathrm{N,leach,nit}}(h)$ is NO_3^- leaching. In contrast to NH_x, vertical transport of NO_3^- in PaSim occurs only through leaching, which is calculated as:

$$F_{\mathrm{N,leach,nit}}(h) = \frac{N_{\mathrm{nit}}(h)}{(z_{\mathrm{s}}(h) - z_{\mathrm{s}}(h-1))\theta_{\mathrm{s}}(h)}F_{\mathrm{H_2O,Drainage}}(h) - \frac{N_{\mathrm{nit}}(h+1)}{(z_{\mathrm{s}}(h+1) - z_{\mathrm{s}}(h))\theta_{\mathrm{s}}(h+1)}F_{\mathrm{H_2O,CapRise}}(h) \quad \text{(A12)}$$

Partitioning of soil N fluxes among different soil layers

Because soil NH_4^+ and NO_3^- have been divided among the different soil layers in this new version of PaSim, the associated N fluxes (Eqs. (13) and (A11)) were also partitioned among the different layers. For N mineralization, $F_{N_{min}}(h)$, a vertical distribution according to the root dry matter profile $f_{root}(h)$ was assumed, and for root NH_4^+ and NO_3^- uptake, $U_{N,amm}(h)$, and $U_{N,nit}(h)$, distributions according to the product of the root dry matter profile and the profile of soil ammoniacal N and soil NO_3^-, respectively. Nitrification, $F_{N,nitrif}(h)$, and NO_3^- used in denitrification, $F_{N,nitdenitrif}(h)$, are calculated separately for each soil layer (Schmid, 2001). NH_4^+ and NO_3^- immobilisation for each layer h, $F_{N,immob,amm}$ (kg N m^{-2} per day) and $F_{N,immob,nit}$ (kg N m^{-2} per day) are given by:

$$F_{N,immob,nit}(h) = \frac{(N_{amm}(h) + N_{nit}(h)) \times f_{root}(h)}{\sum_h (N_{amm}(h) + N_{nit}(h)) \times f_{root}(h)} \times \frac{f_{immprefamm} \times N_{amm}(h)}{(f_{immprefamm} \times N_{amm}(h) + N_{nit}(h))} F_{N,immob} \quad \text{(A13)}$$

$$F_{N,immob,nit}(h) = \frac{(N_{amm}(h) + N_{nit}(h)) \times f_{root}(h)}{\sum_h (N_{amm}(h) + N_{nit}(h)) \times f_{root}(h)} \times \frac{N_{nit}(h)}{(f_{immprefamm} \times N_{amm}(h) + N_{nit}(h))} F_{N,immob} \quad \text{(A14)}$$

where the parameter $f_{immprefamm}$ accounts for the observation that the associated micro-organisms favour NH_4^+ over NO_3^- for soil N immobilisation, $F_{N,immob}$ (kg N m^{-2} per day) (Recous and Mary, 1990).

References

Aneja, V.P., Roelle, P.A., Murray, G.C., Southerland, J., Erisman, J.W., Fowler, D., Asman, W.A.H., Patni, N., 2001. Atmospheric nitrogen compounds II: emissions, transport, transformation, deposition and assessment. Atmos. Environ. 35, 1903–1911.

Bull, K.R., Sutton, M.A., 1998. Critical loads and the relevance of ammonia to an effects based Nitrogen Protocol. Atmos. Environ. 32, 565–573.

Chen, D.-X., Hunt, H.W., Morgan, J.A., 1996. Responses of a C_3 and C_4 perennial grass to CO_2 enrichment and climate change: comparison between model predictions and experimental data. Ecol. Model. 87, 11–27.

Duyzer, J.H., 1994. Dry deposition of ammonia and ammonium aerosols over heathland. J. Geophys. Res. 99, 18757–18763.

Erisman, J.W., 2001. De Vliegende Geest. Ammoniak uit de landbouw en de gevolgen voor de natuur. BetaText, Bergen, p. 271.

Fangmeier, A., Hadwiger-Fangmeier, A., van der Eerden, L., Jaeger, H.J., 1994. Effects of atmopheric ammonia on vegetation—a review. Environ. Pollut. 86, 43–82.

Finnemann, J., Schjoerring, J.K., 1998. Ammonium and soluble amide-bound nitrogen in leaves of *Brassica napus* as related to glutamine synthetase activity and external N supply. Plant Physiol. Biochem. 36, 339–346.

Finnemann, J., Schjoerring, J.K., 1999. Translocation of NH_4^+ in oilseed rape plants in relation to glutamine synthetase isogene expression and activity. Physiologia Plantarum 105, 469–477.

Flechard, C.R., Fowler, D., Sutton, M.A., Cape, J.N., 1999. A dynamic chemical model of bi-directional ammonia exchange between semi-natural vegetation and the atmosphere. Q. J. R. Meteorol. Soc. 125, 2611–2641.

Foy, J.K., Teague, W.R., Hanson, J.D., 1999. Evaluation of the upgraded SPUR model (SPUR2.4). Ecol. Model. 118, 149–165.

Frolking, S.E., Mosier, A.R., Ojima, D.S., Li, C., Parton, W.J., Potter, C.S., Priesack, E., Stenger, R., Haberbosch, C., Dorsch, P., Flessa, H., Smith, K.A., 1998. Comparison of N_2O emissions from soils at three temperate agricultural sites: simulations of year-round measurements by four models. Nutr. Cycl. Agroecosyst. 52, 77–105.

Genermont, S., Cellier, P., Flura, D., Morvan, T., Laville, P., 1998. Measuring ammonia fluxes after slurry spreading under actual field conditions. Atmos. Environ. 32, 279–284.

Harper, L.A., Bussink, D.W., van der Meer, H.G., Corre, W., 1996. Ammonia transport in a temperate grass system: I. Seasonal transport in relation to soil fertility and crop management. Agron. J. 88, 614–621.

Husted, S., Schjoerring, J.K., 1995. Apoplastic pH and ammonium concentration in leaves of *Brassica napus* L. Plant Physiol. 109, 1453–1460.

Husted, S., 1997, Physiological mechanisms controlling the exchange of ammonia between plants and the atmosphere.

Ph.D. Thesis, The Royal Veterinary and Agricultural University Copenhagen.

Kleiner, D., 1985. Bacterial ammonium transport. FEMS Microbiol. Rev. 32, 87–100.

Lande, M.B., Donovan, J.M., Zeidel, M.L., 1995. The relationship between membrane fluidity and permeabilites to water, solutes, ammonia, and protons. J. Gen. Physiol. 106, 67–84.

Lee, R.B., Ayling, S.M., 1993. The effect of methionine sulphoximine on the absorption of ammonium by maize and barley roots over short periods. J. Exp. Bot. 44, 53–63.

Li, C., Frolking, S., Frolking, T.A., 1992. A model of nitrous oxide evolution from soil driven by rainfall events. 1. Model structure and sensitivity. J. Geophys. Res. Atmos. 97 (D9), 9759–9776.

Louahlia, S., Laine, P., Thornton, B., Ourry, A., Boucaud, J., 2000. The role of N-remobilisation and the uptake of NH_4^+ and NO_3^- by *Lolium perenne* L. in laminae growth following defoliation under field conditions. Plant Soil 220, 175–187.

Loubet, B., Milford, C., Hill, P.W., Tang, S.Y., Cellier, P., Sutton, M.A., 2002. Seasonal variability of apoplastic NH4+ and pH in an intensively managed grassland. Plant Soil 238, 97–110.

Mattsson, M., Schjoerring, J.K., 1996. Ammonia emission from young barley plants: influence of N source, light/dark cycles and inhibition of glutamine synthetase. J. Exp. Bot. 47, 477–484.

Mattsson, M.E. Schjoerring, J.K., 1999. Controlled environment chamber measurements of ammonia exchange in two grass species, In: Proc. 10th Nitrogen Workshop, Copenhagen, August 1999. II.46. RVAU, Copenhagen.

Mattsson, M., Lundborg, T., Larsson, C.-M., 1993. Nitrogen utilisation in N-limited barley during vegetative and generative growth. IV. Translocation and remobilisation of nitrogen. J. Exp. Bot. 44, 537–546.

Mattsson, M., Husted, S., Schjoerring, J.K., 1998. Influence of nitrogen nutrition and metabolism on ammonia volatilisation in plants. Nutr. Cycl. Agroecosyst. 51, 35–40.

Menzi, H., Frick, R., Kaufmann, R., 1997. Ammoniak-Emissionen in der Schweiz: Ausmass und technische Beurteilung des Reduktionspotentials. Schriftenreise der FAL 26 FAL, Zürich-Reckenholz, Switzerland, p. 107.

Milford, C., Theobald, M.R., Nemitz, E., Sutton, M.A., 2001. Dynamics of ammonia exchange in response to cutting and fertilising in an intensively-managed grassland. Water Air Soil Poll Focus 1, 167–176.

Nemitz, E., Sutton, M.A., Schjoerring, J.K., Husted, S., Wyers, G.P., 2000. Resistance modelling of ammonia exchange over oilseed rape. Agric. Forest Meteorol. 105, 405–425.

Nemitz, E., Milford, C., Sutton, M.A., 2001. A two-layer canopy compensation point model for describing bi-directional biosphere/atmosphere exchange of ammonia. Q. J. R. Met. Soc. 127, 815–833.

Nielsen, K.H., Schjoerring, J.K., 1998. Regulation of apoplastic NH_4^+ concentration in leaves of oilseed rape. Plant Physiol. 118, 1361–1368.

Parton, W.J., Schimmel, D.S., Cole, C.V., Ojima, D.S., 1987. Analysis of factors controlling soil organic matter levels in great plains grassland. Soil Sci. Soc. Am. J. 51, 1173–1179.

Parton, W.J., Stewart, J.W.B., Cole, C.V., 1998. Dynamics of C, N, P and S in grassland soils—a model. Biogeochemistry 5, 109–131.

Priver, N.A., Rabon, E.C., Zeidel, M.L., 1993. Apical membrane of the gastric parietal cell: water, proton and nonelectrolyte permeabilites. Biochemistry 32, 2459–2468.

Singh, R., Nye, P.H., 1984. Diffusion of urea, ammonium and soil alkalinity from surface applied urea. J. Soil Sci. 35, 529–538.

Raven, J.A., Wollenweber, B., Handley, L.L., 1992. Ammonia and ammonium fluxes between photolithotrophs and the environment in relation to the global nitrogen cycle. New Phytol. 121, 5–18.

Recous, S., Mary, B., 1990. Microbial immobilisation of ammonium and nitrate in cultivated soils. Soil Biol. Biochem. 22, 913–922.

Riedo, M., Grub, A., Rosset, M., Fuhrer, J., 1998. A pasture simulation model for dry matter production, and fluxes of carbon, nitrogen, water and energy. Ecol. Model. 105, 141–183.

Riedo, M., Gyalistras, D., Fischlin, A., Fuhrer, J., 1999. Using an ecosystem model linked to GCM-derived local weather scenarios to analyse effects of climate change and elevated CO_2 on dry matter production and partitioning, and water use in temperate managed grasslands. Global Change Biol. 5, 213–223.

Riedo, M., Gyalistras, D., Fuhrer, J., 2000. Net primary production and carbon stocks in differently managed grasslands: simulation of site-specific sensitivity to an increase in atmospheric CO_2 and to climate change. Ecol. Model. 134, 207–227.

Riedo, M., Gyalistras, D., Fuhrer, H., 2001. Pasture responses to elevated temperature and doubled CO_2 concentration: assessing the spatial pattern across an alpine landscape. Clim. Res. 17, 19–31.

Ritchie, R.J., 1987. The permeability of ammonia, methylamine and ethylamine in the charophyte *Chara corallina* (*C. australis*). J. Exp. Bot. 38, 67–76.

Schjoerring, J.K., 1991. Ammonia emission from the foliage of growing plants. In: Sharkey, T.D., Mooney, H.A., Holland, E.A. (Eds.), Trace Gas Emissions by Plants. Academic Press, New York, pp. 267–292.

Schjoerring, J.K., Husted, S., Mattsson, M., 1998. Physiological parameters controlling plant–atmosophere ammonia exchange. Atmos. Environ. 32, 491–498.

Schmid, M., Neftel, A., Riedo, M., Fuhrer, J., 2000a. Process-based modelling of nitrous oxide emissions from different nitrogen sources in mown grassland. Nutr. Cycl. Agroecosyst. 60, 177–187.

Schmid, M., Neftel, A., Fuhrer, J., 2000b. Lachgasemissionen aus der Schweizer Landwirtschaft. Schriftenreihe der FAL 33 FAL, Zürich-Reckenholz, Switzerland p. 131.

Schmid, M., 2001. Nitrous oxide emissions from managed grasslands – development and tests of a dynamic model. PhD thesis, University of Bern.

Shiyomi, M., Takahashi, S., Kirita, H, 2000. Roles of plant biomass and vegetational heterogeneity, and energy-matter cycling in grassland sustainability. Ecol. Model. 132, 135–149.

Sutton, M.A., Fowler, D., 1993. A model for inferring bidirectional fluxes of ammonia over plant canopies. In: Proc. WMO Conf. on the Measurement and Modelling of Atmosphere Composition Changes Including Pollutant Transport, WMO/GAW-91, Sofia, 4–8 October 1993, World Meteorological Organisation, Geneva, pp. 179–182.

Sutton, M.A., Fowler, D., Moncrieff, J.B., Storeton-West, R.L., 1993a. The exchange of atmospheric ammonia with vegetated surfaces. II: fertilised vegetation. Q. J. R. Meteorol. Soc. 119, 1047–1070.

Sutton, M.A., Pitcairn, C.E.R., Fowler, D., 1993b. The exchange of ammonia between the atmosphere and plant communities. Adv. Ecol. Res. 24, 301–393.

Sutton, M.A., Asman, W.A.H., Schjoerring, J.K., 1994. Dry deposition of reduced nitrogen. Tellus 46B, 255–273.

Sutton, M.A., Fowler, D., Burkhardt, J.K., Milford, C., 1995a. Vegetation atmosphere exchange of ammonia: canopy cycling and the impacts of elevated nitrogen inputs. Water Air Soil Poll. 85, 2057–2063.

Sutton, M.A., Schjoerring, J.K., Wyers, G.P., 1995b. Plant-atmosphere exchange of ammonia. Phil. Trans. R. Soc Lond. Series A 351, 261–278.

Sutton, M.A., Burkhardt, J.K., Guerin, D., Nemitz, E., Fowler, D., 1998a. Development of resistance models to describe measurements of bi-directional ammonia surface-atmosphere exchange. Atmos. Environ. 32, 473–480.

Sutton, M.A., Milford, C., Dragosits, U., Place, C.J., Singles, R.J., Smith, R.I., Pitcairn, C.E.R., Fowler, D., Hill, J., ApSimon, H.M., Ross, C., Hill, R., Jarvis, S.C., Pain, B.F., Phillips, V.C., Harrison, R., Moss, D., Webb, J., Espenhahn, S.E., Lee, D.S., Hornung, M., Ullyett, J., Bull, K.R., Emmett, B.A., Lowe, J., Wyers, G.P., 1998b. Dispersion, deposition and impacts of atmospheric ammonia: quantifying local budgets and spatial variability. Environ. Poll. 102, 349–361.

Sutton, M.A., Milford, C., Nemitz, E., Theobald, M.R., Hill, P.W., Fowler, D., Schjoerring, J.K., Mattsson, M.E., Nielsen, K.H., Husted, S., Erisman, J.W., Otjes, R., Hensen, A., Mosquera, J., Cellier, P., Loubet, B., David, M., Genermont, S., Neftel, A., Blatter, A., Herrmann, B., Jones, S.K., Horvath, L., Führer, E., Mantzanas, K., Koukoura, Z., Gallagher, M., Williams, P., Flynn, M., Riedo, M., 2001. Biosphere–atmosphere interactions of ammonia with grasslands: experimental strategy and results from a new European initiative. Plant Soil 228, 131–145.

Thornley, J.H.M., 1998. Grassland Dynamics. An Ecosystem Simulation Model. CAB International, Oxon.

Thornley, J.H.M., Verberne, E.L.J., 1989. A model of nitrogen flows in grassland. Plant Cell Environ 12, 863–886.

van der Molen, J., Beljaars, A.C.M., Chardon, W.J., Jury, W.A., van Faassen, H.G., 1990. Ammonia volatilisation from arable land after application of cattle slurry. 2. Derivation of a transfer model. Neth. J. Agric. Sci. 38, 239–254.

van der Weerden, T.J., Jarvis, S.C., 1997. Ammonia emission factors for N fertilisers applied to two contrasting grassland soils. Environ. Poll. 95, 205–211.

Whitehead, D.C., Lockyer, D.R., 1989. Decomposing grass herbage as a source of ammonia in the atmosphere. Atmos. Environ. 23, 1867–1869.

Whitehead, D.C., 1995. Grassland Nitrogen. CAB International, Wallingford.

Wyers, G.P., Erisman, J.W., 1998. Ammonia exchange over coniferous forest. Atmos. Environ. 32, 441–451.